Enhanced Osteogenic Differentiation via Chemically Engineered Aggregation of Mouse Embryonic Stem Cells

David Gothard, MBiolSci

Thesis submitted to the University of Nottingham

for the degree of Doctor of Philosophy

February 2009

Abstract

The formation of embryoid bodies has long been utilized to initiate differentiation of embryonic stem cells *in vitro*. The embryoid body provides an effective means of recapitulating early stages during embryogenesis and formation of the three germ layers. Current methodology for embryoid formation is extensive but exhibits a lack of standardisation and coherence. Here is shown a 3D culure system for controlled embryonic stem cell aggregation via a non-cytotoxic cell surface modification and cell-cell cross-linking. Embryoid body formation was found to be a complex relationship between embryonic stem cell aggregation, proliferation, death, cluster agglomeration, extracellular matrix deposition and structural reorganisation. Engineered embryoid bodies formed more rapidly and were significantly larger than those in control samples. Embryoid body characterisation revealed a layered internal structure resulting from poor nutrient and gaseous diffusion and consequent core necrosis after ≥ 5 days in suspension culture. Immuno-labelling and PCR amplification analysis of Brachyury, Nestin, Gata-4 and Oct-4 showed differentiation of mesoderm, ectoderm and endoderm on the embryoid body surface and internal undifferentiated cells, respectively. Engineering appeared to enhance mesoderm differentiation, a progenitor of the osteogenic lineage. Embryoid bodies in settled culture spread outwards to form a plateau of collagen matrix which was later mineralized through differentiated osteoblast function. Quantification through Alizarin Red stained bone nodules and alkaline phosphatase activity demonstrated osteogenic differentiation enhancement within engineered samples. Dex-loaded poly-(lactic co-glycolic) acid polymer microparticles were found to be an effective method for delivery of osteo-inductive factors to internal undifferentiated embryonic

stem cells within the embryoid bodies. These findings show that the proposed 3D culture system provides reliable and repeatable methodology for the controlled formation of embryoid bodies which exhibit enhanced osteogenic differentiation. It is hoped that these engineered embryoid bodies could be used to efficiently generate homogeneous bone tissue for clinical application.

Acknowledgements

I would like to thank both my supervisors, Dr. Lee Buttery and Prof. Kevin Shakesheff for their guidance, time and help with all aspects of the practical and written work undertaken during my 3 year PhD. Their encouragement and belief in my abilities contributed greatly to the success of this study. I would also like to thank Dr. Felicity Rose for being my internal assessor. Her advice and recommendations were invaluable in the development of a logically structured scientific investigation and the resultant interpretation.

I wish also to thank everyone within the Tissue Engineering group for all their help, inspiration and friendship during my studies. Special thanks to Dr. Magdalen Self for showing me, as it were, the ropes and getting me acquainted with everyone, Dr. Daniel Howard for his expert opinion and help, Dr. Matthew TomLinson for provision of essential biological materials, Dr. Scott Roberts for his critique, Dr. Glen Kirkham for his help with cell culture and Mrs Teresa Marshall for all her help and equipment training.

Thanks and appreciation to the staff of the Histopathology department of the Queens Medical Centre for their help with embryoid body sectioning and H&E staining, Prof. Phil Williams for confocal microscopy-training and Mrs Christine Grainger-Boultby for SEM-training. Thank you to the BBSRC for funding this research.

Special thanks to Dr. Andrew Olaye and Mr. Christopher Wright for their practical work and data collection concerning microparticle fabrication and incorporation within embryoid bodies (Chapter 6), Mr. David Carter for PCR-training, Mrs Zahia Derouiche for PSS-training and Miss Ruby Majani for plasma-coating-training.

I would like to thank all of the friends I made for their support and advice when experiments did not work and encouragement to keep at it. Thanks specifically to Dr. Samuel Pygall, Dr. Lucy Johnson, Dr. Gerard Byrne, Dr. Jeff James, Dr. Shailesh Mistry, Mr. Hywel Williams, Miss Claire Jarvis, Miss Racheal Embrey, Dr. Carl Bond and Miss Katy Wilkinson for their friendship and company over the course of my PhD. They each provided no end to humorous and entertaining evenings, whether they were indoor gatherings or outdoor ventures into Nottingham city centre. Their distractions have generated many memories which will amuse me for years to come and that I will keep quiet from here on.

Thank you to my parents, Mr. John and Mrs Julie Gothard, and brothers, Mr. Neil and Mr. Paul Gothard, for their nurture and support in all my academic aspirations. Their love and encouragement fueled my determination to succeed at everything I put my mind too. This thesis represents the culmination of many years of hard work and dedication to an education in science.

I would also like to thank Mr. Roy and Mrs Sheila Howe and Miss Laura Howe for allowing me to stay in their home during the months it took to write this thesis. Their kindness and patience was much appreciated as I turned their dining room into my study.

I wish also to say thank you to my partner Miss Kate Howe for her love and support during my research endeavors. She has shown patience and understanding when I had to work late and on weekends. Her help and advice have been both welcome and constructive. She has tended to my every need whilst I spent many hours writing this thesis and I could not have completed my PhD without her.

A final thanks to all those people not mentioned by name, who have at one time or another provided help with either the practical or theory work during my research.

I would like to dedicate this thesis to both my grandmothers, Mrs Joyce Gothard and Mrs Jenny Edwards, who are not here today to see my achievements and graduation at the highest academic level. They would be very proud of what I have accomplished.

Declaration

I declare that this thesis is the result of my own work which has been mainly undertaken during my period of registration for the degree of Doctor of Philosophy at the University of Nottingham.

Table of Contents

List of Figures

List of Tables

List of Abbreviations

2D	Two Dimensional
3D	Three Dimensional
β-Mercap	β-Mercaptoethanol
µg	Microgram
µl	Microlitre
µm	Micrometer
AIDA	Advanced Image Data Analyzer
ALP	Alkaline phosphatase
AM	Aggregation Media
AP	Acid Phosphatase
AS cell	Adult Stem cell
Asc	Ascorbate-2-phosphate
Asp	Aspartate
ATPase	Adenosine Tri-Phosphatase
BBSRC	Biotechnology and Biological Sciences Research Council
BD	Becton and Dickinson
bFGF	Basic Fibrobast Growth Factor
BGP	β-Glycerophosphate
BMP	Bone Morphogenetic Protein
BSA	Bovine Serum Albumin
BSP	Bone Sialo Protein
Ca^{2+}	Calcium ion

CAD	Computer Aided Design
CAM	Computer Aided Manufacture
Cbfa-1	Core binding factor alpha-1
cDNA	Complementary DNA
CEE	Columnar Epiblast Epithelium
CM	Conditioned Media
CPC	Cetyl-Pyridinium Chloride
CPM	CryoPreservation Media
CNTF	Ciliary NeuroTrophic Factor
CO_2	Carbon dioxide
CT-1	CardioTrophin-1
Cys	Cysteine
DAPI	4, 6-DiAmidino-2-PhenylIndole
DCM	DiChloroMethane
Dex	Dexamethasone
dH_2O	Distilled Water
DMEM	Dulbecco's Modified Eagles Medium
Dmp-1	Dentin matrix protein-1
DMSO	DiMethyl-SulphOxide
DNA	DeoxyriboNucleic Acid
dNTP	DeoxyriboNuleotide TriPhosphate
dsDNA	Double Stranded DNA
EB	Embryoid Body
EC cell	Embryonic Carcinoma cell

ECM	ExtraCellular Matrix
EDTA	EthyleneDiamineTetraacetic Acid
EG cell	Embryonic Germ Cell
ES cell	Embryonic Stem cell
ESM	Embryonic Stem cell Media
FCS	Foetal Calf Serum
FGF	Fibroblast Growth Factor
FITC	Fluorescein IsoThioCyanate
g	Gram
GAG	GlycosAminoGlycan
GAPDH	GlycerAldehyde 3-Phosphate DeHydrogenase
GFP	Green Fluorescent Protein
Gly	Glycine
H^+	Hydrogen ion
H_2O	Water
HA	HydroxyApatite
HBSS	Hanks Balanced Salt Solution
HCl	HydroChloric acid
HEPA	High Efficiency Particulate Air
HEPES	N-2-HydroxyEthylPiperazone-n-2-EthaneSulfonic acid
HF	Human Fibroblast
His	Histidine
HMDS	HexaMethylDiSilazane
HPLC	High Pressure Liquid Chromatography

hr	Hour
HS cell	Haematopoietic Stem cell
Hyp	Hydroxyproline
ICM	Inner Cell Mass
IGF	Insulin-like Growth Factor
iPS cell	Induced Pluripotent Stem cell
IVF	*In Vitro* Fertilization
LIF	Leukemia Inhibiting Factor
LIFR	LIF Receptor
LPA	LysoPhosphatidic Acid
kV	Kilo-Volts
M-CSF	Macrophage Colony-Stimulating Factor
MEF	Mouse Embryonic Fibroblast
Mepe	Matrix Extracellular Phospho-glycoprotein
mg	Milligram
mGCS	Mitochondrial Glycine Cleavage System
min	Minute
mL	Millilitre
mm	Millimeter
MMC	MitoMycin C
MMP	Matrix Metallo-Protease
mRNA	Messenger RiboNucleic Acid
MS cell	Mesenchymal Stem cell
mSNLs	Mitotically inactivated SNLs

Mw	Molecular Weight
NAD+	Nicotinamide Adenine Dinucleotide
NaOH	Sodium Hydroxide
NF-κB	Nuclear Factor – κB
NIH	National Institue of Health
OC	OsteoCalcin
OCIF	OsteoClast Inhibiting Factor
OF45	Osteoblast/Osteoclast Factor 45
OMS cell	Olfactory Mucosa Stem cell
ON	OsteoNectin
OPG	OsteoProteGrin
OPN	OsteoPontiN
OSF-2	Osteoblast Specific Factor-2
OSM	OncoStatin M
OTA	Orthopaedic Trauma Association
PBA	PBS supplemented with 0.1% BSA
PBS	Phosphate Buffered Saline
PBT	PBS supplemented with 1% BSA and 0.1% Triton X-100
PCR	Polymerase Chain Reaction
PDGF	Platelet Derived Growth Factor
PEG	Poly-Ethylene Glycol
Pen/Strep	Penicillin/Streptomycin
PG cell	Primordial Germ cell
PGA	Poly(Glycolic Acid)

PLA	Poly(Lactic Acid)
PLGA	Poly(Lactic co-Glycolic Acid)
PNPP	p-NitroPhenyl Phosphate
ppAAm	Plasma Polymerised AllylAMine
Pro	Proline
PSS	Particle Sizing System
PTS	PBS supplemented with 0.1% Triton X-100
PTSF	PTS supplemented with 10% FCS
PVA	Poly-Vinyl Acetate
QMC	Queens Medical Centre
RANK	Receptor Activator of Nuclear Factor κB
RANKL	RANK Ligand
RNA	RiboNucleic Acid
rpm	Revolutions Per Minute
RT	Reverse Transcriptase
SCM	Standard Culture Media
S.E.M.	Standard Error of the Mean
sec	Second
SEM	Scanning Electron Microscope
SIM	Sandoz Inbred Mouse
SLS	Scientific Laboratory Supplies
SNL	STO Neo Leukemic
SSC	Saline-Sodium Citrate
ssDNA	Single Stranded DNA

SSEA	Stage Specific Embryonic Antigen
STAT	SH2 domain-containing signaling molecule
STEM	Stem cells, Tissue Engineering and Modelling
STO	SIM Thioguanine-resistant and Ouabain-resistant
TBE	Tris-Borate EDTA
TGF-β	Transforming Growth Factor-β
TNF	Tumor Necrosis Family
TRAP	Tartrate-Resistant Acid Phosphatase
U.V.	UltraViolet
UCS cell	Umbilical Cord Stem cell
VEGF-A	Vascular Endothelial Growth Factor-A

Chapter 1

1. Introduction

1.1. Stem Cell Research

1.1.1. Background

The term 'stem cell' was first coined by the Russian histologist Alexander Maksimov in 1908 when he postulated the existence of haematopoietic stem (HS) cells. It took over 50 years before the first stem cells were discovered (Altman, 1962). Ensuing discoveries expanded the field of stem cell research and its potential applications. Since the discovery of embryonic stem (ES) cells over 20 years ago, the field has generated much promise in regenerative and reparative medicine (Martin, 1981, Evans and Kaufman, 1981). ES cells are highly proliferative *in vitro* and therefore provide an ideal abundant and sustainable cell source for tissue engineering (Tsai et al., 2000). Researchers endeavour to recapitulate *in vivo* growth and development of ES cells *in vitro* to better understand the mechanisms involved in their differentiation and organogenesis. Their intention is the elucidation of novel approaches to the repair or replacement of damaged tissue resulting from disease and trauma (Watt and Hogan, 2000, Moon et al., 2006). This would ultimately eliminate the need for many of the drugs currently used to maintain failing tissues and organs, revolutionizing medicine as we now know it (Keller and Snodgrass,

1999). Transplantation would be advanced to the stage where tissues and organs are generated according to demand using a combination of differentiated ES cells and biomaterial scaffold supports.

1.1.2. Stem Cell Types and Derivation

1.1.2.1. Adult Stem Cells

ES and embryonic germ (EG) cell research is controversial because most resultant cell lines are established from the destruction of an embryo. There is no such controversy surrounding adult stem (AS) cells. They are derived directly from the individual into whom the engineered tissue would be implanted (Ratajczak et al., 2007). Their isolation is non-destructive and therefore accepted by most people. They provide a renewable source of stem cells for *ex vivo* tissue engineering without the hinderance of immune-rejection observed in other stem cell-based therapies (Barrileaux et al., 2006). However, as they are genetically identical to the recipient they are redundant when repairing tissue damage caused by genetic disorders.

Unlike ES cells, AS cells do not possess pluripotency. They are multipotent cells which can differentiate into any cell type of the tissue from which they are isolated. Many AS cells have been discovered from various organs and their related tissues. Each type of AS cell carries a prefix referring to its origin tissue, such as mesenchymal stem (MS) cells, HS cells, umbilical cord stem (UCS) cells and olfactory mucosa stem (OMS) cells (Lee, 2008, Kent et al., 2007, Park et al., 2008c, Murrell et al., 2005). This assortment of AS cells has shown regenerative capabilities in tissues corresponding to those from which they were derived, including heart, bone, muscle, cartilage and liver amongst others (Tateishi et al., 2008, Valenti et al., 2008, Bhagavati, 2008, Goessler et al., 2008, Huang, 2007). MS cells specifically, have been

utilized for many years to regenerate bone and related tissues, but like other AS cells their medical application is restricted (Summer and Fine, 2008). However, some AS cells have been shown to exhibit limited plasticity. These special AS cells can transdifferentiate to form cells outside the lineage of their origin tissue, i.e. pancreatic stem cells forming epithelial cells (Meier et al., 2008, Chim et al., 2008, Filip et al., 2005).

1.1.2.2. Embryonic Carcinoma Cells

Some of the earliest cells to exhibit true pluripotency were embryonic carcinoma (EC) cells, derived from malignant germ cell tumors called teratocarcinomas (Martin, 1975, Martin, 1980, Lehman et al., 1974, Finch and Ephrussi, 1967). Teratocarinomas account for 40% of testicular tumors and can occur in the ovaries of prepubescent and teenage girls, although rarely. EC cells are just one of a number of cell types derived from these teratocarcinomas, and have been characterised extensively (Bluthmann et al., 1983). Recent publications have illustrated the isolation of EC cells from embryonic testis and oocytes (Kerr et al., 2008b, Kerr et al., 2008a). Particular EC cell lines have been found to contribute to chimeras upon transplantation into developing embryos (Brinster, 1974, Andrews, 2002). However, most EC cells do not contribute to chimeras, they form clonal teratocarcinomas (Chambers and Smith, 2004). Epigenetic differences between EC cells and ES cells are thought to confer these observed characteristics (Table 1.1) (Bulic-Jakus et al., 2006).

1.1.2.3. Embryonic Germ Cells

The existence of EG cells was first reported nearly 20 years ago (Matsui et al., 1991, Resnick et al., 1992). Mouse EG cells were isolated directly from a specific part of the fetus/embryo called the gonadal ridge, usually 8 weeks following fertilization

Surface Marker	Mouse			Human		
	ES	EG	EC	ES	EG	EC
SSEA-1	+	+	+	-	+	-
SSEA-2	-	-	-	+	+	+
SSEA-4	-	-	-	+	+	+
TRA-1-60	-	-	-	+	+	+
TRA-1-81	-	-	-	+	+	+
ALP	+	+	+	+	+	+
Oct4	+	+	+	+	?	+
Properties						
Feeder-cell dependent	+	+	Some EC cell lines	+	+	Some (poor proliferation)
Stem cell renewal factors	LIF and other factors that act through gp130			bFGF feeders and serum/serum -free media	LIF, bFGF, forskolin	Unknown
Normal karyotype	+	+	-	+	-	+
Teratoma formation	+	+	+	+	-	+
Chimera formation	+	+	limited	?	?	?
				contribute to chimeras in mice		
Telomerase activity	+	-	+	+	?	+
Growth characteristics	form tight, rounded, multi layer clumps; form EBs			form flat, loose aggregates; form EBs	form rounded, multi layer clumps; form EBs	form flat, loose aggregates; form EBs

Table 1.1: Comparison of mouse and human ES, EG and EC cells.

(Labosky et al., 1994, McLaren and Durcova-Hills, 2001). Isolation of human EG cells came soon after in the late 1990s (Shamblott et al., 1998). EG cells were found to originate from primordial germ (PG) cells in the gonadal ridge. During normal embryogenesis PG cells give rise to the germ cells, whether that be sperm or egg. EG cells have also been isolated from adolescent testicular teratomas (Kimura et al., 2003, Kimura et al., 2008). This supports current consensus methodology for the isolation of EG cells from PG cells. Embryoid bodies (EBs) provide a crude recapitulation of *in vivo* teratomas, which can be cultured *in* vitro, and from which PG cells are isolated.

EG cells are very similar to ES cells, exhibiting the ability to differentiate into multiple cell types. EG cells have also been shown to exhibit normal karyotypes over prolonged population doublings (Shamblott et al., 2001). Differences include *in vitro* growth characteristics (Pera et al., 2000), abnormalities in genome imprinting (Labosky et al., 1994, Thomson and Odorico, 2000, Onyango et al., 2002), X chromosome inactivation (Migeon et al., 2001) and failure to form teratomas *in vivo*.

1.1.2.4. Embryonic Stem Cells

ES cells are isolated from the blastocyst of an early pre-implantation embryo, resulting in its destruction (Goumans et al., 1998). However, recent work has shown the derivation of ES cell lines without embryo destruction (Klimanskaya et al., 2006). The blastocyst is the first definitive developmental structure that is readily accessible during embryogenesis (Rathjen et al., 1998). It is composed of a microscopic ball of cells which include three individual cellular architectures. The first structure is the trophoblast which surrounds the blastocyst and gives rise to all extra-embryonic tissues such as the placenta and umbilical cord (Nichols et al.,

1996). The second is the hollow space within the blastocyst called the blastocoel. The third and final structure is the inner cell mass (ICM) which is situated to one side of the blastocyst adhered to the trophoblast.

Cells which constitute the ICM possess pluripotency which is the ability to form all three embryonic germ layers including mesoderm, endoderm and ectoderm (Bain et al., 1995, Keller, 1995, Bishop et al., 2002, Odorico et al., 2001, Wiles and Johansson, 1999). The ICM also gives rise to the germ cells, which differentiate and develop into oocytes and spermatocytes (Fig 1.1). It is from the ICM that ES cells are derived, usually isolated from day 5 to 8 blastocysts prior to gastrulation (Kim et al., 2005, Stojkovic et al., 2004, Thomson et al., 1998, Reubinoff et al., 2000, Mitalpova et al., 2003).

1.1.2.5. Induced Pluripotent Stem Cells

Stem cells can be generated via nuclear reprogramming of somatic cells. Induced pluripotent stem (iPS) cells were first created in mice via retroviral delivery of four defined genes incuding Oct-4, Sox2, Klf4 and c-Myc (Takahashi and Yamanaka, 2006). These cells are similar to ES cells but exhibit differences in DNA methylation and do not contribute to chimeras. Original selection was for Fbx15, however, selection for Nanog generated germLine-competent iPS cells; able to contribute to chimeras (Okita et al., 2007, Maherali et al., 2007, Wernig et al., 2007).

Human iPS cells were created using the same four genes as those in mouse (Takahashi et al., 2007, Park et al., 2008b, Lowry et al., 2008). Specific methodology has been published for their generation through retroviral transfection (Park et al., 2008a). However, other research groups published work describing the generation of human iPS cells using a different combination of genes delivered not by

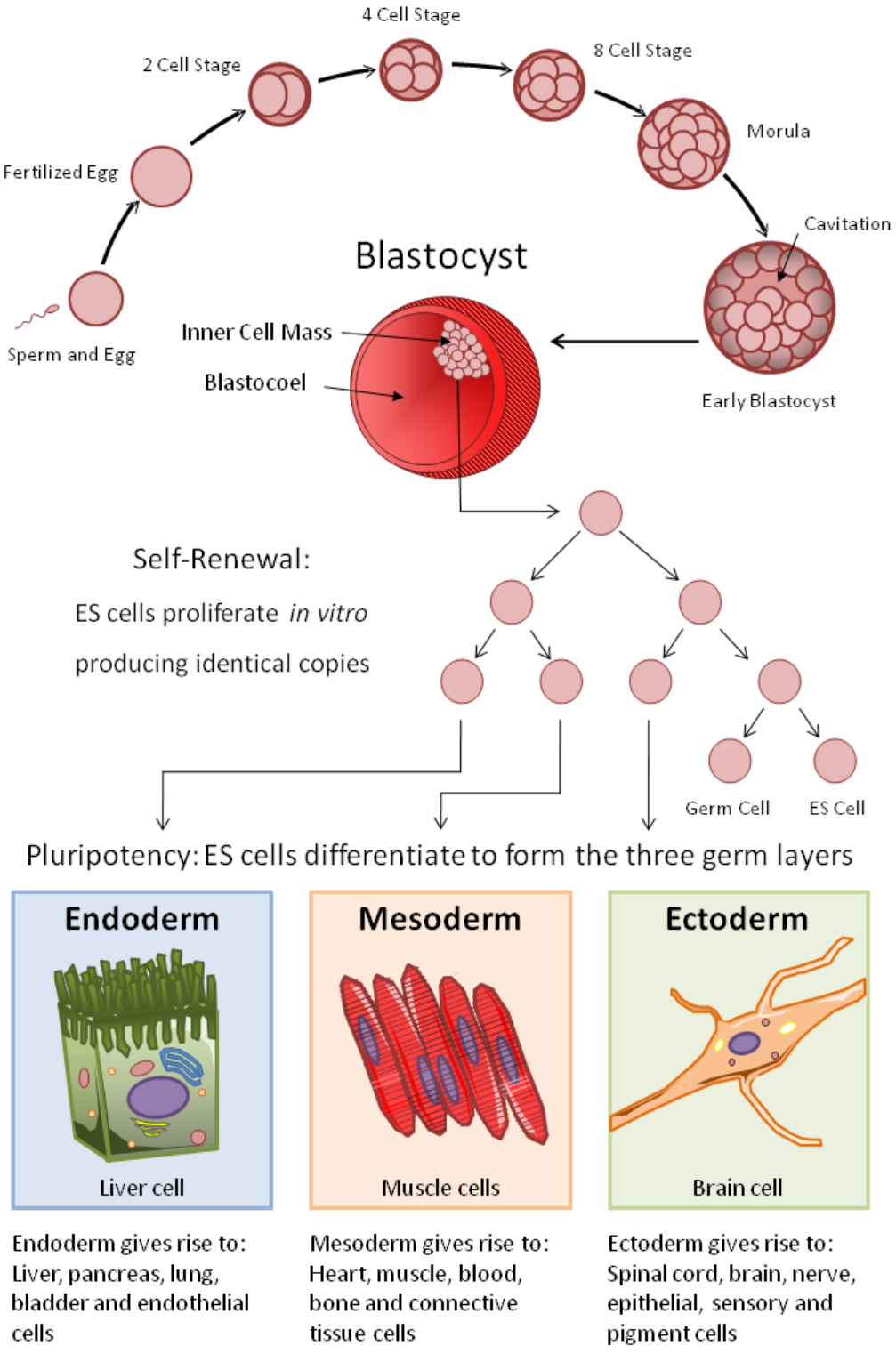

Figure 1.1: ES cell differentiation and germ layer formation.

retroviruses, but by lentiviruses. These new human iPS cells were transfected with Oct-4, Sox2, NANOG, and LIN28 (Yu et al., 2007). Cutting edge research has generated iPS cells without the c-Myc gene. Chimeric mice did not develop cancer when implanted with these c-Myc $^{(-/-)}$ iPS cells, demonstrating significant relevance for medical application (Nakagawa et al., 2008).

1.1.3. Embryonic Stem Cells

1.1.3.1. Definition

Originally, ES cells were loosely defined as cells which could undergo sustained proliferation *in vitro*, self-renewal and differentiate towards any cell lineage within the body. However, other cells fulfil this definition due to observations of transdifferentiation in AS cells and the discovery of self renewing EG and EC cells. The definition of an ES cell was subsequently updated to incorporate more stringent and precise properties that potential ES cells had to exhibit (Bishop et al., 2002).

ES cells must be derived from the ICM of a blastocyst. They must exhibit and maintain a stable diploid karyotype without X-chromosome inactivation during unlimited proliferation consisting of symmetrical divisions without differentiation. ES cells must be able to differentiate and give rise to all three germ layers and the germ line. They should contribute to chimeras and form teratomas upon ectopic transplantation *in vivo*, which resemble *in vitro* EBs (Nichols et al., 1990, Nagy et al., 1993, Iannaccone et al., 1994). However, this is not possible when concerned with human ES cells. A fully differentiated teratoma should resemble the a developing blastula stage embryo, exhibiting a variety of cell types including bone, cartilage, skin, heart, gut, hair, brain and muscle (Odorico et al., 2001).

1.1.3.2. Identification

ES cells are isolated from embryos through selection for pluripotency markers which reside on the cell surface (Shamblott et al., 2001). ES cell markers include stage specific embryonic antigen (SSEA) 3 and SSEA-4 (expressed only on human ES cells), Oct-3/4, Sox2, Rex-1 and NANOG (Bielby et al., 2004, Hatano et al., 2005). The corresponding ligands of these markers are exploited in efforts to isolate pure ES cell cultures. If the isolated ES cells are not pure they can quickly differentiate and also potentially cause teratoma formation when ectopically grafted *in vivo* (Koller et al., 1995, Burdon et al., 1999). Another distinguishing property of ES cells is *de novo* methylation activity which causes hypomethylation of the embryo genome. Hypomethylation may have a direct effect upon genome reformatting in ES cells for preparation of the proliferation and differentiation processes that occur during embryogenesis (Lei et al., 1996). Other markers which can be used in a negative manner are those for differentiation, as opposed to pluripotency. These markers select for trophoectoderm, germ layers and germ cells (Ginis et al., 2004). Representative markers are listed overleaf (Table 1.2).

1.1.3.3. Pluripotency

In vitro proliferation of mouse ES cells currently involves their 2D growth and expansion in co-culture with a feeder layer (Nichols et al., 1990, Cheng et al., 1994). The feeder layer consists of mouse embryonic fibroblasts (MEFs). The specific fibroblast cell line utilized in this study was SNL (STO (SIM (Sandoz Inbred Mice) Thioguanine-resistant and Ouabain-resistant) Neo Leukemic). MEFs support mouse ES cell growth and maintain pluripotency (Bishop et al., 2002, Boontheekul et al., 2005). Pluripotency is maintained by the action of a secreted polypeptide called

Trophoectoderm	Mesoderm	Endoderm	Ectoderm	Germ Cells
CDX2	α-Actin	α –fetoprotein	CRABP2	Axdazl
EOMES	CBFA1	Activin RIB	GFAP	BMP15
GCM1	Brachyury	Amylase α2B	ISL1	DAZL1
KRT1	VE-Cadherin	BMP2	MAP2	GCNA1
	CD31 and CD34	FABP2	MSII	GDF9
	Collagen I and II	FGF-8	Nestin	GP90-MC301
	Dermin	FOXA2	NeuroD1	MATER
	HAND1	GATA-4 and 6	Olig-2	Podoplanin
	Hemoglobin β and ζ	HHEX	PAX-6	Tesmin
	MSX1	HNF4A	SOX1	TEX101
	MYF5	IAPP	Synaptophysin	ZAR1
	NPPA	Laminin α1, β1, γ1	TH	
	VEGFR1	LHX1	TUBB3	
	WT-1	Nodal	Vimentin	
		Otx2		
		PAX-4		
		PDHX		
		PTF1A		
		Smad2		
		SOX7		
		Somatostatin		
		TAT		
		Wnt-1		

Table 1.2: List of selective markers for trophoectoderm, germ layers and germ cells.

leukemia inhibiting factor (LIF) (Piquet-Pellorce et al., 1994, Keller, 1995, Furue et al., 2005). LIF acts to suppress differentiation rather than maintain pluripotency (Zandstra et al., 2000, Niwa, 2001, Oka et al., 2002).

LIF functions via heterodimerization of the low-affinity LIF receptor (LIFR) and a membrane bound signaling complex gp130 (Starr et al., 1997, Smith, 2001, Viswanathan et al., 2002). This heterodimerization causes the transcription of self-renewal genes within the nuclei of the mouse ES cells. A number of steps involving two main signaling molecules called Jaks (non-receptor cytoplasmic protein tyrosine kinase) and STATs (SH2 domain-containing signaling molecules) are activated as a result of this heterodimerization reaction (Fukada et al., 1996, Niwa et al., 1998, Burdon et al., 1999, Matsuda et al., 1999). LIFR and gp130 are receptor complexes for a number of other cytokines including LIF, such as ciliary neurotrophic factor (CNTF), oncostatin M (OSM) and cardiotrophin-1 (CT-1), each of which has the capacity to substitute for LIF and maintain a proliferative state (Thomson et al., 1995, Yoshida et al., 1996, Dani et al., 1998, Nichols et al., 2001). However, the extent to which these alternative factors maintain a proliferative state in mouse ES cells varies compared to LIF (Ware et al., 1995, Nichols et al., 1996). A current study provided evidence that LIF maintains a proliferative, self-renewing state in mouse ES cells in a synergistic manner with Wnt (Ogawa et al., 2006). This finding suggests that LIF may not be sufficient for maintaining pluripotency long term alone. Alternatives exist for maintenanc of human ES cell culture.

1.1.3.4. Differentiation

Although ES cells have been shown to exhibit pluripotency, they have to this day not been employed in clinical trials (Deb et al., 2008). This is mainly due to the present

lack of knowledge concerning their appropriate and efficient differentiation *in vitro* or *in vivo*. Current differentiation methodologies are effective but highly inefficient (Wiles and Johansson, 1999, Schuldiner et al., 2000). Investigations of ES cell cultures that have undergone directed differentiation were found to contain contaminating cells of lineages unintentionally induced. These anomalous cells (1) lower the efficacy of directed differentiation, (2) illustrate a lack of knowledge concerning the factors involved in ES cell differentiation, and (3) demonstrate that current engineered tissue is not ready for clinical application in regenerative and reparative medicine (Polak and Mantalaris, 2008).

Once the problems associated with efficient ES cell differentiation have been resolved, the potential medical use of ES cells covers a plethora of regenerative and reparative applications. The clinical successes in treatment of type I diabetes (Voltarelli et al., 2007), autoimmune diseases (Burt et al., 2006, Burt et al., 2002), leukemia (Marks, 2008, Sierra et al., 2008) and osteonecrosis (Tauchmanova et al., 2002, Kawate et al., 2006) Kawate K. 2006) with human AS cells hints at the therapeutic potential of human ES cells.

1.1.3.5. Feeder Free Culture

As well as problems with differentiation concerning the advancement of ES cells into clinical trials, the use of feeders within *in vitro* culture poses a similar dilemma. To be acceptable for transplantation into the body ES cells must be pure and exhibit uniform differentiation. By co-culturing with feeders it is inevitable that some will be carried through into clinical transplants. The presence of feeders could trigger an immune response which could consequently cause immune-rejection.

In response to this dilemma researchers have developed alternative culture methodology based on the removal of feeders (Matsubara et al., 2004). Initial feeder free culture systems concerning mouse ES cells, simply removed conventional MEF feeders and cultured on residual MEF extracellular matrix (ECM) (Klimanskaya et al., 2005). This removed live MEFs from the culture system but the presence of xeno-ECM still posed a problem. Matrigel (laminin, collagen IV, heparan-sulphate-proteoglycan complex) subsequently replaced MEF-derived ECM and has been widely used in feeder free culture systems (Navarro-Alvarez et al., 2008). However, some studies have published data showing that Matrigel and its individual components can actually induce ES cell differentiation (Ma et al., 2008, Domoqatskaya et al., 2008, Prokhorova et al., 2008). Another problem was the use of conditioned media (CM) from MEFs. Since CM contains unidentified factors essential to ES cell maintenance, its removal from the system was not a viable option. Instead, MEF-CM was substituted with human fibroblast (HF) CM. This completely resolved the problem of xenogeneic material contamination. ES cells were now cultured in a xeno-free system on human feeders in HF-CM (Vemuri et al., 2007). However, risks still existed with potential genetic disease transmission through the allogeneic HF feeder layer, and contamination of engineered tissues with HFs carried over from ES cell culture. Current research has developed a culture system based on feeder layers from autogeneic HFs (Choo et al., 2008). The latest research has demonstrated a human ES cell culture system which is both feeder-free and ECM-free (Bigdeli et al., 2008). This system however, still employs the use of HF-CM. In future, researchers could abrogate the necessity of CM for ES cell culture by replacing it with a completely defined media.

1.1.4. Ethical Stem Cell Research

1.1.4.1. Background

Both derivation and utilization of ES cells are highly regulated and accordingly restricted in specific areas by the legal and ethical issues surrounding them. There are four primary sources of ES cells including current ES cell lines, cloned embryos, aborted embryos and unused *in vitro* fertilisation (IVF) embryos (Thomson et al., 1998). Each source has its own regulatory laws and ethical codes, i.e. the law states that aborted embryos can only be used for research purposes with the explicit consent of the donor *and* if the donor's decision to abort had no relevance to the embryo's potential application in stem cell research. A report written by the 'Human Embryo Research Panel' to the director of the 'National Institute of Health' (NIH) and published in 1994, helped resolve many issues surrounding the derivation of ES cells and their application (Meyer, 2000). Mitigation of inhibitory laws and resolution of ethical constraints would give researchers freedom to develop new stem cell based therapies for regenerative and reparative medicine under effective but not restrictive regulation (Griffith and Naughton, 2002).

1.1.4.2. The Debate

The use of ES cells has ignited an intense national and international ethical debate between government-funded regulatory bodies of stem cell research and pro-life-groups. The crux of the debate is the 'sanctity of life'. Pro-life groups use this to highlight contentious issues surrounding the opportunistic retrieval of ES cells from unused IVF embryos. Their argument is that by destroying the embryo you are in fact committing murder. To counteract this argument, utilitarians raise the question of what constitutes murder. Murder can be interpreted in various ways and the law

reflects this. Execution of murderers is legal in the USA, but yet it is still murder. Manslaughter verdicts simply make murder a scale of intent. Ethically and legally sound benefits arise from murder in the form of available transplants (Robertson, 2001). The only ethical and legal concern to be addressed in the determination of whether someone has committed murder is innocence (Meyer, 2000). A common misconception is that 'legal' is interpreted as 'ethical'. Since the law is subject to interpretation it has no place in the decision-making process concerning ethics. Law is essential for issuing guidelines and setting restrictions but is ultimately flawed when debating ethical concerns (Chu, 2003).

1.1.4.3. Definition of a Human

The ethical controversy surrounding the use of ES cells derived from embryos is fundamentally concerned with the question of how to define a human. To commit murder, the supposed victim would have to be a human being in the eyes of the law. Utilitarians exploit this legal incongruity by arguing that an embryo can not be considered a person, as it does not show any indication of a discernable brain and a phenotype or ability to express self-consciousness, personality, intellect, will and emotion. This may seem at first a strong argument for ES cell research, but approaching the same principles from a different perspective changes the entire argument on its head. Individuals who suffer Alzheimers, Parkinsons disease or who have lost parts of their neural cortex function from stroke are considered no less human than they were beforehand. The diminished capacity to express these qualities is therefore not a justifiable cause to waver the statutory rights of an individual (Chu, 2003).

1.1.4.4. Utilitarianism 'vs' Pro-Life

Democracy, a method that governs our country and many others, has great merit when decisions are to be made in an honest and fair way. Many people, especially utilitarians, support this method. However, public consensus is where democracy becomes tainted and fails; the general consensus may not reflect the majority decision of a nation, rather the opinion of a powerful and influential minority (Fox, 1999). Before public consensus can be trusted for its views and opinions to reflect the majority decision, numerous factors have to be accounted for, or better yet, removed. These include the media, politics, economics, influential personalities and most importantly, the way in which the facts are portrayed to the public so that the content is highlighted, not the manner of its presentation. The utilitarian view and pro-life view should both aim for a balance, not a victory. The arguments are both built on the same premise, but each have taken different routes and drawn separate conclusions about ES cell research.

1.1.4.5. Ethical Research Continues

As a result of this ethical dilemma, progression from laboratory based research to clinical trials is tightly regulated (Thomson et al., 1995). The balance between benefits of ES cell research and the inherent risks has consequently been thoroughly evaluated and is routinely monitored. Despite protests by pro-life groups, stem cell research continues because of scientific benefit, commercial demand on biotechnology and the demand for new therapeutic strategies to treat patients with severe disorders. Ethical concerns should not hinder progress, but provide stem cell research with a moral compass.

1.2. Tissue Engineering

1.2.1. Background

Tissue engineering is an interdisciplinary field which combines the principles of biology with engineering and medicine (Horch, 2006, Vacanti, 2006). More specifically, tissue engineering involves the combination of cells (allogeneic or autogeneic), engineered biomaterial scaffolds and biochemical factors for the regeneration, repair and replacement of damaged tissue due to disease and trauma (Dunn, 2008, Langer and Vacanti, 1993). The field has progressed rapidly over the last two decades, and current research approaches involve the use of early progenitor cells such as ES cells (Habib et al., 2008). ES cells are expanded *in vitro*, seeded onto a suitable scaffold and implanted *in vivo* (Handschel et al., 2008b). ES cells are differentiated inefficiently *in vitro* prior to implantation. Alternatively, they are differentiated in response to biochemical cues delivered via the scaffold (Inanc et al., 2008).

1.2.2. Biomaterial Scaffolds

1.2.2.1. Biomimetics

Biomimetics is the study of models and systems in nature for the generation of bioinspired solutions to human problems (Green, 2008). The field of tissue engineering uses biomimetics to produce scaffolds which replicate one or more advantageous characteristics found in their natural counterparts (Ma, 2008). Successful scaffolds provide 3D architecture and mechanical support for engineered tissue whilst recapitulating the *in vivo* microenvironment. Essentially, the scaffold

replicates the ECM and therefore influences cell attachment, migration, proliferation, differentiation and resultant tissue organization (Shin et al., 2003). The use of biomimicry has aided the synthesis of appropriated scaffolds for engineered tissues including brain (Panseri et al., 2008, Potter et al., 2008), heart (Radisic et al., 2006), liver (Karamuk et al., 1999), blood (Panoskaltsis et al., 2005) and bone (Yang et al., 2003, Green et al., 2002).

1.2.2.2. Biocompatibility

The accepted definition of biocompatibility encompasses two major factors. The scaffold should not provoke an immunological nor inflammatory response, whether locally or systemically. However, recent studies have found that an inflammatory response can be useful for induction of angiogenesis (Levenberg, 2005). Dependent on the medical purpose of the implant, the scaffold should exhibit long or short term integration eliciting appropriate and beneficial tissue responses. PLA and PGA monomeric subunits occur naturally within the body, however they are acidic and cause alteration to physiological conditions at the implant site.

The body can remove lactic acid via the Cori or Krebs cycle (Fig 1.2). Lactic acid enters the blood and dissociates to form lactate and a hydrogen ion. The hydrogen ions can be removed intracellularly via nicotinamide adenine dinucleotide (NAD+) and eventually expelled as H_2O. Lactate enters the Cori cycle where it is converted to glucose in the liver via gluconeogenesis. Alternatively, blood lactate forms lactic acid in the heart and is oxidized to form pyruvic acid via NAD+. The high concentration of oxygen stored in the heart cells allows metabolism via the Krebs cycle.

Glycolic acid undergoes sequential enzymatic reactions in the liver involving glycolate oxidase and glycine transaminase to form glycine. Glycine is converted to

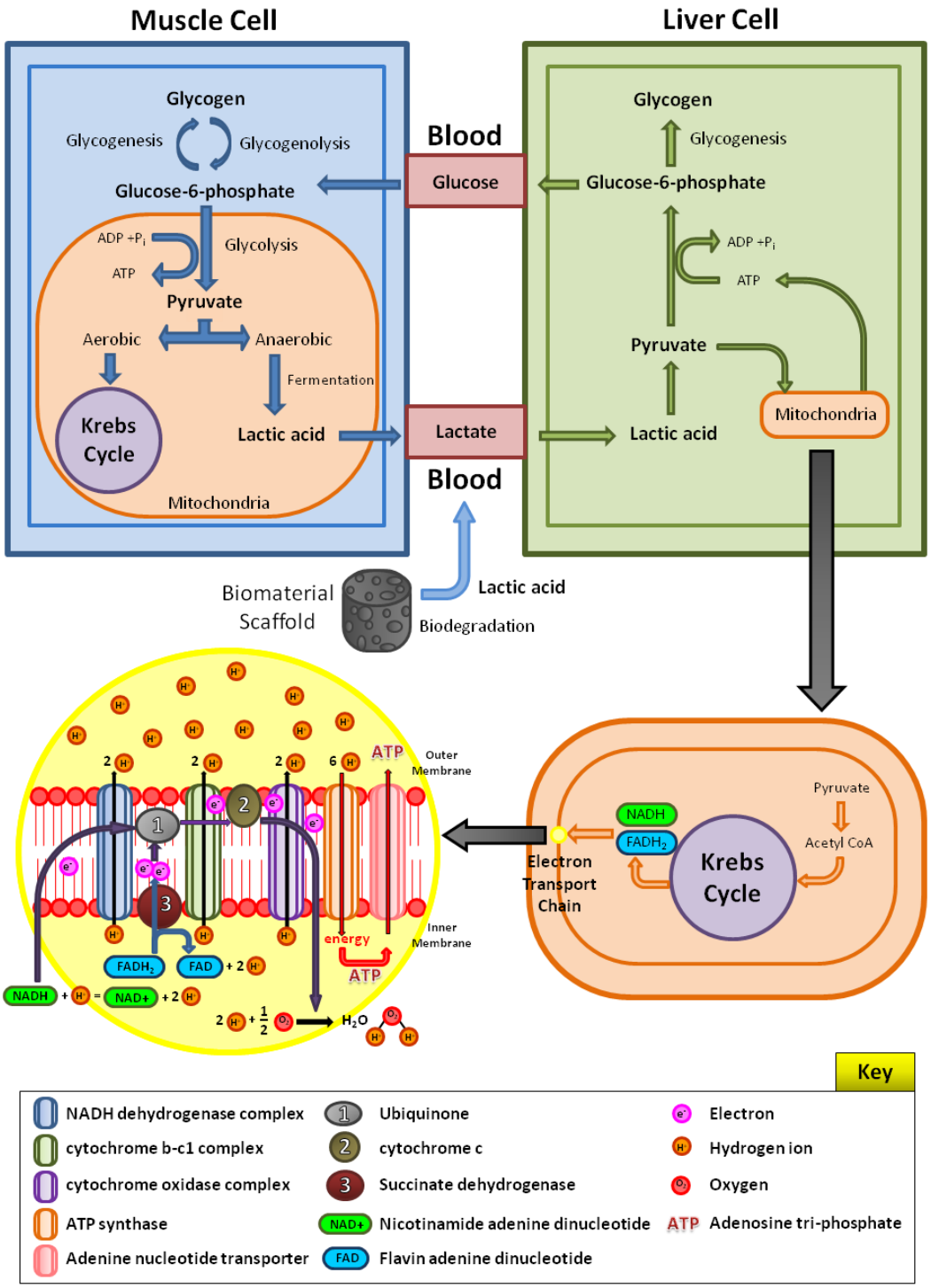

Figure 1.2: Metabolism of lactic acid from scaffold biodegradation, via the Cori and Krebs Cycle.

serine and then pyruvate which enters the Krebs cycle (Hollinger, 1983, Xue et al., 1999). Alternatively, glycine enters the mitochondrial glycine cleavage enzyme system (mGCS) where it is eventually expelled via the lungs as CO_2 and excreted in urine as urea (Fig 1.3) (Hiraga and Kikuchi, 1980, Kikuchi and Hiraga, 1982).

1.2.2.3. Biodegradability

Synthetic polymer scaffolds used for *in vivo* delivery of cells are only a transient step in the regeneration of a target tissue. Scaffolds are made from polymers which can be readily broken down by the body. The byproducts of degradation should be non-toxic so as to not damage newly regenerated tissue. Current polymers used as scaffolds are degradable polyesters including poly(lactic acid) (PLA) and poly(glycolic acid) (PGA) (Freed et al., 1994). These polymers are broken down in the body to their monomer subunits, lactic and glycolic acid. The mode of degradation is commonly accepted to be non-enzymatic hydrolysis of the ester backbone (Anderson and Shive, 1997). However, the action of esterases within the body could also have an unsubstantiated effect on polymer degradation. Degradation rate differs between PLA and PGA, with PLA degrading the slower of the two. Implants are often composites of two or more substances to allow for tailored degradation of subsequent scaffolds (Young et al., 2005). One co-polymer is poly(lactic co-glycolic acid) (PLGA), which has been routinely employed for the production of scaffolds within the field of tissue engineering. However, polymer scaffolds and implants do not always need to be biodegradable. Biomaterial implants have been utilized for heart valve (Stamm et al., 2004) and hip replacement(Schauss et al., 2006). These implants have to be durable and strong enough to withstand the physical stresses associated with the replaced body part function, and last the

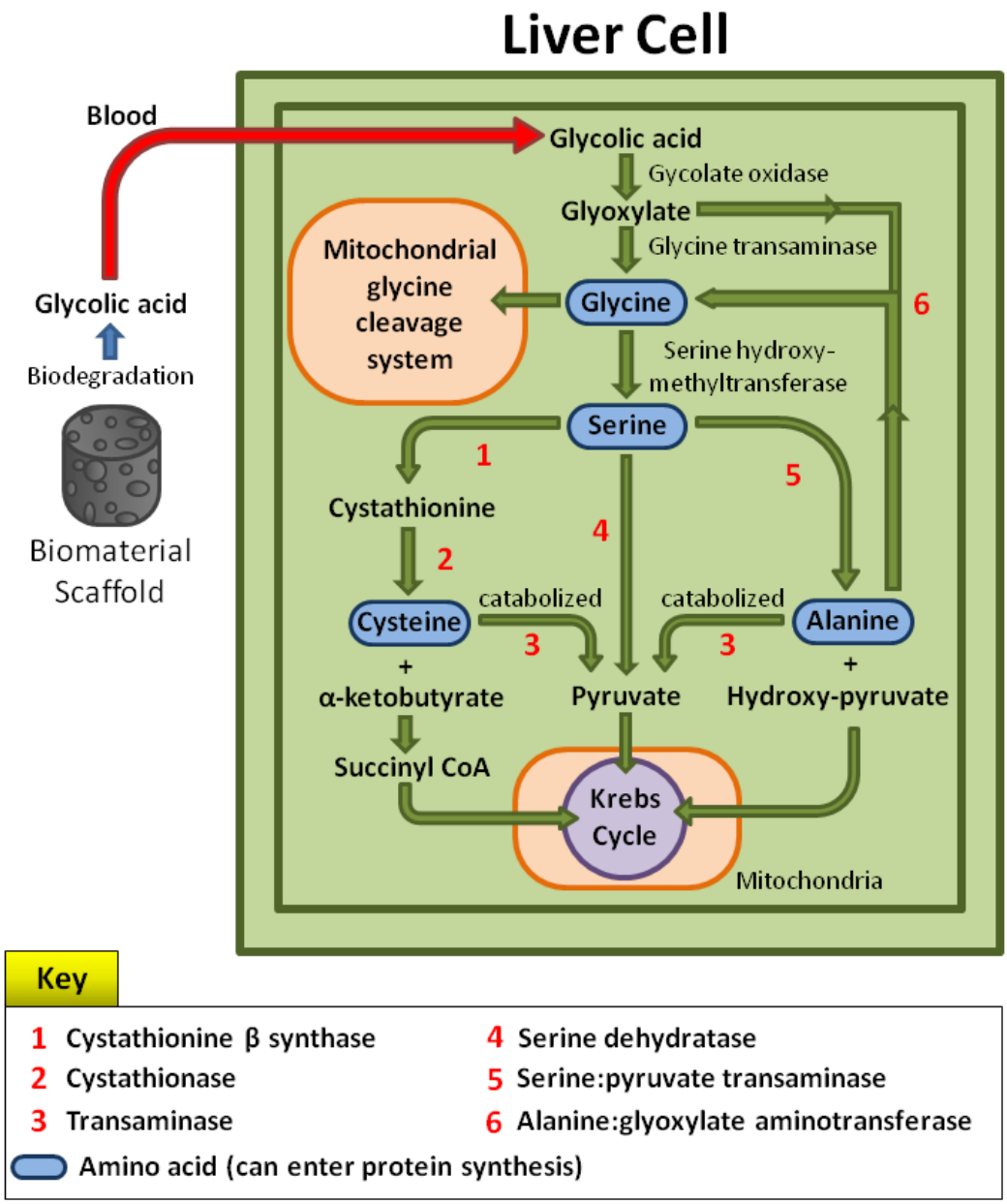

Figure 1.3: Metabolism of glycolic acid from scaffold biodegradation, via the Krebs Cycle.

lifetime of the patient.

1.2.2.4. Biomechanics

The complexity of regenerating tissues *in vivo* demands scaffolds capable of exhibiting multifactorial properties (Butler et al., 2000). Scaffolds must be capable of enduring mechanical and physiological stresses evoked by the body after implantation (Ghosh and Ingber, 2007, Semino, 2008). Biomechanical properties of potential scaffolds that require consideration include elasticity, thermostability, and tensile strength of the constituent polymer(s) (Guan et al., 2004, Lendlein et al., 1998).

Scaffold biomechanics can be tailored to aid regeneration, repair or replacement of existing *in vivo* structures, and more importantly their function. Current scaffold applications include the replacement of heart valves (Sarraf et al., 2005, Stamm et al., 2004), blood vessels (Shum-Tim et al., 1999, Shinoka et al., 1998, Shinoka and Breuer, 2008), and the repair and regeneration of skin (Blackwood et al., 2008, Cai et al., 2005) and bone (Nesti et al., 2008, Duty et al., 2007, Dyson et al., 2007). The regeneration of bone places many demands on the mechanical properties of a suitable scaffold. These include support of physiological loads (McMahon et al., 2008), bone remodeling (El Haj et al., 2005), accommodation of physiological strains (Howard et al., 2008) and suitability to bone type (Babis and Soucacos, 2005).

The method of manufacture is critical when considering what mechanical properties resultant scaffolds should exhibit. A range of methods exist including porogen deposition/leaching (Liao et al., 2002), liquid-liquid phase separation (Goh and Ooi, 2008, Budyanto et al., 2008), molecular self assembly (Schneider et al., 2008, Semino, 2008), supercritical CO_2 gas foaming (Barry et al., 2006, Zhu et al., 2008),

emulsion/freeze drying (Sultana and Wang, 2008, Uttarwar and Aswath, 2008) nanofibre electrospinning (Ngiam et al., 2008, Zhang et al., 2008) and computer aided design/manufacture (CAD/CAM) (Park et al., 2008d, Sun et al., 2004).

1.2.2.5. Cell Organization and Growth

Polymer scaffolds should exhibit a bioactive surface able to interact with biological tissues conducive to cell attachment, spreading and function (Takimoto et al., 2003, Sales et al., 2007). The surface can be bioactive due to the biomaterial used to make the scaffold, functionalized with a bioactive coating or impregnated with bioactive molecules (Murphy and Mooney, 1999, Zhang et al., 2009). However, when treating the polymer surface to enhance cellular adhesion, consideration must be invested so as to not also enhance bacterial adhesion and colonization (Woo et al., 2002).

To achieve successful long-term integration *in vivo*, scaffold porosity must support cell migration and vascularization (Bonfield, 2006, Laschke et al., 2008). 3D architecture of scaffolds should aid this complex growth and the organization of multiple cell types involved in tissue regeneration and organogenesis (Karageorgiou and Kaplan, 2005). As the temporary scaffold degrades, cells within and/or cells surrounding the scaffold post implantation should proliferate and replace the 3D architecture.

Surface topography of potential scaffolds is also critical to the successful attachment, proliferation and survival of cells whether *in vivo* or *in vitro* (Cohen and Bano, 1993, Engel et al., 2008). Surface topographies have been shown to enhance cell attachment and spreading on the micro and even nano-scale. Surface topography and chemistry must therefore be considered in unison to ensure successful scaffold integration.

1.2.2.6. Tissue Support

Correct growth and development of engineered tissue is dependent on environmental cues, both physical and chemical (Quaglia, 2008, Chan and Mooney, 2008). Implanted scaffolds are designed as a delivery system for essential growth factors and hormones critical to cellular proliferation and differentiation. Chemical cues are tailored to support the development of functional tissues (Burdick and Vunjak-Novakovic, 2008). To date, tissues which have been successfully regenerated, either partially or wholly, include cartilage (Park and Na, 2008, Mohan et al., 2008), lung (Nichols and Cortiella, 2008), smooth muscle (Baker and Southgate, 2008), bone (Basmanav et al., 2008, Cartmell, 2008, Kanczler and Oreffo, 2008), heart (Wissink et al., 2000, Huang et al., 2008) and liver (Zhu et al., 2008).

1.2.3. Cell Types

1.2.3.1. Autogeneic

Autogeneic cells are derived from the patient into whom the engineered tissue will be implanted. They are genetically identical to the patient and therefore reduce the risk of immune-rejection and disease transmission. Cells are isolated and expanded *in vitro* to obtain appropriate numbers for transplantation. These cell cultures are delivered back into the patient via a biomaterial scaffold implant. Alternatively, an engineered scaffold itself is implanted to provide support, promote angiogenesis and recruit adjacent cells to initiate tissue regeneration. Cartilage, skin and bone repair are just few examples of the use of autogeneic cells in conjunction with a supporting scaffold (Dounchis et al., 2000, He et al., 2007, Menderes et al., 2004). However, there are obvious disadvantages to the use of autogeneic cells. Their derivation may cause problems at the site of isolation such as chronic pain and infection. Sufficient

quantities may not be available, such as skin cells from severe burns victims, or harvestable, such as neural cells. *In vitro* expansion is costly and takes time. Finally, autogeneic cells are redundant in the regeneration of damaged tissue caused by genetic disease.

1.2.3.2. Allogeneic

Allogeneic cells are derived from donors of the same species. The most prevalent area in which allogeneic cells have been utilized is skin regeneration. Many studies depict the effective application of foreskin cells cultured *in vitro* for the bioengineered substitution of wounded skin (Hirt-Burri et al., 2008, Kellouche et al., 2007). One advantage of using allogeneic cells is that they can be used to regenerate damaged tissue due to genetic disease. The problem of shortages with autogeneic cells is significantly reduced when using allogeneic cells. However, the chances of disease transmission and immune-rejection are increased.

1.2.3.3. Xenogeneic

Xenogeneic cells are isolated from donors of a different species. The use of xenogeneic cells bypasses many issues related to the isolation of human cells, but raises issues of xenozoonosis (Prabha and Verghese, 2008). Examples of the application of xenogeneic cells include the regeneration of liver (Wilson et al., 2006) and bone (Xie et al., 2007). However, the biggest demand is not for xenogeneic cells, but xenogeneic material such as ECM and decellularized tissue (Badylak, 2004). Xenogeneic material has been used extensively in the replacement of heart valves using acellular porcine substitutes (Korossis et al., 2002).

1.2.3.4. Syngeneic / Isogeneic

The terms syngeneic and isogeneic pertain to cells that are isolated from genetically identical individuals such as twins or donors exhibiting a similar genotype. A typical example would be the transplantation of bone marrow from one twin to another, or donor tissue which has been matched to the recipient.

1.2.3.5. Stem Cells

Numerous types of stem cells exist which were described previously. However, all stem cells share similar attributes and are employed due to their ability to differentiate into the necessary cell types for regeneration of damaged tissue (Fodor, 2003, Cedar et al., 2007). Stem cells can be autogeneic or allogeneic in the form of AS cells or ES cells respectively. A major problem accompanying stem cell-based therapy is their complete and efficient differentiation. A plethora of published methodology exists for the directed differentiation of stem cells with varying efficacy (Gruen and Grabel, 2006). Stem cells are highly proliferative and without efficient differentiation could cause teratoma formation *in vivo* (Blum and Benvenisty, 2008).

1.2.3.6. Genetically Engineered

Cells can be genetically engineered to exhibit phenotypes and characteristics advantageous to their application in regenerative medicine. Dependent on their intended use they can be engineered to produce vital proteins and growth factors for enhanced differentiation of cell types such as chondrocytes (Feng et al., 2008). Other cell types include bone mineralising and cardiovascular cells (Phillips and Garcia, 2008, Phillips et al., 2007, Rosenstrauch et al., 2007). Alternatively, cells can be engineered to exhibit increased compatibility for long term integration and survival without provoking an immune response.

1.2.3.7. Immuno-modulated

The method of immuno-modulation involves the alteration of a particular cell type's activity to control immune-response. One approach includes the administration of immuno-modulatory factors to improve native cellular responses and tolerance levels to implants (O'Neill, 2006, Irvine et al., 2008). The introduction of cells such as mesenchymal and neural stem cells has also been shown to exhibit immuno-modulatory function in hepatic, pancreatic and neural tissues (Parekkadan et al., 2007, Pluchino and Martino, 2008, Abdi et al., 2008). A combination of immuno-modulatory factors and immuno-modulated cells can also be used to enhance tissue regeneration, i.e. engineered bone (Haisch et al., 2004, Marcu et al., 2007).

1.3. Bone Physiology

1.3.1. Development / Formation

1.3.1.1. Cartilage

During embryogenesis large portions of a connective tissue called the mesenchyme condense and differentiate to form cartilage in the shape of ensuing bone. Cartilage can be broken into three separate types comprising hyaline, elastic and fibrocartilage. Hyaline cartilage consists mainy of type II collgen (~40%) and proteoglycans. Proteoglycans are glycoproteins covalently attached to gylcosaminoglycans (GAGs) such as chondroitin sulfate. Chondroitin sulfate provides both structure and organization for collagen fibrils and an overall negative charge which promotes electrostatic repulsion and increases matrix integrity and resilience to compression (Stuart and Panitch, 2008). Exhibited glycoproteins promote matrix/cell interactions and appropriate differentiation. Elastic cartilage is composed of chondrocytes surrounded by both type II collagen and elastic fibres of which elastin is the major constituent. Elastic cartilage provides support for external structures such as the ear and nose and also the epiglottis and can withstand repetative bending and flexing. Fibrocartilage is intermediary between hyaline cartilage and dense connective tissue, primarily comprising collagen fibres (Benjamin and Evans, 1990). Collagen fibres are bundled together in parallel and surrounded by fibroblasts. Lacunae, containing chondrocytes, are spread throughout the cartilage inbetween the collagen fibres. Collagen fibres form and orientate themselves in the direction of stress, and chondrocytes synthesize additional collagen fibres. Fibrocartilage aids transfer of load stress between tendons and

bones. Most cartilage that acts as a template for bone development is surrounded by a dense fibrous tissue called the perichondrium. The perichondrium is composed of two layers, the first comprises of fibroblasts spread through a dense collagen matrix. The second layer is composed of chondrogenic progenitor cells.

1.3.1.2. Endochondral Ossification

The mesenchyme tissue condenses and progenitor cells differentiate to form chondrocytes. These chondrocytes begin to secrete and deposit ECM largely consisting of type II collagen and GAGs. Chondrocytes trapped within the collagen become hypertrophic. They cease to produce type II collagen and begin to secrete type X collagen. Hypertrophic chondrocytes adjacent to the perichondrium differentiate to form osteoblasts which secrete bone matrix and form the bone collar around the template. The cartilage template begins to elongate through interstitial growth; hypertrophic chondrocytes continually produce more ECM which pushes adjacent cells further apart. The template also widens through appositional growth; the chondrogenic layer of the perichondrium secretes additional ECM. Altogether this forms the growth plate of endochondral bone (Kronenberg, 2003). The growth plate lies in parallel to the direction of extension between the epiphysis (rounded end of long bone) and diaphysis (shaft of long bone). At the extending end of the growth plate lies the resting zone; chondrogenic progenitor cells that are not proliferating. At the opposite end of the proliferative zone reside hypertrophic chondrocytes. The proliferating chondrocytes stack into columns separated by longitudinal and transverse septa consisting of collagen and proteoglycans (Fig 1.4) (Mitchell et al., 1982, Eggli et al., 1985, Gregory et al., 2001).

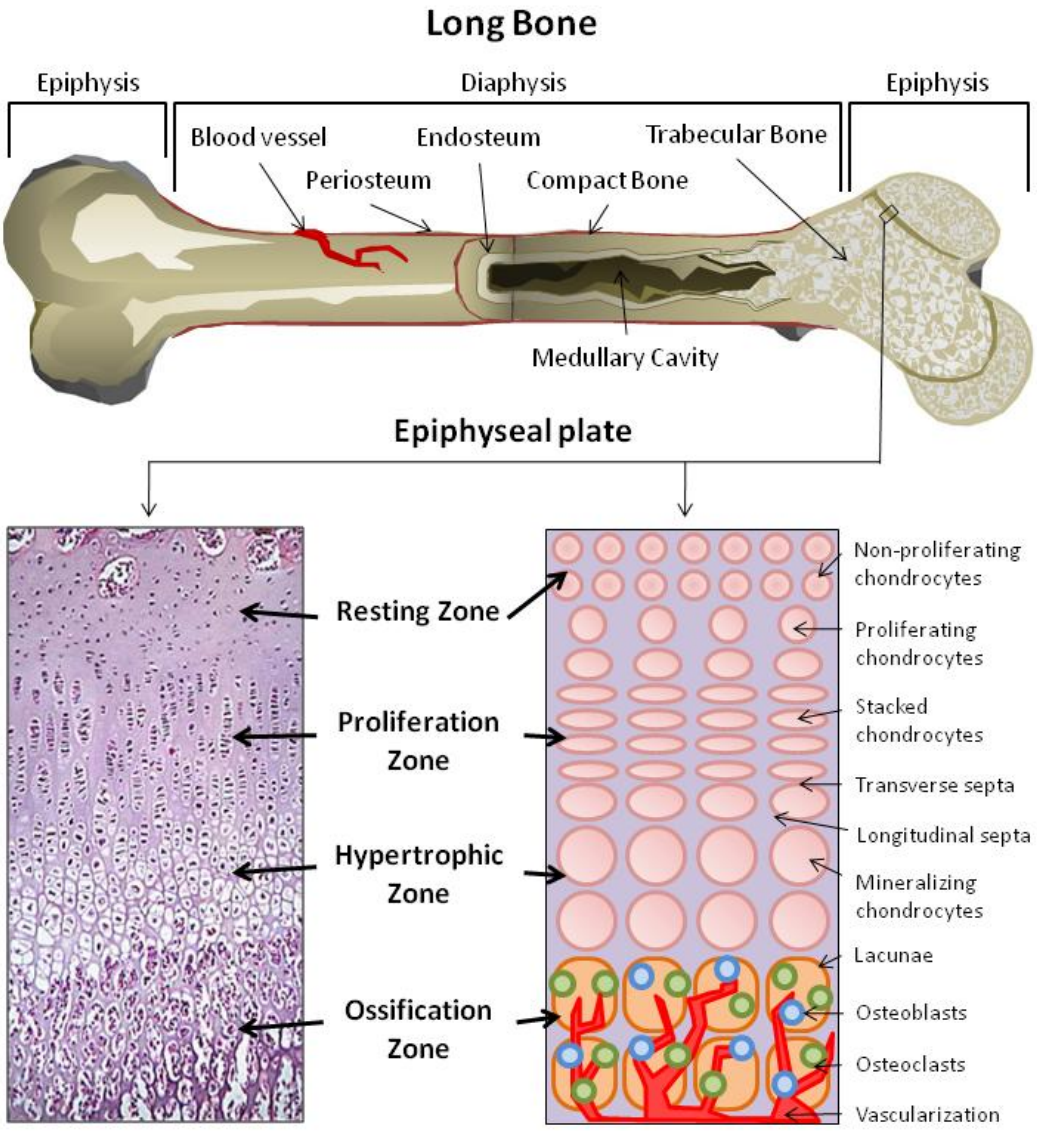

Figure 1.4: Epiphyseal plate (growth plate) of long bone during endochondral ossification. Photograph taken from www.kumc.edu.

Hypertrophic chondrocytes produce alkaline phosphatase (ALP) and begin to mineralize surrounding matrix. These mineralising chondrocytes also secrete vascular endothelial growth factor-A (VEGF-A) which chemotactically attracts blood vessels and promotes angiogenesis (Dai and Rabie, 2007, Murata et al., 2008). Eventually, chondrocytes within the hypertrophic zone undergo programmed cell death or apoptosis leaving voids within the ECM called lacunae. Vascularization introduces HS cells, osteoclasts and osteoblasts into the hypertrophic zone through the lacunae forming the primary ossification centre. HS cells act as progenitor cells for bone marrow differentiation within what will eventually become the medullary cavity. Osteoclasts completely resorb the transverse septa, hypertrophic and dead chondrocytes, and partially resorb longitudinal septa. Osteoblasts replace the ECM with osteoid (un-mineralized organic matrix consisting of type I collagen and proteins such as osteocalcin (OC), osteopontin (OPN) which binds hydroxyapatite (HA), osteonectin (ON), bone sialo-protein (BSP), chondroitin sulphate and GAG (Sommerfeldt and Rubin, 2001). Osteoblasts also mineralize osteoid to form the primary spongiosa. The primary spongiosa comprises of trabeculae (calcified osteoid) which continue to thicken to form the secondary spongiosa. Osteoblasts eventually fill the gaps between trabeculae to form compact bone. As they fill in the gaps they become encased within the bone and form osteocytes. The perichondrium which surrounds compact bone now becomes periosteum. Periosteum consists of two layers called the fibrous layer (thick connective tissue and fibroblasts) and the cambium layer (osteoblast and chondrocyte progenitor cells). Whilst the periosteum provides an outer sheath, the endosteum provides an inner sheath. The endosteum comprises a layer of osteoblasts and progenitor cells sandwiched with a layer of connective tissue, and lies between the medullary cavity and compact bone.

At either end of the bone lies more hyaline cartilage (epiphysis region) which undergoes the same process as above and constitutes the secondary ossification centre. The diaphysis is separated from the epiphysis by the epiphyseal plate (metaphysis or growth plate). In adults, chondrocytes within the epiphyseal plate cease mitosis and stop bone elongation. The hypertrophic zone catches up with the forefront of the epiphyseal plate and eventually invading osteoblasts mineralize the whole tissue fusing the epiphysis and diaphysis to create a complete bone. Articular cartilage remains on the peripery of the epiphysis.

1.3.1.3. Intramembranous Ossification

Intramembranous ossification is very similar to endochondral ossification but does not involve the replacement of hyaline cartilage with bone. Instead, the formation of bone comes directly from the condensed mesenchyme. Cells within the condensed mesenchyme differentiate to form osteoblasts which begin to secrete osteoid. The long type I collagen fibres of the osteoid become mineralized to form bone spicules. Bone spicules increase in size and join to form trabeculae. Successive osteoid deposition and mineralization by osteoblasts forms concentric rings called lamellae which widen the trabeculae. The trabeculae continue to grow until they begin to touch one another and form an internal lattice structure. Further deposition and mineralization fills in the gaps between trabeculae to form woven bone. Woven bone comprises a network of interlacing calcified fibres, also known as nonlamellar bone. These fibres are irregular in orientation and are later remodelled into compact bone. The areas which remain as a lattice are referred to as primary cancellous or trabecular bone.

1.3.1.4. Mineralization

In 1855 a German pathologist named Dr. Rudolf Karl Ludwig Virchow first documented the process of mineralization, also known as calcification. He documented metastatic calcification of soft tissues during pathologies of the kidney such as chronic renal failure. Also now known as calciphylaxis, calcium is precipitated into cutaneous tissue forming benign bone nodules. However, it took over another 100 years for the mechanism of mineralization to be elucidated.

It was discovered that extracellular calcium and phosphate concentrations were too low for calcium precipitation. This formed the idea of a nucleator to increase the concentration at the mineralizing front of the cell membrane (Howell et al., 1968). It was later found that lipids were highly concentrated at the mineralizing front, and further investigation identified the presence of matrix vesicles (Wuthier, 1968, Ali et al., 1970). These matrix vesicles were found to exhibit intense phosphatase activity which regulates lumenal phosphate concentration (Anderson, 2003). Lumenal calcium concentration is regulated by calcium binding proteins such as annexin I and phosphatidylserine (Nie et al., 1995). The concentration of calcium phosphate within the matrix vesicle lumen increases to a level that is permissive to precipitation. Calcium phosphate crystals are converted to an intermediary form called octa-calcium phosphate before final conversion to HA (Sauer and Wuthier, 1988, Garimella et al., 2006). The formation of HA is the first of two phases for complete mineralization. The first phase ends with the HA crystals piercing the matrix vesicle membrane causing it to collapse and release into the extracellular space. The second phase involves epitaxial growth of the HA crystals in the extracellular space. Growth is radial and culminates in the formation of HA spherules (Tarallo et al., 2008). These fuse together at the mineralization front parallel to the longitudinal septa coating the

triple helix of type I collagen fibres. This gives bone its characteristic strength, resilience to compression and flexibility.

1.3.2. Types of Bone

1.3.2.1. Long Bones

Long bones are characterised by a long diaphysis in comparison to its width. The epiphysis is located at either end and the whole bone is surrounded by the periosteum. The outermost parts are compact bone and the innermost parts are trabecular bone containing red bone marrow within the medullary cavity. The centremost part of the medullary cavity contains yellow bone marrow. The bones extend via endochondral ossification of the epiphyseal plate. Typical long bones include the humerous, radius and ulna of the arm, femur, tibia and fibula of the leg, and the metacarpals, metatarsals and phalanges of the hands and feet.

1.3.2.2. Short Bones

Short bones are characterised by their length and width being similar and resulting in a cube shape. These bones are predominantly made of trabecular bone with a thin crust of compact bone. Consequently, short bones are more susceptible to fracture than long bones. Carpal and tarsal bones of the wrist and ankle are examples of short bones.

1.3.2.3. Flat Bones

Flat bones are characterised by two broad layers of compact bone sandwiched either side of a thin layer of trabecular bone filled with red bone marrow. Their function is

to provide either shielding or larger surface area for muscle attachment. Typical examples include the skull, sternum, ribs, pelvis and scapula.

1.3.2.4. Irregular Bones

Irregular bones include the occipital, parietal, frontal, nasal, temporal, vomer, maxilla, echmoid, sphenoid, zygomatic and lacrimal bones of the skull, sacrum (triangular bone of the pelvis), hyoid (located in the neck and supports the root of the tongue), palatine (roof of the mouth), mandible (jawbone) and vertebrae. These are characterised by their lack of similarity to any long, short or flat bone within the body. Their function is the support or protection of organs and nerves such as the brain and spinal cord. They comprise predominantly of trabecular bone with a thin crust of compact bone.

1.3.2.5. Sesamoid Bones

Sesamoid bones are typically located within tendons spanning a joint. Examples include the patella and pisiform (pea shaped bone in the wrist). They are primarily composed of trabecular bone with a thin layer of compact bone. They act to hold the tendon away from the joint and enhance the mechanical action of the tendon. By holding the tendon at an increased angle to the joint, the force exerted by muscles through the tendon is also increased.

1.3.3. Bone Structure

1.3.3.1. Compact Bone

Compact bone, also known as cortical bone, accounts for ~80% of the weight of a human skeleton and gives bones their characteristic white, smooth and solid

appearance. Initial bone formation involves deposition and random orientation of mineralized collagen fibres. Cortical bone exhibits a highly ordered structure called the Haversian system which comprises predominantly of closely packed osteons. Osteons lie in parallel to one another along the length of the diaphysis. Each osteon comprises a central cavity called the Haversian canal, in which resides the artery and vein supplying blood to the bone. This is surrounded by concentric rings of compact bone called lamellae. Each lamella comprises of mineralized type I collagen fibres that are in parallel to one another along the length of the osteon in various orientations (Weiner et al., 1999). X-ray diffraction and electron microscopy studies of the osteon structure have found that mineralized collagen fibres lie in parallel within a single lamella, and within a 90° difference in adjacent lamellae (Ascenzi and Bonucci, 1976, Ascenzi et al., 1978). This has led to the discovery of three structural orientations within osteons which resemble 'twisted plywood' (Fig 1.5) (Martin and Ishida, 1989). This plywood structure confers the characteristic strength of cortical bone. Within each lamella lie osteocytes encased in lacunae, thought to have mechano-sensory function. Osteocytes signal to one another and dispose of wastes via cytoplasmic extensions termed dendrite termini. These occupy channels called canaliculi which transect lamellae linking to the Haversian canal (Blumer et al., 2008). Haversian canals are connected by transecting channels called Volkmann's canals. The space between osteons is filled with interstitial lamellae. Osteoclast function also creates resorption cavities. Fig 1.5 illustrates the structure of cortical bone.

1.3.3.2. Trabecular Bone

Also known as spongy or cancellous bone, trabecular bone accounts for the

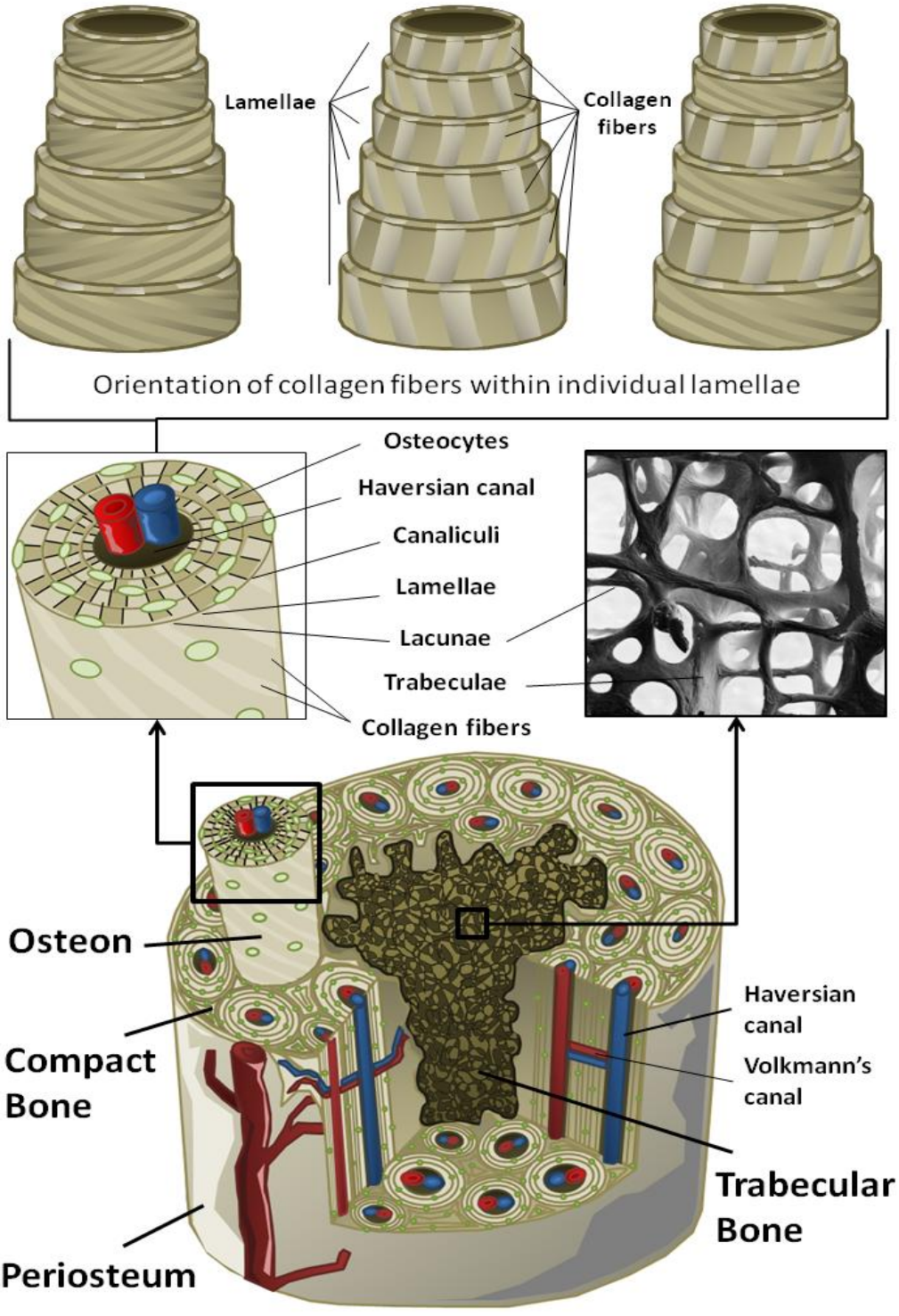

Figure 1.5: Structure of compact and trabecular bone. Photograph taken from www.archive.nyu.edu. Individual images are adapted from wikipedia.

remaining 20% of the weight of a complete adult human skeleton. Trabecular bone lies within bones surrounded by cortical bone. Unlike cortical bone, trabecular bone is oriented irregularly and exhibits reduced strength and increased porosity. It comprises an irregular lattice structure of flat and rod shaped trabeculae. This reduces weight of the bone and allows space for blood vessels and bone marrow. The lattice structure acts like braces in a building, helping to distribute load along the bone to be supported by cortical bone. Trabeculae can also realign to support changes in stress. Canaliculi transect trabeculae connecting lacunae and blood vessels. Fig 1.5 illustrates the structure of trabecular bone.

1.3.3.3. Cells of the Bone

Osteoblasts

Osteoblasts are mature bone forming cells, characteristically cuboid in shape and are thought of as complex fibroblasts. They originate from differentiated from multipotent MS cells within the periosteum (Duque et al., 2008). These same progenitor cells give rise to both adipocytes and chondrocytes (Muruganandan et al., 2008, Choi et al., 2008b). Osteoblasts are located on the surface of bone where they form a thick layer alongside their progenitor cells which block osteoclast activity at the same location. Osteoblasts produce osteoid which is regulated by fibroblast growth factor (FGF) and insulin-like growth factor (IGF) I and II. IGF-I and IGF-II which inhibit the expression of collagenase and thus aid type I collagen synthesis (Wang et al., 2008). Other factors that control osteoblast differentiation and activity include Runx2, also known as osteoblast specific factor-2 (OSF-2) or core binding factor alpha 1 (Cbfa1), bone morphogenetic proteins (BMPs), transforming growth factor-β (TGF-β) and platelet derived growth factor (PDGF) (Lavery et al., 2008).

Runx2 also directly inhibits differentiation of adipocytes and chondrocytes. Overexpression of another factor called osterix was found to increase osteoblast proliferation, ALP activity and bone nodule formation (Tai et al., 2004). Osterix was found to be important in bone formation when osterix $^{(-/-)}$ mice were discovered not to exhibit osteoblasts (Nakashima et al., 2002).

Osteoclasts

Osteoclasts originate from differentiated HS cells within the bone marrow. Progenitor cells differentiate towards mononuclear pre-fusion osteoclasts which then fuse to form characteristic giant multinucleated osteoclasts (MacDonald et al., 1987, Jimi et al., 1999). They are located in resorption pits or Howships lacunae where they produce a localised acidic environment conducive to bone de-mineralization (Boyde et al., 1990). Osteoclastogenesis requires macrophage colony-stimulating factor (M-CSF) and receptor activator of nuclear factor κβ (RANK) ligand (RANKL). RANK is a member of the tumor necrosis family (TNF) and activates nuclear factor κβ (NF- κβ). Osteoblasts positively regulate development and activation of osteoclasts through exhibiting RANKL (Schoppet et al., 2002). Another TNF member is osteoprotegrin (OPG) also known as osteoclast inhibiting factor (OCIF). OPG is produced by osteoblasts and binds RANKL inhibiting osteoclastogenesis (Drugarin et al., 2003).

Osteoclasts are recruited to the bone by VEGF-A or M-CSF (Niida et al., 1999). Osteoclasts attach to the bone via specific adhesion structures called podosomes located at sealing zones (Lakkakorpi and Vaananen, 1991). Podosomes specifically attach to OPN and type I collagen through expression of numerous integrins (Helfritch et al., 1992, Horton et al., 1995). Once attached, osteoclasts become

polarised with membrane adjacent to the bone becoming convoluted and forming a 'ruffled border'. Activated osteoclasts secrete hydrogen ions through an H^+ pump called vacuolar ATPase, matrix metalloproteases (MMPs), tartrate-resistant acid phophatase (TRAP) and hydrolytic enzymes such as cathepsin K. The acidic environment solubilizes mineralized calcium. MMPs are a family of endopeptidases which are important in bone resorption. For example, MMP-9 is a gelatinase and MMP-13 $^{(-/-)}$ mice show decreased numbers of osteoclasts. TRAP is involved in the de-phosphorylation of OPN which enables osteoclast migration. Cathepsin K is a collagenolytic cysteine protease secreted from membrane vesicles called lysosomes. As a result of these secretions bone is de-mineralized, degraded and finally phagocytosed by osteoclasts.

Osteocytes

Osteocytes are formed when osteoblasts become trapped within the mineralized osteoid they secrete. When osteoblasts become osteocytes they exhibit increased expression of dentin matrix protein 1 (Dmp1), matrix extracellular phosphogylcoprotein (Mepe) in complex with osteoblast/osteoclast factor 45 (OF45), and Phex. These factors control phosphate metabolism through regulation of the phosphaturic factor FGF23 (Bonewald, 2006). Osteocytes are mitotically arrested and smaller than osteoblasts exhibiting minimal endoplasmic reticulum and reduced golgi apparatus. They have many functions including bone formation, matrix maintenance and calcium homeostasis. They also have a mechano-sensory function involved in sensing and transducing signals from stress and loading. Osteocytes are located within lacunae and exhibit dendrite termini which occupy canaliculi. Through these dendrite termini osteocytes communicate with one another and

osteoblasts via formation of transient gap junctions (Doty, 1981). This communication is thought to regulate bone remodelling in response to stress and loading. Dendrite termini growth is regulated by a lipid growth factor called lysophosphatidic acid (LPA) (Karagiosis and Karin, 2007). Although osteocytes are thought of as trapped osteoblasts, they are actually mobile. Green fluorescent protein (GFP) labelled osteocytes have been found to move along canaliculi (Kalajzic et al., 2004, Veno, 2006). A final function termed osteocytic osteolysis involves the destruction of surrounding mineralized matrix within osteocyte-containing lacunae (Belanger, 1969). Osteocytic osteolysis is a rapid and transient mechanism involved in mineral homeostasis, not bone remodelling (Cullinane, 2002).

1.3.4. Bone Function

1.3.4.1. Movement

Bones provide solid structures for muscles and tendons to attach to. Muscles, tendons and bones function together to generate and transfer forces which allow movement of the whole body or individual parts. The human skeleton provides support for the body and enables movement through 3D space. Bones are specific to the type of movement they accommodate. For example, the femoral head of the femur and the acetabulum of the pelvis fit like a ball and socket allowing flexion, extension, abduction, adduction, medial or lateral rotation and circumduction motions.

1.3.4.2. Protection and Shape

An important function of bone is the protection of soft tissues and organs. Bones provide strong shielding against impacting forces, but also exhibit a certain degree of

flexibility. The skull, spine, scapula, ilium, patella, carpals and tarsals protect the brain, spinal cord, shoulder, urogenital system, knee joint, wrist and ankle, respectively. The ribs and sternum provide protective casing for the heart, lungs, stomach, liver, pancreas, spleen and major blood vessels. Bones are specially adapted to their protective function. For example, the shoulder covers a large area and accordingly, the scapula is large and flat so as to provide maximum protection of the joint. The skeleton also acts as internal scaffolding, supporting the weight of the body. It provides anatomical shape and 3D spacing for internal organs.

1.3.4.3. Blood

Within bone lies both red and yellow bone marrow, the difference being ~50% red marrow is converted to yellow marrow in adults and contains mainly adipocytes. The bones of infants only contain red marrow. Red marrow contains HS cells which undergo haematopoiesis to form the three major cell types of blood; erythroid, lymphoid and myeloid cells. These cells include erythrocytes, thrombocytes, platelets, mast cells, neutrophils, eosinophils, basophils, macrophages, megakaryocytes, T and B lymphocytes and natural killer cells. Some HS cells within the bone marrow remain in a multipotent state. These provide a cell source for future proliferation and differentiation.

1.3.4.4. Detoxification

It has been known for many years that heavy metals such as lead and cadmium are adsorbed and stored within bones (Wiechula et al., 2008). This has marked toxicological effects on the Haversian remodelling system (Anderson and Danylchuk, 1977, Anderson and Danylchuk, 1978). Consequently, a significant amount of blood lead is prevented from adsorption into vital organs such as the liver and heart. Their

storage within bone is transient and they can be gradually excreted in the urine. This is a slow process and increases the chance of physiological damage. Diseases and conditions which affect bone can mobilize lead and other heavy metals, reintroducing them into the blood (Silbergeld et al., 1993, Silbergeld et al., 1988).

1.3.4.5. Mineral Storage

Bones act as a reservoir of essential minerals for biological processes and cellular function. There are two types of stored minerals called macro and micro-minerals. Macro-minerals (bulk elements) include calcium, iron, magnesium, phosphorus, potassium and sodium. Micro-minerals (trace elements) include boron, chromium, copper, iodine, manganese, selenium and zinc. Storage within bone helps reduce toxic levels occurring within the blood.

1.3.4.6. Acid-Alkali Balance

Blood can accommodate changes in pH via acceptance of H^+ ions through plasma cells, circulating bicarbonate, phosphate in erythrocytes and haemoglobin. Muscles can also help to buffer changes in pH. However, the major buffering capacity of the body lies within bones. Bones balance pH by releasing or adsorbing H^+ ion acceptors in the form of carbonates. Sodium carbonate is first to be released from bone. Calcium carbonate is released over longer periods. Further available carbonate is located within HA crystals of mineralized osteoid.

1.3.4.7. Sound Transduction

The smallest bones in the human body are located within the middle ear and transduce vibrational signals from the tympanic membrane (eardrum) to the fenestra ovalis of the cochlea. These bones are called the ossicles and include the

malleus (hammer), incus (anvil) and stapes (stirrup). The ossicles function together as a leveraging system to intensify the force of airborne sound vibrations collected at the eardrum. The purpose of intensifying the vibrations is to efficiently transduce airborne sounds into the fluid of the cochlea. Imagine being underwater and someone is talking to you. Their voice is muffled because the water does not transduce vibrational signals as well as air. The signal has to be intensified to travel through the water.

1.3.4.8. Modulatory Adaptation

Natural bone homeostasis through osteoclast/osteoblast function remodels bone shape and density. Collagen fibres are successively realigned and deposited in an orientation parallel to the direction of stress exerted on the bone. Continuous remodelling enables structural adaptation to environmental changes. Bone structure is altered according to the forces exerted upon it. For example, professional tennis players exhibit thicker and denser bones in their playing arm. Professional runners and cyclists would have femurs more dense than average.

1.3.5. Bone Injury and Repair

1.3.5.1. Reactive Stage

Upon bone fracture, blood vessels are broken filling the site of injury with extravascular blood cells. Blood vessels then constrict to stem the flow. Within hours to days a hematoma forms to clot the site of injury. Cells within the hematoma degenerate and die. Prostaglandins chemotactically attract the infiltration of inflammatory cells and fibroblasts. Primary nutrients and oxygen supply are

provided by exposed cancellous bone and surrounding muscle. Vascularization and ECM deposition by fibroblasts forms granulation tissue.

1.3.5.2. Reparative Stage

The periosteum generates chondrocytes which migrate into the granulation tissue and begin depositing hyaline cartilage. Chondrocytes and invading osteoblasts introduced through newly formed blood vessels mineralize the hyaline cartilage to form a fracture callus. The callus is soft and provides minimum support to the fracture site for the first 4 to 6 weeks. Osteoblasts convert deposited hyaline cartilage to osteoid which later becomes calcified forming woven bone. Trabeculae within woven bone consist of irregularly orientated mineralized collagen fibres. Woven bone affords stability to the fracture until osteoblasts replace it with lamellar bone. The lamellar bone is in the form of trabecular bone strengthening the fractured bone enough to begin supporting compressive forces.

1.3.5.3. Remodeling Stage

Complete healing of the fractured bone occurs during the remodelling stage. Bone homeostasis remodels the bone to its original shape. Trabecular bone is converted to cortical bone according to mechanical stresses. Bone is deposited where it is needed and adsorbed from where it is not. The fractured bone is usually completely healed in 3 to 6 months.

1.3.6. Bone Damage

1.3.6.1. Fracture

During life bones experience a multitude of forces, some of which may cause trauma in the form of fracture. Bone fractures are classified using the orthopaedic trauma association (OTA) classification system (Marsh et al., 2007). The OTA classification system comprises five parts for accurate identification of fractured bone (Table 1.3). Bone fractures can be simple or complicated and require detailed definition in order to assess the best treatment. Fractures are classified by the bone in which they reside, location on the bone, whether it is simple or multi-fragmentary, geometry and bone functionality.

1.3.6.2. Disease/Disorder

A plethora of diseases and disorders exist which can cause bone damage. Certain infections such as syphilis and periodontitis cause erosion and loss of bone matrix. Other bone infections (osteomyelitis) can lead to osteonecrosis via constriction or blockage of blood capillaries to the bone causing hypoxia and eventual necrosis. Numerous disorders involve an imbalance in bone homeostasis resulting in the gaining or reduction and hardening or softening of the bone mass. These disorders include osteoporosis, osteopetrosis, osteomalacia and rickets. Other disorders such as osteogenesis imperfecta, also known as 'brittle bone disease', affect the growth plate and cause bones to be easily broken. Osteoarthritis causes bone damage as a result of wearing within joints due to loss of cartilage. There are also many types of bone cancer such as osteosarcoma which cause varying degrees of bone damage.

OTA Classification				
(1) Bone	**(2) Region**	**(3) Type**	**(4) Group**	**(5) Subgroup**
1. Humerus	1. Proximal	A. Simple Fracture	Spiral	Stability
1.4. Clavicle				
1.5. Scapula				
2. Radius/Ulna	2. Diaphyseal	B. Wedge Fracture	Oblique	Angulation
3. Femur/Patella				
4. Tibia/Fibula				
5. Spine			Transverse	Displacement
6. Pelvis/Acetabulum	3. Distal	C. Complex Fracture		
7. Hand				
8. Foot			Segmental	Rotation
9. Craniomaxillofacial bones				

Common Fractures			
Fracture Type	**Description**	**Fracture Type**	**Description**
Complete	The fractured ends are completely separate	Linear	The fracture is parallel to the length of the bone
Incomplete	The fractured ends are partially connected	Transverse	The fracture is 90° to the length of the bone
Open	The fractured bone is exposed to the air; pierces the skin	Oblique	The fracture is diagonal to the length of the bone
Comminuted	The fracture generates multiple fragments	Spiral	One or both of the fractured ends are twisted
Compacted	Ends of the fractured bone are pushed into one another	Compression	Fractures which usually occur within the spine

Table 1.3: The OTA classification system and common bone fractures.

1.3.6.3. Surgery

Birth defects such as cleft lip and palate, clubfoot, arthrogryposis multiplex congenital (locked joints) and hip dysplasia require corrective surgery in which bones are surgically dissected and realigned. Scoliosis (curved spine) is commonly associated with conditions such as spina bifida and cerebral palsy. It is corrected by use of rods to fuse the spine in place, which are drilled directly into the spine. This again employs deliberate surgical damage to the bone. Elective or cosmetic surgeries cause damage to bone to improve aesthetics of the body and face. For example, malarplasty and rhinoplasty involve alteration of the cheek, jaw, chin and nose. Individuals who suffer from achondroplasia or dwarfism electively undergo bone lengthening surgery.

1.4. Engineered Aggregation

1.4.1. Background

Much research has been focussed on the control of ES cell differentiation to produce homogeneous cell cultures for therapeutic applications (Curtis and Riehle, 2001, Fodor, 2003, Cedar et al., 2007, Raikwar et al., 2006). However, advances in the efficiency of directing differentiation and producing desired cell types suitable for clinical application have been somewhat troublesome (Gruen and Grabel, 2006). ES cells are often differentiated in a series of steps involving both physical and chemical cues. One of the foremost steps is the production of cell clusters or aggregates known as EBs (Dang et al., 2002, Hwang et al., 2006a, Schuldiner et al., 2000). EBs provide a crude but effective method of recapitulating natural 3D interaction and proliferation of ES cells *in vitro*. All three germ layers have been identified within these structures (Fok and Zandstra, 2005, Itskovitz-Eldor et al., 2000, Ling and Neben, 1997, Wiles and Johansson, 1999). The benefit of including the EB step has been published repeatedly, whether its effect had been direct or indirect (Wenger et al., 2004, Abe et al., 1996, Bagchi et al., 2006). However, studies have also shown that ES cells can be effectively differentiated without prior EB formation (Hwang et al., 2008b, Hwang et al., 2008a).

Although the use of EBs to control ES cell differentiation has become accepted practice, consensus methodology for their generation remains elusive. Many methods exist for the generation of EBs, each having its own advantages and disadvantages with respect to aggregation efficiency (Carpenedo et al., 2007, Gerecht-Nir et al., 2004, Ng et al., 2005, Dang et al., 2002). The variation between EB formation methods results in variable ES cell differentiation (Koike et al., 2007,

Kurosawa, 2007). Table 1.4 illustrates the variety EB formation methods and associated cell types. Consequently, it is hypothesized that control of EB formation may also control differentiation of constituent ES cells and enable generation of homogeneous cultures (Ungrin et al., 2008, Raikwar et al., 2006, Karp et al., 2007). The first step would be to collate current knowledge and produce standardised methodology wherein EB formation, ES cell differentiation, process scalability and cost effectiveness could be assessed (Placzek et al., 2009).

1.4.2. In Vitro Culture

1.4.2.1. 2D Culture

ES cells are maintained *in vitro* through 2D culture. 2D culture involves the proliferation of ES cells in a monolayer under defined conditions (Ying et al., 2008, Amit, 2007). The main purpose of 2D culture is cell expansion whilst maintaining ES cell pluripotency (Trish et al., 2006). The monolayer format minimizes ES cell-ES cell contact and interaction, which consequently reduces intercellular signalling. Monolayer culture enables sufficient spatial orientation of proliferating ES cells so that the majority are exposed to the defined exogenous conditions. Defined conditions such as temperature, humidity and media composition are adapted to mimic the *in vivo* environment and reduce the chance of differentiation during continuous culture.

1.4.2.2. 3D Culture

ES cells are usually allowed to proliferate in 3D culture for the purpose of initiating differentiation. As previously stated, ES cells are suspended in culture media to allow EB formation. It is thought that the increased ES cell-ES cell contact and decreased

Method	Description	Controlled Shape	Aggregation Time	Associated Cell Type	Reference
Mass Suspension	Static or rotary culture, non-adherent surfaces, multiple EBs, non-uniform EBs	-	Days	Pancreas Liver	Micallef *et. al.*, 2007; Drobinskaya *et. al.*, 2008
Stirred Suspension	Rotation culture, non-adherent surfaces, Multiple EBs, partially uniform EBs	+	Hours	Heart	Zandstra *et. al.*, 1994; Fok *et. al.*, 2005; Carpenedo *et. al.*, 2007
Spinner Flask	Large volume, non-adherent surfaces, multiple EBs, non-uniform EBs	-	Days	Liver Heart	Yin *et. al.*, 2007; Niebruegge *et. al.*, 2008
Bioreactor	Rotary culture, large volume, multiple EBs, recapitulate in vivo conditions, non-uniform EBs	-	Days	Muscle Endothelium Brain	Botta *et. al.*, 2007; Abilez *et. al.*, 2006; Come *et. al.*, 2008
Hanging Drop	Small volume, single EBs, uniform EBs	+	Hours	Heart Bone	De Smedt *et. al.*, 2008; Duplomb *et. al.*, 2007; Dang *et. al.*, 2002
Polymer Encapsulation	Multiple EBs, growth factor delivery system, uniform EBs	+	Days	Brain Bone	Tanaka *et. al.*, 2004; Rohani *et. al.*, 2008; Kanczler *et. al.*, 2008
Centrifugation	Single EBs, small volume, uniform EBs	+	Minutes	Heart	Burridge *et. al.*, 2007
Microwell	Single EBs, small volume, non-adherent surfaces, uniform EBs	+	Days	Pluripotency maintenance	Karp *et. al.*, 2007; Moeller *et. al.*, 2008
Peptide Conjugation	Chemical modification, large volume, multiple EBs, non-uniform EBs	+	Hours	Brain Bone	Dai *et. al.*, 1996; Dai *et. al.*, 1994; Belcheva *et. al.*, 1998; Tosatti *et. al.*, 2004
Biotin-Avidin	Chemical modification, large volume, multiple EBs, non-uniform EBs	+	Hours	Bone	De Bank *et. al.*, 2007
Co-culture	Heterotypic culture, large volume, multiple EBs, non-uniform EBs	-	Days	Liver	Thomas *et. al.*, 2006; Lu *et. al.*, 2005

Table 1.4: List of aggregation methods currently used in ES cell research.

exposure to pluripotency maintenance factors such as LIF in mouse and basic FGF (bFGF) in human, promotes adequate intercellular signalling to induce differentiation (Parekkadan et al., 2008). However, differentiation is random with the appearance of many cell types. Elucidation of the mechanisms involved in cell-cell signalling and control of 3D culture would greatly benefit our understanding of differentiation pathways.

1.4.2.3. Co-culture

Co-culture involves *in vitro* proliferation and/or differentiation of ES cells with one or multiple other cell types. ES cell culture remains far from ideal. Most ES cells are cultured on feeder cells or in CM since feeder cells produce unidentified factors important to pluripotency maintenance (Amit et al., 2003). Alternatively, ES cells are cultured with a second cell type to provide differentiation cues. For example, ES cell co-culture with endothelial cells, hepatic cells, periodontal ligament fibroblasts and visceral endodermal cells have induced neurogenesis, chondrogenesis, osteogenesis and cardiomyogenesis, respectively (Lai et al., 2008, Lee et al., 2008a, Inanc et al., 2007).

1.4.3. Natural Aggregation

1.4.3.1. Tissue Organization

Many factors influence natural aggregation and growth of ES cells and their subsequent differentiation. It is well established that normal cell function is directly correlated with tissue organization and the 3D intercellular orientation of constituent cells (Roskelley et al., 1995). Atypical tissue structures and cell morphologies may lead to abnormal cell growth and tumorigenicity (Weaver et al.,

1997, Wang et al., 1998). 3D orientation is dictated by both cell-cell and cell-ECM interaction. Fibroblasts are responsible for the production of large amounts of connective tissue. *In vitro* studies have found fibroblast ECM exhibits morphology akin to that observed *in vivo*, and that it stimulates cell migration and proliferation (Cukierman et al., 2001). Analyzing cell-cell and cell-ECM interactions in more natural 3D settings offers a relevant paradigm of natural cell aggregation and tissue development in living systems (Yamada and Clark, 2002).

1.4.3.2. Cadherins

In vitro, cells naturally coalesce to form aggregates after ~3 to 5 days of removing proliferation maintenance factors (Itskovitz-Eldor et al., 2000). Homotypic cell-cell adhesion is largely mediated through cadherins. For example, cells expressing epithelial cadherins (E-cadherins) only bind other cells expressing E-cadherins. This enables alike cells to adhere to one another and form tissues during development. Cadherins are a class of transmembrane protein responsible for cell-cell adhesions (Pokutta and Weis, 2007). Cadherins bind intracellular anchorage proteins called catenins (abundantly α and β-catenin) which bind to actin filaments of the cytoskeleton, effectively anchoring one cell to another (Hartsock and Nelson, 2008). In the epithelium, these complexes form adherens junctions which occur as bands or spots between cells (Ko et al., 2001). The action of cadherins is dependent on calcium ion signaling due to their extracellular calcium binding domain (Courjean et al., 2008).

1.4.3.3. Integrins

Integrins are proteins which have a single transmembrane helical domain. They are involved mainly in cell-ECM adhesion and signal transduction. The helix is composed

of two chains called the α and β subunit, each of which has numerous types (Schneider and Engelman, 2004). The combination of these two subunits dictates the binding capacity of integrins. Ligands of integrins include collagen, fibronectin, laminin and vitronectin (Reyes et al., 2008). They form adhesion complexes through interaction with cytoplasmic proteins such as talin, vinculin and α-actin (Ziegler et al., 2008, Bois et al., 2006). Through the recruitment and action of phosphotransferases (kinases) integrins anchor the actin cytoskeleton to the surrounding ECM. These adhesion complexes provide important signals pertaining to the surrounding environment. Signal transduction from integrin binding is critical for cell attachment, migration, differentiation or apoptosis (Arnaout et al., 2007).

1.4.4. Engineered Aggregation

1.4.4.1. Surface Modification

Surface modification creates reactive residues on the ES cell surface that can be used to control 3D aggregation. The surface of an ES cell naturally exhibits a monosaccharide called sialic acid (Martin et al., 2005, Schwarzkopf et al., 2002). These residues are biochemically altered by a periodate oxidation step to exhibit reactive aldehyde groups (De Bank et al., 2003). These groups are then biotinylated through reaction with biotin hydrazide. Biotin molecules are subsequently cross-linked with a protein called avidin (Yarema et al., 1998, Jacobs et al., 2000). Surface modification enables the construction of a controlled model for investigation of cell-cell interaction, EB formation and subsequent differentiation.

1.4.4.2. Control of Aggregation

The system provides many levels of manipulation, applicable in different ways for control over ES cell aggregation and subsequent EB formation (Kellam et al., 2003). Aggregation kinetics including formation process, size, rate of development and differentiation pathway can be fine-tuned by the adjustment of factors such as initial cell seeding density, avidin concentration, degree of biotinylation and addition of environmental cues at specific concentrations and at different stages. Initial cell seeding density has a direct effect upon differentiation. Inter-EB agglomeration has been shown to have effects on ES cell proliferation and differentiation (Gerecht-Nir et al., 2004, Dang et al., 2004). However, this method provides a solution to the problem by inhibiting EB-EB interaction with the addition of biotin-poly-ethylene gylcol (PEG). Biotin-PEG coats the surface of an engineered EB and blocks adhesion to other engineered EBs through non-adhesion of PEG molecules.

1.4.4.3. Microparticle Incorporation

As previously stated, biomaterial scaffolds have been used for the purpose of delivering cell cultures *in vivo* whilst providing growth factors and surface topography conducive to morphogenesis (Drury and Mooney, 2003, Lutolf and Hubbell, 2005, Levenberg et al., 2003). Previously scaffolds have been large structures for the purpose of space filling *in vivo*. However, scaffolds can also be in the form of individual microparticles which incorporate within the EB structure. Microparticles still provide surface for cell attachment and proliferation but act more as a delivery system for growth factors during degradation (Weber et al., 2002, Awad et al., 2004). Efficient delivery of growth factors and other environmental cues directly to differentiating ES cells within the EB structure is essential for eventual

tissue formation and vascularization (Dawson and Oreffo, 2008, Shamblott et al., 2001, Balakrishnan and Jayakrishnan, 2005, Boontheekul et al., 2005). The hypothesis is that microparticles would deliver growth factors directly to internal ES cells. This would abate the problem of only exposing the EB surface to inductive factors, and aid uniform differentiation throughout the EB structure.

1.5. Aims and Objectives

The main aim of this study was to characterize ES cell aggregation and subsequent EB formation using a chemically engineered 3D culture system (De Bank et al., 2003). The hypothesis that control of early ES cell aggregation via surface modification may provide control over downstream ES cell differentiation was also investigated with respect to osteogenic differentiation. Specific objectives of this study included:

1. Assess ES cell viability after surface modification
2. Investigate aggregation kinetics
3. Characterize physical properties
4. Determine differentiation potential
5. Investigate osteogenic potential
6. Generate microparticle incorporated EBs

Chapter 2

2. Methods and Materials

All chemicals were obtained from Sigma-Aldrich Ltd (Poole U.K.) unless stated otherwise.

2.1. Mammalian Cell Culture

2.1.1. Culture Media

2.1.1.1. SNL Fibroblast Media

SNL fibroblasts were cultured in a standard culture media (SCM) containing Dulbecco's Modified Eagles Medium (DMEM) (Invitrogen, Paisley U.K.), 10% Fetal Calves Serum (FCS), 1% Penicillin/Streptomycin (Pen/Strep) (Invitrogen), 2mM L-glutamine and 500μM β-mercaptoethanol (β-Mercap). DMEM acts a buffered liquid-culture support for *in vitro* proliferation of cells. The main ingredients are glucose (energy source), L-glutamine (essential amino acid), and N-2-hydroxy-ethylpiperazone-N-2-ethanesulfonic acid (HEPES) (buffer). FCS was added to supply nucleotides and other various factors required for proliferation. Pen/Strep was added to minimize risk of bacterial infection. Additional L-glutamine was added to

cope with the rate of cell growth. β-Mercap acts as a reducing agent to control the detrimental effects of harmful metabolites produced as byproducts of cell proliferation. SCM was made fresh every 1 to 2 months.

2.1.1.2. Embryonic Stem Cell Media

ES cells were cultured in SCM supplemented with 500units/mL LIF (Chemicon, Hampshire U.K.). LIF was added to the culture media as a maintenance factor of ES cell pluripotency. ES cell media (ESM) was made fresh every month.

2.1.1.3. Aggregation Media

Initial aggregation of engineered and control ES cells in mass suspension, was carried out in aggregation media (AM) (DMEM, 1% FCS, 2mM L-glutamine and 1% Pen/Strep). DMEM acts as a support, L-glutamine is an essential amino acid and Pen/Strep reduces risk of bacterial infection. The reduced FCS minimized ES cell proliferation to allow for maximum aggregation immediately after seeding.

2.1.1.4. Cryopreservation Media

Stock aliquots of both SNL fibroblasts and ES cells were prepared and frozen in cryopreservation media (CPM) (DMEM, 20% FCS and 10% dimethyl-sulfoxide (DMSO)). DMSO is a polar aprotic solvent which exhibits hydrogen bonding and can stabilize ions in solution. It is routinely used as a cryoprotectant as it minimizes the formation of damaging ice crystals intracellularly and extracellularly. During freezing, water molecules move into the extracellular space, reducing water content and risk of ice crystal formation intracellularly. DMSO hydrogen bonds to the cells displacing water molecules, reducing risk of ice crystal formation extracellularly.

2.1.2. Culture Apparatus and Reagents

2.1.2.1. Equipment

Mammalian cell culture was performed in a sterile environment in a Class II cabinet (Envair, Lancashire U.K.) fitted with high efficiency particulate air (HEPA) filters. Air is drawn into the cabinet to protect the user from the samples. This is then circulated under the internal working area and passed through a HEPA filter before being directed on top of the working area to protect the samples. Dispensable lab-ware utilized for routine cell culture included plugged serological pipettes (Fisher, Leicestershire U.K.), T25cm^3 and T75cm^3 flasks (Nunc, Fisher, Leicestershire U.K.), syringes (Becton Dickinson (BD) Biosciences, Oxford U.K.), 15mL and 50mL tubes (BD Falcon, Oxford U.K.), 30mL universals and 7mL bijouxs (Sterilin, Caerphilly U.K.), sterile glass Pasteur pipettes (Costar, Fisher), 1.5mL Eppendorfs (Sarstedt Ltd., Leicestershire U.K.), 100mL beakers (Scientific Laboratory Supplies (SLS), Nottingham U.K.), cell scrapers (Fisher), cryovials (Fisher), pipette tips (SLS) and weighing boats (SLS). A lab coat and sterile nitrile gloves (SLS) were worn throughout to protect work from contamination and waste plastic-ware was disposed of in autoclave bags (SLS). Sterilization of reagents was either by filtration using 0.22μm filters (Sartorius, Epsom U.K.) or by autoclaving using a Prestige Medical 20100 autoclave (SLS). All cell cultures were kept in a Sanyo incubator (Gaithersburg U.S.A.) at 37°C and 5% CO_2 in a humidified atmosphere.

2.1.2.2. Chemicals

All used and/or contaminated plastic-ware was disinfected by overnight immersion in diluted trigene (SLS) before incineration. 70% ethanol in dH_2O was used to sterilize the working area within the Class II cabinet and any items prior to their

transfer into the cabinet to reduce risk of contamination. Trypsin/ethylenediaminetetraacetic acid (EDTA) was used to break cell-cell adherens junctions, cell-matrix adhesions and aid cell detachment from plastic-ware. Trypsin is a serine protease which predominantly targets and cleaves peptide chains at the carboxyl-terminus of amino acids lysine and arginine, except when either has an adjacent proline towards the amino-terminus. Specificity is imparted by an aspartate residue (Asp 189) which is located in the S1 catalytic pocket. EDTA is a chelating agent that binds metal ions via four carboxylate and two amine groups. It is used in conjunction with trypsin in cell culture to bind calcium and prevent formation of adherens junctions between cells.

2.1.2.3. Buffers

Buffers regularly used in cell culture, engineering and assays included phosphate buffered saline (PBS) (1 tablet per 100mL dH_2O), biotinylation buffer (0.1% FCS in PBS, pH 6.5 with HCl), avidin buffer (0.1% FCS in PBS, pH 7.0), papain buffer (0.1M dibasic sodium phosphate, 0.005M cysteine hydrochloride and 0.005M EDTA in dH_2O, pH 6.5), and Hoescht buffer (0.01M Trizma base, 0.01M EDTA and 0.1M sodium chloride (VWR International, Poole U.K.)).

2.1.3. Cell Types

2.1.3.1. Embryonic Stem Cells

Mouse ES cells were a kind gift from Miss Magdalen Self, Wolfson Centre for Stem Cells, Tissue Engineering and Modelling (STEM), Division of Drug Delivery and Tissue Engineering, Centre for Biomolecular Sciences, University of Nottingham, U.K. The ES cell line was originally derived from mouse columnar epiblast epithelium

(CEE). It is unknown when the ES cells were first isolated and therefore, the passage number was also unknown. However, they are a well characterized and immortalized stem cell line. Their differentiated and undifferentiated states have both been shown in this and previous studies. All ES cells utilized in experimentation were between passages 1-30 post receipt.

2.1.3.2. SNL Fibroblasts

The SNL fibroblasts were again, a kind gift from Miss Magdalen Self. It is unknown how many passages the SNLs had been through prior to receipt. However, they are a well established feeder layer for *in vitro* support of ES cell proliferation and pluripotency maintenance. They were used between 1-50 passages post receipt.

2.1.3. *In Vitro* Proliferation and Maintenance

2.1.3.1. SNL Fibroblast Culture

SNL fibroblasts were proliferated in a SCM. Cultures were incubated at 37°C and 5% CO_2 in a humidified atmosphere in T75cm^3 flasks. Flasks were incubated under stationary conditions until cell cultures were ~80-90% confluent. Confluency was judged by eye on a compact inverted microscope (Olympus CKX-31).

Once confluent, media was carefully aspirated using a sterile glass Pasteur pipette, cultures were washed twice with 5mL room temperature PBS and treated with 2mL trypsin/EDTA. Cells were treated with trypsin/EDTA for no longer than 5mins at room temperature to minimize cell damage and gently agitated. Once the cells had fully detached from the flask surface, the suspension was transferred to a 15mL Falcon tube. The suspension was repeatedly pipetted to disperse cell clumps before the addition of 3mL SCM to inactivate the trypsin/EDTA. Specifically, FCS within SCM

causes inactivation through competition; FCS provides more proteins for the trypsin to target. Suspensions were centrifuged for 5mins at 1000rpm in a Mistral 1000 centrifuge (MSE, London U.K.). Supernatant was then aspirated, carefully avoiding the cell pellet.

Pellets were suspended in 4mL SCM and passaged in a typical ratio of 1:4. 9mL SCM was added to each of 4 x T75cm^2 flasks before the cell suspension was added, 1mL to each. SNLs were cultured for ~3 to 4 days until confluent, prior to subsequent passage. Passage ratio was adjusted as required to accommodate time taken to reach confluency. Media was changed when the phenol indicator turned yellow or every 2 to 3 days.

2.1.3.2. Embryonic Stem Cell Culture

ES cells were proliferated in ESM. ES cells were cultured in T25cm^2 flasks on a feeder layer of mitotically inactivated SNL fibroblasts (mSNLs) under stationary conditions at 37°C and 5% CO_2 in a humidified atmosphere until ~80% confluent or until individual colonies were about to touch one another. Confluency was judged by eye on a compact inverted microscope.

Media was carefully aspirated once confluent and cultures were washed twice with 5mL PBS. Subsequently, cultures were treated at room temperature for 5mins with 2mL trypsin/EDTA. Cultures were gently agitated until gaps appeared in the confluent layer indicating detachment of ES cells from the feeder layer. The cell suspension was then transferred to a 15mL Falcon tube. The suspension was pipetted gently to disperse any cell clumps before the addition of 3mL ESM to inactivate the trypsin/EDTA. Cell suspensions were centrifuged for 5mins at 1000rpm and supernatant was then aspirated.

Pellets were suspended in ESM and passaged in a typical ratio of 1:5. SCM media was aspirated from 5 x T25cm^2 flasks of mSNLs and replaced with 4mL ESM. The cell pellet was suspended in 5mL ESM and distributed evenly between the 5 flasks. Cultures were incubated at 37°C and 5% CO_2 in a humidified atmosphere for 2 days under stationary conditions prior to subsequent passage.

Media was changed when the phenol red indicator began to turn yellow; ~1 to 2 days, dependent on confluency. Passage ratio was adjusted as required to accommodate time taken to reach confluency. Cellular morphology was monitored over passage number for visual alterations. If changes were observed, fresh cells were reanimated and old cultures disposed of.

2.1.3.3. Cryopreservation and Reanimation

Confluent cells, either SNL fibroblasts or ES cells were washed twice in 5mL room temperature PBS and treated with 2mL trypsin/EDTA. After cell detachment, suspensions were transferred to a 15mL Falcon tube, trypsin inactivated with 3mL CPM and centrifuged for 5mins at 1000rpm. Supernatant was aspirated and cells suspended in CPM. Cells were subsequently seeded in 1mL suspensions of CPM in cryovials and placed in a polystyrene box. This was then stored at -80°C where cells were slowly frozen at a rate of 1°C per hour. This allows time for DMSO to displace water molecules. Once cooled to -80°C, cryovials were transferred to liquid nitrogen (-196°C to -210°C) for long term storage.

Cells were reanimated by immediate transfer from liquid nitrogen storage to 37°C. Once thawed, the suspensions were quickly centrifuged and supernatant was aspirated. Cells were suspended in appropriate media pre-heated to 37°C and seeded into T75cm^2 flask for SNL fibroblasts and T25cm^2 flasks for ES cells. Cells reanimated

at varying rates, usually ranging between 1 week for ES cells and 2 weeks for SNL fibroblasts.

2.1.4. Mitotic Inactivation

2.1.4.1. SNL Fibroblast Inactivation

Confluent cultures of SNL fibroblasts were treated with a 10mL solution of 0.01mg/mL mitomycin C (MMC) and incubated for 2hrs at 37°C and 5% CO_2 in a humidified atmosphere. MMC solution was then removed and cultures were washed with 2 x 10mL PBS. Cultures were treated with 2mL trypsin/EDTA at room temperature and gently agitated. After the confluent cell layer dissociated from the flask, the cell suspension was transferred to a 15mL Falcon tube. 3mL SCM was added to the tube to inactivate the trypsin/EDTA before the suspension was centrifuged for 5mins at 1000rpm. Supernatant was aspirated and the pellet suspended in 2mL SCM.

MMC is isolated from *Streptomyces lavendulae* and is a potent deoxyribonucleic acid (DNA) cross-linker. It prevents DNA replication and halts treated cells in G1 phase of the cell cycle. Cells are consequently mitotically inactivated.

2.1.4.2. Cell Number Quantification

10µl of a cell suspension was seeded into an improved neubauer hemocytometer and viewed under an inverted light microscope. The hemocytometer displayed a 5 by 5 square grid. All cells within the 4 corner and central squares were counted. Only cells which were positioned fully within the square and those which were situated on two sides of each square were counted (Fig 2.1). Cell concentration was calculated by the following equation;

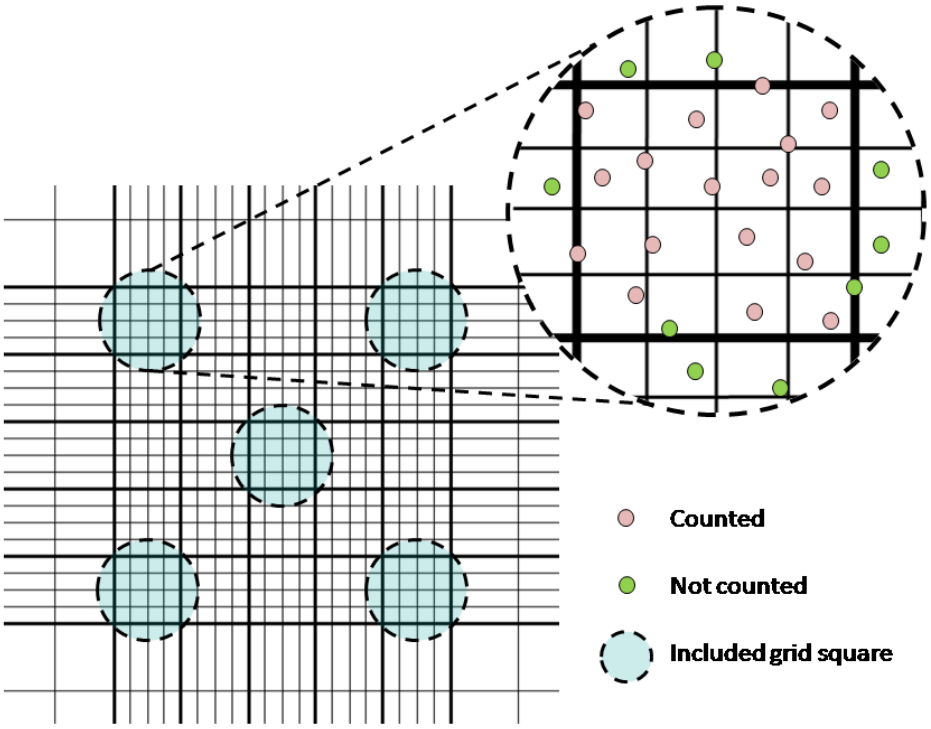

Figure 2.1: Diagrammatic representation of a cell count using an improved neubauer hemocytometer. ES cells are trypsinized to ensure full dissociation into single cell suspensions. 10µl aliquots are carefully loaded onto the hemocytometer on either side so that the aliquot in trapped between the hemocytometer and cover slip. The reference grid is composed of a 5 by 5 square grid, and each of the 25 squares is further separated into a 4 by 4 square grid. All cells within the four corners and central squares of the 5 by 5 square grid are counted and an average calculated. Specifically, all cells lying completely within each and those overlapping two of the four sides are included. Dilution factor of the loaded suspension and the inherent dilution factor of the hemocytometer are then used to calculate ES cell number within the original suspension.

$$A \times B \times C \times D = \text{number of cells/mL}$$

A = number of cells counted in all 5 squares

B = 5 (number of cells in the 25 square grid)

C = 100 (inherent dilution factor of the hemocytometer)

D = 100 (dilution factor of the volume added)

2.1.4.3. Feeder Layer Preparation

T25cm^2 flasks were prepared for mSNL culture via incubation at room temperature with 2-3mL 0.1% bovine gelatin in PBS for 20-30mins. Excess gelatin was aspirated and replaced with 5mL SCM. mSNLs were seeded into the flasks at 8 x 10^4 cells/mL (1.6 x 10^4 cells/cm^2). The appropriate volume of cell suspension required to seed at 8 x 10^4 cells/mL was calculated as follows;

$$(A / B) \times C = \text{volume } (\mu l)$$

A = 8 x 10^4 cells/mL (desired cell concentration)

B = number of cells/mL (cell suspension concentration)

C = 1000 (conversion factor from mL to µl)

The correct volume of cell suspension was then added to each flask and gently mixed to ensure homogeneity. Flasks were incubated overnight to allow adhesion of the mSNL fibroblasts to the flask surface prior to their use for ES cell culture. MMC solution was used at 37°C, and mSNL coated T25cm^2 flasks were replenished every 2 weeks due to cell death and detachment from the flask.

Gelatin is the subunit of denatured collagen whose natural structure is a left-handed helix composed of three hydrogen bonded gelatin strands (tropocollagen). Gelatin can be extracted by either acidic, alkali or neutral treatment of tropocollagen. Bovine collagen is complex and contains chemical cross-linkages such as covalent bonding

between tropocollagen fibrils. Alkali treatment is used to break these bonds and denature bovine collagen producing type-B gelatin (alkali extracted). Gelatin has a highly repetitive structure consisting of three amino acid subunits. The amino acid sequence of the basic subunit is Gly-X-Hyp or Gly-Pro-Y, where X and Y can be any amino acid. Gelatin is soluble in dH_2O and forms a hydro-colloidal mixture which is used to coat the polystyrene flasks. Gelatin adsorbs to the polystyrene flasks providing a base layer which binds integrins on the cell surface.

2.1.4.4. Embryonic Stem Cell Inactivation

ES cells were inactivated with a solution of 0.01mg/mL MMC and incubated for 2hrs at 37°C and 5% CO_2 in a humidified atmosphere. MMC solution was removed with 2 x 5mL PBS washes at room temperature prior to experimentation, i.e. aggregate formation.

2.2. Engineered Embryonic Stem Cells

2.2.1. Sodium Periodate Oxidation

Confluent ES cell cultures were washed twice with 5mL room temperature PBS, after removal of ESM. Cultures were then treated with 2mL trypsin/EDTA and agitated gently until breaks appeared in the monolayer. 3mL AM was added to inactivate the trypsin/EDTA and then cell suspensions were transferred to 15mL Falcon tubes and centrifuged for 5mins at 1000rpm. Supernatant was aspirated and the pellet suspended in 5mL PBS. The cell suspension was centrifuged again, supernatant aspirated and the pellet suspended in 5mL 1mM sodium periodate solution (sodium periodate powder in PBS). Cell suspensions were incubated for 15mins at 4°C in the

dark with agitation after 5mins. Sodium periodate solution was used at 4°C and made fresh every week.

Sodium periodate is used to target the terminal vicinal diol groups of cell surface saccharides. The target saccharide was sialic acid. Loss of the terminal carbon atom creates a non-native reactive aldehyde group. The reaction is carried out at 4°C to minimize intracellular uptake of the exogenous sodium periodate by slowing membrane transport. This oxidation reaction is also exothermic and the cool environment is required to dispel the released heat energy. Heat can also cause decomposition of sodium periodate to form sodium iodate and oxygen, altering the oxidation kinetics. The reaction is carried out in the dark as light can cause oxidation, introducing an uncontrolled variable which reduces reproducibility of the modification. Light can cause photoactivation of periodate to form reactive intermediaries that act over a range of pH (Tang and Weavers, 2007). Dark conditions minimize the generation of these intermediaries, reducing the risk of cell damage via organic degradation by iodine radicals.

2.2.2. Embryonic Stem Cell Biotinylation

Sodium periodate-treated ES cells were removed from incubation at 4°C and centrifuged for 5mins at 1000rpm. Sodium periodate solution was aspirated and the pellet suspended in 5mL biotin buffer. Cell suspensions were centrifuged again and suspended in 5mL 5mM biotin hydrazide solution (lyophilized biotin hydrazide powder in biotin buffer) then incubated for 30mins at 37°C. During incubation cell suspensions were under constant rotational agitation on a Stuart Roller Mixer SRT6 (Scientific Laboratories Supplies, Nottingham U.K.). Biotin hydrazide solution was used at room temperature and made fresh every week.

The reactive aldehydes are joined with biotin groups via a hydrazone linkage. The hydrazide group of biotin hydrazide replaces the oxygen atom of the aldehyde. The reaction is carried out at 37°C to simply speed up the whole procedure and minimize stress to the cells before being placed back in culture.

2.2.3. Control Embryonic Stem Cells

Control ES cells were processed identically to engineered ES cells, except that all chemical washes were replaced with PBS washes. Two controls were employed, (1) non-engineered ES cells without avidin supplementation, and (2) non-engineered ES cells with avidin supplementation (to assess any non-specific binding of avidin).

2.3. Mass Suspension

Both engineered and control ES cell suspensions were centrifuged for 5mins at 1000rpm after incubation with biotin hydrazide solution. Supernatant was aspirated and pellets were suspended in 5mL avidin buffer, then centrifuged. Pellets were suspended in AM and cell concentration was calculated using an improved neubauer hemocytometer as previously stated. ES cells were then seeded into non-tissue-culture treated 6 well plates (Falcon) in AM supplemented with 10μg/mL avidin (lyophilized avidin powder from chicken egg white in PBS). All suspensions were 2mL final volume (Fig 2.2). Avidin incorporation study employed avidin-FITC conjugate (buffered aqueous solution).

Avidin is a 66-69kDa tetrameric protein composed of four identical subunits, each of which can bind covalently to biotin. Due to the size of the ES cells, only two subunits of an individual avidin molecule bind the biotin groups attached to the cell surface.

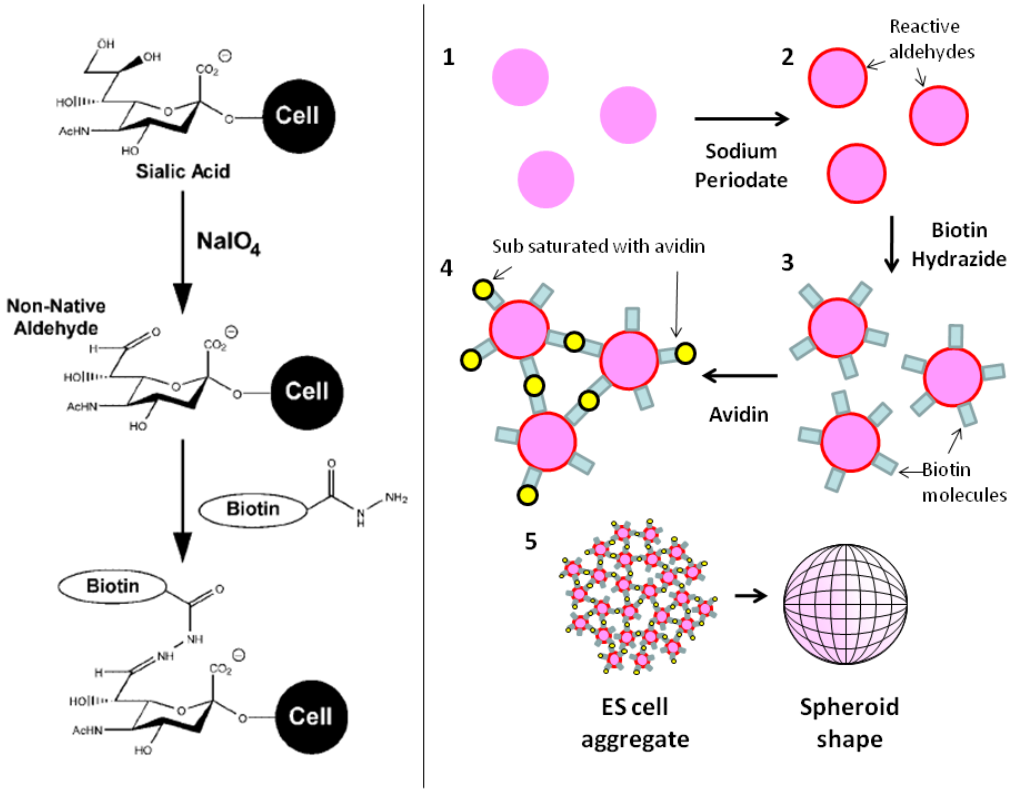

Figure 2.2: Chemically engineered ES cell aggregation (De Bank et al., 2003). Engineering is based on modification of surface glycoforms. ES cells are treated with 1mM $NaIO_4$ for 10mins at 4°C in the dark. NaIO4 is an oxidizing agent which specifically targets the vicinal diol of sialic acid residues which is invariably the terminal or penultimate sugar residue in most glycoforms. NaIO4 treatment creates a non-native reactive aldehyde group. ES cells are then treated with 5mM biotin hydrazide which results in the ES cell surface becoming effectively biotinylated via a hydrazone bond between biotin hydrazide and the reactive aldehyde groups. Biotinylated ES cells are then cross-linked with exogenously added avidin, exploiting the known binding affinity of avidin for biotin.

Seeding densities used were 0.05, 0.1, 0.25, 0.5, 0.75 and 1 x 10^6 cells/mL. Plates were incubated for 6hrs at 37°C and 5% CO_2 in a humidified atmosphere and constant agitation using a gyrotwister 3D-shaker (Labnet International Inc., Dorset, U.K.) set between 0 and 30rpm. After 6hrs incubation, FCS concentration was increased to 10% and suspensions placed under stationary conditions. Aggregation was allowed for up to 9 days and media was changed every 2 to 3 days with SCM pre-warmed to room temperature. FCS concentration was kept at 1% for the first 6hrs to encourage aggregation between ES cells with minimum proliferation.

2.4. Trypan Blue

EBs were fully dissociated with trypsin/EDTA, centrifuged and suspended in SCM. Before cell counting, an aliquot of the cell suspension was mixed with trypan blue in equal volumes, i.e. 20µl of each. 10µl was then added to the haemocytometer and a cell count was carried out as stated previously. However, cells which stained blue were not included as these cells were dead. This was repeated prior to all experiments to ensure that cell concentrations were calculated for live cells only.

Trypan blue is a derivative of toluidine (an isomeric derivative of toluene) which is capable of entering cells without intact membranes such as necrotic cells and cells undergoing apoptosis. These cells therefore appear blue under a microscope. Live cells have intact membranes which trypan blue cannot permeate.

2.5. Alamar Blue Assay

After 2hrs incubation with 0.01% MMC solution, ES cell cultures were washed twice with 5mL PBS to thoroughly remove the MMC. PBS was then aspirated and 1mL Alamar Blue working solution (Alamar Blue diluted 1:10 in HBSS (Hanks Balanced Salts Solution)) was added to the cultures. Cultures were incubated at 37°C and 5% CO_2 in a humidified atmosphere for 1hr. 100µl of the supernatant was transferred to a 96 well plate (Nunc) and absorbance was read at 570nm using a KC4 plate reader (Labtech International, East Sussex U.K.).

Alamar Blue has previously been identified as resazurin (7-hydroxy-3H-phenoxazin-3-one 10-oxide). Resazurin is normally used for testing spoilage of milk, indicated by a colour change. The removal of oxygen and formation of reducing agents during cellular proliferation are thought to cause the reduction of resazurin (blue and non-fluorescent) to resorufin (pink and fluorescent) (O'Brien et al., 2000). However, continued reduction generates hydroresorufin, which is not coloured and non-fluorescent. This hints at a possible draw back of using Alamar Blue as a proliferation assay in long term cultures. Alamar Blue was specifically used to give continuous measurement of ES cell viability over MMC concentration. Rather than showing whether the cells were alive or dead due to increasing MMC concentration, Alamar Blue assay allowed identification of a graded response.

2.6. Live/Dead™ Stain

ES cells/EBs were incubated at 37°C and 5% CO_2 in a humidified atmosphere for 1hr in Live/Dead™ solution (2µM calcein AM and 4µM ethidium homodimer-1 in SCM). Samples were then allowed to settle or they were centrifuged briefly at 200rpm for

30secs before being washed with 2mL PBS. PBS suspended samples were imaged at excitation/emission 495/515nm for calcein AM and 495/635nm for ethidium homodimer-1 using fluorescence microscopy. Samples were viewed on an inverted-microscope (Leica DM IRE2), and images were captured using 'Volocity' imaging software. Live/Dead™ solution was either prepared fresh each time, or used within 1 freeze-thaw cycle. Live/Dead™ solution was pre-heated to 37°C to avoid cold shocking the samples.

Calcein AM is the acetomethoxy derivate of calcein, also known as fluorescein complex. It is membrane permeable and enters both living and dead cells. However, only living cells have functional esterases which remove the acetomethoxy group. Once removed, the calcein chelates intracellular calcium ions to give bright green fluorescence. Ethidium homodimer-1 is a membrane-impermeable red fluorescent dye. The dye intercalates with DNA, highlighting dead cells under U.V. light.

2.7. Microscopy

2.7.1. Light Microscopy

During aggregation EBs were measured by phase contrast microscopy on a stereo-microscope (Nikon Eclipse TS100) at 10x magnification. Photographs were taken using an attached imaging screen with built in software (Nikon Digital Sight DS-L1).

2.7.2. Fluorescence Microscopy

Fluorescently immuno-labelled EB sections were viewed using an inverted-microscope (Nikon Eclipse 90i). Photographs were captured using a Hamamatsu digital camera and imaged using 'Volocity' imaging software.

2.8. Scanning Electron Microscopy

2.8.1. Preparation for SEM

EBs were transferred to 15mL Falcon tubes and allowed to settle for 20mins at room temperature. Medium was aspirated and the EBs suspended in 5mL PBS. After settling again the EBs were suspended and fixed overnight at 4°C in 3% glutaraldehyde. EBs were allowed to settle and then suspended in 1% osmium tetroxide (TAAB, Berkshire U.K.) for 2hrs at room temperature. These were then washed in 5mL dH_2O and allowed to settle. After washing they were dehydrated through a series of ethanol washes (25%, 50%, 70%, 90%, 95% in dH_2O, and 100% ethanol) each lasting 2-5mins. Once dehydrated, EBs were chemically dried twice with 5mL hexa-methyldisilazane (HMDS) for 5mins at room temperature. HMDS was removed and EBs were allowed to air dry overnight in an externally vented fume hood.

Glutaraldehyde is a fixative which in its monomeric form exhibits two aldehyde groups, each of which can bind the amino groups on proteins. Consequently, glutaraldehyde cross-links intracellular proteins quickly killing the cells. Osmium tetroxide cross-links and stabilizes all cell and organelle membrane lipids. It binds the double bonds found in lipoproteins depositing heavy metal in the cell membranes. Membrane deposited osmium also enhances bulk conductivity of the biological samples which increases image contrast by reducing localized electrostatic build up of electrons fired from the scanning electron microscopy (SEM) tungsten element. HMDS consists of ammonia substituted with two trimethylsilyl groups. It readily displaces the organic solvent ethanol allowing for removal by evaporation. Also, it binds organic surfaces leaving a ‘single molecule thick’ coating which

terminates at a methyl group. Methyl groups are relatively inert and do not easily attach to each other or other molecules (Nation, 1983). Excess HMDS evaporates and leaves behind thinly-coated EBs that are prevented from adhering to one another.

2.8.2 SEM Imaging

Desiccated EBs were carefully removed from the Falcon tubes and adhered to carbon discs (Agar Scientific Ltd., Essex U.K.) mounted on aluminium stubs (Agar). These were gold-coated using a Balzers SCD 030 gold sputter coater (Balzers Union Ltd., Leichtenstein) for 3mins under argon atmosphere. Coated EBs were then imaged using a JEOL 6060L scanning electron microscope (JEOL Ltd., Hertfordshire U.K.). Images were initially taken at 12kV, and later at 14kV dependent on higher resolution images. Magnification was balanced with working distance from element to reduce the voltage required for imaging and hence, ionization of the sample. Repeat gold sputtering was applied to EBs imaged at 14kV for long periods as ionization build up reduced contrast resolution.

Gold sputtering involves the thin-layer deposition of ionized gold atoms on a target sample. Gold is electron dense, thus providing a source of secondary electrons for SEM imaging (Ludwig et al., 1976). Biological samples are carbon based and poor emitters of secondary electrons. Secondary electrons collide with surrounding electrons creating a detectable electrical current. Gold also enhances conductivity of the biological samples. Sputtering was carried out in an argon atmosphere due the inert property of argon and that argon can be easily ionized to create conductive plasma for transmission of gold ions.

2.9. Histology

2.9.1. Paraffin Embedding

EB suspensions were transferred to 15mL Falcon tubes and allowed to settle for 20mins at room temperature. The media was aspirated and the EBs carefully suspended in 5mL PBS. After settling, PBS was aspirated and EBs were suspended and fixed in 5mL 10% formalin (formaldehyde in dH_2O) for 20mins at room temperature. After a second wash with 5mL PBS the EBs were allowed to settle for 20mins and then they were suspended in a solution of 3% (w/v) agarose (low gelling temperature). EBs were carefully positioned adjacent to one another, opposed to evenly distributed throughout the gel suspension. The agarose was allowed to gel and then cooled to 4°C for 30-60mins. Using a Fireboy Bunsen burner (INTEGRA Biosciences AG, Zurich Switzerland) to heat a scalpel blade, the cone tip of the Falcon tube holding the gel suspended EBs was carefully removed. A syringe needle was used to remove the gel cone from the Falcon tube tip. A second scalpel blade at room temperature was used to slice the gel cone in half. Sliced gel halves were placed in a histology cassette and stored in 10% formalin before being processed at the Histopathology department of the Queen's Medical Centre (QMC, Nottingham U.K.) where the EBs were finally embedded in paraffin wax.

Formalin is formaldehyde in aqueous solution and causes fixation of biological tissues through covalent bonding and cross-linking of proteins to each other and the cytoskeleton. All intracellular biochemical reactions are stopped immediately upon exposure to the formalin, effectively killing the cell and preventing decay. The cross-links also provide rigidity, preventing structural collapse of the cells. Agarose is one of two polysaccharides which make agar, the other (more complex) polysaccharide

being agaropectin. It consists of a galactose-based backbone exhibiting far less complex side chains as those of agaropectin. Due to this low degree of chemical complexity and neutral charge, agarose provides an ideal support for suspension of cells. Agarose also exhibits reduced risk of biochemical interaction with cell proteins. 3% agarose has sufficient pore size to trap cells in a stationary position once cooled and allowed to gel. Paraffin wax helps to harden and secure the EBs in a stationary position ready for sectioning.

2.9.2. Microtome Sectioning

Once embedded, EBs were sectioned on a Leica RM2165 microtome (Leica Microsystems Ltd., Buckinghamshire U.K.). The section diameter was set to 4μm. Successive sections were collected as a ribbon and carefully placed into a water-bath set approximately at 60˚C. When ribbons became shredded, the blade was either cleaned with UltraClear (TAAB) or replaced. If the ribbon continued to shred, the paraffin block was removed and placed on ice to cool for 10-15mins. The ribbon was carefully separated into individual sections with ice cold forceps and tweezers. Sections were adhered to SuperFrost® Plus glass slides (Laboratory Sales Ltd., Rochdale U.K.) and excess water was gently dabbed off. These slides were dried using a Hearson hot-bed set at 60˚C for 30-60mins. Sections were allowed to cool to room temperature and stored under dark and dry conditions.

SuperFrost® Plus glass slides are treated to exhibit a permanently positive surface. This electrostatically attracts formalin-fixed tissue sections and binds them through covalent bonding.

2.10. Haematoxylin and Eosin Stain

Sections were placed in a glass holder and washed twice in a bath of xylene for 3mins to de-wax. Sections were rehydrated through a series of ethanol washes (100%, 90%, 70% and 50% in dH_2O) and a final rinse in dH_2O, each for 2-3mins. Once hydrated, sections were treated with enough Mayers haematoxylin to cover the sample for 5-10mins at room temperature then washed with dH_2O. Sections were washed with Scott's tap water (2% magnesium sulphate and 0.35% sodium bicarbonate in dH_2O) and partially dehydrated through 50%, 70% and 90% ethanol in dH_2O washes, 2-3mins each. After being dipped in alcoholic 1% eosin (eosin in ethanol), dehydration was completed with a 2-3min wash of 100% ethanol and a final wash in xylene. Stained sections were left to air dry on a hot-bed for 30-60mins and mounted with DPX. Sections were stored in a cool, dark and dry place.

Xylene is essentially a mix of three dimethyl benzene isomers including ortho, meta and para-xylene. It acts as a solvent for the removal of paraffin wax. Haematoxylin is a compound derived from logwood trees which binds and stains basophilic structures within biological sections. Basophilic structures include the nucleus and ribosomes which contain nucleic acid. Once oxidized, haematoxylin forms haematein which has a deep blue/purple colour. Haematein binds nuclear histones in chromatin, specifically lysine residues, and exhibits a blue colour as a result of metallic ion mordant formation through linkage to iron and aluminium salts. The linkage creates insoluble aluminium hydroxide (mordant) in the alkaline conditions provided by the Scott's tap water. This reaction darkens the colour of the stain via a process called blueing. Eosin is a compound which stains eosinophilic structures within biological samples such as collagen and the cytoplasm. It is used as a counter-stain in conjunction with haematoxylin. Eosin is a mixture of two derivates resulting

from the chemical reaction between bromine and fluorescein; eosin Y (tetrabromo) and eosin B (dibromo dinitro). Alcoholic eosin is used to give a deeper red stain, opposed to the pink colour in non-alcoholic eosin. DPX contains a plastic resin dissolved in xylene supplemented with di-N-butyl phthalate as a plasticizer for dissolved resin flexibility. It acts as a transparent shield to protect the stained biological sections during imaging and storage.

2.11. Immuno-Histochemistry

2.11.1. Citrate Buffer

Citrate buffer was prepared by mixing equimolar sodium citrate and citric acid solutions (41mL to 9mL, respectively), diluting with dH_2O to 100mL and adjusting the pH to 6.0. Both sodium citrate and citric acid solutions were 0.1M in dH_2O with 0.05% Tween 20 and adjusted to pH 6.0. All solutions were stored at 4°C.

Tween 20 is a polysorbate surfactant used to solubilize and create holes in the cell membrane. It is a polyoxyethylene derivative of sorbitan monolaurate.

2.11.2. Section Preparation

Sections were washed in xylene twice for 5mins to de-wax, hydrated in 100% ethanol twice for 3mins, 95% and 80% ethanol in dH_2O twice for 1min, all sequentially. After a final wash in dH_2O for 1min, sections were immersed in citrate buffer pre-heated to 95-100°C for 20-40mins for antigen retrieval. Sections were then allowed to cool at room temperature for 20mins.

2.11.3. Antibody Labelling

2.11.3.1. Blocking Solution

Once cooled, sections were loaded into a slide holder and rinsed with PBS containing 0.1% Tween 20. Sections were then washed and incubated with 100µl 0.1% Triton X-100 and 1% bovine serum albumin (BSA) in PBS (PBT) for 30mins at room temperature. After 3 x 5 min washes with 100µl 0.1% BSA in PBS (PBA), 100µl blocking solution (10% donkey serum in PBS) was added for 30mins at room temperature.

Triton X-100 is a nonionic surfactant which causes cell membrane permeabilization. BSA is a serum albumin protein that is used as a stabilizer and for its lack of biochemical interaction during the labelling procedure.

2.11.3.2. Primary Antibody

Blocking solution was rinsed away with 3 x PBA washes, 5mins each. Sections were incubated for 1hr at room temperature with 100µl primary antibody (1:50 dilution in PBA). Alternatively, if target epitopes were internal markers, samples were incubated at 4°C overnight. A list of the primary antibodies used is shown overleaf (Table 2.1).

2.11.3.3. Secondary Antibody

Primary antibody solution was washed away with 3 x 100µl PBA rinses, 5mins each. Sections were incubated at room temperature with 100µl fluorescently-labelled secondary antibody (1:250 dilution in PBA) for 1hr in the dark (Table 2.1). Sections were rinsed with 3 x 5min washes of 100µl PBA. Finally, sections were washed for 10mins in PBS before being removed from the slide holder. Before the sections began

Primary Antibodies		Secondary Antibodies			
Specific for:	Raised in:	Specific for:	Raised in:	Conjugated to:	Excitation/ Emission
• Oct-4	Rabbit	Rabbit	Goat	FitC	495/575nm
• Brachyury	Goat	Goat	Sheep	PE (phycoerytherin)	495/521nm
• Gata-4	Rabbit	Rabbit	Goat	FitC	495/575nm
• Nestin	Rabbit	Rabbit	Goat	FitC	495/575nm
• Cadherin-11	Goat	Goat	Sheep	PE (phycoerytherin)	495/521nm

Table 2.1: List of primary antibodies and corresponding fluorescently-conjugated secondary antibodies.

to air dry they were mounted with 'Vectashield® with DAPI' (Vector Laboratories Ltd., Peterborough U.K.) and incubated overnight at 4°C in the dark. Fluorescence images were taken on a Leica DMIRE2 inverted microscope using the appropriate filters. Stained sections were stored at 4°C in the dark.

Vectashield® preserves fluorescence by scavenging free radicals produced upon exposure to U.V. light. DAPI is a fluorescent stain that binds strongly to DNA via intercalation in the minor groove of the helical structure. Its excitation and emission wavelengths are 358nm and 461nm respective.

2.12. Hoescht Assay

2.12.1. Papain Digestion

Cells were collected in 15mL Falcon tubes and centrifuged for 5mins at 1000rpm. Pellets were suspended in 0.5-1mL papain solution (1.06mg/mL papain powder in papain buffer) pre-heated to 60°C. Papain solution was pre-heated to 60°C to dissolve papain powder prior to addition of cells. Cells were rigorously mixed by pipetting in papain solution prior to overnight incubation in a Grant waterbath (JB4 mid-sized 16litre, Cambridgeshire U.K.) set at 60°C.

Papain is derived from *Carica papaya* and the latex of its tree. Papain is a cysteine protease which has two structural domains and a cleft in between which hosts the active site. The active site consists of three amino acid residues including Cys-25, His-159 and Asp-158. Papain function involves deprotonation of Cys-25 by His-159 which is spatially orientated by Asp-158. Cys-25 then nucleophilically attacks the

carbonyl carbon of peptides. Over a prolonged period papain completely digests ECM and lyses cells.

2.12.2. DNA Quantification

Once digested, 34µl of each digested sample solution was mixed with 0.5mL Hoescht buffer and 0.75mL of Hoescht working solution (Hoescht stock solution in Hoescht buffer, 1:2000). Hoescht stock solution was made by mixing 1mg/mL bis-benzimide with single-strength SSC buffer. 300µl of this mixture was then transferred to a 96 well plate and fluorescence was read at excitation/emission 360nm/460nm using a KC4 plate reader. All solutions and samples were kept under minimal light conditions throughout.

Bis-benzimide is a fluorescent dye which intercalates with DNA and can be used to quantify DNA content from plotting a standard emission-to-content curve. Two bis-benzimides are regularly used including Hoescht 33258 (pentahydrate) and Hoescht 33342 (trihydrate). The difference between them is an additional ethyl group on Hoescht 33342 making it more lipophilic.

2.13. Osteo-Induction

EB suspensions were transferred to 15mL Falcon tubes and allowed to settle. Alternatively, suspensions were centrifuged briefly at 200rpm to pellet the EBs. Media was removed and EBs were suspended in either osteo-inductive media (DMEM, 15% FCS, 1% L-glutamine, 1% Pen/Strep, 500µM β-Mercap, 10µM dexamethasone (Dex), 50µg/mL ascorbate-2-phosphate (Asc), and 10mM β-glycerophosphate (BGP)) or control media (no Dex or BGP). EBs suspensions were

then transferred to tissue-culture treated 6 well plates, pre-coated with 0.1% gelatin for 30-60mins at room temperature. Plates were incubated at 37°C and 5% CO_2 in a humidified atmosphere for 3-4 days before changing media to allow time for EBs to adhere. Cultures were grown for 4 weeks and media was changed every 2-3 days with fresh osteo-inductive and control media pre-heated to 37°C. Dex, Asc and BGP were freshly added to stock culture media every week.

Dex is a synthetic member of the glucocorticoid class of steroid hormones. The mechanism and signaling involved in dex-induced osteogenic differentiation is not fully understood. However, its ability to induce osteoblast differentiation has been reported extensively (Zalman et al., 1979, Bellows et al., 1987, Bellows et al., 1990, Grigoriadis et al., 1988). Bone nodule formation occurs initially through secretion of ECM followed by the deposition of calcium phosphate crystals by osteoblasts. Asc induces ECM secretion including collagen and GAG deposition (Poliard et al., 1993, Choi et al., 2008a). GAG is a chain of repeating disaccharide subunits which are unbranched. It is important in fibrous connective tissue and can covalently bond to proteins to form proteoglycans which are constituents of bone matrix. Asc has also been found to maintain the proliferative capacity of stem cells (Choi et al., 2008a). BGP is an organic phosphate added to induce mineralization of the collagen matrix through calcium phosphate deposition (Garimella et al., 2006). It serves as an inorganic phosphate reservoir once hydrolyzed by acid phosphatase (AP) (Fratzl-Zelman et al., 1998, Lee et al., 1992, Ecarot-Charrier et al., 1983, Chang et al., 2000).

2.14. Alizarin Red Stain

Cultures were washed in 3mL PBS, fixed in 1mL 10% formalin for 20-30mins at room temperature and washed twice in 2mL dH_2O. Cultures were treated with 1mL Alizarin Red solution (2% w/v Alizarin Red powder in dH_2O) for 5-10mins at room temperature under continuous agitation. Alizarin Red solution was removed and cultures were washed repeatedly with dH_2O until no further colour leached out. Images were taken under wet conditions (in dH_2O) using the Nikon Eclipse TS100 stereo-microscope described previously. Plates were then desiccated and stored in the dark.

Alizarin Red is a derivative of anthracene (three fused benzene rings) which exhibits two hydroxyl groups at positions 7 and 8, and two ketone side chains at positions 9 and 10 on the central ring. Originally extracted from the root of the madder plant, synthetic Alizarin Red is used today to stain calcium deposition in bone nodules formed by osteoblast function. Specifically, Alizarin Red chelates with calcium phosphate crystals deposited in the ECM to give a bright red/orange colour.

2.15. Alkaline Phosphatase Assay

Cell cultures were washed with 37°C PBS to remove traces of culture media. Alkaline phosphatase (ALP) substrate, p-nitrophenyl phosphate (PNPP) disodium salt hexahydrate in 0.2M Tris buffer, was prepared in dH_2O at a concentration of 1mg/mL. 1mL aliquots were transferred to each well containing cell cultures. Samples were then incubated at 37°C and 5% CO_2 in a humidified atmosphere for a maximum of 15mins until solution began to turn yellow. Incubation time was equal for all samples. Reactions were stopped upon addition of 100µl 3M NaOH after

removal from cell cultures. 300µl aliquots were transferred to a 96 well plate in triplicate per well and absorbance was measured at 405nm using a KC4 plate reader. Averages were taken of the triplicate readings after deducting a blank measurement of fresh PNPP solution. All readings were then equalized for DNA content of 1 x 10^6 cells using accompanying Hoescht data.

PNPP is a non-proteinaceous, non-specific substrate used for the detection of acid and ALPs. ALP acts as a catalyst for PNPP hydrolysis which forms p-nitrophenol. P-nitrophenol is a chromogenic product which has a yellow appearance with an absorbance at 405nm. Absorbance readings therefore give indirect measurement of ALP activity within the cell cultures.

2.16. Alcian Blue Stain

Cell cultures were washed with room temperature PBS and then fixed with 95% methanol solution in dH_2O at room temperature for 1hr. Samples were washed with dH_2O and then incubated with 1mL Alcian Blue solution (1% Alcian Blue powder in 3% glacial acetic acid) at 4°C for a maximum of 10mins. Alcian Blue solution was then removed and cultures were washed with dH_2O repeatedly until no further dye leached out. Samples were then imaged using the Nikon Eclipse TS100 stereomicroscope and Nikon DS-L1 imaging system at 10x magnification.

Alcian Blue is a cationic phthalocyanine dye which contains a central copper atom giving it a blue appearance. It electrostatically binds to the negatively charged regions of GAGs.

2.17. Polymerase Chain Reaction

2.17.1. Primer Design

Go to www.ensembl.org and in the drop down menu choose the desired animal model, i.e. *mus musculus*. Type in the name of the desired gene and click on 'Go'. Choose the correct gene from the list that appears and then click on 'exon info'. Copy and paste two exon codes into an online program called 'Primer 3'. Place a bracket either side of the break between the two exons and keeping all the preset parameters click on 'Pick Primers'. Choose a primer pair from the list and ensure that the 'tm' for both primer sequences match (± 1). Check the primer sequences using the online 'blastn' program found on the website, www.ncbi.nlm.nih.gov. Simply paste the sequence in, choose the correct genome for comparison, i.e. mouse, and click on 'BLAST'. Scroll down the page and check that the only 100% match is the correct gene. If there is another gene which has matched 100%, then refer back to the results in the 'Primer 3' program and choose another primer set. Finally check the sequences for potential hairpin formation using the online 'Oligo Calc' program at www.basic.northwestern.edu/biotools/oligocalc.htmL. Paste in the sequence and click on 'Check Self-Complementarity'. If there are potential hairpins, go back and choose another set of primer sequences. Once the sequences have been chosen and verified they were ordered from www.ecom.mwgdna.com.

Primers are tailored oligonucleotides of specific base sequence complimentary to the target cDNA. Their purpose is to provide a starting position either side of a target gene for polymerase to transcribe the encompassed cDNA derived from mRNA.

2.17.2. RNA Isolation and Purification

Ribonucleic acid (RNA) was extracted using the protocol supplied in the RNeasy mini kit handbook (Qiagen, West Sussex U.K.). Samples were lysed in 300µl RLT lysis solution and stored at -80°C. Once thawed, the solution was transferred to an RNeasy mini spin column and the volume doubled with 70% ethanol. The columns were spun in a centrifuge (Spectrafuge 24D, Labnet) at 9400rpm (800*g*) for 15-30secs. The waste liquid in the collection tube was removed. 700µl of RPE buffer (supplemented with ethanol) was added and the columns centrifuged again. The collection tubes were emptied, 500µl of RW1 buffer was added and the columns centrifuged for 15-30secs. After a second wash with RW1 buffer the columns were centrifuged for 2mins. Collection tubes were replaced and the columns centrifuged for 1min to ensure all liquid was collected. Columns were transferred to Eppendorf tubes and 30-50µl RNase free water was added. The columns were centrifuged for 1min before adding another 30-50µl and centrifuging again. RNA solutions were kept on ice throughout and frozen at -80°C.

2.17.3. cDNA Reverse Transcription

RNA solutions were thawed and their concentration measured on a NanoDrop® spectrophotometer (ND-1000, Labtech) at 260nm. The RNA solutions were reverse transcribed to form stable cDNA for polymerase chain reaction (PCR) amplification. The total volume for reverse transcription was 40µl. Maximum volume of RNA solution added to the reaction was up to 28µl (dependent on RNA concentration and made up to volume with RNase free water). The reaction required 1µg RNA. Oligo-dT primers constituted 1µl of the total volume (25ng/µl), and the 'master mix' constituted the other 11µl. The 'master mix' comprised 8µl reverse transcriptase

(RT) buffer, 2µl deoxyribonucleotide triphosphates (dNTPs) (1mM), 0.5µl RNase inhibitor (20ng/µl) and 0.5µl RT (20ng/µl). 1µg of RNA was made to a volume of 28µl with RNase free water and transferred to a 0.2mL thin walled PCR tube (STARLAB, Milton Keynes U.K.). The tubes are thin walled to minimize insulation and aid heat transfer. 1µl of stock oligo-dT primers was added to the tubes and centrifuged at 5000rpm for a pulse-spin in a microfuge (Sigma 1-14, SLS). Tubes were transferred to a PCR machine (Px2 Thermal Cycler, Thermo Scientific, Surrey U.K.) and heated to 65°C for 10mins. This denatures any secondary structures to expose the RNA sequence to oligo-dT primer adhesion. 11µl of the prepared 'master mix' was added to each tube and the tubes were pulse-spun. The tubes were transferred back into the PCR machine and heated for 2hrs at 55°C then 10mins at 85°C. Reverse transcriptase binds the oligo-dT primers and reverse transcribes the RNA sequence to form cDNA. The high temperature spent at 85°C denatures the reverse transcriptase and ceases cDNA synthesis. Resultant cDNA transcripts were stored at -20°C.

2.17.4. PCR Amplification

cDNA transcripts were subsequently used as templates for PCR amplification of targeted markers. Two PCR 'master mixes' were prepared and combined with a cDNA template in a thin walled PCR tube. PCR 'master mix 1' consisted of 0.2mM dNTPs, 0.5µM forward primer, 0.5µM reverse primer and RNase free water. Total volume was made to 20µl per sample. PCR 'master mix 2' consisted of 0.25µl Taq polymerase, 5µl of 10x PCR buffer and 19.75µl RNase free water, per sample. 20µl PCR 'master mix 1' and 25µl PCR 'master mix 2' were added together in a thin walled PCR tube. 5µl of the cDNA transcript was added and the tubes were pulse-spun. The

reaction solutions were loaded into a PCR machine and run on an appropriate amplification program. The PCR amplification programs included an initial denaturation step at 94°C for 5mins before a cycling step including denaturation and annealing, and a final extension phase. The exact cycling step was dependent on the primer pair being used (Table 2.2). The last step involved a final extension at 72°C for 10mins. The cycling step involves 30secs at 94°C to denature the cDNA transcripts breaking double strand DNA (dsDNA) into single strand DNA (ssDNA). The temperature then decreased according to the annealing temperature of the primer pair for 30secs. Once the primers had annealed to their targets, Taq polymerase bound the primers and transcribed the cDNA during the extension phase at 72°C for 1min. These three steps were repeated 30-35 times to amplify the DNA to a detectable level. Amplified DNA transcripts were stored at -20°C.

2.17.5. Gel Electrophoresis

A 2% (w/v) agarose gel was prepared by mixing 1.5g multipurpose agarose (agarose MP) (Roche, Hertfordshire U.K.) in 75mL Tris-Borate-EDTA (TBE) buffer. The solution was mixed in a glass 200mL Duran bottle (SLS) and heated in a microwave on full power for 1min to dissolve the agarose MP. The solution was heated for another 15secs and then supplemented with 0.5µg/mL ethidium bromide. The solution was poured into a mould holding two combs, each with 20 prongs, and allowed to set for 20mins at room temperature. Once set the gels were placed in a gel electrophoresis tank (Fisher) and submerged in TBE buffer. Additional ethidium bromide (~0.1µg/mL) was added to the buffer to counteract leaching from the gel. The combs were removed and 10µl PCR amplified DNA was loaded per sample per well, once mixed with 5µl of gel loading solution. The lid was placed on the gel

Primer	Sequence	Annealing Temperature	Cycle Number
Oct-4 (forward)	AGC ACG AGT GGA AAG CAA CT	60°C	30
Oct-4 (reverse)	AGA TGG TGG TCT GGC TGA AC	60°C	30
Brachyury (forward)	GCT GTT GGG TAG GGA GTC AA	60°C	30
Brachyury (reverse)	CCC CGT TCA CAT ATT TCC AG	60°C	30
Gata-4 (forward)	CTG GAA GAC ACC CCA ATC TC	55°C	30
Gata-4 (reverse)	GTA GTG TCC CGT CCC ATC TC	55°C	30
Nestin (forward)	AGG CGC TGG AAC AGA GAT CT	55°C	30
Nestin (reverse)	CTT CAC GAT CTG AGC GAT CT	55°C	30
Runx2 (forward)	CTT CAC AAA TCC TCC CCA AG	57°C	35
Runx2 (reverse)	GAG GCG GGA CAC CTA CTC TC	57°C	35
Osteopontin (forward)	TGC TGT GTC CTC TGA AGA AAA	57°C	35
Osteopontin (reverse)	CAG ACT CAT CCG AAT GGT GA	57°C	35
GAPDH (forward)	TGA GGC CGG TGC TGA GTA TGT CG	60°C	30
GAPDH (reverse)	CCA CAG TCT TCT GGG TGG CAG TG	60°C	30

Table 2.2: Primer pair sequences, corresponding annealing temperatures and optimized cycle number.

electrophoresis tank and connected to a power 300 - gel electrophoresis power supply (Fisher) then run for ~20 to 30mins at 100volts.

Gel loading buffer contained 0.05% (w/v) bromophenol blue, 40% (w/v) sucrose, 0.1M EDTA pH 8.0 and 0.5% (w/v) sodium lauryl sulphate (SLS). Bromophenol blue acts as a visible colour indicator to track samples during electrophoresis. Sucrose makes the solution dense and therefore enables the solution to sink into the well rather than diffusing in the buffer. EDTA denatures any contaminating enzymes and SLS dissociates any potential DNA-protein complexes and also imparts a negative charge on the DNA surface. The negative charge is essential for the electrical current to pull the sample through the gel.

2.17.6. Gel Imaging

Once finished, the tanks were drained of TBE buffer and the gels dabbed dry of excess liquid. The gels were imaged in a Fujifilm intelligent dark box using Fujifilm LAS-1000 imager (Bedfordshire U.K.) and Win TV2000 (Hauppage, London U.K.) software. The gels were illuminated with ultra violet (U.V.) light which excited ethidium bromide intercalated with DNA, therefore highlighting the sample bands. Advanced image data analyzer (AIDA) 2D densiometry software v3.28.001 (Raytest Inc., Sheffield U.K.) was used to convert the images into a usable format such as bitmap. The density of triplicate bands were quantified using ImageJ version 1.35i (NIH, USA). These measurements were normalised to the corresponding GAPDH value of that sample and expressed as a mean ± standard deviation. Waste gels were disposed of in toxic waste due to the ethidium bromide content.

2.18. May-Grünwald and Giemsa Stain

After ES cells had attached to the microparticle surface and spread out, samples were removed from culture media, washed in room temperature PBS and fixed with 4% (w/v) paraformaldehyde in PBS for 30mins at room temperature. Samples were washed with PBS to remove fixative solution and incubated in 0.1% (v/v) Triton X-100 in PBS for 15mins at room temperature to permeabilize the cell membrane. After another wash in PBS samples were incubated at room temperature in 0.25% (w/v) May-Grünwald solution in methanol for 15mins to stain the cell cytoplasm. After a wash in PBS, samples were incubated at room temperature in 0.4% (w/v) Giemsa solution in methanol for 20mins to stain the cell nucleus. Samples were then washed twice in dH_2O and left to air dry overnight. Samples were imaged using light microscopy.

Paraformaldehyde is formed by polymerising formaldehyde molecules to make a chain. It cross-links amino groups within biological samples effectively sterilising and fixing the tissue protecting it from decay and structural collapse. May-Grünwald stain is a solution of methylene blue eosinate in methyl alcohol. Giemsa stain is a solution of methylene azure eosinate in methyl alcohol. Azure of methylene is the oxidized version of methylene blue. Methylene blue/azure of methylene cations (basic dye) mix with eosin Y anions (acid dye) to form a salt. The salt is dissolved in methyl alcohol as an inactive solution. Contact with acidic or basic water causes colouring of the solutions via redox reactions. The cell cytoplasm and nucleus are stained with a pink and blue colour, respectively.

2.19. Statistical Analysis

EB populations did not follow a Gaussian distribution as determined by a Kolmogorov Smirnov test, and were subsequently analyzed using non-parametric methods. Significant variation among means within individual samples was assessed by one-way ANOVA, specifically a Kruskal Wallis test. Significant difference between the means of any two individual data sets within the same sample was determined by Dunns multiple comparison test. Significance between two data sets from different samples was assessed by a Mann Whitney U test. Significance is depicted as *** $P \leq 0.001$, ** $P \leq 0.01$, * $P \leq 0.05$.

Chapter 3

3. Results

Aggregation Kinetics

3.1. Introduction

Much methodology currently exists with regards to EB formation encompassing a range of techniques (Kurosawa, 2007, Carpenedo et al., 2007). Each technique affects various properties of resultant EBs including size, stability, viability and density, but more importantly constituent ES cell differentiation. Previous studies have portrayed a direct link between the aggregation method and downstream ES cell differentiation (Ng et al., 2005, Burridge et al., 2007, Kim et al., 2007a, Gerecht-Nir et al., 2004). Consequently, research is now being heavily invested in the elucidation of how EB formation exhibits control over ES cell differentiation. However, due to a lack of standardized methodology, comparison between studies is convoluted and difficult to decipher. We hypothesize that by controlling early ES cell-ES cell interaction and aggregation, ES cell differentiation within resultant EBs can be efficiently and effectively directed towards desired cell types. The controlled generation of specific cell types in potentially homogeneous populations is a crucial step in the advancement of ES cell research from the laboratory to clinical application (Karlsson et al., 2008, Zweigerdt et al., 2003). Controlled ES cell-ES cell interaction could allow

for more detailed investigation of variables affecting EB formation and ES cell differentiation which may have previously not been identified or quantified. These variables include constitutive ES cell number, cell-cell attachment and signalling, resultant EB size, number and density, and aggregation time prior to the addition of exogenous biochemical cues (Koike et al., 2007, Dang et al., 2004). Here is shown how a non-cytotoxic modification to the cell surface which is then biotinylated and cross-linked with avidin, provides control over ES cell-ES cell aggregation and subsequent EB formation. This proposed methodology is reliable, repeatable and robust, and has the potential to be expanded to an industrial scale.

3.2. Methods and Materials

3.2.1. Engineered Aggregation and Avidin

The effect of avidin concentration on EB formation and incorporation within the EB structure was investigated. Both engineered and control ES cells were seeded into mass suspension over a range of densities (5×10^4 to 1×10^6 cells/mL). Suspensions were then rotated for 6hrs at 15rpm with 5, 10, 20, 50 and 80μg/mL exogenously added avidin. Control samples were rotated without avidin. ES cell suspensions were cultured for 24hrs prior to EB measurements. Avidin incorporation was visualised by fluorescence microscopy looking for avidin-FITC. Duplicate ES cell suspensions over the same seeding density range were rotated for 6hrs at 15rpm and incubated for 48hrs with 10μg/mL avidin-FITC conjugate. After 24 and 48hrs incubation, EBs were washed thoroughly with room temperature PBS to remove any unbound avidin-FITC from suspension, and imaged at ex/em of 495/515nm on a stereo-microscope (Nikon SMZ1500) with Nikon Digital Sight DS-L1.

3.2.2. Particle Sizing System

To investigate the effect of rotation speed on ES cell aggregation and EB formation, both engineered and control ES cells were seeded into mass suspension and rotated at 5, 10, 15, 20, 25 and 30rpm for the first 6hrs of 24hrs incubation. Control samples were left stationary for the first 6hrs. Rotation was applied only for the first 6hrs to encourage cell-cell interactions and aggregation of individual EBs. Observations revealed that suspensions rotated beyond 6hrs began to show inter-EB adhesion. After incubation, EB formation was quantified by high throughput analysis afforded by Particle Sizing System (PSS) analysis.

After aggregation, the whole sample suspension was carefully transferred to a 15mL Falcon tube so as to minimize EB disruption and fragmentation. The suspension was kept at room temperature whilst remaining suspensions were transferred. Suspensions were made to a volume of 10mL with PBS. The glass holding vial of a PSS (Accusizer™ 780A Autodiluter^{PAT}, PSS.NICOMP, California U.S.A.) was washed through with 50mL aliquots of dH_2O. Once the PSS measured ≤ 5 particles/second dH_2O was allowed to drain until the last few millilitres so as to not allow air bubbles to enter the measuring chamber. A 50mL aliquot of PBS (inclusive of 2mL SCM) was poured into the glass holding vial and analyzed using accompanying software (CW780md Version 1.55). Measurements provided blank controls to be subtracted from sample measurements. Individual sample suspensions were subsequently poured into the glass holding vial, one at a time. The volume was made to 50mL with PBS and gently stirred for 10secs then analyzed. Between each sample suspension the glass holding vial was washed through continuously with dH_2O until the PSS measured ≤ 5 particles/sec.

3.2.3. Mitomycin C Toxicity

To investigate the toxicity of MMC, ES cells were incubated for 2hrs with a range of MMC concentrations (0.001, 0.005, 0.01, 0.05 and 0.1mg/mL). ES cell viability was assessed by Alamar Blue assay (Chapter 2). ES cells incubated with 0.001, 0.01 and 0.1mg/mL were seeded onto a SNL feeder layer in SCM for continuous culture. After 1hr and 60hrs incubation, ES cells were imaged for colony formation and ES cell viability was assessed by live/dead™ stain (Chapter 2).

3.2.4. Embryoid Body Formation

Engineered and control ES cells were seeded at 0.05, 0.1, 0.25, 0.5, 0.75 and 1 x 10^6 cells/mL in mass suspension and rotated between 0 and 30rpm for the first 6hrs of a 24hr period. Only data from the lowest (5 x 10^4 cells/mL) and highest (1 x 10^6 cells/mL) seeding densities is shown, highlighting major differences with relation to initial seeding density. After every 4hrs, ES cell suspensions were photographed to assess EB formation. EBs were observed in both engineered and control suspensions after 6hrs rotation. All subsequent experiments involved an initial rotational period of 6hrs. To assess EB formation further and surface cell morphology, EBs after 1, 3 and 5 days incubation were imaged using SEM (Chapter 2).

3.2.5. Embryoid Body Quantification

A 0.25cm square grid was printed onto an acetate sheet. Discs were cut from the sheet to match the well size of a 6 well plate (2cm diameter circle) and externally adhered in identical orientations prior to seeding of ES cell suspensions. Three squares spanning the well in a diagonal line were marked on each grid in the same locations.

ES cell suspensions were seeded into 6 well plates and cultured for a period of 9 days. At each time point plates were removed from incubation, gently agitated to homogenize EB suspensions and viewed using a Nikon Eclipse TS100 microscope at 10x magnification. All EBs observed within the three squares were counted and measured using the attached imaging screen and Nikon Digital Sight DS-L1 imaging software. EB diameter was measured between the sides closest to one another across the EB centre to reduce the error of measuring two connected EBs. An average of EB number and diameter was calculated for all EBs falling within the

three sample squares. Plates were then placed back into incubation ready for the next time point. EBs were counted and measured over time and seeding density in both engineered and control ES cell samples. Duplicate samples using mitotically inactivated ES cells were also measured using this method.

Initial aggregation formed randomly orientated ES cell clusters which later reorganized to form compact EBs. Compact EBs appeared to have a diameter ≥ 40μm. Consequently, ES cell clusters with a diameter < 40μm were not included within EB measurements. Previous studies have also encountered the issue of when to call an ES cell aggregate and EB, and have defined an EB as having a diameter ≥ 40μm and ES cell aggregates with diameter < 40μm defined as primitive EBs (Carpenedo et al., 2007).

3.2.6. Aggregation and Cell Populations

3.2.6.1. Numbers of Cells in Sample Suspension

Multiple samples were prepared to provide one per time point. At each time point EB suspensions were transferred to a 15mL Falcon tube and centrifuged for 5mins at 1000rpm. Supernatant was removed and pellets were suspended in 5mL PBS. Suspensions were centrifuged a second time and the DNA content of the pellets was assessed by Hoescht assay. Cell number was calculated from fluorescence readings using a standard curve (Fig 3.1).

3.2.6.2. Numbers of Cells within Embryoid Bodies

Suspensions were washed through a 40μm cell strainer (Falcon) with 5mL PBS. Flow-through was collected in a 50mL Falcon tube and centrifuged for 5mins at 1000rpm. Supernatant was removed and the DNA content of resultant pellets was

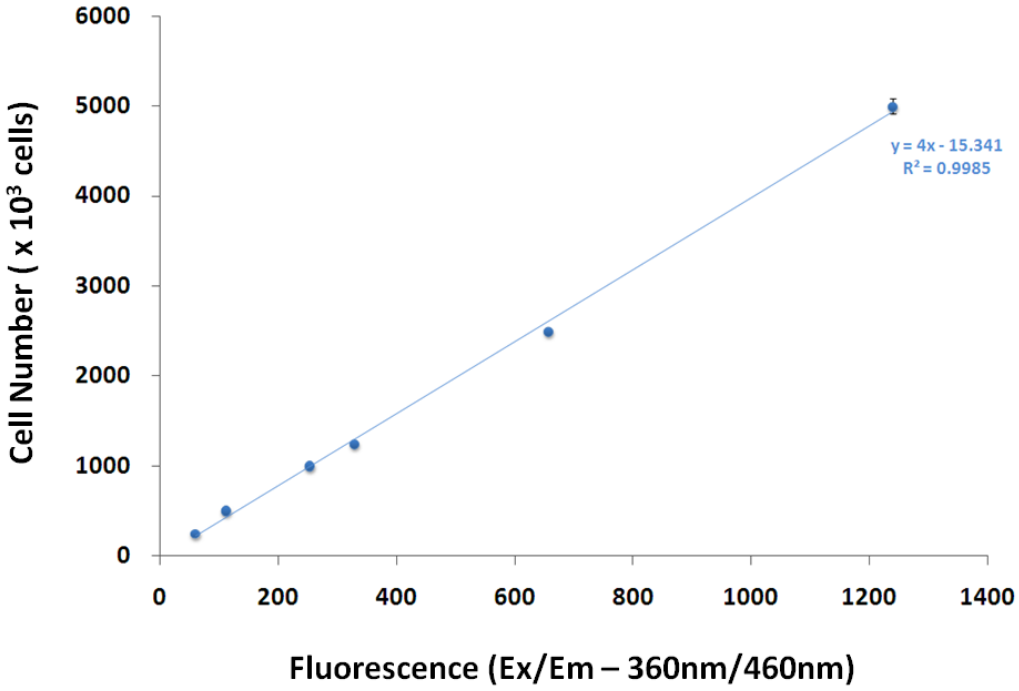

Figure 3.1: Standard curve of fluorescence against cell number using Hoescht assay. ES cells were trypsinized from continuous culture flasks into suspension and cell number quantified by haemocytometer-based cell count. 250, 500, 1000, 1250, 2500 and 5000 x 10^3 cells were treated with papain solution at 60°C overnight and DNA content was quantified the following day by Hoescht assay. The experiment was repeated in triplicate and each experiment consisted of 3 fluorescence measurements; *n* = 9. Error bars = S.E.M.

assessed by Hoescht assay. Fluorescence readings were converted to cell numbers using a standard curve (Fig 3.1). Cells and clusters smaller than 40μm were washed through the filter leaving behind EBs. 'Cells within the whole sample' minus 'cells washed through the filter' gave a representative number of cells within EBs.

3.3. Results: Critical Factors

3.3.1. Avidin Cross-linker

3.3.1.1. Avidin Incorporation

Avidin-FITC was clearly visibly spread throughout the structure of both engineered and control EBs, indicated by fluorescence when observed under an epi-fluorescent microscope (Fig 3.2). Fluorescence within engineered EBs was speckled and not uniformly distributed (Figs 3.2A and C). Conversely, fluorescence within control EBs did appear uniformly distributed (Figs 3.2B and D). Samples incubated for 48hrs exhibited greater amounts of fluorescence than those incubated for 24hrs. Engineered EBs within Figs 3.2E and G, cultured without avidin-FITC conjugate, were smaller in size than equivalent control EBs in Figs 3.2F and H. The lack of fluorescence observed in Figs 3.2E, F, G and H revealed that EBs themselves did not auto-fluoresce. Therefore, any fluorescence observed was due solely to exogenous avidin-FITC conjugate.

3.3.1.2. Avidin Concentration

Engineered EBs were significantly ($P \leq 0.001$) larger in size than corresponding control EBs at 5×10^4 cells/mL and 1×10^6 cells/mL over a range of avidin concentrations (Figs 3.3A and B). Interestingly, similar sized EBs were observed at low avidin concentration of 5μg/mL as what were observed at high avidin concentration of 80μg/mL. Engineered EBs were significantly ($P \leq 0.001$) smaller in size without exogenous avidin at low seeding density (Fig 3.3A) demonstrating the importance of avidin for engineered ES cell aggregation, and that natural aggregation

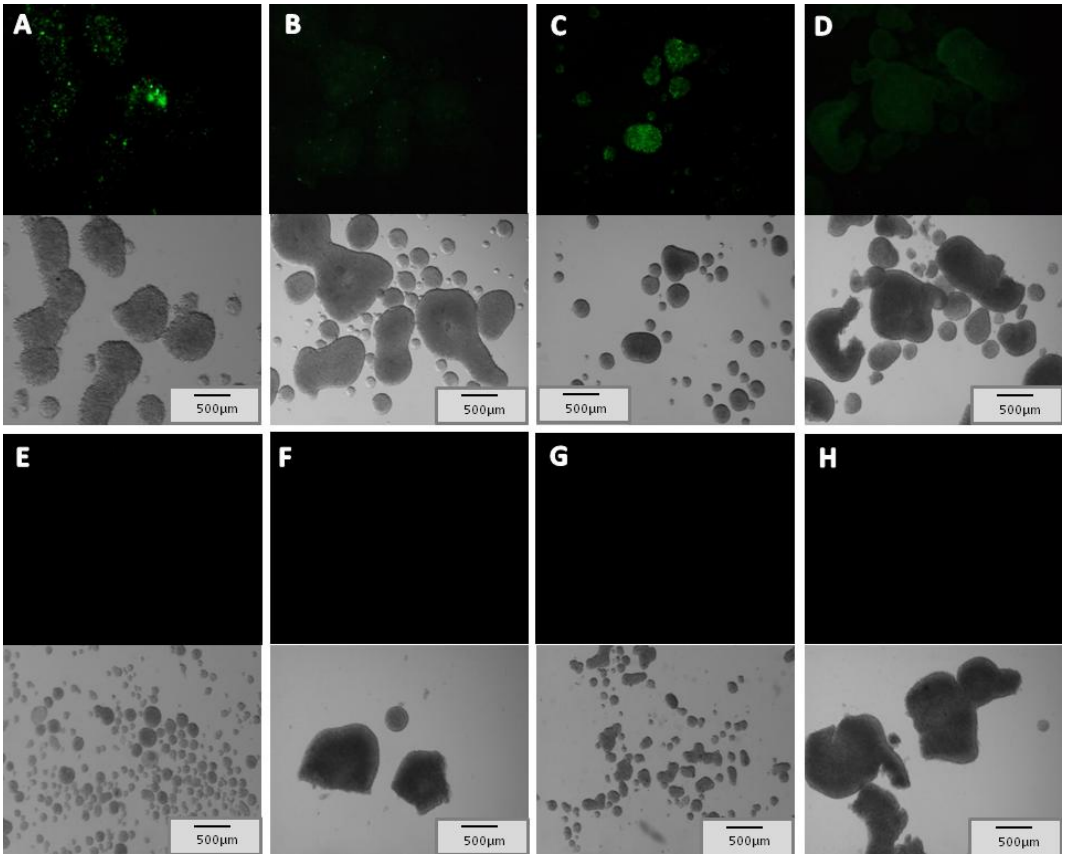

Figure 3.2: Avidin-FITC conjugate incorporation within engineered and control EBs. Engineered (A, C, E and G) and control ES cells (B, D, F and H) were rotated at 15rpm for the first 6hrs of a 24hr (A, E, B and F) and 48hr (C, G, D and H) incubation period. Both engineered and control EBs were incubated in SCM supplemented with 10µg/mL avidin-FITC conjugate (A to D) or SCM without avidin-FITC conjugate (E to H). All images were of ES cells seeded at 1 x 10^6 cells/mL. Both brightfield and fluorescence (ex/em - 495/515nm) images were taken at each time point. Scale bar measures 500µm.

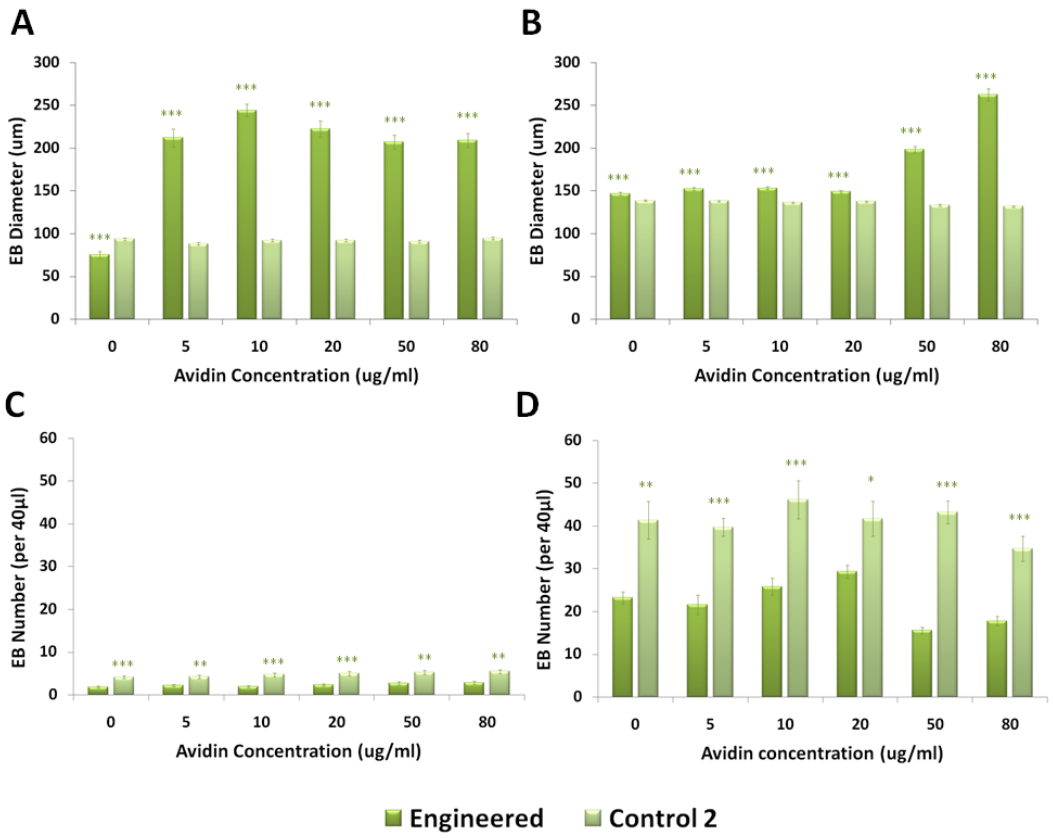

Figure 3.3: ES cell aggregation and EB formation over a range of avidin concentrations. Engineered and control 2 ES cells were seeded into mass suspension in SCM supplemented with exogenous avidin over a range of concentrations (0 to 80µg/mL) at 5 x 10^4 cells/mL (A and C) and 1 x 10^6 cells/mL (B and D). Suspensions were then rotated at 15rpm for the first 6hrs of a stationary 24hr incubation period. Suspensions were subsequently sampled and analyzed for average EB diameter (A and B) and EB number (C and D). Engineered and control 1 ES cells were also incubated without exogenous avidin, shown in all graphs at 0µg/mL. When calculating mean EB number, *n* = 9. When calculating mean EB diameter, *n* ranges from 16 to 49 (5 x 10^4 cells/mL) and *n* ranges from 140 to 415 (1 x 10^6 cells/mL). *** $P \leq 0.001$, ** $P \leq 0.01$, * $P \leq 0.05$. Error bars = S.E.M.

may be temporarily hindered by engineering. However, engineered ES cells without exogenous avidin at 1 x 10^6 cells/mL aggregated to form EBs of equivalent size to those with exogenous avidin (Fig 3.3B). Avidin concentration had no effect on control 2 EB diameters at either seeding density. No significant differences were observed between different control EBs cultured with and without avidin (Fig 3.3A and B). Avidin concentration also had no significant effect on engineered ES cell aggregation at low seeding density. However, at 1 x 10^6 cells/mL engineered EBs were significantly ($P \leq 0.001$) larger when cultured with avidin ≥ 50μg/mL, indicating a potential threshold concentration of avidin required to efficiently aggregate 1 x 10^6 cells/mL (Fig 3.3B).

EB numbers were significantly ($P \leq 0.001$) reduced at 5 x 10^4 cells/mL, concurrent with the idea of more ES cells available for aggregation more EBs can be formed (Fig 3.3C). Significantly ($P \leq 0.05$) more control EBs were observed at both seeding densities. Avidin concentration had no significant effect on EB number in both engineered and control samples. However, there was a significant ($P \leq 0.05$) decrease in engineered EB number at 1 x 10^6 cells/mL when incubated with avidin ≥ 50μg/mL (Fig 3.3D).

3.3.2. Rotation Speed

Engineered and control ES cells were seeded at 5 x 10^4 and 1 x 10^6 cells/mL (Figs 3.4A and B, respective) and either left stationary or rotated for 6hrs at 5 to 30rpm with increasing increments of 5. After 6hrs of rotation the suspensions were left stationary overnight and analyzed using PSS. Greater numbers of EBs were observed at 1 x 10^6 cells/mL over all rotation speeds investigated until speed reached 30rpm. At 30rpm individual EBs adhered to one another and resulted in mass agglomeration

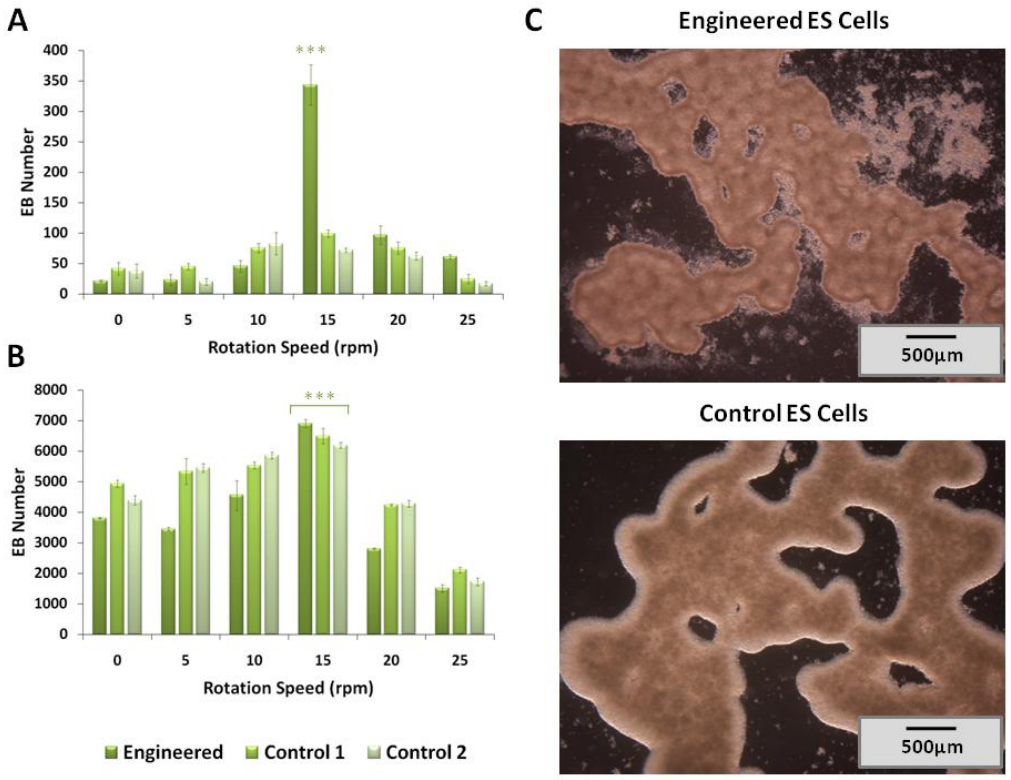

Figure 3.4: Effect of rotation speed on ES cell aggregation. ES cells were seeded at 5 x 10^4 cells/mL (A) and 1 x 10^6 cells/mL (B) into mass suspension, rotated between 0 and 30rpm for 6hrs and incubated for 24hrs to establish EB formation. EB suspensions were washed with PBS and analyzed using PSS to calculate average EB number. Cultures rotated at 30rpm resulted in mass agglomeration of ES cells and EBs (C) and were therefore not analyzed by PSS. Images were taken of cultures seeded at 1 x 10^6 cells/mL. Experiments were repeated in triplicate and each experiment consisted of 3 duplicate suspensions; *n* = 9. Error bars = S.E.M.

(Fig 3.4C). Both engineered and control EBs appeared to follow the same trend over rotation speed. Suspensions rotated at 15rpm formed the greatest number of EBs with a diameter ≥ 40μm. At 1 x 10^6 cells/mL engineered ES cells formed significantly ($P \leq 0.05$) less EBs than control ES cells (Fig 3.4B).

3.3.3. Mitomycin C Concentration

A range of MMC concentrations from 0.001 to 0.1% were investigated and their effect on sustained ES cell culture assessed. Confluent ES cells were removed from feeder layers and treated with MMC solution for 2hrs prior to re-seeding. Increasing MMC concentration directly resulted in decreased ES cell viability (Fig 3.5J). At the lowest concentration of 0.001%, ES cells continued to proliferate and form colonies (Figs 3.5A and D). At the highest concentration of 0.1%, most ES cells had detached from the feeder layer and floated into a single cell suspension, indicative of cell death (Figs 3.5C and F). ES cells treated with 0.01% MMC solution neither proliferated nor detached from the feeder layer (Figs 3.5B and E). Figs 3.5G to I revealed remaining cells adhered to the feeder layer were viable. The green fluorescence in Fig 3.5I was possibly due to the underlying SNL feeder layer with only a few remaining viable ES cells.

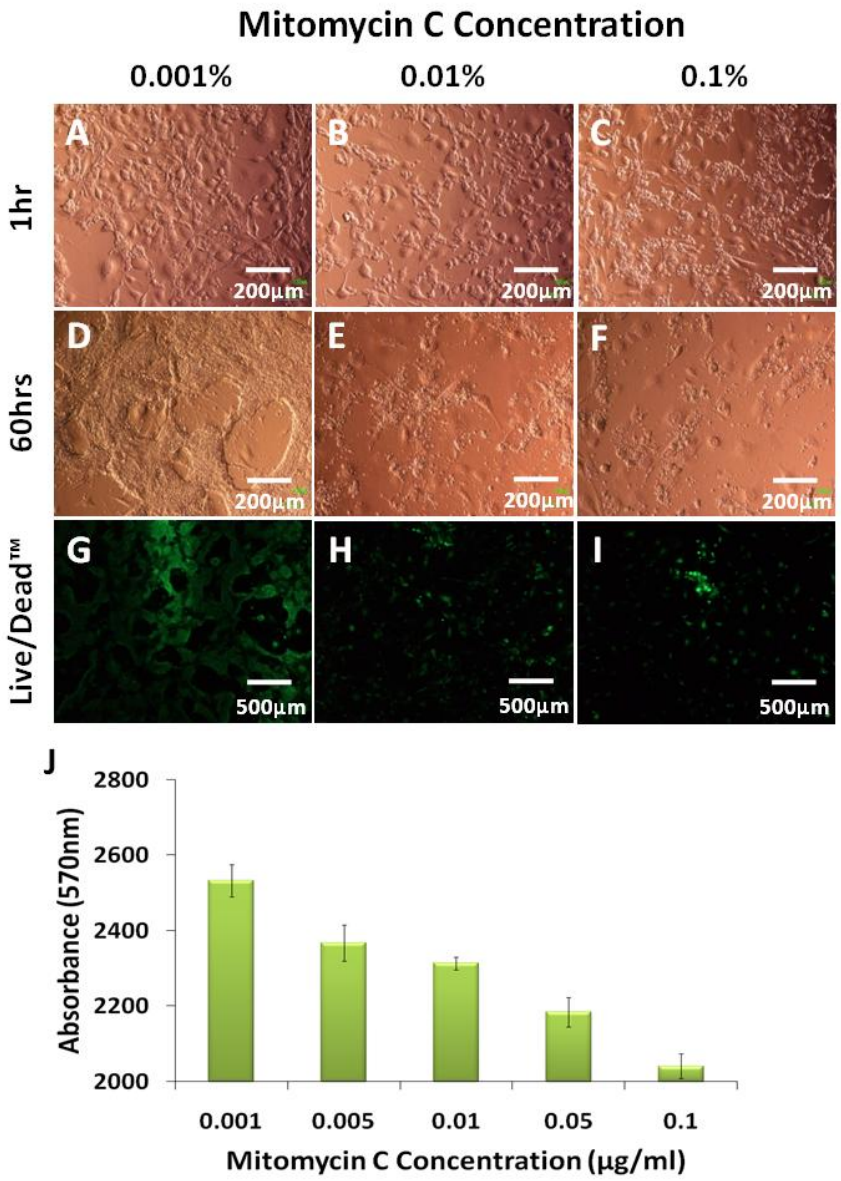

Figure 3.5: Effect of MMC concentration on ES cell viability. ES cells were incubated at 37°C and 5% CO_2 in a humidified atmosphere with a range of MMC concentrations (0.001, 0.005, 0.01, 0.05 and 0.1µg/mL) for 2hrs. Cell viability was assessed by metabolic activity via Alamar Blue assay (J). ES cells from duplicate cultures were passaged after MMC treatment onto fresh SNL feeder layers and cultured for up to 60hrs. Efficient mitotic inactivation was assessed by absence of colony formation (A to F). Viability of ES cells adhered to the feeder layer was also assessed by Live/Dead™ stain (G to I). *n* =9. Error bars = S.E.M.

3.4. Results: Aggregation

3.4.1. Embryoid Body Formation

3.4.1.1. Aggregation Time

Engineered and control ES cells were both seeded over a range of densities. Fig 3.6A shows images of ES cell suspensions seeded at 5 x 10^4 cells/mL. ES cells were seeded into suspension and rotated at 15rpm continuously for 12hrs. At 1hr both engineered and control samples appeared as single cell suspensions, and at 12hrs both had formed large EBs (Fig 3.6A). Engineered ES cells had aggregated to form initial EBs resembling loose clusters after just 4hrs of incubation which later appeared as tightly packed structures after 8hrs. Control ES cells began to show signs of aggregation after 8hrs and tightly packed structures resembling EBs after 12hrs.

3.4.1.2. Cell Morphology

Engineered ES cells were seeded at 5 x 10^4 and 1 x 10^6 cells/mL and allowed to aggregate for 5 days in SCM. Resultant EBs were removed from suspension and processed for SEM imaging after 1, 3 and 5 days (Fig 3.6B). ES cells seeded at 5 x 10^4 cells/mL after 1 day formed randomly orientated ES cell aggregates. These early aggregates resembled loose clusters of ES cells rather than tightly packed cell structures. They also exhibited a rough and uneven surface morphology. ES cell aggregates seeded at 1 x 10^6 cells/mL after 1 day appeared as tightly packed cell clusters exhibiting a smooth and uniform surface morphology. After 5 days of aggregation, ES cells at both seeding densities had formed tightly packed EBs similar

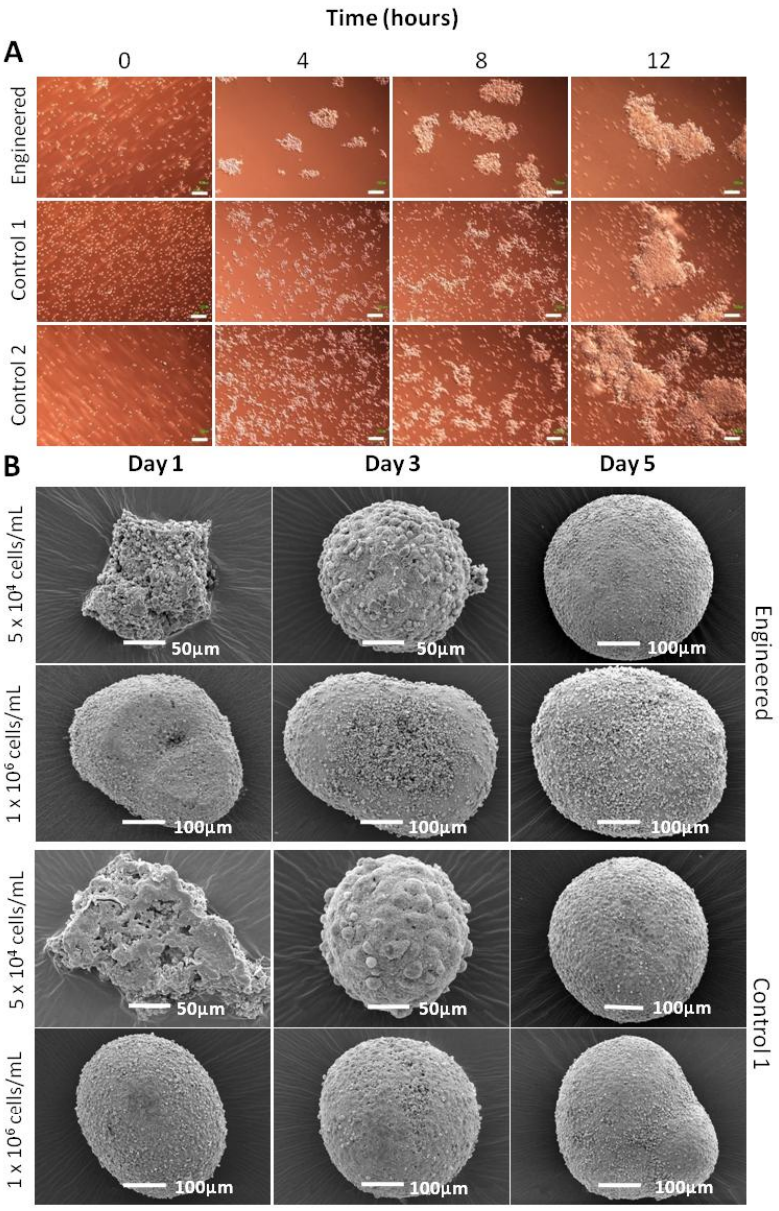

Figure 3.6: Effect of engineering on ES cell aggregation and EB formation. Engineered and control ES cells were seeded into mass suspension at 5 x 10^5 cells/mL and continuously rotated for 12hrs. Brightfield images were taken of the suspensions every 4hrs (A). Scale bars in Fig A measure 100µm. Engineered and control 1 ES cells were seeded into mass suspension at 5 x 10^4 and 1 x 10^6 cells/mL, rotated at 15rpm for 6hrs and cultured for 5 days. EB surface morphology was analyzed by SEM after 1, 3 and 5 days aggregation (B).

in surface morphology. EBs at 1 x 10^6 cells/mL after 1 day of aggregation resembled EBs seeded at 5 x10^4 cells/mL after 5 days of aggregation. This indicated an acceleration of ES cell aggregation with increased seeding density. Minimal difference was observed between engineered and control samples, indicating that engineering merely accelerates EB formation rather than altering the mode of aggregation.

3.4.2. Effect of Engineering on Embryonic Stem Cell Aggregation

Fig 3.7 shows ES cell aggregation over 9 days of aggregation at 5 x 10^4 cells/mL and 1 x 10^6 cells/mL. Engineered ES cells formed EBs with significantly ($P \leq 0.001$) larger diameter than control EBs at 5 x 10^4 cells/mL (Fig 3.7A). EBs continued to increase in diameter over time indicating cell proliferation and sustained aggregation. Control EBs at 5 x 10^4 cells/mL did not significantly increase in diameter over 9 days of culture. At 1 x 10^6 cells/mL the difference between engineered and control EB diameters was insignificant (Fig 3.7B). Consequently, the positive effect of engineering on ES cell aggregation was lost with increasing seeding density. Fig 3.7B depicted a significant ($P \leq 0.001$) increase in both engineered and control EB diameters at 1 x 10^6 cells/mL. Therefore, at 1 x 10^6 cells/mL engineered and control EBs exhibited continued ES cell proliferation and aggregation.

3.4.3. Effect of Mitotic Inactivation on Embryoid Body Formation

Engineered ES cells formed EBs of a significantly ($P \leq 0.05$) larger diameter than control ES cells at 5 x 10^4 cells/mL (Fig 3.8A). This was concurrent with findings in Fig 3.7 indicating mitotic inactivation did not detrimentally affect the ability of ES cells to be engineered. However, EB augmentation via engineering was not observed when ES cells were seeded at 1 x 10^6 cells/mL (Fig 3.8B). Both engineered and

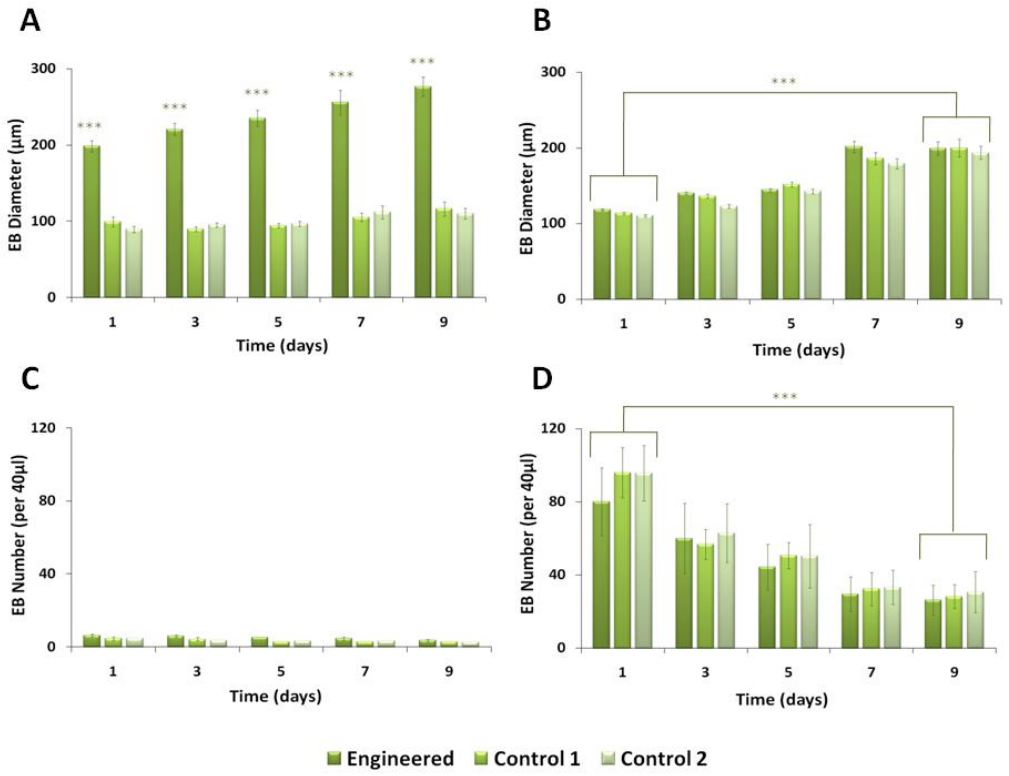

Figure 3.7: Effect of engineering on ES cell aggregation and resultant EB diameter and number. Engineered and control ES cells were seeded into mass suspension at 5 x 10^4 cells/mL (A and C) and 1 x 10^6 cells/mL (B and D) in SCM with or without avidin supplementation of 10µg/mL. Cell suspensions were rotated ay 15rpm for 6hrs then cultured for a period of 9 days at 37°C and 5% CO_2 in a humidified atmosphere. Mean EB diameter (A and B) and number (C and D) were calculated after 1, 3, 5, 7 and 9 days of aggregation. Experiments were repeated in triplicate, and in each experiment all EBs within 3 representative areas were quantified. When calculating mean EB number, *n* = 3. When calculating mean EB diameter, *n* ranged from 9 to 19 (5 x10^4 cells/mL) and 79 to 288 (1 x 10^6 cells/mL). *** P ≤ 0.001, ** P ≤ 0.01, * P ≤ 0.05. Error bars = S.E.M.

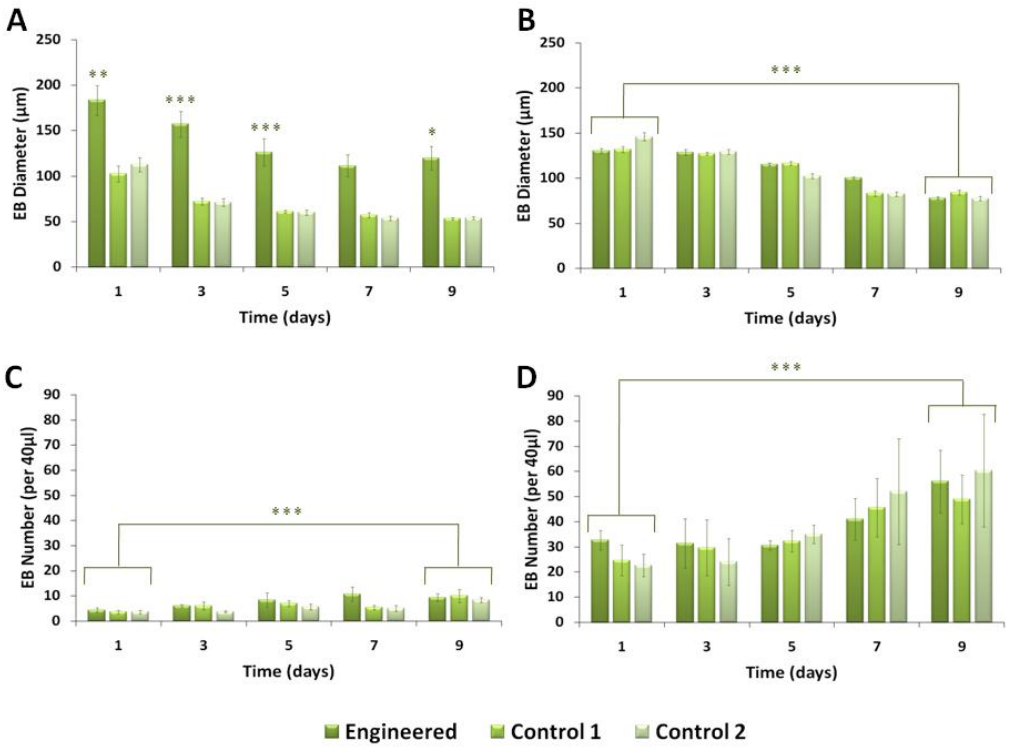

Figure 3.8: Effect of engineering on MMC treated ES cell aggregation and resultant EBs. Engineered and control ES cells were treated with 0.01% MMC solution for 2hrs prior to seeding into mass suspension at 5 x 10^4 cells/mL (A and C) and 1 x 10^6 cells/ mL (B and D). ES cell suspensions were rotated at 15rpm for 6hrs prior to 9 days incubation at 37°C and 5% CO_2 in a humidified atmosphere in SCM with or without avidin supplementation of 10µg/mL. Mean EB diameter (A and B) and number (C and D) were calculated after 1, 3, 5, 7 and 9 days aggregation. Experiments were repeated in triplicate. When calculating mean EB number, *n* = 3. When calculating mean EB diameter, *n* ranged from 11 to 32 (5 x 10^4 cells/mL) and 68 to 181 (1 x 10^6 cells/mL). *** P ≤ 0.001, ** P ≤ 0.01, * P ≤ 0.05. Error bars = S.E.M.

control EBs exhibited a significant ($P \leq 0.001$) decrease in diameter over 9 days of incubation. Engineered EBs maintained a significant ($P \leq 0.001$) difference in diameter to control EBs over the 9 days of culture. EB number increased significantly ($P \leq 0.001$) as their diameter decreased, at both 5×10^4 and 1×10^6 cells/mL (Figs 3.8C and D). No significant difference in EB number between engineered and control EBs was observed.

3.4.4. Effect of Engineering on Cell Populations

3.4.4.1. Cells in Suspension

Figs 3.9A and B show the number of cells in suspension over 9 days of culture in both engineered and control samples seeded at 5×10^4 cells/mL and 1×10^6 cells/mL, respectively. There was a significant ($P \leq 0.001$) decrease in the number of cells in suspension over the 9 day culture period at 5×10^4 cells/mL (Fig 3.9A). The number of cells in suspension at 1×10^6 cells/mL showed no significant change during 9 days of culture. The number of engineered cells in suspension was significantly ($P \leq 0.001$) less than the numbers of control cells at 5×10^4 cells/mL. However, the number of engineered cells in suspension showed no significant difference to the number of control cells in suspension after 5 days of culture (Fig 3.9A). There was no significant difference between the numbers of engineered and control cells in suspension over the 9 day culture period at 1×10^6 cells/mL (Fig 3.9B).

3.4.4.2. Cells Constituting Embryoid Bodies

At 5×10^4 cells/mL, the number of cells constituting engineered EBs was significantly ($P \leq 0.001$) greater than the number of cells constituting control EBs (Fig 3.9C). Therefore, engineered EBs consisted of more cells than control EBs indicating

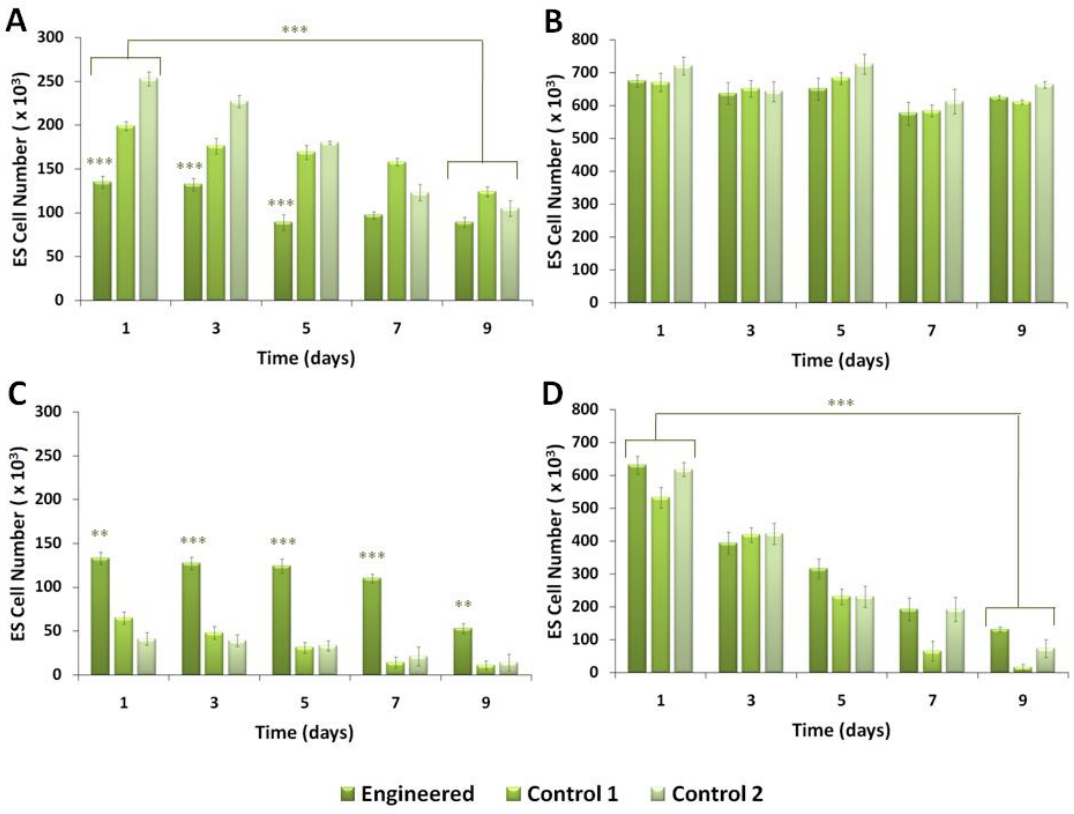

Figure 3.9: Effect of engineering on cell populations during aggregation. ES cells were seeded into mass suspension at 5 x 10^4 cells/mL (A and C) and 1 x 10^6 cells/mL (B and D). Cell suspensions were rotated at 15rpm for 6hrs prior to 9 days in culture at 37°C and 5% CO_2 in a humidified atmosphere. After 1, 3, 5, 7 and 9 days, suspensions were filtered through a 40µm sieve. Cell numbers washed through the sieve were quantified by Hoescht assay, representing the proportion of cells not constituting EBs (A and B). Duplicate samples were also analyzed after 1, 3, 5, 7 and 9 days without prior filtering; cell numbers were quantified by Hoescht assay. Flow-through cell numbers were subtracted from total suspension cell numbers to give constituent cell number within EBs (C and D). Experiments were performed in triplicate and each experiment consisted of 3 repeat measurements. *n* = 9. *** P ≤ 0.001, ** P ≤ 0.01, * P ≤ 0.05. Error bars = S.E.M.

enhanced cell- cell interaction and aggregation at 5 x 10^4 cells/mL. No significant difference was observed between the numbers of engineered and control cells in samples seeded at 1 x 10^6 cells/mL (Fig 3.9D). The number of cells in suspension in both engineered and control samples at 5 x 10^4 and 1 x 10^6 cells/mL significantly ($P \leq 0.001$) decreased between 1 and 9 days of culture.

3.5. Discussion

Ever since ES cells and their pluripotency were first discovered researchers have endeavoured to control their differentiation using a plethora of *in vitro* methodology. However, directed differentiation remains highly inefficient with the formation of contaminating cell types resulting in heterogeneous populations. A general consensus between studies is the use of EB formation for ES cell differentiation (Hamazaki et al., 2004). An EB comprises ES cells which adhere to one another to form a 3D cluster. ES cells then produce ECM which stabilizes and cements the 3D structure. Close proximity between ES cells causes differentiation, along with exogenously added growth factors (Mohr et al., 2006). However, there is currently a distinct lack of standardisation for EB formation (Kurosawa, 2007). It has been repeatedly documented that methodology used to produce EBs has a direct effect on ES cell differentiation and consequently on their potential clinical application (Fig 1.4) (Rathjen et al., 1998). This lack of standardisation and consequent variability in ES cell differentiation makes comparison between studies immensely difficult. Here is proposed a simple, repeatable and reliable chemical process involving cell surface engineering and intercellular cross-linking, for the efficient production of EBs using the mass suspension method (De Bank et al., 2007, De Bank et al., 2003).

3.5.1. Investigation of Critical Factors

Prior to investigating the effect of chemical modification on ES cell aggregation and EB formation in mass suspension, certain variables were analysis tested. These variables included avidin concentration, rotation speed and MMC concentration.

3.5.1.1. Avidin Concentration and Embryoid Body Formation

ES cells were incubated with avidin-FITC conjugate to investigate avidin incorporation (Fig 3.2). Avidin was incorporated within the EB structure. However, fluorescence was speckled within engineered EBs and uniform within control EBs. Speckled fluorescence was most likely the result of accumulated avidin-FITC conjugate specifically located at ES cell-ES cell cross-links within the engineered EB structure. Alternatively, speckling could simply have been due to cell dense regions (Fig 3.2A). The uniform fluorescence observed in control EB samples was indicative of non-specific binding of avidin and/or physical entrapment between ES cells and ECM (Fig 3.2B). Similar observations were made after 48hrs incubation between engineered and control samples (Figs 3.2C and D, respectively). Fluorescence was still observed showing persistence of avidin-FitC within the EB.

To investigate the effect of avidin on ES cell aggregation, engineered and control ES cells were incubated with varying concentrations ranging from 0 to 80μg/mL (Fig 3.3). Control ES cells incubated with and without avidin formed EBs of equal diameter, at 5 x 10^4 and 1 x 10^6 cells/mL (Figs 3.3A and B). Increasing the concentration of exogenous avidin therefore had no significant effect on control EB diameter, indicating non-specific binding of avidin. Engineered ES cells formed significantly ($P \leq 0.001$) larger EBs than control samples at 5 x 10^4 cells/mL, but showed no significant difference over avidin concentration (Fig 3.3A). This shows the importance of engineering, since large EBs can be produced with minimal levels of exogenous avidin. However, without avidin engineered ES cells formed significantly ($P \leq 0.001$) smaller EBs than control samples. Engineering may therefore have had a negative or inhibitory effect on natural ES cell adhesion. If so,

engineering provides precise control over EB formation as ES cell-ES cell interaction can only occur upon addition of exogenous avidin.

At 1 x 10^6 cells/mL, engineered ES cells formed EBs of equal diameter whether incubated with or without exogenous avidin (Fig 3.3B). The fact that engineered ES cells formed EBs without exogenous avidin demonstrated that they could still aggregate through natural adhesion. High ES cell density increased the occurrence of ES cell-ES cell collisions and subsequent interactions within the given suspension volume generating EBs of equivalent diameter to those incubated with avidin. Engineered EBs significantly ($P \leq 0.001$) increased in diameter when avidin concentration reached ≥ 50μg/mL (Fig 3.3B). At this concentration there may have been a sufficient amount of avidin in ratio to engineered ES cells to cause measurable enhancement of ES cell-ES cell interaction and adhesion. Alternatively, the high concentration of avidin may have enabled or enhanced EB agglomeration. EB agglomeration is discussed later, but the increase in EB diameter correlated with a significant ($P \leq 0.001$) decrease in EB number at 1 x 10^6 cells/mL (Fig 3.3D). The same increase in EB diameter and decrease in EB number was not observed at 5 x 10^4 cells/mL (Figs 3.3A and C). 10μg/mL avidin was chosen as the ideal working concentration for all subsequent experiments.

3.5.1.2. Rotation Speed and Embryoid Body Formation

The second variable which required analysis was rotation speed. To investigate the effect of rotation on ES cell aggregation, a range of speeds were investigated in comparison to stationary culture. Suspensions rotated at 15rpm generated the most EBs with a diameter ≥ 40μm (Figs 3.4A and B). At 5 x 10^4 cells/mL engineered ES cell suspensions rotated at 15rpm generated more EBs than control ES cell suspensions.

Rotation ≤ 15rpm increased chance collisions resulting in ES cell-ES cell interaction and EB formation. Above 15rpm rotation became too vigorous and disrupted ES cell-ES cell interactions. Also, increased kinetic energy could have caused inter-EB collisions resulting in EB fragmentation into < 40μm diameter ES cell clusters. However, this seems unlikely since increasing the rotation speed to 30rpm generated EBs which had mass agglomerated in both engineered and control samples (Fig 3.4C).

There was a significant ($P \leq 0.001$) decrease in both engineered and control EBs formed in stationary cultures. However, EBs still formed demonstrating that rotation was not essential to, but enhanced EB formation. Engineered EBs showed no significant difference in diameter to control EBs without rotation. It is difficult to say whether EBs in stationary culture resulted from ES cell aggregation alone or simply proliferation and adhesion between daughter cells. 15rpm was chosen as the optimum rotation speed for all subsequent experiments.

3.5.1.3. Mitomycin C Concentration and Embryonic Stem Cell Viability

A third variable that required analysis was MMC concentration. A series of concentrations were investigated ranging from 0.001 to 0.1%. After 60mins incubation in Alamar Blue solution, ES cell metabolic activity was found to decrease with increasing MMC concentration (Fig 3.5J). However, ES cells remained viable, so prolonged culture after MMC treatment was investigated. After 60hrs incubation ES cells had proliferated to form distinct colonies, showing that ES cells were not mitotically inactivated after treatment with 0.001% MMC (Fig 3.5D). ES cells treated with 0.1% MMC solution did not form colonies due to cytotoxic effects and cell death. Few ES cells remained adhered to the feeder layer as many had dissociated and

floated into suspension (Fig 3.5F). ES cells treated with 0.01% MMC were viable and mitotically inactivated, as indicated by attached ES cells but absence of colony formation (Fig 3.5E).

3.5.2. Embryonic Stem Cell Aggregation

3.5.2.1. Embryoid Body Formation

To investigate EB formation the first step was to assess rotation time required to initiate ES cell aggregation (Fig 3.6). Evidently, engineered ES cells formed aggregates after only 4hrs, demonstrating accelerated aggregation (Fig 3.6A). Control ES cells formed aggregates after 8hrs incubation, taking up to twice as long. After 12hrs incubation both engineered and control aggregates appeared to have formed dense, compacted EB structures. This may be the result of simple restructuring and/or constituent ES cell proliferation. Consequently, initial rotation phase was defined as 6hrs.

Aggregation occurs through the random collisions of ES cells in suspension which result in ES cell-ES cell interaction and adhesion. These collisions produce small loosely packed clusters of ES cells, which initially exhibited a rough surface morphology and uneven structure after 1 day at 5 x 10^4 cells/mL (Fig 3.6B) (Song et al., 2003). After 5 days, aggregation had progressed and tightly packed EB structures emerged exhibiting a smoother surface morphology and an organized spherical composition. It appeared that ES cells at 5 x 10^4 cells/mL aggregated rapidly and formed randomly oriented branched structures. These structures reorganized after 5 days into a less chaotic spherical orientation, possibly through compaction. The smooth surface morphology could be the effect of strained adhesion between surface ES cells. Surface ES cells encase central ES cells which continually proliferate

increasing the size of the core exponentially compared to the surface. This would have the effect of stretching the surface making it appear smooth. Alternatively, the smooth morphology was the result of spontaneous differentiation of surface ES cells. Surface cell morphology resembled cells of the primitive endoderm, found to occur in other studies (Fok and Zandstra, 2005).

EBs at 1 x 10^6 cells/mL exhibited a spherical composition and smooth surface morphology after just 1 day (Fig 3.6B). This may have been due to the elevated number of ES cells in suspension which increased the chance of ES cell-ES cell collisions, enabling accelerated EB formation. Similarity between engineered and control 1 samples merely indicated that engineered ES cells aggregated in an accelerated fashion, rather than a different mode of aggregation. However, engineered EBs did show signs of advanced compaction after 3 days at 5 x10^4 cells/mL compared to control 1 EBs (Fig 3.6B). It is therefore possible that analysis or surface morphology over shorter time intervals may help resolve differences between engineered and control EBs. Similar results were observed in control 2 samples (data not shown).

3.5.2.2. Engineered Embryonic Stem Cell Aggregation

Engineered ES cells formed EBs of a significantly ($P \leq 0.001$) larger diameter than control EBs at 5 x 10^4 cells/mL (Fig 3.7A). Engineered EBs continued to increase in diameter over time demonstrating that enhancement was not lost even though natural membrane renewal would have been active (Mahmutefendic et al., 2007, De Bank et al., 2007). This is to be expected as membrane recycling would not be able to break the avidin/biotin bond and internalize the modified sugar residues. However, enhancement was not observed at 1 x 10^6 cells/mL where engineered EBs were not

significantly larger than control EBs (Fig 3.7B). This could be due to the increased number of ES cells within the same volume. More ES cells would mean two things, increased chance of ES cell-ES cell collisions, and a reduced ratio of avidin to engineered ES cells. Therefore, limited avidin would reduce the size of engineered EBs, and increased collisions would enhance the size of control EBs. Also, engineered EBs may have been reduced in size due to inter-EB collisions and EB fragmentation before ES cell clumps had time to restructure and exhibit a stable spherical conformation (Sachlos and Auguste, 2008, Carpenedo et al., 2007).

Both engineered and control EBs increased in diameter over time at 1 x 10^6 cells/mL but not at 5 x 10^4 cells/mL. At 1 x 10^6 cells/mL more ES cells were available for aggregation which resulted in increased ES cell-ES cell collisions and interactions, adhesion and resultant EB growth. The increase in EB diameter over time indicated that the population of single ES cells in suspension at 1 x 10^6 cells/mL were inexhaustible. At 5 x 10^4 cells/mL, aggregation may have exhausted the limited number of available ES cells within 1 day, after which further aggregation became restricted or ceased. The lack of significant increase in diameter over time in control EBs indicated that ES cell proliferation contributed minimally to EB growth; constituent ES cells were actively proliferating but the EB was not significantly increasing in diameter.

There were no significant differences between the numbers of engineered and control EBs at 5 x 10^4 and 1 x 10^6 cells/mL (Figs 3.7C and D). This was concurrent with engineered and control EBs being of similar diameter at 1 x 10^6 cells/mL. However, at 5 x 10^4 cells/mL engineered EBs were significantly ($P \leq 0.001$) larger than control EBs (Fig 3.7A). If available ES cells in suspension were exhausted after 24hrs and the numbers of EBs were similar between samples, then logically,

engineered EBs should have been of similar diameter to control EBs. Engineered EBs may be larger in diameter due to internal structure and orientation of constituent ES cells (Karbanova and Morkry, 2002). Alternatively, the set number of ES cells within control samples generated a population of ES cell clusters with diameters measuring < 40μm. The number of ES cells tied up in these clusters may have accounted for the difference between engineered and control EB diameters and numbers. The number of EBs did not increase over time at 5 x 10^4 cells/mL, indicating there was no generation of new EBs. The hypothetical ES cell clusters with diameter < 40μm should have increased the number of control EBs over time as they themselves grew. However, as described earlier, proliferation rate of constituent ES cells over 9 days was insufficient to significantly increase EB diameter. Therefore, these clusters were still below the measurable diameter threshold of 40μm. ES clusters were not regarded as EBs due to a diameter < 40μm. Aggregates of ES cells have previously been identified as EBs when nucleated and cell dense (observed to occur in EBs with a diameter ≥ 40μm) (Bauwens et al., 2008, Zandstra et al., 1994, Chen et al., 2008).

In fact, the number of engineered and control EBs at 5 x 10^4 and 1 x 10^6 cells/mL significantly ($P \leq 0.001$) decreased over time (Figs 3.7C and D). A decrease in EB number can mean one of two things; EB fragmentation, which is unlikely since EBs increased in diameter, or EB agglomeration (Fig 3.10). EB agglomeration occurs when two individual EBs come into close proximity through chance collisions and interact. As with single ES cell-ES cell interactions, EB-EB interactions result in temporary adhesion. As constituent ES cells migrate and re-structure the two EBs begin to merge together (Carpenedo et al., 2007). Over time the two EBs become one larger EB via cohesion. EB agglomeration therefore raised problems concerning investigation of individual EB development. Growth of individual EBs was masked by

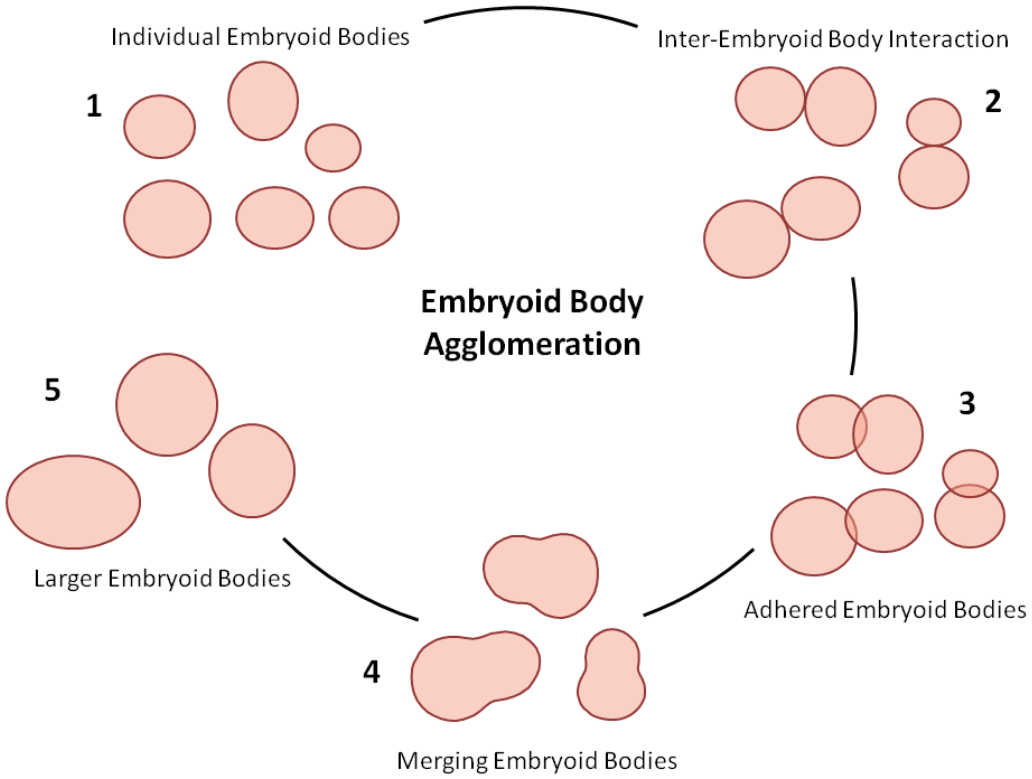

Figure 3.10: Inter-EB collision, cohesion and eventual agglomeration in mass suspension. Individual EBs free floating in mass suspension randomly collide with adjacent EBs resulting in inter-EB adhesion. Adhered EBs slowly reorganize during further cell proliferation and aggregation exhibiting a merged appearance. Eventually the two individual EBs are no longer distinguishable and exhibit a smooth spherical individual EB morphology. EB agglomeration results in decreased EB numbers and increased EB diameters.

EB cohesion interactions, and inter-EB signalling interfered with differentiation of ES cells within individual EBs. Studies have emerged described EB formation specifically targeted at minimizing EB agglomeration such as physical separation of EBs in separate compartments (Karp et al., 2007, Burridge et al., 2007, Moeller et al., 2008). However, EB agglomeration required a high number of EBs to have a significant effect on EB diameter and number measurements. Also, EB agglomeration was only observed when ES cell suspensions were rotated at 30rpm, and suspensions in Fig 3.7 were rotated at 15rpm. Since suspensions were stationary after the first 6hrs, it is unlikely that resultant EBs had sufficient kinetic energy to move around compared to rotated suspensions. Therefore, the observed decrease in EB number appeared to have been the result of fragmentation or dissociation due to cell death. The fact that EB diameter continued to increase even though EB number decreased was probably due to the fact that EB fragments or dissociated EBs were amalgamated into surviving EBs. Alternatively, the residual EB components were themselves < 40μm in diameter and thus not included within measurements, maintaining the average diameter. Consequently, this would leave measurements of thriving EBs unaffected. The increase also indicated that the population of single ES cells in suspension were not exhausted after 24hrs. Engineered EBs increased in size due to enhanced aggregation at 5 x 10^4 cells/mL (Fig 3.7A). Control EBs may have increased in size, but not at a measurable rate over the aggregation time period investigated, at 5 x 10^4 cells/mL. The increase in EB diameter at 1 x 10^6 cells/mL would therefore be an outcome of increased ES cell-ES cell interactions.

3.5.2.3. Aggregation of Mitotically Inactivated Embryonic Stem Cells

EB formation is the consequence of chance collisions between ES cells in suspension and resultant aggregation. However, EB growth is the result of continued ES cell aggregation *and* constituent ES cell proliferation. To investigate EB formation and growth as a direct result of ES cell aggregation, ES cell proliferation was removed. ES cells were mitotically inactivated with 0.01% MMC prior to engineering. Engineered EBs were significantly ($P \leq 0.05$) larger in diameter than control EBs at 5×10^4 cells/mL (Fig 3.8A). Since ES cells were non-proliferative this showed that ES cell proliferation played a minor role, if any, in EB growth. At 1×10^6 cells/mL enhancement was no longer observed. This was most likely due to the same reasons stated previously for aggregation of proliferating ES cells; avidin became a limiting factor as ES cell number increased and increased chance collisions accelerated control EB formation.

Evidently, engineered aggregation was not detrimentally affected by mitotic inactivation. However, EBs significantly ($P \leq 0.001$) decreased in diameter over time in both engineered and control suspensions despite change in seeding density (Figs 3.8A and B). Mitotically inactivated ES cells have a shorter lifespan than proliferating ES cells, accelerating constituent ES cell death. Consequently, dead ES cells would have separated causing the EB diameter to become diminished. Engineering simply provided a stronger interaction between ES cells than natural adhesion which only slowed observed EB dissociation.

Proliferation may not have contributed largely to EB growth but it appears that it had a major role to play in EB stability. Upon ES cell-ES cell collision a temporary bond is formed. This temporary bond becomes long term adhesion upon ECM production and deposition. Mitotically inactivated ES cells produce reduced amounts

of ECM (Occleston et al., 1997). Therefore, the lack of ECM required to bind ES cells together long term could explain the observed decrease in EB diameter (Figs 3.8A and B). The number of EBs in suspension significantly ($P \leq 0.001$) increased over time at 5×10^4 and 1×10^6 cells/mL. This increase correlated with the observed decrease in EB diameter (Figs 3.8C and D). However, dissociation due to cell death would cause diminished EB diameter and an increase of single cells in suspension, not an increase in EB number. The most likely cause of increased EB number was fragmentation. EBs would have been structurally weak due to mitotic inactivation. This instability on top of cell death would have made EBs become easily fragmented as a result of any significant movement applied to the suspension, such as when cultures were measured. There was no significant difference between EB numbers in engineered and control samples regardless of seeding density. Once membrane recycling removed the surface modification, engineered EBs would have been expected to dissociate completely. However, engineered EB number remained equivalent to control samples, possibly indicating some degree of natural adhesion. Similar trends were observed during aggregation of proliferative ES cells. This illustrated that engineering is possibly a temporary step for the formation of EBs and not persistent during their growth.

3.5.2.4. Cell Number and Embryoid Body Formation

As previously mentioned EBs increase in diameter largely due to the aggregation of additional ES cells during growth (Cormier et al., 2006). Therefore, as both engineered and control EBs increased in diameter over time it would be expected that constituent cell number increased as a function of cell aggregation and proliferation (Figs 3.7A and B). However, the number of cells within both engineered

and control EBs significantly ($P \leq 0.001$) decreased over time at 5×10^4 and 1×10^6 cells/mL (Figs 3.9C and D). The decreased constituent cell number was most likely the result of natural cell death in combination with core necrosis (Wartenberg et al., 1998, Carpenedo et al., 2007, Boyd et al., 1984, Conley et al., 2005, Kurosawa, 2007), discussed in Chapter 4. Increase in EB diameter was therefore not simply the result of ES cell aggregation. 3D conformation of constituent cells may also have had a direct effect on EB diameter. Initial aggregation of ES cells formed loosely packed clusters which later reorganized to form compact EBs (Enmon et al., 2001). It was possible that restructuring did not involve compaction. Cell aggregation caused cell-cell adhesion in a random spatial orientation and cell proliferation may have filled in the gaps. This would explain why cell proliferation has minimal effect on EB growth, since gap filling would not increase overall EB diameter. Even though constituent cell number decreased, remaining cells within the EB maintained 3D structure. Continuous aggregation of additional cells increased the diameter. Alternatively, ECM production and deposition from constituent cells would have acted to fill in the gaps. Therefore EB diameter becomes a function of cell aggregation, proliferation and ECM production. ECM deposition would maintain existing EB diameter whilst aggregation of additional cells would increase the diameter. The decrease in constituent cell number could have been the result of internal cells becoming trapped within ECM. Trapped ES cells may have undergone apoptosis or necrosis, either of which would cause a decrease in constituent cell number (Abe et al., 1996). The decrease in constituent cell number appeared to occur more rapidly at 1×10^6 cells/mL (Fig 3.9D). This would be concurrent with the hypothesized aggregation system described above. A greater number of cells in suspension available for aggregation would have caused an increase in the number of cells within EBs

becoming trapped in deposited ECM. Therefore, more cells would become necrotic and decrease the overall constituent cell number (Kurosawa, 2007).

At 5 x 10^4 cells/mL the number of constituent cells within engineered EBs was significantly ($P \leq 0.001$) greater than control EBs (Fig 3.9C). This showed that the diameter was directly related to the number of constituent cells. Engineering enhanced aggregation between ES cells and increased EB size without affecting EB number (Fig 3.7C). The difference in number of constituent cells within engineered and control EBs was insignificant at 1 x 10^6 cells/mL (Fig 3.9D). This was expected since there was also no significant difference in EB diameter (Fig 3.7D).

EB formation and growth depends on the availability of additional cells in surrounding suspension. As aggregation progresses, the set number of available cells seeded into suspension would be expected to decrease. At 5 x 10^4 cells/mL the number of single cells in suspension gradually decreased over time supporting this idea. However, cells were continuously proliferating and increasing available numbers. The fact that the number still decreased showed that aggregation rate outweighed proliferation rate. At 1 x 10^6 cells/mL the number of single cells in suspension showed no significant change over time even though aggregation continued. It was possible that at 1 x 10^6 cells/mL proliferation rate exceeded aggregation rate and thus provided an inexhaustible supply of additional cells. Alternatively, the high number of cells in suspension could have been due to the hypothesized cell death and diminishing EB number observed at 1 x 10^6 cells/mL. Also, the higher the proportion of cells per given volume, the faster the nutrient supply is utilized. Consequently, cells may have died rapidly from starvation maintaining a high single cell population in suspension. However, trypan blue stains

revealed that the majority of cells were still alive. A minority had taken up the stain, thus cell death played a minor role in the population of single cells in suspension.

A possible explanation for the lack of a significant change in suspended cell number was that the data collected did not represent the true single cell population. EB suspensions were washed through a < 40μm sieve and a Hoescht assay quantified the DNA content of flow-through cells. Initial ES cell clusters and true individual ES cells were not distinguishable using this technique. Ultimately, true single ES cells in suspension may have decreased in number over time due to aggregation. Most cells at 1 x 10^6 cells/mL would have formed EBs due to increased chance collisions. However, many cells would have collided with adjacent cells to form small cell clusters with a < 40μm diameter. Some cell clusters would have continued to accumulate additional cells and eventually form EBs (Kim et al., 2007b, Come et al., 2008, Cormier et al., 2006). EBs would also have grown through amalgamation of adjacent cell clusters. Remaining cells clusters that had escaped amalgamation would have slowly increased in diameter mainly due to cell proliferation since single cell availability for aggregation would have been limited. Since the contribution of cell proliferation to EB diameter was insignificant over the time period investigated, cell clusters may have remained < 40μm in diameter adding to the true population of single cells.

The number of engineered cells in suspension was significantly ($P \leq 0.001$) less than control samples for the first 5 days of aggregation at 5 x 10^4 cells/mL (Fig 3.9A). This was concurrent with engineered EBs being significantly ($P \leq 0.001$) larger than control EBs (Fig 3.7A). Larger EBs required more ES cells to form causing the observed decrease in overall ES cell number in suspension. However, by day 7 engineered samples contained a similar number of single cells in suspension to

control samples. Initially, engineered aggregation enhanced ES cell-ES cell interaction and adhesion which rapidly decreased available cells in suspension. However, the surface modification was removed over time and further aggregation slowed to the same rate of control samples. It was possible that control aggregation took 7 days to accumulate as many single cells from suspension as what engineered aggregation accumulated in only 5 days. At 1 x 10^6 cells/mL the difference between engineered and control samples was insignificant (Fig 3.9B). This was simply because at 1 x 10^6 cells/mL engineered cells did not exhibit enhanced aggregation. Therefore, the number of cells from single cell populations in suspension which aggregated to form EBs was the same in both engineered and control samples.

3.6. Conclusions

In summary, engineering provided influence over ES cell-ES cell interaction, adhesion and subsequent EB formation. Engineered EBs were both significantly ($P \leq 0.001$) larger and more stable than control EBs. Interestingly, enhancement due to engineering was only observed at 5×10^4 cells/mL. EB number reflected the average diameter of both engineered and control EBs, such that EB number decreased as EB diameter increased. Consequently, the relationship illustrated that ES cell aggregation may not have been responsible for initial ES cell clusters, but continued EB growth and development was dependent to an extent on cluster-cluster interactions. Engineered EBs were composed of a significantly ($P \leq 0.001$) higher number of cells than control EBs showing cell number was directly related to EB diameter. However, over time constituent cell number decreased whilst diameter increased or remained unchanged. Structural arrangement of constituent cells therefore played a major role in determining EB diameter, able to counter potential detrimental effects of decreasing cell number as a result of apoptosis/necrosis. EB formation was found to be a complex relationship between ES cell aggregation, proliferation, death, cluster agglomeration, and ECM deposition.

Chapter 4

4. Results

Embryoid Body Characterization

4.1. Introduction

For many years ES cells have been cultured via EB formation to induce and sometimes control differentiation (Itskovitz-Eldor et al., 2000, Bratt-Leal et al., 2009, Mansergh et al., 2009). Numerous aggregation methods have generated a variety of results with previous studies having repeatedly documented a direct relationship between EB formation method and resultant ES cell differentiation (Mogi et al., 2009, Dang et al., 2004, Chen et al., 2008). For example, EBs formed individually in separate wells with and without centrifugation have exhibited enhanced cardiomyogenesis (Burridge et al., 2007, Kurosawa, 2007). Alternatively, EBs formed through 3D hydrogel culture have exhibited enhanced chondrogenesis, adipogenesis and osteogenesis (Kanczler and Oreffo, 2008, Hwang et al., 2008a, Rohani et al., 2008, Hillel et al., 2009). EBs formed by hanging drop have exhibited enhanced neurogenesis (Kuo et al., 2003), hepatogenesis (Takashimizu et al., 2009) and vasculogenesis (Kim et al., 2008) (Table 1.4).

This high degree of variability impedes our understanding of how the EB confers control and influence over ES cell differentiation. Due to a lack of standardization fro EB formation, inherent mechanisms during ES cell aggregation and resultant EB characteristics which affect differentiation are difficult to decipher and remain convoluted. One possible solution would be to standardize aggregation methodology. An ideal standardized method should provide control over aspects of EB formation known to affect ES cell differentiation, such as size, number, growth, morphology and density. However, we first need to understand how and why these particular parameters of EB formation cause differentiation towards specific cell types.

Chapter 3 has described a novel aggregation method for EB formation. Here is shown a detailed characterization of resultant engineered EBs in comparison to control EBs, identifying key aspects of the EB affected by aggregation method and affecting differentiation.

4.2. Methods and Materials

4.2.1. Embryoid Body Cell Density

At each time point EB sections were processed through haematoxylin and eosin stain described in Chapter 2. Cross sections were photographed at 10x magnification using the Nikon Eclipse TS100 and attached Nikon Digital Sight DS-L1 imaging system. 50μm by 50μm squares were positioned on top of EB cross-section images in similar locations (Fig 4.1). Three squares were positioned over the centre and three more around the surface. Squares were positioned at equal distances from one another where possible. ES cell nuclei within each square were counted and an average taken. As with haemocytometer based counts, only ES cell nuclei lying within the squares or those overlapping two of the four sides were included in the count. This is because two of the sides would constitute a side of an adjacent square. Since square measurements were 50μm width, 50μm depth and 4μm height, the number of ES cell nuclei counted were in a total volume of 10,000μm^3. EB cross-section images showed a clear structural difference between the surface and the core. As a result, two separate sets of squares were used to evaluate ES cell density within the EB core and at the EB surface. Three individual EB cross-section images were used to calculate an average core and surface ES cell density measurement.

4.2.2. Embryoid Body Necrosis

At each time point during the 9 day period of aggregation, duplicate EB samples were removed from culture and washed through a 40μm cell strainer. Single ES cells and ES cell clusters were rinsed through the cell strainer with 5mL room temperature PBS. Flow through was collected in a 50mL Falcon tube and discarded. EBs were

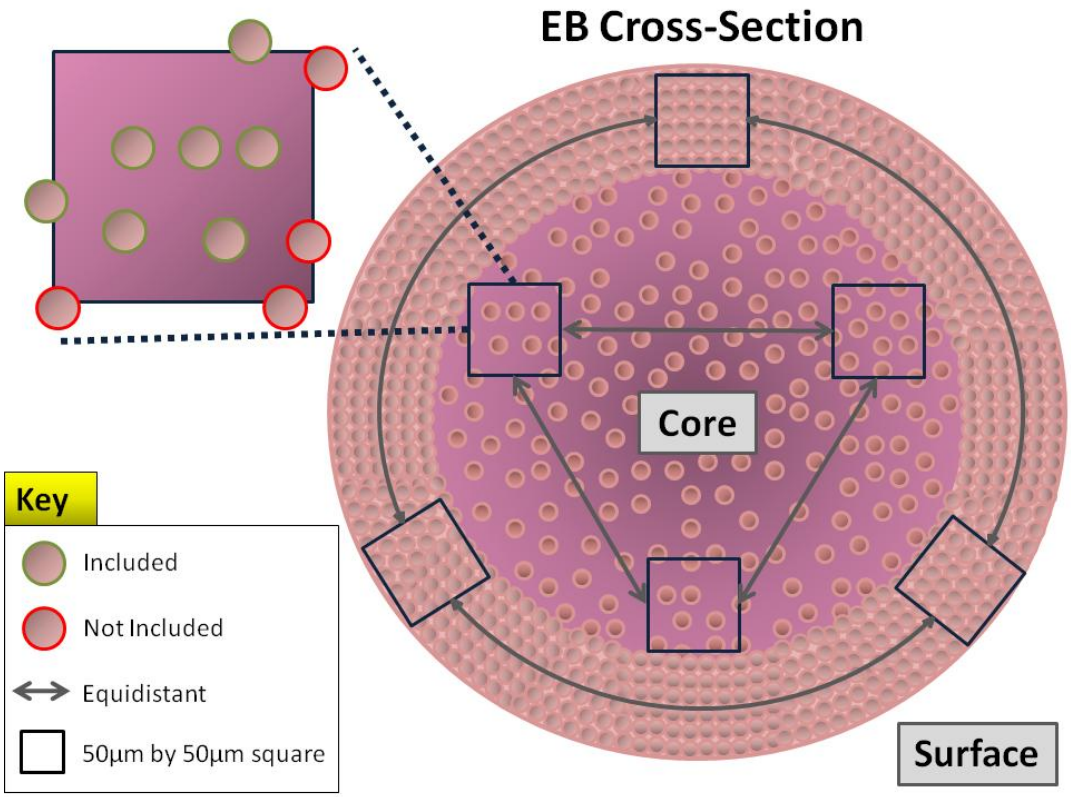

Figure 4.1: Measuring cell density using EB cross-sections. EB cross-sections were treated with H&E stain to highlight cell nuclei. Squares measuring 50µm by 50µm were positioned equidistantly (where possible) on the stained cross-sections. Three squares were positioned at the surface and three more at the core. Individual cell nuclei within each square were counted and an average calculated representing cell density and the surface and core. Cell densities were taken from 3 separate EBs per sample.

carefully washed from the filter into a Falcon tube with PBS and centrifuged briefly at 1000rpm to pellet the EBs. PBS was subsequently aspirated and the pellet suspended in 2mL trypsin/EDTA. The suspension was pipetted carefully to dissociate intact EBs. 3mL SCM was added to inactivate the trypsin/EDTA and the suspension centrifuged at 1000rpm for 5mins. Supernatant was aspirated and the pellet suspended in Live/Dead™ solution in SCM. Single cell suspensions were incubated for 30-60mins at 37°C and 5% CO_2 in a humidified atmosphere. After incubation, suspensions were centrifuged and washed twice with PBS to remove the Live/Dead™ solution. Pellets were finally suspended in 2mL PBS and a 10µl aliquot loaded onto an improved neubauer hemocytometer. A cell count was taken under fluorescence (refer to Live/Dead™ stain in Chapter 2). All ES cells were counted under brightfield imaging. ES cells which fluoresced red were subsequently counted. All cells within 5 squares were counted and an average was calculated. Few ES cells were visible at 5 x 10^4 cells/mL. Therefore, all ES cells lying within the 25 square-grid were counted. The number of ES cells which fluoresced red was calculated as a percentage of the whole EB suspension using the whole ES cell counts.

Isolation of EBs without ES cell clusters and single ES cells was achieved by cell straining. This allowed analysis of EBs alone. Trypsinisation time was similar for all samples at a maximum of 5mins. Green fluorescence highlighted ES cells which were alive and thriving. Red fluorescence highlighted ES cells that were dead or necrotic. Tracking the number of dead ES cells within EBs allowed analysis of core necrosis within the EB structure over time.

4.3. Results

4.3.1. Embryoid Body Structure and Viability

4.3.1.1. Internal Structure

Both engineered and control EBs appeared to exhibit a layered internal structure (Fig 4.2). On closer analysis four different layers could be distinguished, each representing hypothetical stages of ES cell aggregation and EB formation. From the outermost layer towards the core the four distinguishable layers have been labelled as surface, outer and inner shells, and core. A distinct difference in ES cell density could be seen between the surface and the core. ES cells were less densely packed at the core than those near the surface due to the reduced number of cell nuclei observed in Fig 4.2C. This observation was conserved at both 5×10^4 and 1×10^6 cells/mL. The core was sparsely populated with ES cell nuclei spaced apart randomly. The surface also appeared to consist of disorganised ES cell nuclei, but at a higher density. The inner and outer shells appeared to be transition stages between the surface and the core. The outer layer resembled a condensed version of surface ES cell nuclei. The inner shell resembled a dense version of core ES cell nuclei. The relative thickness of each layer appeared to decrease from the inner shell to the surface.

4.3.1.2. Cell Viability

The core and surface of EBs exhibited both red and green fluorescence respectively, indicating that cells within the EB core were dead or necrotic, and cells on the EB surface were alive and thriving. Similar observations were made in both

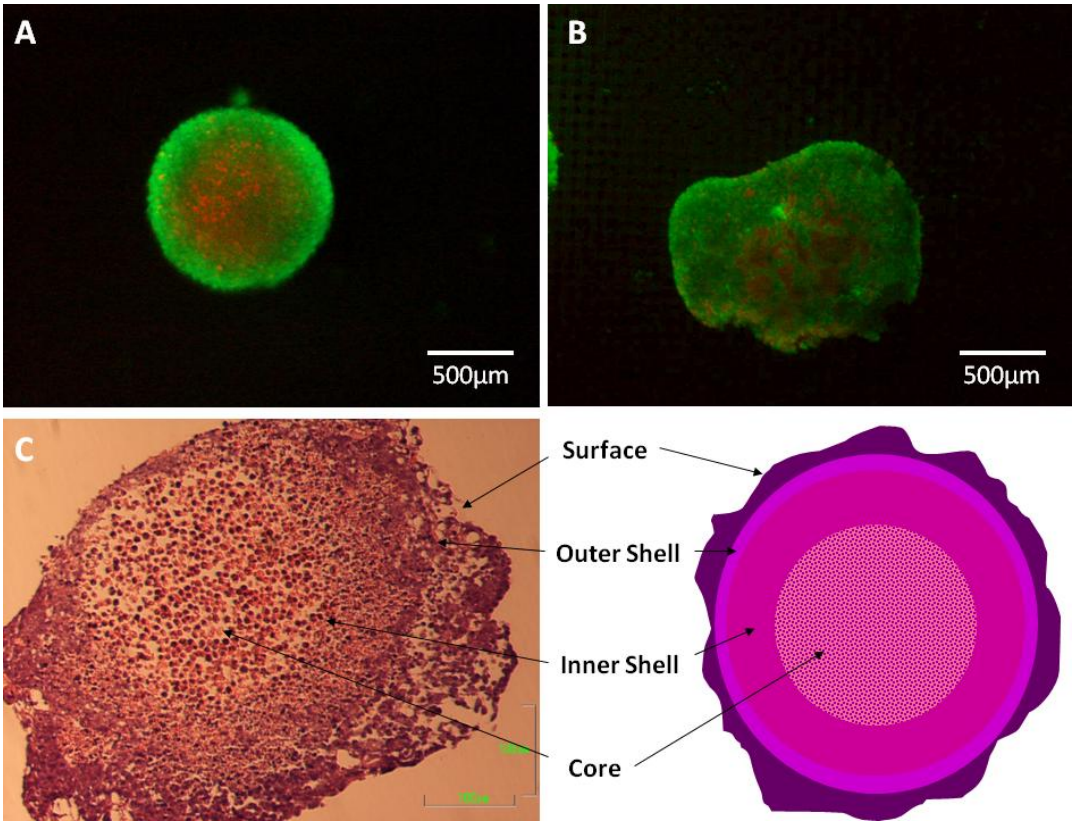

Figure 4.2: EB structure and constituent cell viability. Engineered and control 1 ES cells were seeded at 1 x 10^6 cells/mL into mass suspension, rotated at 15rpm for 6hrs prior to 9 days incubation at 37°C and 5% CO_2 in a humidified atmosphere. After 9 days, cell viability within engineered (A) and control 1 (B) EBs was assessed by Live/Dead™ assay. EBs were taken from duplicate samples after 9 days of aggregation and prepared for microtome-sectioning. EB cross-sections were then stained with H&E. Fig C shows an H&E stained cross-section of an engineered EB and a diagrammatic representation of its structure. Cell nuclei within the core appeared swollen and enlarged indicating necrosis, rather than apoptosis where cell nuclei effectively shrink. Also, core cells did not show typical characteristics of apoptosis such as membrane blebbing.

engineered and control samples at 5 x 10^4 and 1 x 10^6 cells/mL (Figs 4.2A and B). Only EBs aggregated and cultured for 9 days were sampled due to structural instability of earlier stage EBs during repeat PBS washing to remove excess Live/Dead™ stain.

4.3.2. Embryoid Body Density and Necrosis

4.3.2.1. Cell Density

Engineered EBs appeared to exhibit dense populations of cells at both the surface and core (Figs 4.3A and B). Surface and core cell densities within engineered EBs were significantly ($P \leq 0.05$) greater than those in corresponding control EBs. Cell density showed minimal change over increasing seeding density in engineered and control EBs within the surface layer and the core (Fig 4.3). Both engineered and control EBs exhibited significantly ($P \leq 0.05$) denser cell populations within their surface layer in comparison to their core layer (Figs 4.3C and D). Surface to core cell density data for control 2 EB samples is not shown in Fig 4.3. However, results were not significantly different to those of control 1 EB samples (Fig 4.3D).

4.3.2.2. Cell Death

High seeding density of 1 x 10^6 cells/mL was reduced to 2.5 x 10^5 cells/mL for all subsequent experiments because 2.5 x 10^5 cells/mL was the maximum seeding density investigated that did not show measurable EB agglomeration (data not shown). EB agglomeration increases EB diameter and decreases constituent cell viability. The average proportion of dead cells within all EBs was not significantly different between engineered and control samples (Fig 4.4). There was no significant difference over seeding density from 5 x 10^4 cells/mL (Fig 4.4A) to 2.5 x 10^5 cells/mL

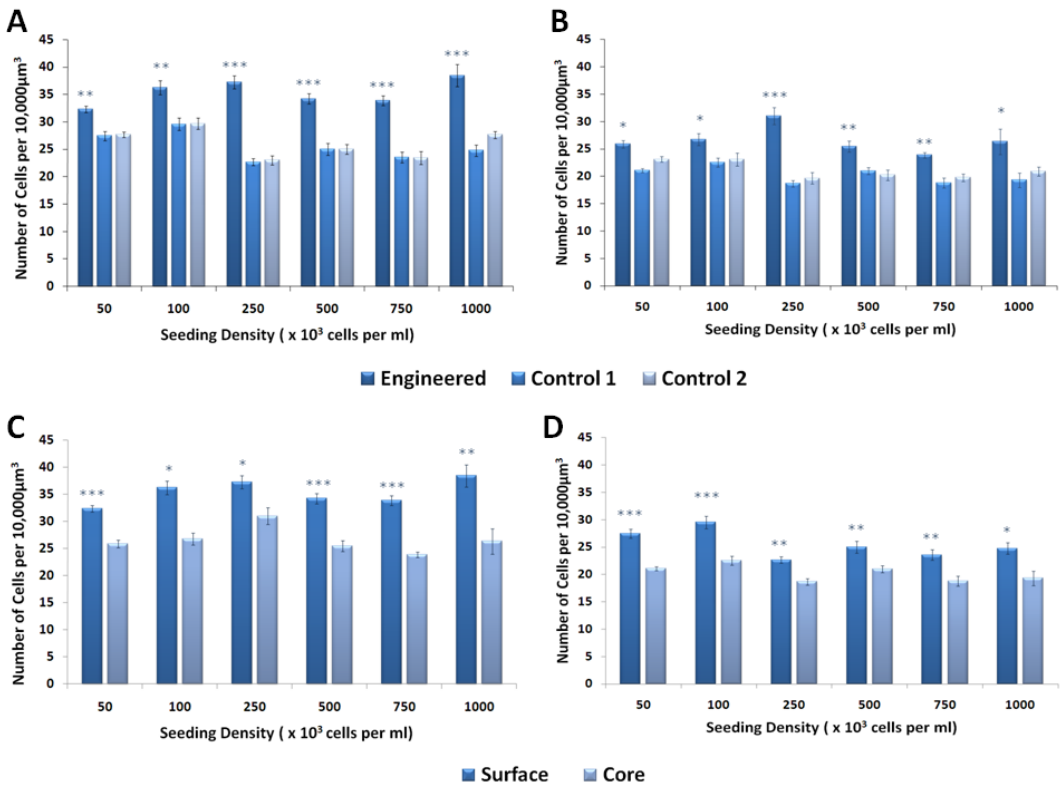

Figure 4.3: Effect of engineering on cell density within EBs. Engineered and control ES cells were seeded into mass suspension over a range of densities ranging 50, 100, 250, 500, 750 and 1000 x 10^3 cells/mL. Suspensions were rotated at 15rpm for 6hrs then cultured under stationary conditions for 9 days. After 9 days, EBs were fixed, sectioned and H&E stained. Labelled nuclei were counted and used to calculate representative cell densities at the EB surface (A) and core (B). Figs C and D directly compare the surface and core cell densities in engineered and control 1 EBs, respectively. Three EBs were sampled for engineered and control samples and cell density measured in triplicate; n = 9. *** P ≤ 0.001, ** P ≤ 0.01, * P ≤ 0.05. Error bars = S.E.M.

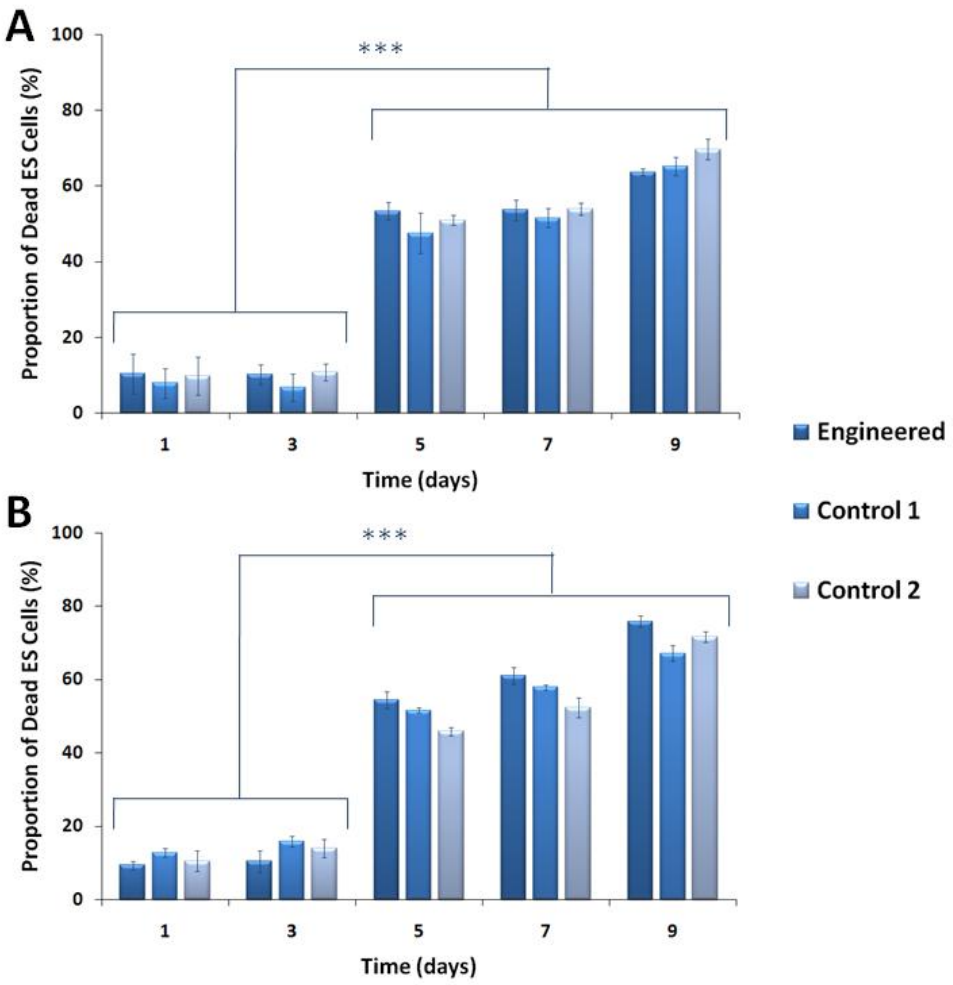

Figure 4.4: Cell viability and EB core necrosis. Engineered and control ES cells were seeded into mass suspension at 5 x 10^4 cells/mL (A) and 2.5 x 10^5 cells/mL (B), rotated at 15rpm for 6hrs and incubated at 37°C and 5% CO_2 in a humidified atmosphere for up to 9 days. After 1, 3, 5, 7 and 9 days, EB suspensions were centrifuged and washed in PBS prior to trypsinization. Single cell suspensions were incubated with Live/Dead™ solution and dead cells were quantified by hemocytometer cell count and calculated as a percentage of the whole. Experiments were conducted in triplicate; *n* = 3. *** P ≤ 0.001, ** P ≤ 0.01, * P ≤ 0.05. Error bars = S.E.M.

(Fig 4.4B) in all samples. Engineered and control samples showed a significant ($P \leq 0.001$) increase in the proportion of dead cells constituting EBs after 5 days of aggregation and growth. The proportion of dead cells increased significantly ($P \leq 0.001$) from day 5 to day 9 in both engineered and control EBs.

4.3.3. Cellular Morphology

Both engineered and control EBs were cultured for 4 weeks in SCM under static conditions. EBs were allowed to spontaneously differentiate without the addition of exogenous cues. After 4 weeks EBs were processed for SEM imaging (refer to Chapter 2). A range of cellular morphologies were observed on the EB surface on both engineered and control samples. A representative selection of cellular morphologies was chosen and photographed (Fig 4.5). Morphologies resembled possible cell types such as endothelial (Fig 4.5A), neuronal (Fig 4.5B), ciliated (Fig 4.5C), adipose (Fig 4.5D), and fibroblastic (Fig 4.5E). Loading processed EBs onto the imaging stubs caused some EBs to break apart. The advantage of this was accessibility to internal ES cell morphology (Fig 4.5F). Internal ES cells showed no change in morphology, remaining small, smooth and spherical.

The surface of the EB appeared to compose of cells embedded in a fibrous mesh (Fig 4.6A). During SEM processing, fragile EBs broke apart revealing cell morphology internally. The broken parts also allowed visualization of a cross section through the surface. Immediately below the surface layer is a mesh of fibrous material, most likely being ECM deposition. Internal cells were not apparent in the image, possibly due to having fallen apart during impact. ES cells in 2D culture prior to engineering and aggregation in suspension were labelled with Oct-4 antibody (Fig 4.6C). The bright green fluorescence illustrated that all cells were pluripotent and remained

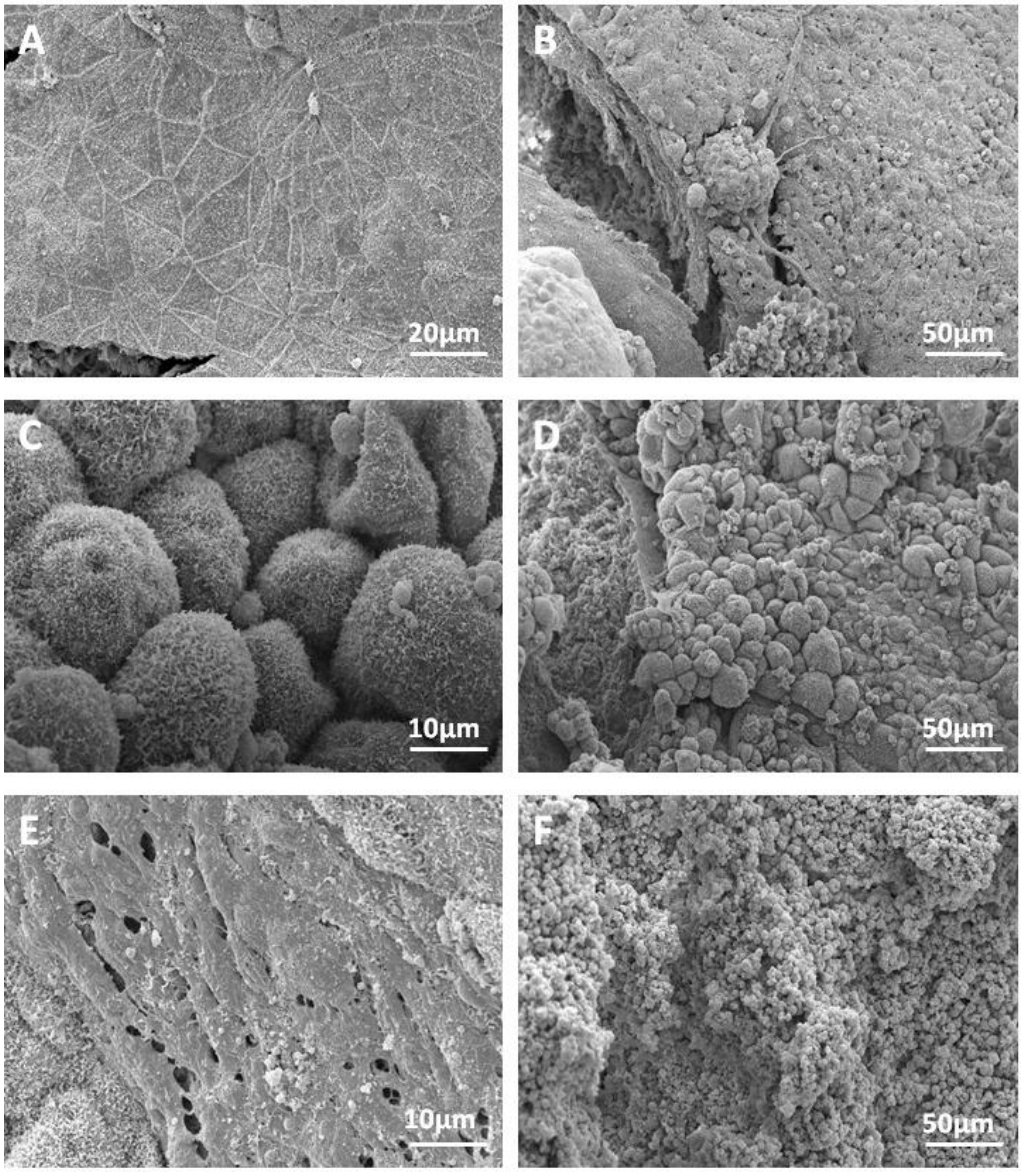

Figure 4.5: Cellular morphologies observed on the EB surface and internally. Engineered and control ES cells were seeded into suspension in SCM for 4 weeks. After 4 weeks, EB suspensions were washed and processed for SEM analysis. Images were taken of engineered samples. Similar morphologies were observed in control samples (data not shown). Morphologies appear to resemble cell types such as endothelial (A), neuronal (B), ciliated (C), adipose (D) and fibroblastic (E). Internal cells resembled undifferentiated ES cells with a small, smooth and spherical morphology (F).

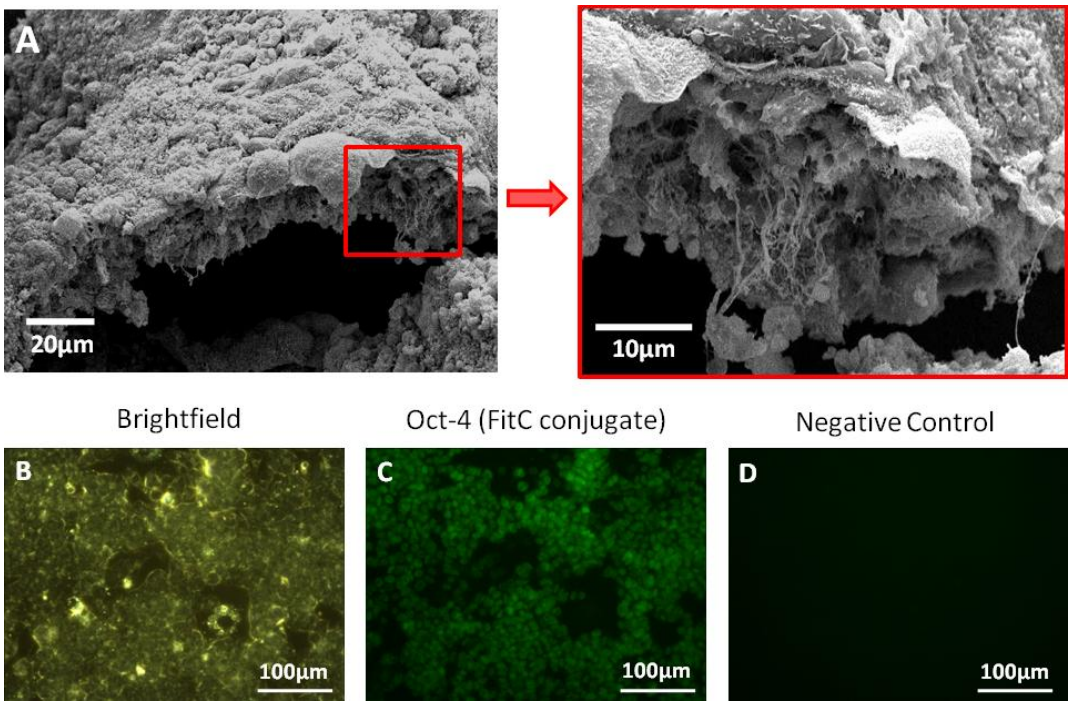

Figure 4.6: ES cell pluripotency and differentiation within the EB. ES cells were seeded into mass suspension and rotated at 15rpm for 6hrs prior to 4 weeks culture at 37°C and 5% CO_2 in a humidified atmosphere. After 4 weeks, EBs were processed for SEM analysis. During loading of SEM prepared EBs onto SEM stubs, the fragile EBs would sometimes break apart. Fig A shows a broken engineered EB. The EB surface can be visualized as cells embedded in a fibrous mesh. To ensure ES cells in continuous culture were pluripotent prior to EB experimentation, ES cell colonies in 2D culture (B) were immuno-labelled with a primary antibody against Oct-4 and FitC-conjugated secondary antibody (C). A negative control was prepared by incubating ES cells with just the FitC-conjugated secondary antibody, not the Oct-4 primary antibody (D).

undifferentiated. Since the morphology of these cells was comparable to those within the EB structure, internal cells appeared undifferentiated. Therefore, the fact that surface cells were distinctly morphologically different to internal cells lends support to surface cells having undergone random differentiation.

4.3.4. Germ Layer Differentiation

4.3.4.1. Embryoid Body Differentiation

Both engineered and control ES cells were aggregated and cultured in SCM without the addition of exogenous growth factors for 9 days. EB sections were immuno-labelled for the three germ layers, mesoderm, endoderm and ectoderm (Fig 4.7). Similar results were observed at 5 x 10^4 cells/mL and 2.5 x 10^5 cells/mL in both engineered and control samples. Engineered EBs exhibited mesoderm differentiation where both control EB samples did not (Figs 4.7A and J). In contrast, both control EB samples exhibited endoderm differentiation where engineered EBs did not (Figs 4.7E, H, N and Q). Mesoderm differentiation appeared both internally and externally (Fig 4.7A). Endoderm differentiation appeared to be restricted to the section periphery indicating differentiation was located at the surface (Fig 4.7Q). Ectoderm differentiation was not observed in any samples, at least to a detectable level (Figs 4.7C, F, I, L, O and R).

4.3.4.2. Germ Layer Formation

Engineered and control ES cells were aggregated for 3 and 9 days. RNA was extracted from the resultant EBs for PCR amplification. Fig 4.8 shows PCR results for undifferentiated cells (Oct-4) and the three germ layers, including mesoderm, endoderm and ectoderm (Brachyury, Gata-4, Nestin, respectively). Nestin expression

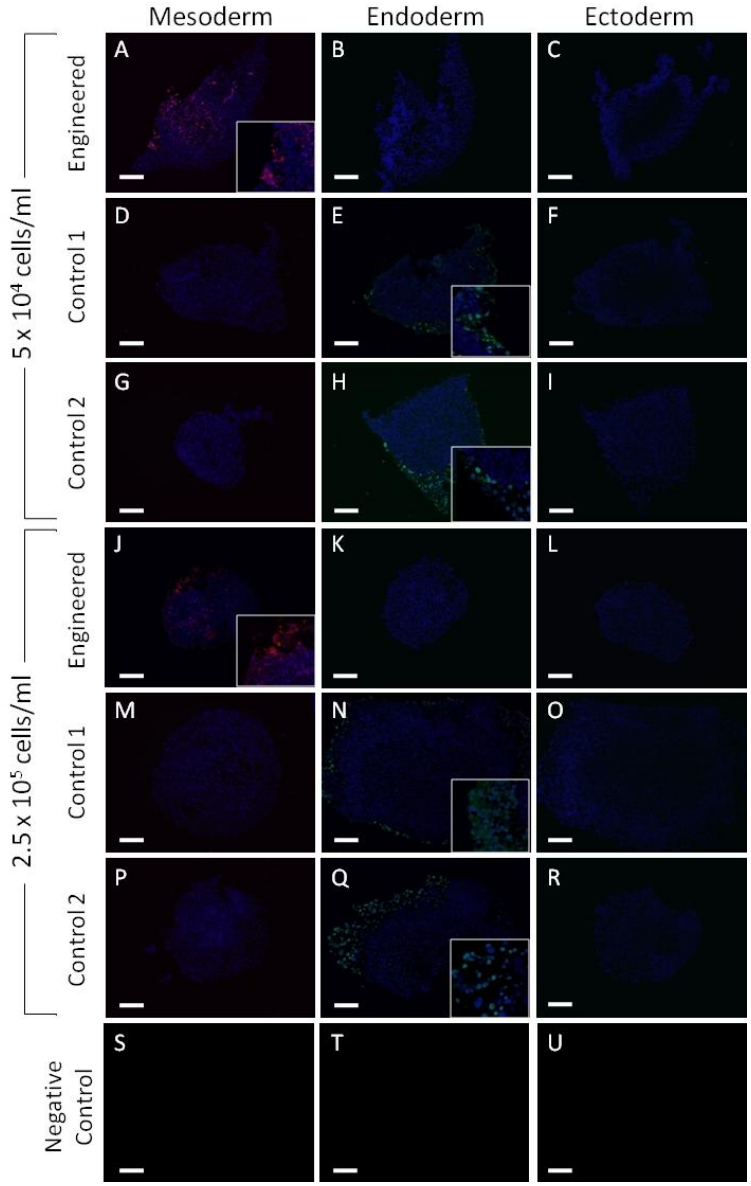

Figure 4.7: EB differentiation and germ layer formation. Engineered and control ES cells were seeded into mass suspension, rotated at 15rpm for 6hrs and aggregated for 9 days in SCM. After 9 days, EBs were fixed, sectioned and fluorescence immuno-labelled for mesoderm (Brachyury), endoderm (Gata-4) and ectoderm (Nestin). Negative controls were prepared by skipping incubation with primary antibodies against the germ layers, and incubation with just fluorescence-conjugated secondary antibodies. DAPI was used as a counter-stain. Scale bars measure 100µm.

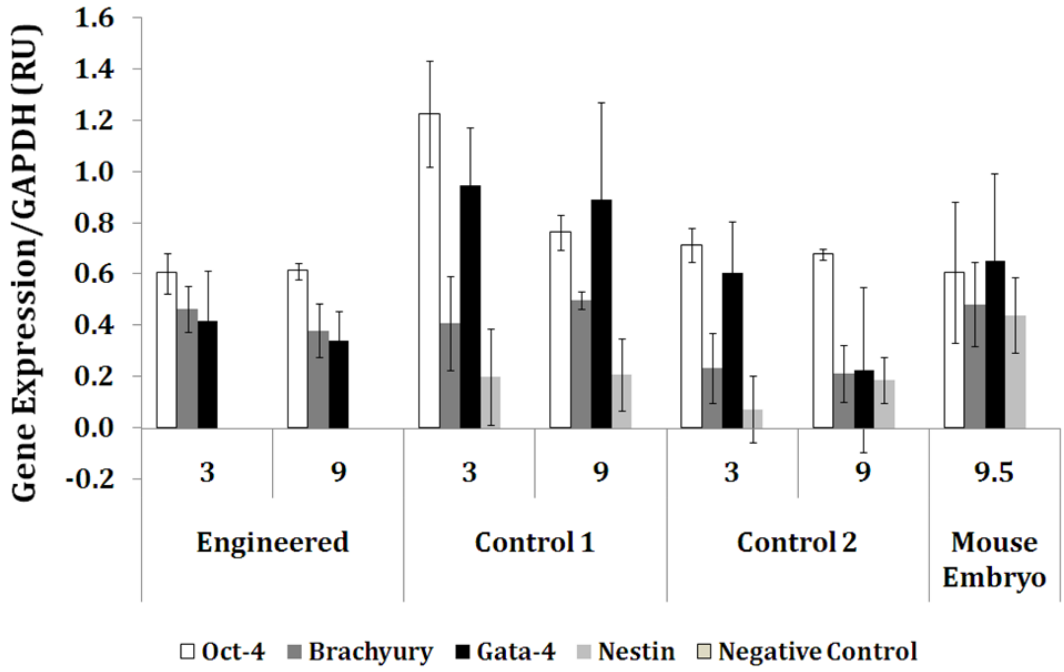

Figure 4.8: Effect of engineering on ES cell differentiation and germ layer formation during the EB stage. Engineered and control ES cells were seeded into suspension at 5 x 10^4 cells/mL, rotated at 15rpm for 6hrs and incubated under stationary conditions for between 3 and 9 days. After 3 and 9 days, EBs were prepared for PCR analysis. EB lysates were analyzed for mesoderm (Brachyury), endoderm (Gata-4) and ectoderm (Nestin) expression. Lysates were also analyzed for pluripotency (Oct-4) to show the presence of undifferentiated ES cells. GAPDH was used as a quality control. Bands were scanned using densiometric analysis and equalized between samples using GAPDH expression levels. Day 9.5 mouse embryos were used as a positive control. Negative controls were prepared by not adding cDNA templates to the PCR mix before amplification. Error bars = standard deviation.

was absent in engineered samples and minimal in control samples. Brachyury and Gata-4 expression was observed in all samples. Brachyury expression appeared to be unaffected by engineering. However, both Gata-4 and Nestin expression appeared reduced within engineered samples in comparison control samples. This indicates an indirect enhancement of mesoderm formation via possible inhibition or downregulation of endoderm and ectoderm expression; possible increased mesoderm homogeneity. All samples exhibited high Oct-4 expression up to 9 days showing a high proportion of the cells within EBs remained undifferentiated. Day 9.5 mouse embryos were used as positive controls and showed Oct-4, Brachyury, Gata-4 and Nestin expression. Presence of bands showed that primer pairs were efficient for PCR amplification. Clear GAPDH expression within all samples showed reverse transcription efficiency. Negative controls revealed no sample contamination.

4.3.5. Cadherin-11 Expression

ES cells were seeded at 5 x 10^4 cells/mL and aggregated for 9 days in SCM. Fig 4.9 shows fluorescence images of engineered and control EBs immuno-labelled for cadherin-11. All samples exhibited cadherin-11 expression. Engineered samples appeared to exhibit more cadherin-11 expression than control samples (Fig 4.9A). However, expression within engineered samples only appeared greater than control samples within small diameter engineered EBs. This indicated a potential correlation between EB diameter and cadherin-11 expression. Cadherin-11 expression within these small engineered EBs appeared below the EB surface. However, without fluorescence quantification from multiple EB sections, the conclusion is that all samples exhibited cadherin-11 expression.

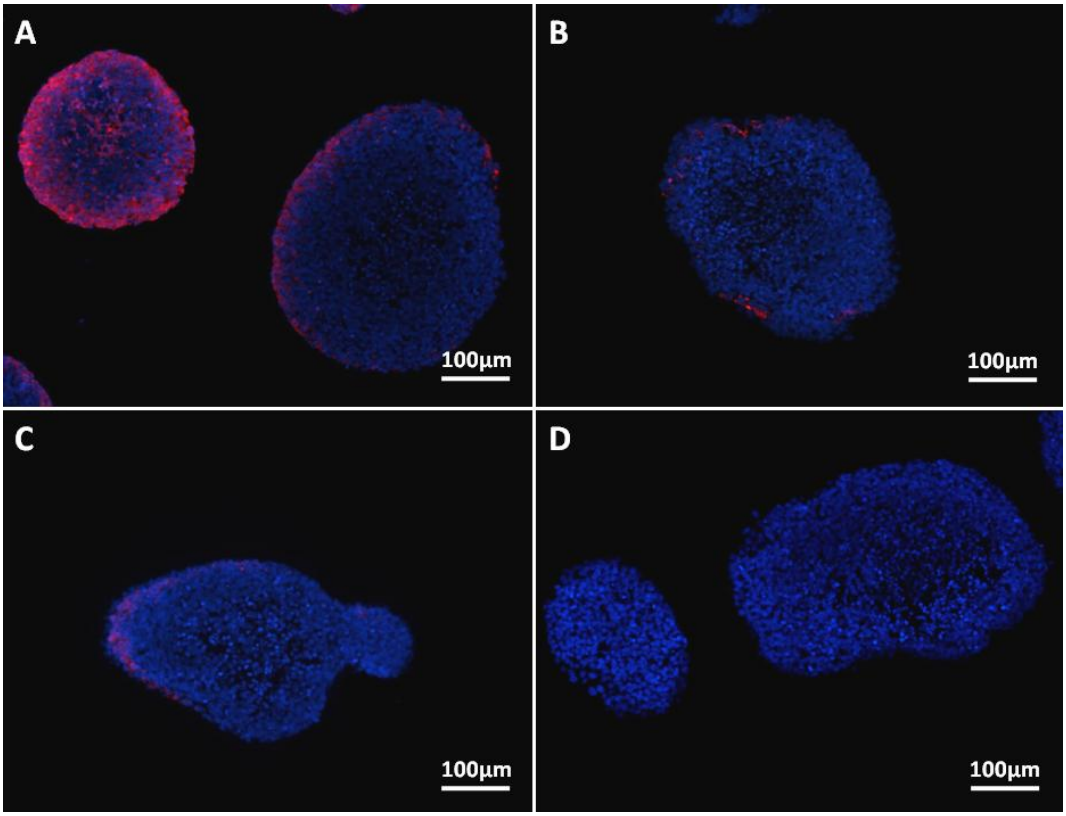

Figure 4.9: Effect of engineering on cadherin-11 expression. Engineered (A), control 1 (B) and control 2 (C) ES cells were seeded into mass suspension at 5 x 10^4 cells/mL rotated at 15rpm for 6hrs and incubated at 37°C and 5% CO_2 in a humidified atmosphere for 9 days. After 9 days, EBs were fixed, sectioned and immuno-labelled with primary antibody against cadherin-11 and phycoerytherin-conjugated secondary antibody. Fig D shows a negative control prepared by incubating the EB cross-section with only the secondary antibody, not the primary antibody. DAPI was used as a counter-stain.

4.4. Discussion

Many individual studies have employed the use of EBs in their differentiation protocols as it provides a means of recapitulating natural 3D embryo growth and development *in vitro* (Conley et al., 2005). Specifically, EBs exhibit the ability to cause and potentially direct ES cell differentiation. Many methods are currently employed for efficient ES cell aggregation and EB formation. Each method of aggregation appears to enhance ES cell differentiation towards a specific cell type. However, minimal work is invested in the characterisation of these EBs (Koike et al., 2007). Mostly, the aggregation method is altered to produce desired ES cell differentiation without adequate analysis of the transitional EB stage. Detailed analysis of the EB stage would provide a closer insight into the formation of differentiated cell types. Identification of trends in both EB structure and constituent cell viability and differentiation could pave the way for efficient production of desired cell types in potentially homogeneous populations. Understanding what properties EBs possess and how these relate to ES cell differentiation would enable standardisation of EB formation protocols. Here we show a detailed analysis of the EB structure and constituent cell viability and differentiation. Both engineered and control EBs were investigated at different seeding densities and over aggregation time.

4.4.1. Embryoid Body Structure

EB formation is extremely complex involving the interaction of many factors. Logic would dictate that EB formation begins with single ES cell-ES cell collisions and resultant adhesion. These interactions progress and eventually ES cell masses,

namely clusters, are generated. These grow in size through further aggregation and constituent cell proliferation. However, logic alone does not provide adequate explanation for how these events take place. The layered EB structure provided insight into EB formation which possibly arose through a build up of ES cell layers (Fig 4.2C). Importantly, this hypothesis implies two things, (1) ES cell proliferation has minimal bearing on overall EB structure and/or (2) cell mobility within the EB structure is extremely limited. If ES cell proliferation had a major effect on EB structure then constituent cells would increase the internal size of EBs exponentially in comparison to the surface. Consequently, the EB would exhibit a large core in comparison to the surface, a cell dense core and possibly surface traits like stretching. Stretching has been indicated by cellular morphology of surface cells in Chapter 3. However, Figs 4.2A and B clearly showed that the core of the EB was necrotic. Therefore ES cell proliferation could not be contributing to the increase in EB core size. As for limited cell mobility within the EB structure, constituent cells would be fixed in place once they became adhered. Additional ES cells would adhere to these in sequential layers hence generation of the observed layered internal EB structure.

The above hypothesis is flawed in its explanation of the observed layered EB structure. The aforementioned hypothesis is based on the internal layered structure arising through physical ES cell-ES cell interaction and subsequent 3D orientation, which is spatially fixed within certain parameters. An alternative hypothesis, supported by ensuing data, describes the generation of layers within the structure as an artefact of cell viability and mobility. It is true that ES cells interacted and adhered to form clusters. These continued to acquire additional ES cells through aggregation, but also interaction with one another. Visual observations of cell clusters showed

them to be irregular in shape and consist of randomly orientated ES cells. Continual aggregation and EB growth resulted in dense spherical aggregates which exhibited a less chaotic organisation. This indicated that cells were more than capable of moving around within the EB structure. They could have potentially traversed the entire EB structure from one side to the other. Consequently, it was unlikely that the layered structure was a direct result of cell mobility. Even though ES cell adhesion would occur in layers, constituent cells within each layer had the ability to move between layers. Eventually, this movement would have blurred the boundaries between layers until they were no longer distinguishable. However, it was possible that the 9 day period of aggregation investigated was insufficient time for this to occur. Therefore, layering as a consequence of cell mobility is not completely excluded.

Constituent cell mobility raised another interesting point concerning core necrosis. It was possible that cells were mobile enough to enable restructuring of the entire EB mass into a less chaotic configuration. This restructuring may have involved internalisation and accumulation of damaged or dead cells within the EB core. Inter-EB collisions or sensitivity to altering environmental conditions may have caused damage to surface cells which then became internalised. The core would have consequently become populated with dead cells. EB diameter would have been maintained but with a large proportion of dead cells, supporting observations in Figs 3.9C and D where constituent cell numbers decreased whilst EB diameter increased. Accumulation of necrotic cells within the core was also exacerbated by hypoxia and starvation within the core.

4.4.2. Embryonic Stem Cell Viability

The layered structure of the EB appeared to arise primarily from different levels of cell viability. Four layers could be distinguished including the surface, the outer and inner shells, and the core. The core was composed of dead or necrotic cells. The surface was composed cells which were alive and thriving but also disorganised as a result of rapid recent attachment. The inner and outer shells illustrated a transitional stage between alive and dead cells. The outer shell was composed of cells which were alive and resembled an condensed version of the surface. The inner shell was composed of cells which were necrotic and resembled the dead cells found at the core. Therefore, layering was simply a visualisation of cell death across the EB structure and not necessarily an artefact of ES cell aggregation. However, cell viability was acutely affected by properties such as cell density and organisation within the EB structure, and these properties were directly under the control of cell-cell aggregation. Therefore, layering was an indirect consequence of ES cell aggregation.

The difference in cell viability across the EB structure was most likely the result of hypoxia and/or starvation. Nutrient and gaseous exchange was made increasingly difficult as the distance between internal cells and the EB surface increased. It may have merely been that surface and outer shell cells had used all available nutrients and gases before they had chance to permeate towards the centre. Alternatively, permeation may have been severely restricted to the surface area due to constituent cell density. Another factor that may have had measurable effect is intercellular signalling which may have initiated apoptosis as a result of surrounding environmental cues (Lee et al., 2005).

Relative core to surface size could not be adequately calculated using the EB cross-sections since it was impossible to tell whether the section was cut through the widest part of the EB. Sections could have been taken from the widest region of all EBs so as to enable calculation of relative core and surface size. However, this would have been immensely difficult and time consuming. Consequently, only core/inner shell and surface/outer shell ES cell densities could be adequately quantified from cross-section images.

Engineered ES cells aggregated at an accelerated rate compared to control samples (Figs 3.7A and B). Logically, the rate of cell death should also have been accelerated. However, engineered EBs did not show signs of advanced necrosis or major structural differences. Therefore, engineering may not have detrimentally affected cell viability or altered the mode of EB formation. Similar results were observed at 5 x 10^4 and 2.5 x 10^5 cells/mL. This showed that increased cell number had no direct effect on cell viability. High numbers of cells in suspension meant increased chance collisions and rapid EB formation. Accelerated EB formation should therefore have conferred increased core necrosis, yet this was not the case. Consequently, seeding density had minimal to no effect on both EB structure and constituent cell viability, at least not directly. However, without knowing the relative sizes of the core and surface, it remains unclear as to what extent, if any, both engineering and seeding density had on cell viability within the EB structure. Core necrosis within engineered EBs may have been more or less advanced compared to that in control samples. The maximum seeding density employed was reduced from 1 x 10^6 to 2.5 x 10^5 cells/mL, to minimize the occurrence of EB agglomeration and ensure the results reflected individual EB dynamics.

4.4.3. Cell Density

As stated previously, ES cells aggregated to form EBs which exhibited a necrotic core and a thriving surface. Structural differences between the core and surface emphasized this distinction. Analysis of constituent cell densities provided insight concerning the discrepancy between surface and core cell viability. Surface density was calculated from the combined surface and outer shell layers, and core density was calculated from the combined core and inner shell layers. This was due to difficulty in definitively distinguishing between all four layers in most EB cross-sections. Both engineered and control EBs were significantly ($P \leq 0.001$) denser at the surface compared to the core (Figs 4.3C and D). The higher the density the more difficult it became for efficient nutrient permeation and gaseous exchange between internal cells and the surrounding environment. Consequently, core cells became starved and hypoxic, supporting the idea that the inner and outer shells represented a transitional stage between alive cells and eventual necrosis (Jiang et al., 2005). Thriving cells at the surface would also have been depositing large amounts of ECM. Layer upon layer of ECM would have trapped constituent cells and eventually prevented adequate penetration of nutrients into the EB structure.

Engineered EBs exhibited significantly ($P \leq 0.001$) greater cell density at both their core and surface compared to control EBs (Figs 4.3A and B). This showed that engineering had a direct effect on EB composition and overall structure. Engineered EBs did not show signs of advanced necrosis, which would have been expected with increased cell density. It is also possible that the increased density was simply not high enough to restrict permeability to a measurable level. Cell density did not significantly change over seeding density in both engineered and control EBs (Fig 4.3). ES cell aggregation kinetics were simply accelerated by high initial cell

numbers, but EB structure and density remained unaltered. In summary, engineered EBs composed of significantly ($P \leq 0.001$) denser ES cell populations compared to control EBs, but without detrimental effect on constituent ES cell viability.

Analysis of necrosis within the EB core via direct diameter measurement was difficult and prone to error. Instead, the degree of necrosis within the core was estimated as a percentage of the whole (Fig 4.4). The downside of this method was that it assumed all necrotic ES cells were positioned within the core. However, since this was concurrent with Live/Dead™ images of EBs showing all necrotic ES cells were within the core, the assumption was accepted. Even though ES cells within surface layers may have died, they were not visible within the Live/Dead™ images. This may have been because the fluorescence from live ES cells masked that from necrotic ES cells. Alternatively, ES cell mobility and reorganisation within the EB structure could have caused accumulation of necrotic ES cells within the core. Fig 4.4 shows no significant difference between engineered and control EBs, indicating that even though engineered EBs are denser than their control counterparts this did not affect constituent cell viability. In fact, it suggested that engineering may have enhanced cell viability. Engineered ES cells aggregated rapidly to form large EBs which one would expect to exhibit signs of advanced necrosis compared to slower aggregating control EBs. However, the percentage of dead cells within engineered EBs equalled that in control EBs. Therefore, engineering allowed for the formation of larger EBs without elevated cell death. It is therefore plausible that if engineering was fine tuned to form EBs of equal size to control samples, engineered EBs may resolve the problem of necrosis within the core completely. Engineering had clearly altered the 'EB size to core necrosis' ratio in a favourable manner, possibly through enhanced nutrient and gaseous exchange. This was emphasized by the fact that

engineered EBs did not show a significant increase in core necrosis until after 5 days, identical to control EBs. If engineering did not improve cell viability we would expect to see the observed increase in core necrosis at an earlier time point. However, the methodology used to calculate the percentage of core necrosis may not have been sensitive enough to highlight small but significant differences between engineered and control EBs. The cell count on a haemocytometer measures a minimum of 5×10^4 cells/mL. This meant that core necrosis was measurable only after the core reached a particular size threshold composing of $\geq 5 \times 10^4$ cells. Due to this, the true point at which necrosis began within the core remains unclear. Alternatively, time intervals between measurements may not have been sufficiently close together to highlight any differences. For example, engineered EBs may have exhibited a significant increase in core necrosis after 4 days, but the time points investigated in Fig 4.4 infer that it took 5 days.

The significant ($P \leq 0.001$) increase in core necrosis after 5 days illustrated that core necrosis was both time and size dependent. After 5 days of aggregation and growth, engineered EBs were ≥ 200μm in diameter and control EBs were ≤ 100μm (Fig 3.7A). This demonstrated that engineering enhanced cell viability in larger EBs. However, dependency on size may not have been an issue with constituent cell viability. There was no significant increase in size from 3 to 5 days in either engineered or control EBs at 5×10^4 and 1×10^6 cells/mL to correlate with the significant ($P \leq 0.001$) increase in core necrosis. The explanation may be that for a linear increase in 3D spherical size the number of constituent cells has to increase non-linearly. It is possible that after 5 days of aggregation the number of core cells had increased massively and consequently become necrotic. The observed cell death prior to day 5 may not have been a sign of core necrosis, but merely damaged cells during the

aggregation procedure. This was indicated by the fact that there was no significant increase in necrosis between 1 and 3 days. If it were true core necrosis then accumulation at the core would have shown an increase. There was a significant ($P \leq 0.001$) increase between 5 and 9 days of aggregation, illustrating that core necrosis increased over time. The percentage of core necrosis increased rapidly because of hypoxic conditions and starvation within the EB structure, but also, further cell damage on the surface and reorganisation towards the centre. Up to 80% of the EB became necrotic by day 9 highlighting a serious problem with extended EB culture (Fig 4.4B). It appeared that 3 days of EB culture was the maximum time allowed to avoid core necrosis. A variety of avenues could be explored to resolve this problem including vascularization of the EB structure (Gerecht-Nir et al., 2005, Goodwin, 2007, Feraud et al., 2001).

4.4.4. Embryoid Body Differentiation

ES cells within the thriving EB surface showed signs of differentiation towards numerous cell types (Fig 4.5). Both engineered and control samples exhibited a similar range of cell morphologies after 4 weeks culture in SCM, indicating that engineering did not detrimentally affect ES cell differentiation potential. Cell morphologies included possible endothelial (Fig 4.5A) and fibroblastic cells (Fig 4.5E) amongst others. Previous studies have shown that primitive endoderm cells are a primary cell type to differentiate during the EB stage (Hamazaki et al., 2004, Capo-Chichi et al., 2005). Concurrent with these findings, the morphology of the most abundant cell type observed on the EB surface matched that of cell derivatives from primitive endoderm (Lee and Anderson, 2008). However, it may simply have been that these primitive endoderm-like cells proliferated more rapidly than other cell

types and therefore spread over the surface quickly. Primitive endoderm cells inherently migrate towards the surface and therefore would be expected to coat the EB (Yang et al., 2007, Plusa et al., 2008, Rula et al., 2007, Chazaud et al., 2006). If this cell type was primitive endoderm cells it would provide some explanation for necrosis within the core. Effectively, they would have acted as a protective skin surrounding the EB and provided a barrier against unregulated nutrient and gaseous diffusion (Hamazaki et al., 2004, Sachlos and Auguste, 2008). This implies that core necrosis may not have been solely dependent on EB size and aggregation time, but on ES cell differentiation. However, since the purpose of EB formation is ES cell differentiation this can not be avoided, albeit directing differentiation during EB formation may have advantageous effects on constituent ES cell viability. As for heart/muscle cell differentiation, cultures of beating cells were observed in EB samples allowed to settle, adhere and spread on tissue culture plastic and grown for ~14 days. Other studies have also demonstrated differentiation of heart cells from EBs (Ng et al., 2005). These have found that factors such as constituent ES cell number have a direct effect on downstream differentiation. As engineering directly affected the number of ES cells involved in EB formation in a controlled manner, it may provide a practical means of differentiation manipulation. Internal ES cells within the core exhibited a small spherical morphology similar to that of undifferentiated ES cells in continuous culture (Figs 4.5E, 4.6B and C). This is simply because core ES cells would have become necrotic and died before having the chance to differentiate. Another indication that ES cells within the core were undifferentiated and necrotic or dead is the distinct lack of ECM deposition. Cells within the surface exhibited extensive ECM deposition as observed by a thick fibrous mesh binding adjacent cells together (Fig 4.6A). This dense layer of ECM deposition

most probably contributed to the decrease in surface permeability for nutrient and gaseous exchange.

The observations above were taken from 4 week old EBs exhibiting advanced stages in formation and differentiation. Analysis of early stage EBs was primarily via immuno-labelling of EB cross-sections after 9 days of aggregation (Fig 4.7). Attempts to investigate EBs from earlier time points were made, however, these EBs were either too small or simply too fragile to withstand processing and/or retrieve high-grade sections. Engineered EBs at both 5×10^4 and 2.5×10^5 cells/mL exhibited mesoderm differentiation at the surface and within the core (Figs 4.7A and J) supporting the presence of heart/muscle cells discussed earlier. Differentiation observed within the core supports the earlier hypothesis that engineering enhanced cell viability within the core. However, it is unclear whether these cells differentiated within the core or simply migrated there after differentiating at the surface as a consequence of primitive endoderm migrating to the surface (Rula et al., 2007). Control EBs at both 5×10^4 and 1×10^6 cells/mL did not show positive labelling for Brachyury, indicating that engineered EBs exhibited a greater propensity for mesoderm differentiation. Control EBs exhibited endoderm differentiation where engineered EBs did not (Figs 4.7E, H, N and O). Endoderm may therefore be the preferred lineage during initial EB differentiation, supporting previous findings (Rust et al., 2006, Yang et al., 2002, Morrisey et al., 2000). Differentiation was potentially isolated at the surface unlike mesoderm differentiation in engineered samples. This may be that cells within control EBs were less mobile than their engineered counterparts, or that engineered EBs were at a more advanced stage of structural reorganisation than control EBs. Neither engineered nor control EBs exhibited ectoderm differentiation at either seeding density. This may be due natural

ectoderm differentiation within the EB taking longer than 9 days of aggregation without exogenous cues such as retinoic acid (Bain et al., 1995). Other reasons include, presence of unknown inhibitory factors or simply that any positive labelling was not at a detectable level (Murashov et al., 2004).

PCR was employed to amplify the same germ layer markers as those labelled for immuno-fluorescence images (Fig 4.8). PCR data at first supported the observations made in Fig 4.7. However, there were a few discrepancies, such as the expression of Brachyury and Nestin in control EBs, and expression of Gata-4 in engineered EBs. Immuno-fluorescence images exhibited no expression of these markers in corresponding EB sections. This could be due to the fact that ES cell differentiation spontaneously occurred in patches rather than a continuous sheet encompassing the EB surface. Cross-sections in Fig 4.7 not exhibiting fluorescence may simply have been cut through regions of the EB where there were no differentiated ES cells. If we hypothesise that an EB is a perfect sphere measuring 100μm in diameter, then a 4μm thick cross-section views ~4% of the entire EB surface area. The surface area of a sphere is $4.\pi.r^2$, where r is radius. The circumference of the circular cross-section is $\pi.d$, where d is diameter. The surface area of the circular cross-section is calculated by multiplying the circumference by the thickness. The surface area of the cross-section is then converted to a percentage of the whole EB surface. This percentage falls as the EB increases in size. It is therefore highly possible that differentiated areas were not included within the cross-sections. Alternatively, discrepancies could be due to the higher sensitivity of PCR. Where fluorescence was too weak to be visible, there were adequate amounts of mRNA for PCR amplification.

Unlike control EBs, PCR revealed that engineered EBs exhibited no ectoderm expression during the 9 day aggregation period. This indicated that engineering may

have had a direct or indirect negative effect on Nestin expression. Both engineered and control samples exhibited mesoderm and endoderm differentiation. This is consistent with the natural sequence of differentiation events in which mesendoderm is primarily and possibly preferentially generated (Vallier et al., 2004, Hamazaki et al., 2004, Izumi et al., 2007, Smith et al., 2008). Interestingly, engineered samples showed reduced levels of endoderm and ectoderm expression compared to control samples. Consequently, mesoderm formation appeared indirectly enhanced, indicating potential for increased homogeneity of mesoderm derived cell types. Strong Oct-4 expression appeared in both engineered and control samples, suggesting that the majority of constituent cells remained undifferentiated (Fig 4.8). This is consistent with only surface ES cells undergoing differentiation.

The potentially enhanced mesoderm differentiation within engineered samples was investigated further by immuno-labelling for cadherin-11 expression (Fig 4.9). It has previously been shown that cadherin-11 mediated ES cell-ES cell interaction has an important role to play in MS cell differentiation towards the osteogenic and chondrogenic lineages (Kii et al., 2004). Osteoblasts have also been successfully isolated by purification of cadherin-11 positive cells via magnetically activated cell sorting (Bourne et al., 2004). Therefore, the potential strong presence of cadherin-11 expression within engineered EBs (Fig 4.9A) indicated that engineering may also exhibit enhanced differentiation of osteogenic lineages compared to control EBs. However, lack of fluorescence quantification meant that difference in cadherin-11 expression between engineered and control samples remained unclear.

4.5. Conclusions

In summary, engineering appeared to enhance cell viability within the EB structure even though they were larger in diameter and exhibited greater cell density at both their core and surface. EBs exhibited a layered structure which could be broken into four sections including the surface, outer shell, inner shell and core. The core composed of dead or necrotic cells possibly resulting from a lack of efficient nutrient and gaseous exchange, whilst the surface composed of thriving cells. Necrosis was indicated by swollen cell nuclei, lack of membrane blebbing and cell debris. The inner and outer shells illustrate transitional stages between surface and core states. The fact that internal cells were necrotic meant that only the EB surface underwent differentiation. A multitude of cell morphologies showed that engineering did not detrimentally affect ES cell differentiation. In fact, engineered EBs showed indirect enhancement of mesoderm formation through possible inhibition or downregulation of ectoderm and endoderm formation. It is possible that increased cell number and density within the engineered EB caused enhanced mesoderm differentiation. However, further analysis would be required to elucidate any direct link. Excitingly, engineering of the ES cell surface has demonstrated a distinct ability to influence aggregation and therefore provides ideal means to investigate these variables further. Mesoderm enhancement has important ramifications for engineered driven differentiation of ES cells towards the osteogenic lineage, such as increasing homogeneity of resultant osteogenic cultures (Mateizel et al., 2008). Positive immuno-labelling for osteoblast cadherin (cadherin-11) within engineered EBs indeed marked potential osteogenic differentiation.

Chapter 5

5. Results

Embryoid Body Osteogenic Potential

5.1. Introduction

Previous studies have demonstrated selective differentiation of osteoblasts from ES cells via EB culture with osteo-inductive factors including Asc, BGP and the glucocorticoid Dex (Bourne et al., 2004, Bielby et al., 2004, Handschel et al., 2008a). *In vitro* cultured osteoblasts hold great promise for tissue repair and regeneration of bone, damaged as a result of disease and trauma (Grayson et al., 2008, Heng et al., 2004). Generating transplantable from ES cells bypasses many problems associated with existing bone repair strategies, such as genetic abnormalities within auto- and allografts, disease transmission from xenografts, micromechanical mismatch and biocompatibility of prosthetic implants, and cell availability (Vaccaro et al., 2002, Marquis et al., 2009, Pappalardo et al., 2007, Patil et al., 2009). Other exciting applications of osteoblast generation include *in vitro* analysis of early bone development and investigative tool for pharmacological and cytotoxic testing of bone-related drugs and biomaterials (Wdziekonski et al., 2006, Cao et al., 2005).

Analysis of cell-cell interaction revealed cadherin-11 expression within engineered EBs, a surface cell-adhesion molecule important in osteogenic differentiation (Kawaguchi et al., 2001, Bourne et al., 2004, Kii et al., 2004). Hypothesizing that surface engineering may induce differentiation towards osteogenic precursors, engineered EBs were cultured in, osteo-inductive (Asc, BGP and Dex) and control (Asc) media. Here is shown that engineered EBs exhibit enhanced osteoblastic differentiation assessed by bone nodule formation, ALP activity and expression of osteogenic markers Runx2 and OPN (Sottile et al., 2003, Chaudhry et al., 2004, Morris et al., 1992, Karner et al., 2007, Garreta et al., 2006). Evidently, engineered cell-cell interactions during EB formation have subsequent effects on ES cell differentiation, apparently influencing intercellular and possibly intracellular signalling pathways in favour of osteogenic differentiation.

5.2. Methods and Materials

5.2.1. Osteogenic Differentiation without the Embryoid Body Formation

Engineered and control ES cells were taken from continuous culture (Chapter 2) and seeded directly into gelatin-coated tissue culture plates in osteo-inductive and control media for 4 weeks. Comparative samples were set up in which ES cells had been allowed to form EBs before culture in osteo-inductive or control media. ES cells were seeded into mass suspension over a range of densities (5×10^4 to 2.5×10^5 cells/mL), rotated for 6hrs at 15rpm and cultured for 3 days. Osteogenic differentiation was quantified after 4 weeks by bone nodule counts and ALP activity (Chapter 2).

5.2.2. Bone Nodule Quantification

Both engineered and control ES cells were cultured in mass suspension at a seeding density ranging from 5×10^4 cells/mL to 2.5×10^5 cells/mL. Resulting EBs were cultured for 1 to 9 days before transfer to tissue-culture treated plates and incubated in either osteo-inductive or control media for a period of 4 weeks. Alizarin Red stain was employed to highlight bone nodules within these cultures after 4 weeks (Chapter 2). Quantification of bone nodules was assessed by colorimetric assay and direct counting.

5.2.2.1. Colorimetric Assay

Once cell cultures were stained with Alizarin Red they were imaged at 10x magnification using a stereomicroscope (Nikon Eclipse TS100). Cultures were covered in 10% cetyl-pyridinium chloride (CPC) and gently rotated at room

temperature for a maximum of 10mins (Gregory et al., 2004, Srouji et al., 2005). Once the red stain had leached from the culture, 300µl aliquots were transferred to a 96well plate. Absorbance was measured at 595nm using a KC4 plate reader. A blank measurement of 10% CPC solution was deducted from all sample readings. An average of three individual readings was taken.

5.2.2.2. Bone Nodule Count

Alizarin Red positively stained calcium deposits also known as bone nodules. Bone nodules within cultures were viewed and counted using a stereomicroscope (Nikon SMZ1500) set between 1x and 4x magnification. All bone nodules were counted in cultures containing minimal stained areas which could be easily distinguished from one another. Cultures that contained many bone nodules made counting very difficult as numbers were 100 to 1000x higher than those with minimal bone nodules. Consequently, a representative area of the whole culture was analyzed to minimize the number of bone nodules counted (Fig 5.1). The entire well was divided into 8 sections and all bone nodules within one section were counted and multiplied by 8. Three individual wells for each sample were quantified and an average taken. Duplicate cultures of all samples were quantified by Hoescht assay for total DNA content (Chapter 2). All readings were subsequently equalized for DNA content of 1 x 10^6 cells.

CPC is a cationic quaternary ammonium compound which is often used as a surfactant. It can cause disruption of the calcium phosphate crystals within bone nodules through solid/liquid phase adsorption (Dutour-Sikiric and Furedi-Milhofer, 2006). Adsorption affects further growth and causes morphological aberrations through competition with Ca^{2+} ions for available phosphate ions

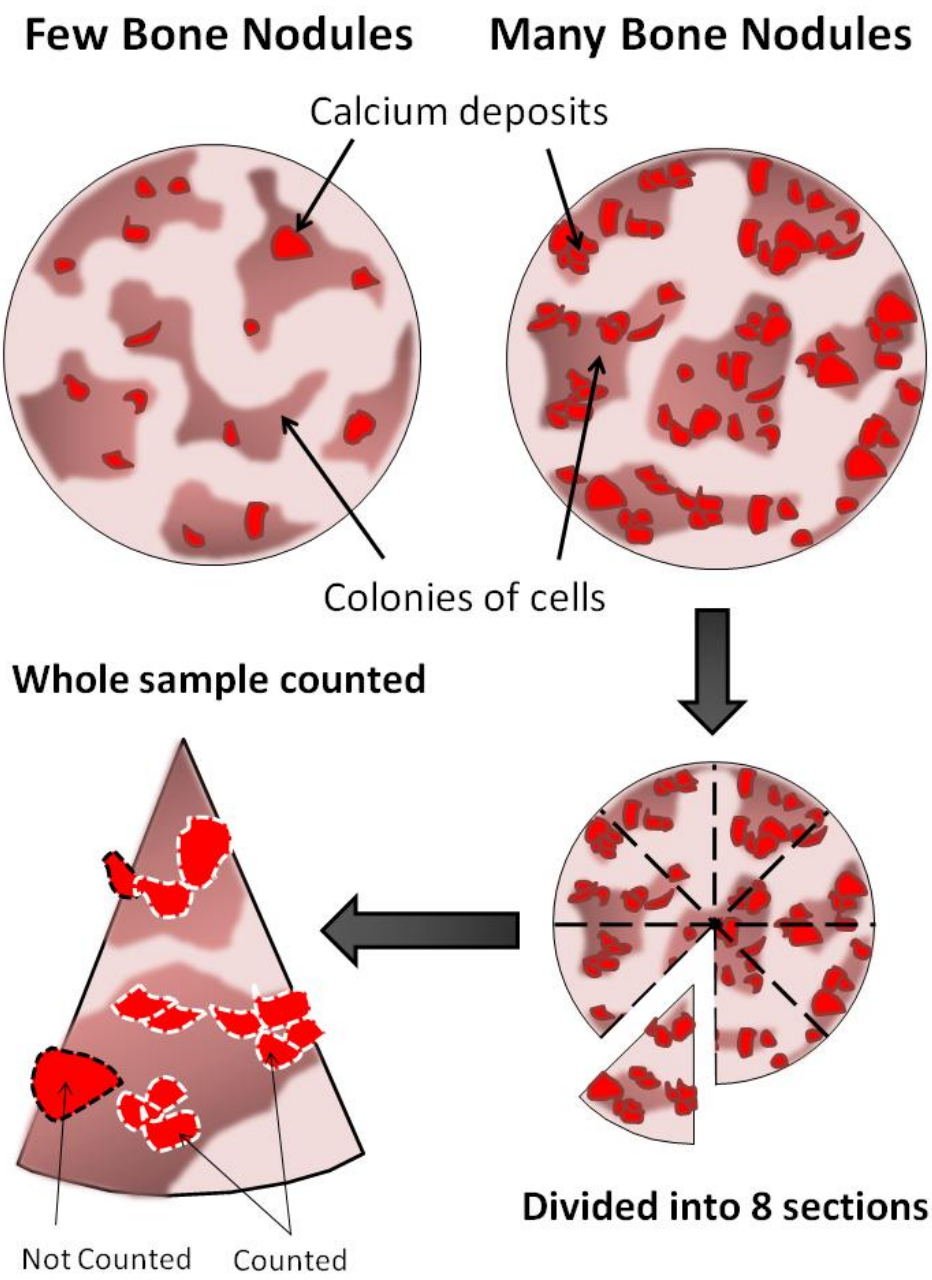

Figure 5.1: Quantification of Alizarin Red stained calcium deposits. Where cultures showed minimal bone nodule formation, the whole sample was analyzed. Where cultures exhibited large numbers of bone nodules, wells were divided into 8 equal sections. All calcium deposits within 3 sections were counted and an average calculated. Values were then multiplied by 8 to represent the total bone nodule number.

(Horvath et al., 2000). The lattice structure of the calcium phosphate crystals can become unstable and eventually end in dissolution. These changes in the structural integrity of calcium phosphate crystals causes precipitation of intercalated Alizarin Red stain into suspension.

5.2.3. Plate Coating

To investigate the interaction between EBs and ECM components, plates in which EB suspensions were cultured for 4 weeks were pre-coated. Plates were removed from packaging and washed briefly with PBS. Four plates were set up for each coating included gelatin, fibronectin and collagen (BD Biosciences) and control uncoated plates. Each coating was applied within the recommended concentration limits quoted by the supplier (50μg/mL in PBS). Wells were covered in 1mL of the appropriate coating suspension for 30mins at room temperature. Excess solution was aspirated and EB suspensions were then directly transferred to the wells. It was found that gelatin-coated plates provided inexpensive enhancement of EB adhesion compared to both fibronectin and collagen-coated plates. All subsequent experiments employed gelatin-coated plates.

5.2.4. Osteogenic Differentiation in Settled and Dissociated Embryoid Bodies

ES cells were seeded into suspension and cultured for up to 9 days before resulting EBs were transferred into either osteo-inductive or control media (Chapter 2). EB suspensions were seeded into new wells pre-coated with 0.1% gelatin for 20mins at room temperature (Bielby et al., 2004, Randle et al., 2007). Suspensions were cultured for 4 weeks in stationary conditions to allow EBs to settle and adhere. Duplicate samples were aggregated for up to 9 days then transferred to a 15mL Falcon tube and centrifuged at 1000rpm for 5mins. Supernatant was aspirated and

the pellet washed in PBS before being suspended in 37°C trypsin/EDTA solution for a maximum of 5mins. The suspension was pipetted gently until EBs were fully dissociated. SCM was added and the suspension centrifuged. Dissociation was checked under a microscope for any large cell clumps. The whole single cell suspension was transferred to a gelatin-coated well in either osteo-inductive or control media and cultured for 4 weeks.

5.2.5. Embryoid Body Differentiation and Osteogenic Differentiation

5.2.5.1. Embryoid Body Stage

To investigate the effect of EB stage on osteogenic differentiation, both engineered and control ES cells were seeded into mass suspension, rotated for 6hrs at 15rpm and cultured between 1 and 9 days. EBs were transferred on days 1, 3, 5, 7 and 9 into gelatin-coated plates in either osteo-inductive or control media and cultured for a further 4 weeks. Osteogenic differentiation was subsequently quantified by bone nodule counts and analysis of OPN and Runx2 expression via PCR amplification (Chapter 2) (Sottile et al., 2003).

5.2.5.2. Osteogenic Differentiation over Time

To investigate osteogenic differentiation over time, engineered and control ES cells were seeded at 5 x 10^4 cells/mL into mass suspension, rotated at 15rpm for 6hrs and cultured for 3 days. All EBs were transferred to gelatin-coated plates in either osteo-inductive or control media and cultured for a further 4 weeks. Duplicate cultures prepared alongside to be analyzed by Hoescht assay. After 1, 2, 3 and 4 weeks, osteogenic differentiation was quantified by bone nodule counts. After 2 and 4 weeks, OPN and Runx2 expression were analyzed by PCR amplification (Chapter 2).

5.2.5.3. Bone Extraction

PCR amplification experiments for osteogenic markers OPN and Runx2 required validation via amplification from positive control samples. Adult mouse femurs were used as positive control samples. The hind legs of an adult mouse were amputated and mechanically stripped of skin and muscle with forceps and a scalpel blade in a PBS bath. Extracted bones were washed thoroughly in PBS and then chopped into smaller sections. Sections were allowed to settle and excess PBS was aspirated. Bone fragments were suspended in enzyme digestion solution (0.14% collagenase 1A and 0.05% trypsin II-S in DMEM), rotated and incubated at 37°C and 5% CO_2 in a humidified atmosphere for 20 to 30mins (Fuller and Chambers, 1995, Sakaguchi et al., 2004, Chambers et al., 1985). Suspensions were rotated until solution appeared cloudy and turbid. Once digested, the suspensions were washed through a 100µm sieve with PBS to remove the bone fragments. Samples were subsequently centrifuged for 5mins at 1000rpm and supernatant was aspirated. Pellets were suspended and washed in PBS. Where samples did not contain adequate amounts of extracted cellular material, bone fragments were incubated a second time with fresh enzyme digestion solution. Large cell pellets were lysed in RLT buffer in preparation for PCR amplification (Chapter 2).

5.3. Results

5.3.1. Embryoid Body Adhesion

To investigate osteogenic differentiation within both engineered and control samples over time, EBs had to first be attached to the wells of cell culture plastic plates. To enhance the adhesive properties of the plastic, wells were pre-coated with ECM components. Components were selected for their cell adhesion properties, cost and availability. Figs 5.2 and 5.3 show images taken of EB adhesion over 28 days of culture on uncoated, fibronectin, gelatin and collagen-coated plates in engineered and control samples, respectively. EBs adhered more rapidly when cultured in osteo-inductive media compared to control media. This is illustrated in Fig 5.2 where EBs had adhered after just 7 days when cultured in osteo-inductive media on fibronectin and gelatin-coated plates. Equivalent EBs cultured in control media had not adhered to fibronectin and gelatin-coated plates until after 14 days. However, control EBs adhered to fibronectin and gelatin-coated plates after 14 days regardless of whether they were cultured in osteo-inductive or control media (Fig 5.3). Another discrepancy between engineered and control samples was observed in EBs seeded onto uncoated plates. Engineered EBs did not adhere to uncoated plates after 28 days in either osteo-inductive or control media. Control EBs had adhered to uncoated plates 7 days after initial seeding when cultured in osteo-inductive media, but had not adhered when cultured in control media up to 28 days later. One clear similarity between engineered and control samples was observed in EBs seeded onto collagen-coated plates. EBs did not adhere to collagen-coated plates up to 28 days after initial seeding whether cultured in osteo-inductive or control media. Both engineered and

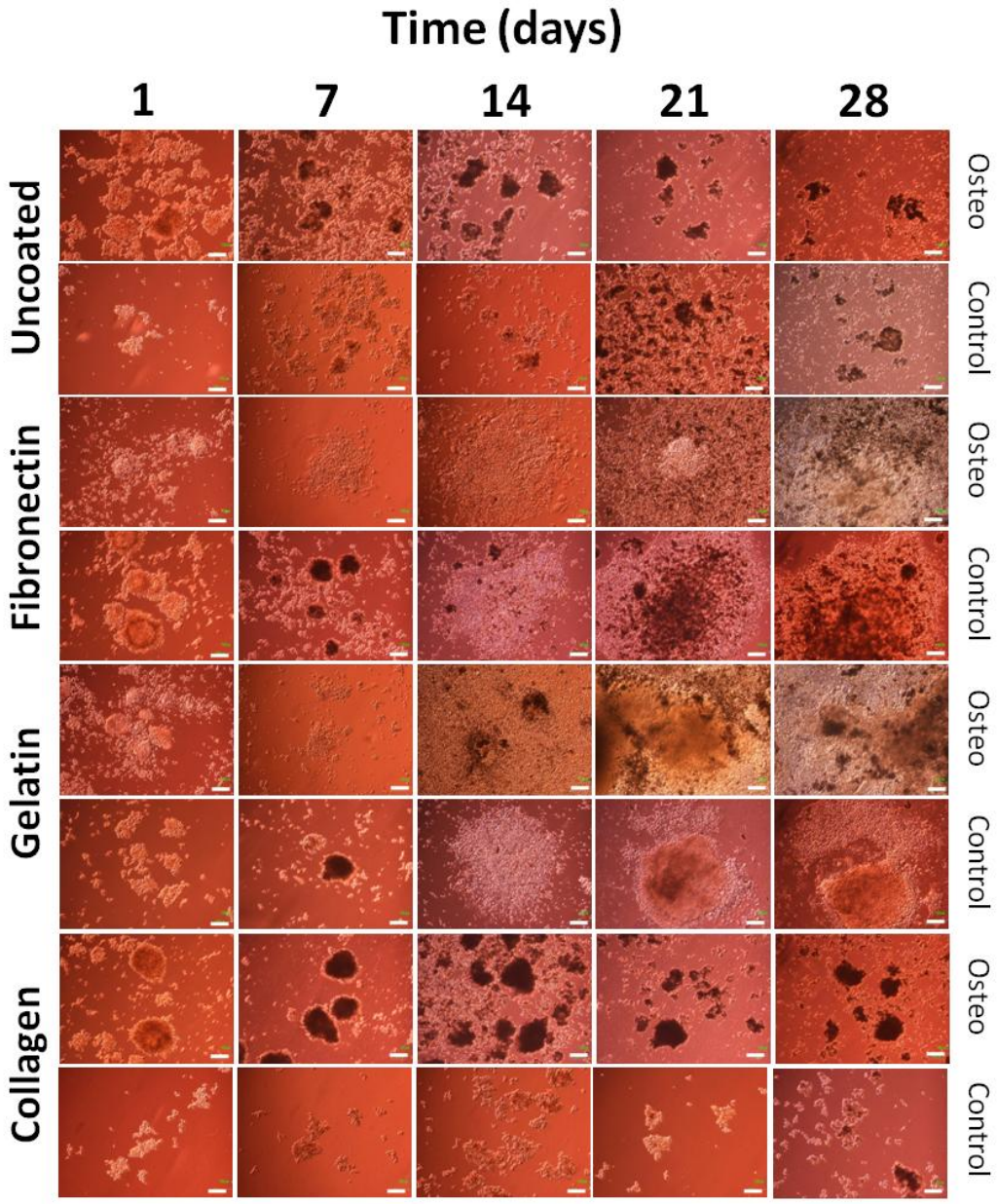

Figure 5.2: EB adhesion and spreading in engineered samples. Engineered ES cells were seeded into mass suspension at 5 x 10^4 cells/mL rotated at 15rpm for 6hrs and cultured for 3 days at 37°C and 5% CO_2 in a humidified atmosphere. After 3 days, EBs were transferred to uncoated, fibronectin, gelatin and collagen-coated plates and cultured in either osteo-inductive or control media for 4 weeks. Cultures were imaged every week during the 4 week incubation. Scale bars measure 100µm.

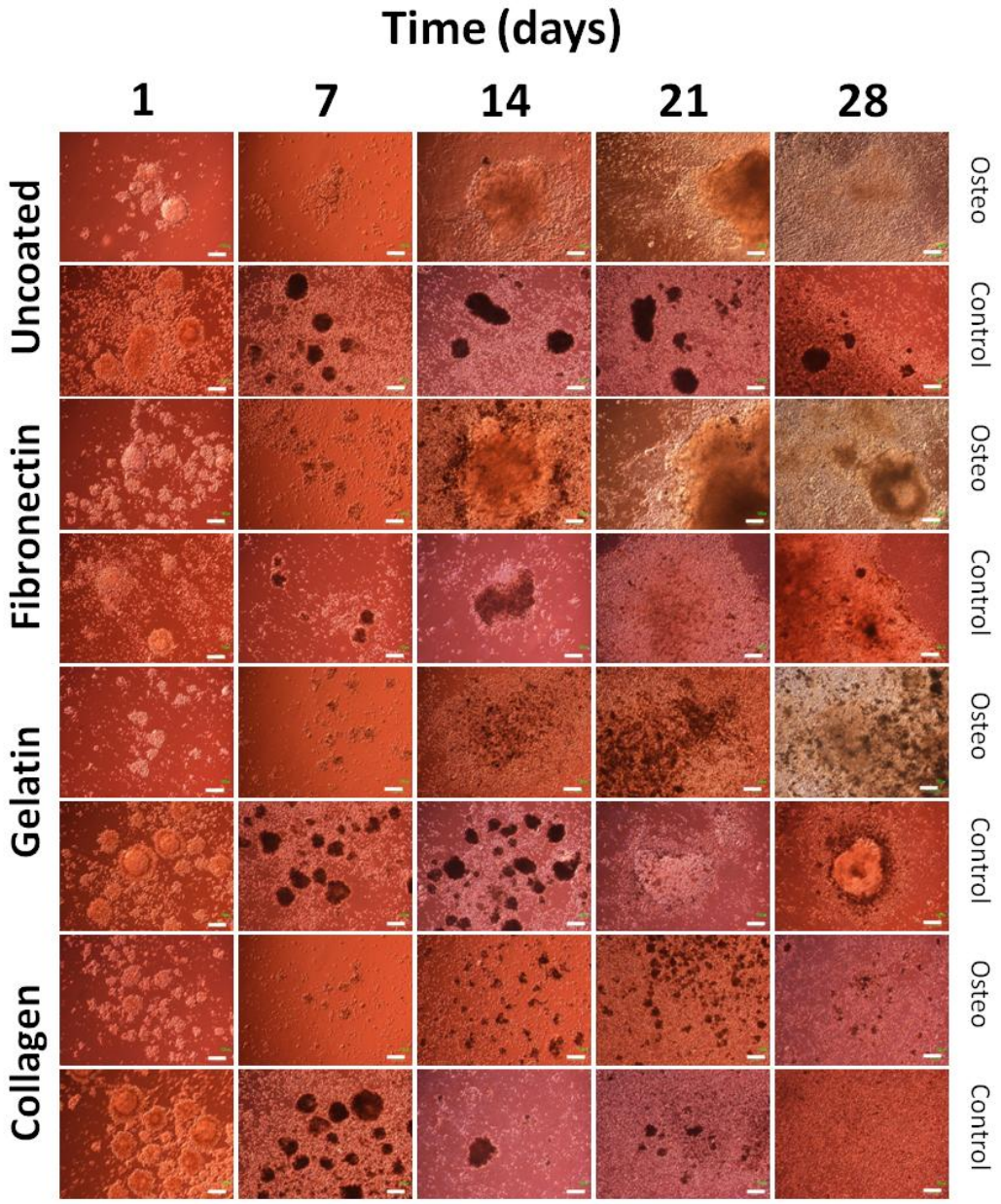

Figure 5.3: EB adhesion and spreading in control 1 samples. Control 1 ES cells were seeded into mass suspension at 5 x 10^4 cells/mL rotated at 15rpm for 6hrs and cultured for 3 days at 37°C and 5% CO_2 in a humidified atmosphere. After 3 days, EBs were transferred to uncoated, fibronectin, gelatin and collagen-coated plates and cultured in either osteo-inductive or control media for 4 weeks. Cultures were imaged every week during the 4 week incubation. Scale bars measure 100µm.

control EBs exhibited a lightly coloured and translucent appearance 1 day after transfer to either osteo-inductive or control media. However, as early as 7 days later, non-adhered EBs began to show a darkened appearance. EBs which had adhered and spread outwards also exhibited darkened areas.

Fig 5.4 shows the individual stages of EB adhesion and spreading in control 1 and engineered samples on gelatin-coated plates. In control 1 samples, free-floating EBs were observed after initial seeding which appeared as translucent spherical cell aggregates. After 3 days in culture, control 1 EBs had made contact with the well surface and had loosely attached whilst maintaining their stereotypical spherical shape (Fig 5.4B). Once attached, control 1 EBs began to flatten and spread outwards. Cells that were morphologically different to initial ES cells, migrated outwards from the central EB mass to form a fringe after 7 days (Fig 5.4D). The cell mass of these flattened control 1 EBs continued to proliferate and spread outwards across this fringe of cells. By day 12 control 1 EBs had spread out completely and formed a thick continuous layer which continued to grow until the well surface was covered (Fig 5.4F). Engineered EBs exhibited a more rapid, but similar attachment process (Figs 5.4G to L). The site of initial attachment could still be distinguished throughout adhesion and spreading.

5.3.2. Embryonic Stem Cell 'vs' Embryoid Body Differentiation

Osteogenic differentiation was quantified by ALP and Alizarin Red assay (Figs 5.5 and 5.6, respectively). ALP activity is a standard marker for osteogenic differentiation however it is also a marker for ES cell pluripotency. Research has shown that ALP activity, whilst high in pluripotent ES cells, decreases at the start of differentiation and becomes elevated within particular differentiated cell types

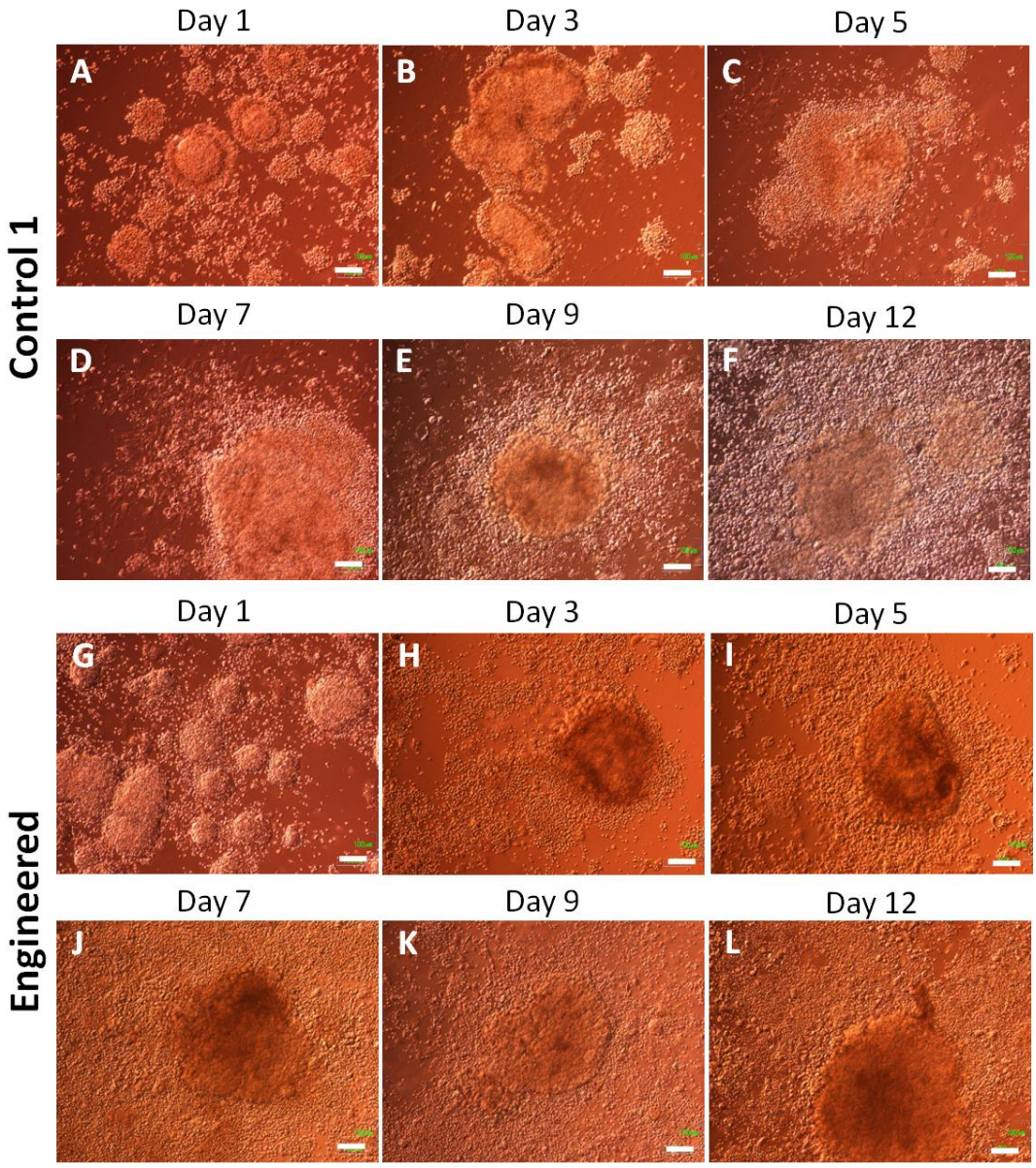

Figure 5.4: EB adhesion and spreading on gelatin-coated plates in engineered and control 1 samples. Control 1 (A to F) and engineered (G to L) ES cells were seeded into mass suspension at 1 x 10^6 cells/mL rotated at 15rpm for 6hrs and cultured for 3 days at 37°C and 5% CO_2 in a humidified atmosphere. After 3 days, EBs were transferred to gelatin-coated plates and cultured for 12 days. Representative images were taken after 1, 3, 5, 7, 9 and 12 days. Scale bars measure 100µm.

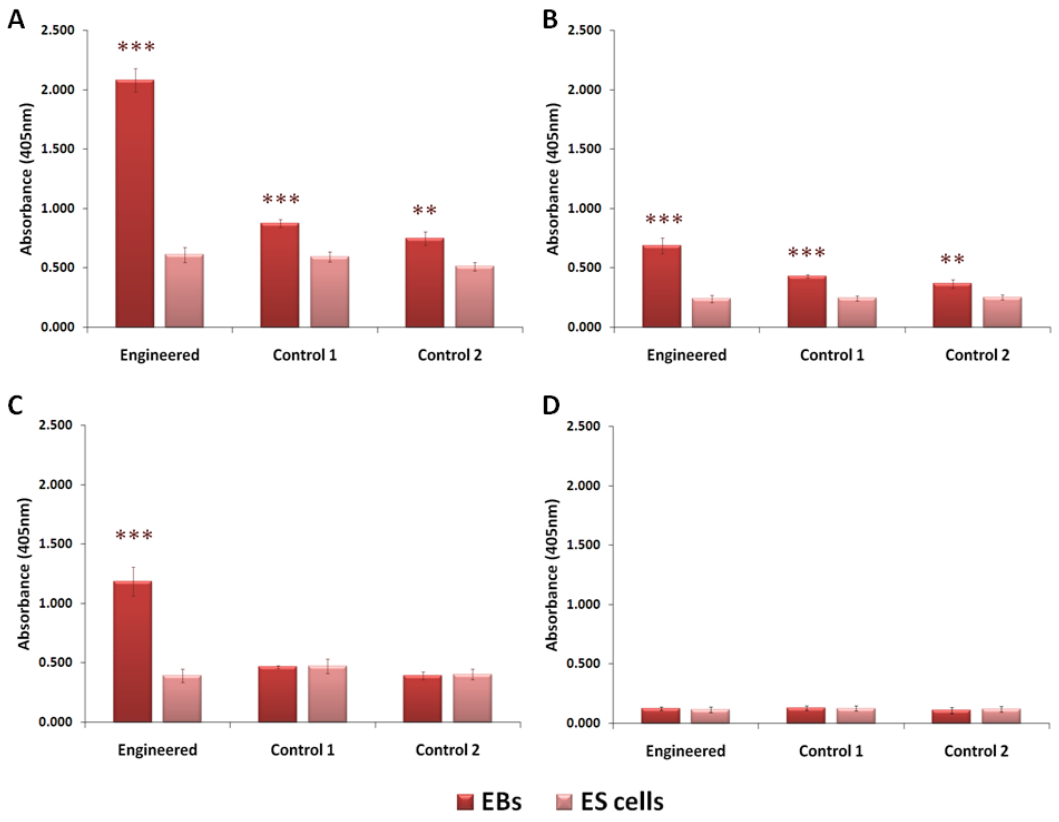

Figure 5.5: EB 'vs' ES cell differentiation and osteogenic differentiation; assessed by ALP assay (Chapter 2). Engineered and control ES cells were seeded directly into either osteo-inductive (A and B) or control (C and D) media directly from continuous culture at 5 x 10^4 cells/mL (A and C) and 2.5 x 10^5 cells/mL (B and D). Alternatively, ES cells were seeded into mass suspension rotated at 15rpm for 6hrs and cultured for 3 days at 37°C and 5% CO_2 in a humidified atmosphere. After 3 days, these EBs were transferred to either osteo-inductive or control media as appropriate. After transfer to osteogenic culture, all samples were cultured for 4 weeks. After 4 weeks, osteogenic differentiation was quantified by ALP activity assay. All experiments were repeated in triplicate and each experiment recorded ALP activity in triplicate; n = 9. *** $P \leq 0.001$, ** $P \leq 0.01$, * $P \leq 0.05$. Error bars = S.E.M.

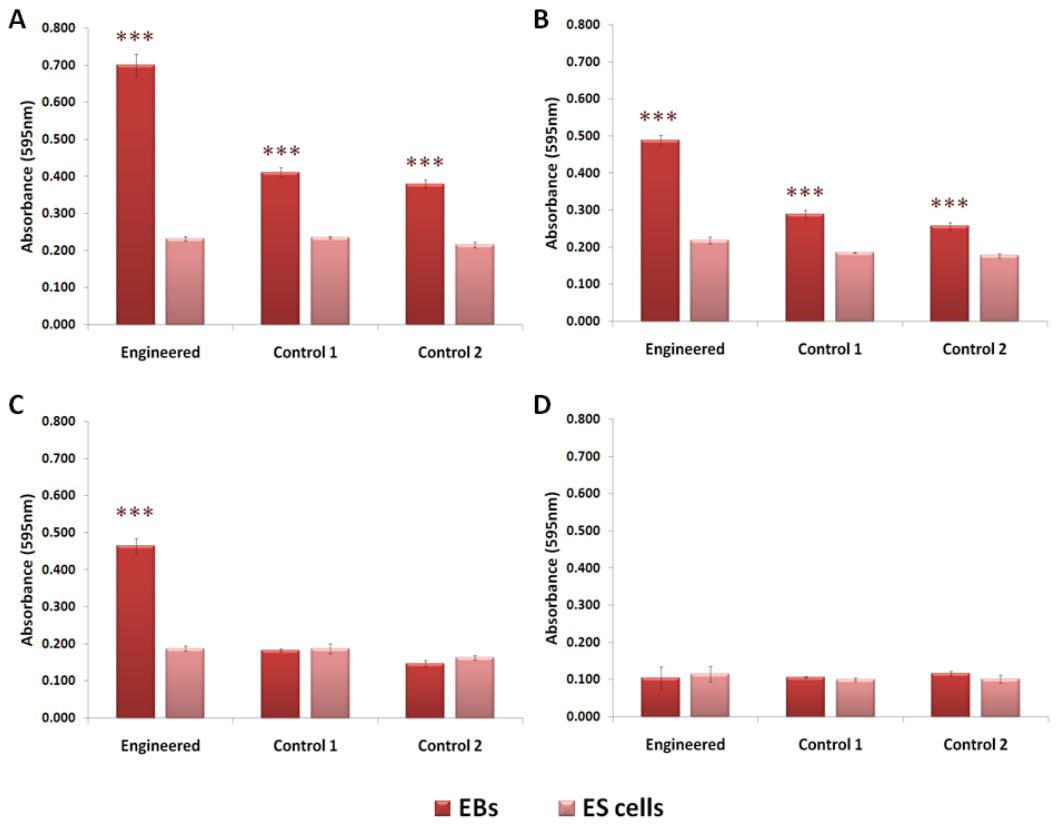

Figure 5.6: EB 'vs' ES cell differentiation and osteogenic differentiation; assessed by Alizarin Red assay. Engineered and control ES cells were seeded directly into either osteo-inductive (A and B) or control (C and D) media directly from continuous culture at 5 x 10^4 cells/mL (A and C) and 2.5 x 10^5 cells/mL (B and D). Alternatively, ES cells were seeded into mass suspension rotated at 15rpm for 6hrs and cultured for 3 days at 37°C and 5% CO_2 in a humidified atmosphere. After 3 days, these EBs were transferred to either osteo-inductive or control media as appropriate. After transfer to osteogenic culture, all samples were cultured for 4 weeks. After 4 weeks, osteogenic differentiation was quantified by Alizarin Red assay. All experiments were repeated in triplicate and each experiment recorded Alizarin Red staining in triplicate; n = 9. *** $P \leq 0.001$, ** $P \leq 0.01$, * $P \leq 0.05$. Error bars = S.E.M.

(Berrill et al., 2004). EB samples cultured in osteo-inductive media showed significant ($P \leq 0.001$) increase in both ALP activity (Figs 5.5A and B) and bone nodule formation (Figs 5.6A and B) compared to ES cell samples. This was observed at both 5×10^4 and 2.5×10^5 cells/mL, respectively. Engineered EB samples exhibited significantly greater osteogenic differentiation than control EB samples when cultured in osteo-inductive media. Where ES cells were cultured in osteo-inductive media, no difference was observed between engineered and control samples. No difference was observed between engineered and control ES cell samples also cultured in control media, regardless of initial seeding density. At 2.5×10^5 cells/mL, EBs cultured in control media also showed no change in osteogenic differentiation between engineered and control samples. However, at 5×10^4 cells/mL engineered EB samples exhibited a significant ($P \leq 0.001$) increase in osteogenic differentiation when cultured in control media (Figs 5.5C and 5.6C). These results indicated that engineered ES cells significantly ($P \leq 0.001$) increased osteogenic differentiation when cultured through the EB stage. This was observed in both osteo-inductive and control media cultures. All samples cultured in osteo-inductive media exhibited greater levels of osteogenic differentiation than comparable samples cultured in control media. This indicated that osteo-inductive media alone, effectively directed ES cell differentiation towards the osteogenic lineage. All of the trends observed in Fig 5.5 were reflected in Fig 5.6 demonstrating a link between ALP activity and bone nodule formation.

5.3.3. Settled 'vs' Dissociated Embryoid Body Differentiation

ES cells were aggregated in suspension for 3 days to form EBs before a 4 week incubation in either osteo-inductive or control media. Duplicate EB samples were

dissociated to single cell suspensions before the 4 week incubation. Figs 5.7 and 5.8 show quantification of osteogenic differentiation within these samples through ALP activity and bone nodule formation, respectively. All samples cultured in osteo-inductive media showed greater osteogenic differentiation than comparable samples cultured in control media (Figs 5.7A and C). This trend was observed in both settled and dissociated EB samples (Figs 5.8A and C). Settled EB samples exhibited significantly ($P \leq 0.001$) increased ALP activity and bone nodule formation in both engineered and control samples compared to dissociated EB samples (Figs 5.7B and 5.8B). This was observed at both 5×10^4 and 2.5×10^5 cells/mL, but only when samples were cultured in osteo-inductive media. No difference was observed between settled and dissociated EB samples when cultured in control media (Figs 5.7D and 5.8D). However, settled EBs from engineered samples did show a significant ($P \leq 0.001$) increase in osteogenic differentiation when cultured in control media at 5×10^4 cells/mL, in comparison to dissociated EBs (Fig 5.7C). Both settled and dissociated EBs exhibited increased ALP activity and bone nodule formation in engineered samples compared to control samples. However, this was only observed in samples originally seeded at 5×10^4 cells/mL. At high initial seeding density in control media, engineered samples did not exhibit a marked increase in either ALP activity or bone nodule formation when compared to control samples (Figs 5.7D and 5.8D). As previously mentioned, all trends observed in Fig 5.7 reflected those in Fig 5.8, again highlighting a link between ALP activity and bone nodule formation. However, the relationship between them is more complicated than first appears. The relative changes in ALP activity were not matched by those in bone nodule formation between samples. For example, the relative decrease in ALP activity between engineered samples cultured in osteo-inductive and control media was greatly

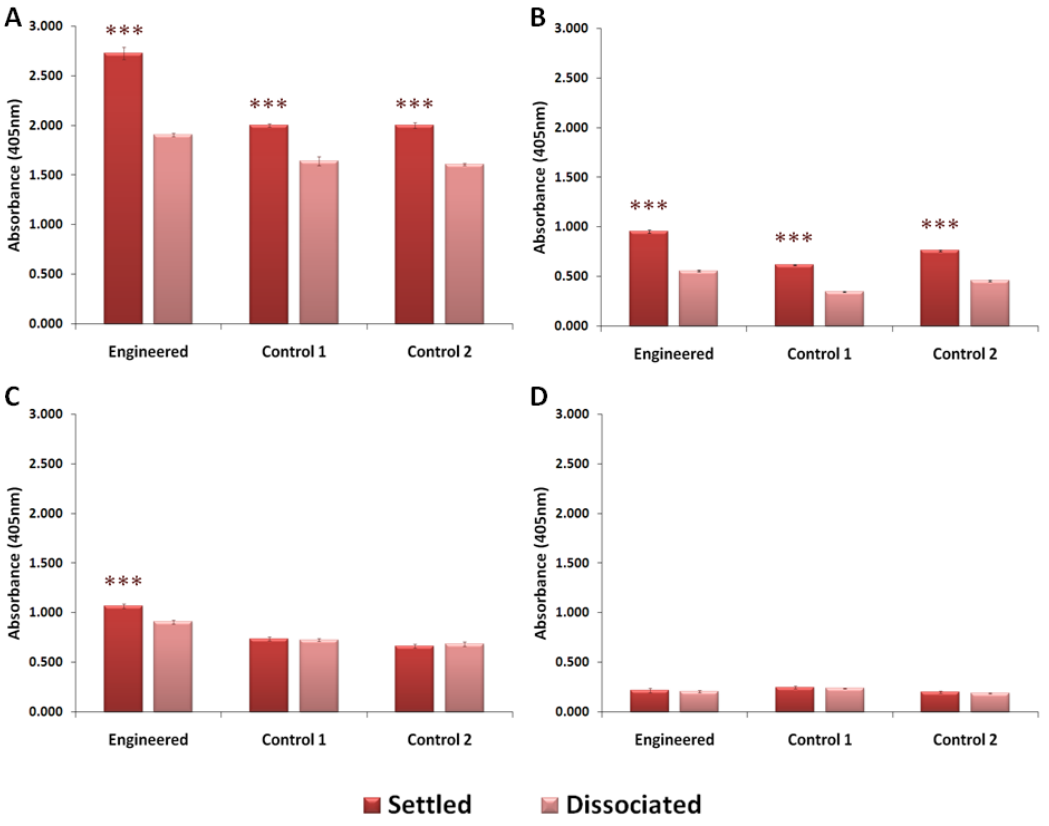

Figure 5.7: Settled 'vs' dissociated EB differentiation and osteogenic differentiation; assessed by ALP assay. Engineered and control ES cells were seeded into mass suspension at 5 x 10^4 cells/mL (A and C) and 2.5 x 10^5 cells/mL (B and D), rotated at 15rpm for 6hrs and cultured for 3 days at 37°C and 5% CO_2 in a humidified atmosphere. After 3 days, these EBs were either transferred directly into osteo-inductive (A and B) or control (C and D) media, or dissociated via trypsinization prior to transfer. After transfer to osteogenic culture, all samples were cultured for 4 weeks. After 4 weeks, osteogenic differentiation was quantified by ALP assay. All experiments were repeated in triplicate and each experiment recorded ALP activity in triplicate; *n* = 9. *** P ≤ 0.001, ** P ≤ 0.01, * P ≤ 0.05. Error bars = S.E.M.

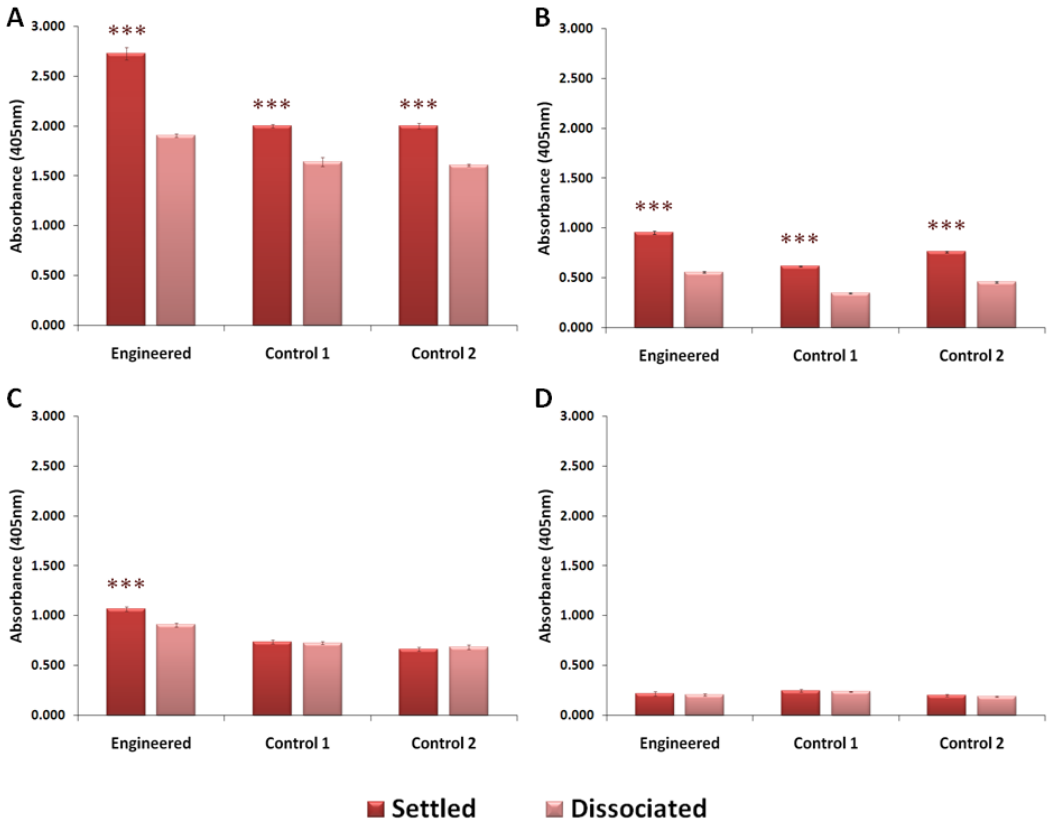

Figure 5.8: Settled 'vs' dissociated EB differentiation and osteogenic differentiation; assessed by Alizarin Red assay. Engineered and control ES cells were seeded into mass suspension at 5 x 10^4 cells/mL (A and C) and 2.5 x 10^5 cells/mL (B and D), rotated at 15rpm for 6hrs and cultured for 3 days at 37°C and 5% CO_2 in a humidified atmosphere. After 3 days, these EBs were either transferred directly into osteo-inductive (A and B) or control (C and D) media, or dissociated via trypsinization prior to transfer. After transfer to osteogenic culture, all samples were cultured for 4 weeks. After 4 weeks, osteogenic differentiation was quantified by Alizarin Red assay. All experiments were repeated in triplicate and each experiment recorded Alizarin Red staining in triplicate; *n* = 9. *** P ≤ 0.001, ** P ≤ 0.01, * P ≤ 0.05. Error bars = S.E.M.

different to the relative decrease in their bone nodule formation. Overall, settled EBs from engineered samples exhibited the greatest increase in osteogenic differentiation compared to dissociated EBs from control samples. However, enhancement was lost at high initial seeding density when cultured in control media.

5.3.4. Effect of Embryoid Body Stage on Osteogenic differentiation

To investigate further the effect that differentiating ES cells through the EB stage had on downstream osteogenic differentiation, ES cells were aggregated for variable lengths of time prior to incubation with osteo-inductive or control media. EBs that were aggregated for only 1 day showed little or no osteogenic differentiation regardless of media and at both seeding densities. There was a significant ($P \leq 0.001$) increase in bone nodule formation after 3 days of aggregation in both engineered and control samples (Figs 5.9A and C). However, this was only observed when samples were cultured in osteo-inductive media. Bone nodule formation decreased significantly ($P \leq 0.001$) with longer aggregation time up to 9 days. Engineered EBs exhibited significantly ($P \leq 0.001$) greater bone nodule formation than control EBs at both 5×10^4 and 2.5×10^5 cells/mL when cultured in osteo-inductive media. This enhancement was observed primarily in samples aggregated for 3 days and then slowly diminished with longer aggregation time. When cultured in control media, only engineered samples seeded at 5×10^4 cells/mL and aggregated for 3 days showed significant ($P \leq 0.001$) bone nodule formation to a detectable level (Fig 5.9B). However, osteogenic differentiation was significantly ($P \leq 0.001$) lower constituting only 6% of that when cultured in osteo-inductive media. Overall, it appeared that ES cells aggregated for 3 days showed the greatest increase in bone nodule formation, and that engineering enhanced this osteogenic differentiation

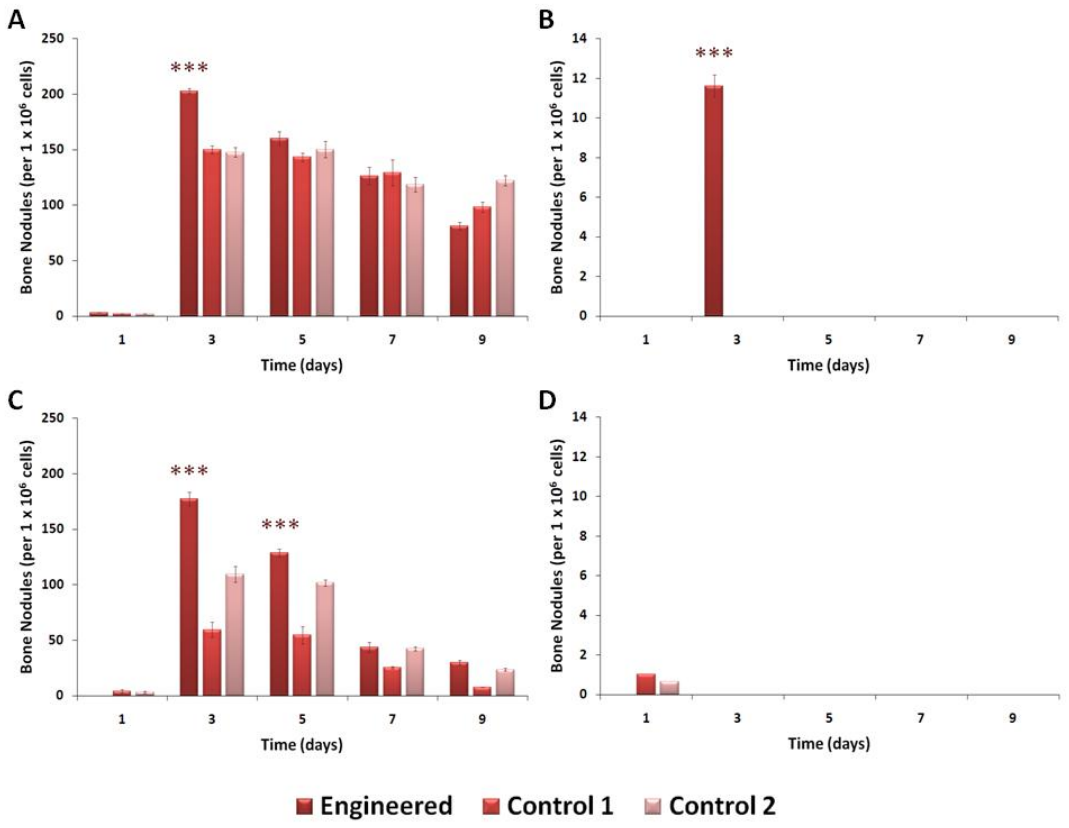

Figure 5.9: Effect of EB stage on ES cell differentiation and osteogenic differentiation: assessed by bone nodule counts. Engineered and control ES cells were seeded into mass suspension at 5 x 10^4 cells/mL (A and B) and 2.5 x 10^5 cells/mL (C and D) rotated at 15rpm for 6hrs and cultured for 1 to 9 days at 37°C and 5% CO_2 in a humidified atmosphere. After 1, 3, 5, 7 and 9 days, EBs were transferred to gelatin-coated plates in either osteo-inductive (A and C) or control (B and D) media and cultured for 4 weeks. After 4 weeks, osteogenic differentiation was assessed via Alizarin Red stained bone nodule counts. Bone nodule numbers were equalized between samples using Hoescht data taken from duplicate samples, and expressed as bone nodules per 1 x 10^6 cells. Important to note is the different y axis scale between Figs A/C and B/D. Experiments were repeated in triplicate and each experiment recorded bone nodules in triplicate; n = 9. *** $P \leq 0.001$, ** $P \leq 0.01$, * $P \leq 0.05$. Error bars = S.E.M.

further. However, enhancement was dependent on both initial seeding density of constituent ES cells and culture media composition.

Fig 5.10 shows images of Alizarin Red stained bone nodules with engineered and control samples originally cultured from EBs aggregated for 3 days. All samples cultured in osteo-inductive media consequently formed bone nodules. However, it was clear that when cultured in control media, only engineered samples seeded at 5 x 10^4 cells/mL exhibited bone nodule formation (Fig 5.10B). It was also clear to see that much of the sample around bone nodules highlighted in red was stained pink/purple. Bone nodules were variable is size and shape between samples.

5.3.5. Aggregation Time and Osteogenic differentiation

Due to osteogenic differentiation results in Fig 5.9, aggregation time for all subsequent experiments was set at 3 days. Osteogenic differentiation within engineered and control EBs was assessed over the 4 week incubation period in either osteo-inductive or control media. Only samples originally seeded at 5 x 10^4 cells/mL were investigated. Osteogenic differentiation was again quantified through Alizarin Red stained bone nodule counts (Fig 5.11). Neither engineered nor control EBs exhibited bone nodule formation after 1 week in culture. Bone nodules were first observed after 2 weeks culture. However, only engineered samples exhibited bone nodule formation after 2 weeks. Control samples first exhibited bone nodule formation after 3 weeks, but only when cultured in osteo-inductive media (Figs 5.12K and O). No bone nodules were observed in control samples cultured in control media over the whole 4 week period investigated (Figs 5.11B, 5.12L and P). After initial occurrence, the number of bone nodules increased significantly ($P \leq 0.001$), then slowed as indicated by a plateau in Fig 5.11A. No difference was observed

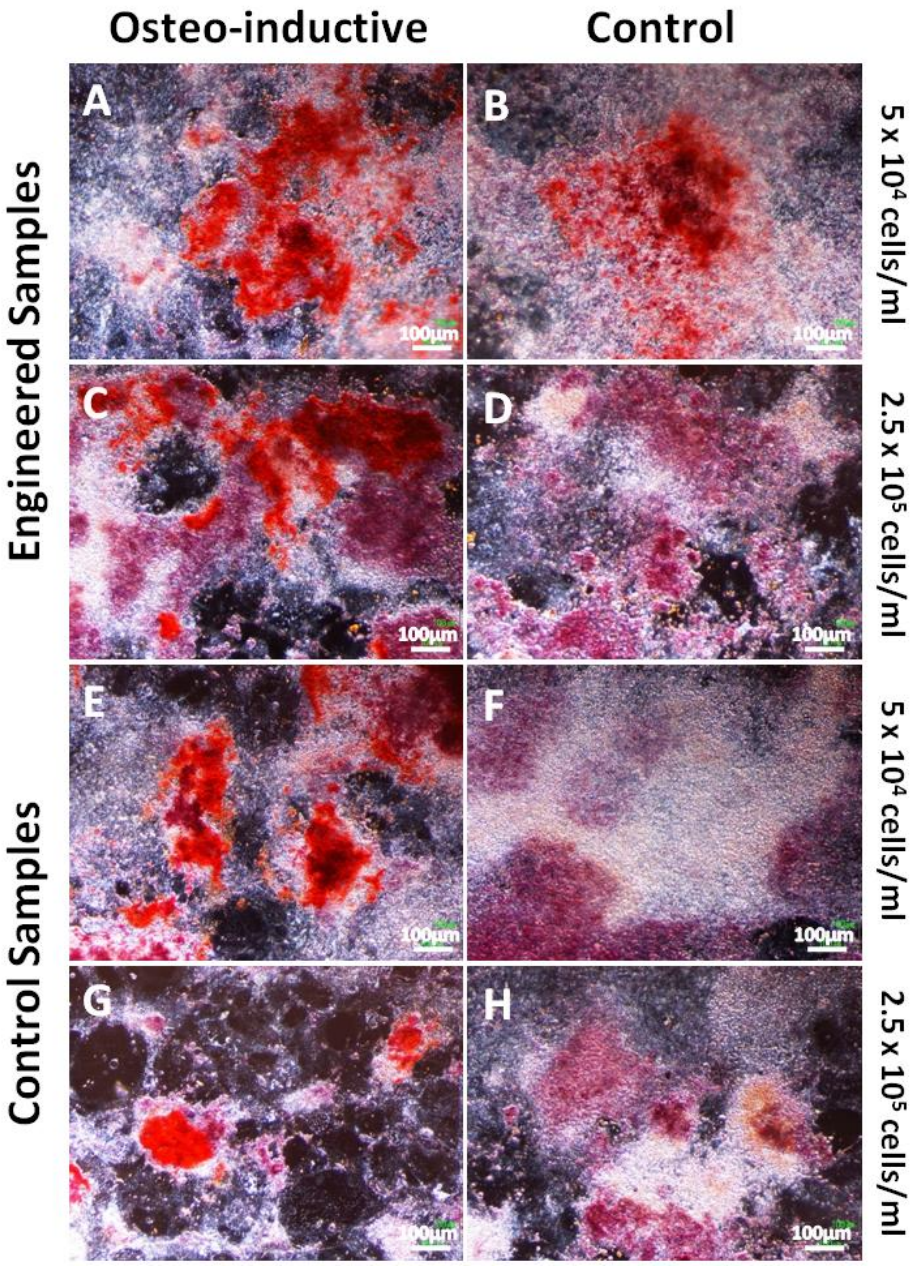

Figure 5.10: Osteogenic differentiation within samples originally aggregated for 3 days; assessed by Alizarin Red stained bone nodules. ES cells were seeded into mass suspension rotated at 15rpm for 6hrs and cultured for 3 days. After 3 days, EBs were transferred to osteogenic culture in either osteo-inductive or control media and cultured for 4 weeks. After 4 weeks, all cultures were stained with Alizarin Red solution to highlight bone nodule formation.

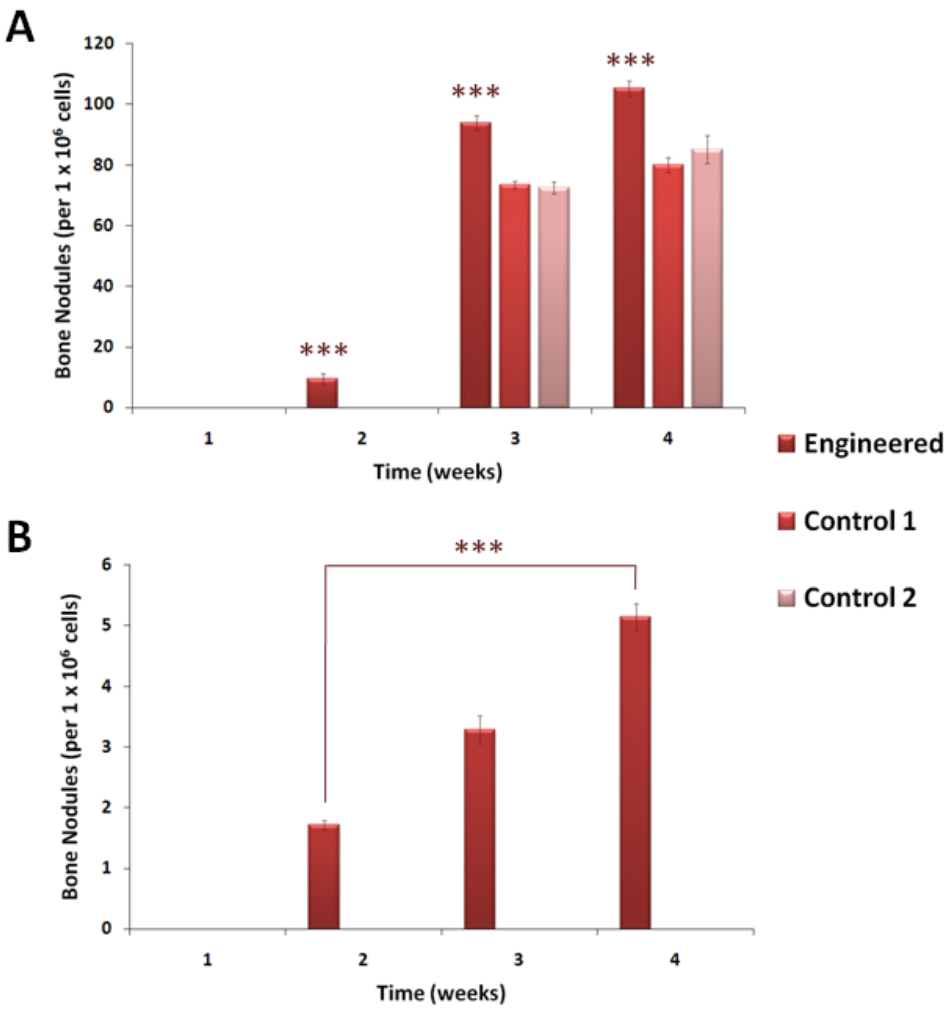

Figure 5.11: Effect of engineering on osteogenic differentiation over time. Engineered and control ES cells were seeded into mass suspension 5 x 10^4 cells/mL rotated at 16rpm for 6hrs and cultured for 3 days at 37°C and 5% CO_2 in a humidified atmosphere. After 3 days, EBs were transferred to gelatin-coated plates and cultured in either osteo-inductive (A) or control (B) media for 4 weeks. After 1, 2, 3 and 4 weeks, osteogenic differentiation was quantified via Alizarin Red stained bone nodule counts. Bone nodule numbers were equalized between samples using Hoescht data taken from duplicate samples, and expressed as bone nodules per 1 x 10^6 cells. Experiments were repeated in triplicate and each experiment recorded bone nodules in triplicate; n = 9. *** $P \leq 0.001$, ** $P \leq 0.01$, * $P \leq 0.05$. Error bars = S.E.M.

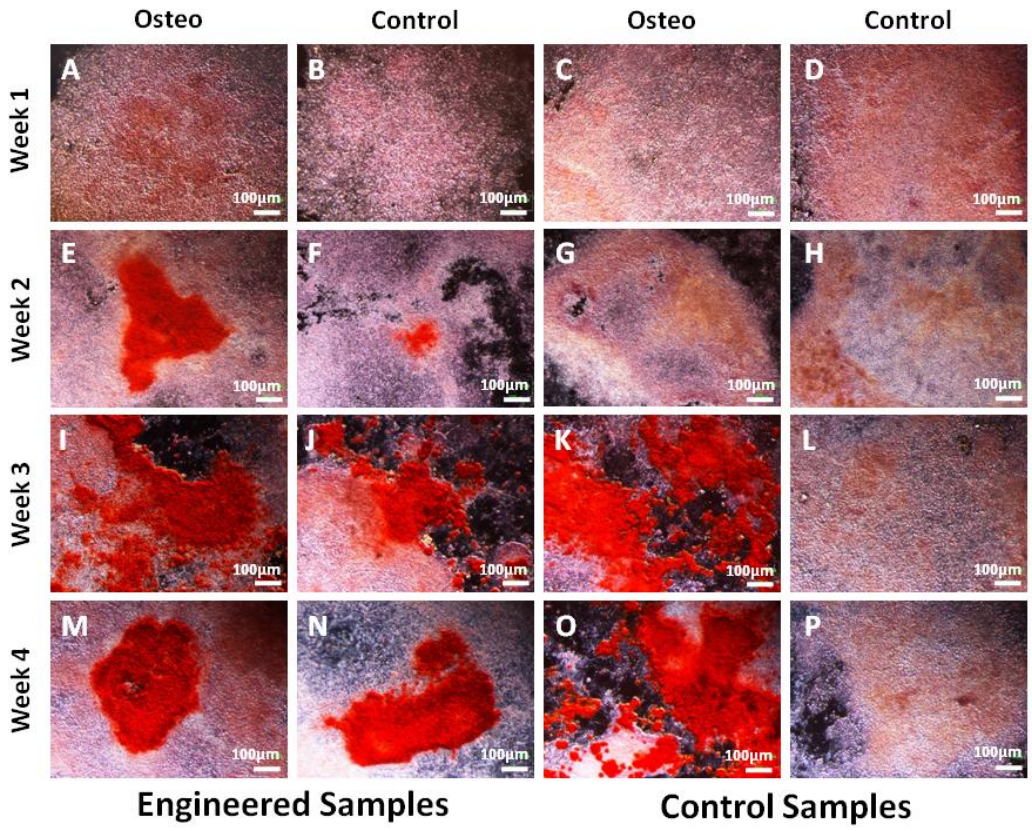

Figure 5.12: Osteogenic differentiation over time; assessed by Alizarin Red stained bone nodules. Engineered and control ES cells were seeded into mass suspension at 5 x 10^4 cells/mL rotated at 16rpm for 6hrs and cultured for 3 days at 37°C and 5% CO_2 in a humidified atmosphere. After 3 days, EBs were transferred to gelatin-coated plates and cultured in either osteo-inductive or control media for 4 weeks. After 1, 2, 3 and 4 weeks, osteogenic differentiation was identified by Alizarin Red stained bone nodules.

between control samples cultured in osteo-inductive media (Fig 5.11A). Samples cultured in osteo-inductive media generated significantly ($P \leq 0.001$) greater numbers of bone nodules than equivalent samples cultured in control media. Overall, engineered samples exhibited bone nodule formation earlier than control samples. When control samples exhibited bone nodule formation, it was significantly ($P \leq 0.001$) less than that in engineered samples. Bone nodules were irregular in shape and variable in size (Fig 5.12). Areas around bone nodules appeared pink/purple as a result of background stain. Bone nodules were observed both within and at the periphery of EBs which had either completely or partially spread out. They also increased in size over time. This occasionally caused the boundaries between individual nodules to become blurred.

Fig 5.13 shows photographs taken of engineered and control cultures at 1x magnification. Bone nodules within engineered and control samples cultured in osteo-inductive media were clearly visible. However, after 4 weeks of culture many nodules had increased in size so much that they had begun to overlap and could have been mistaken as one during quantification. Higher magnification helped resolve bone nodule boundaries. However, some were still indistinguishable. Another problem shown in Figs 5.13A and C was the occurrence of many tiny and positively stained specks located around any large bone nodules. These occurred in both engineered and control samples mainly after 3 weeks incubation in osteo-inductive media.

PCR amplification of osteogenic markers supported bone nodule observations (Fig 5.14). Since bone nodule formation was not observed after just 1 week in culture, samples were taken after a minimum of 2 weeks. Cultures were tested again after the full 4 weeks for comparison to assess osteogenic differentiation over time. Both

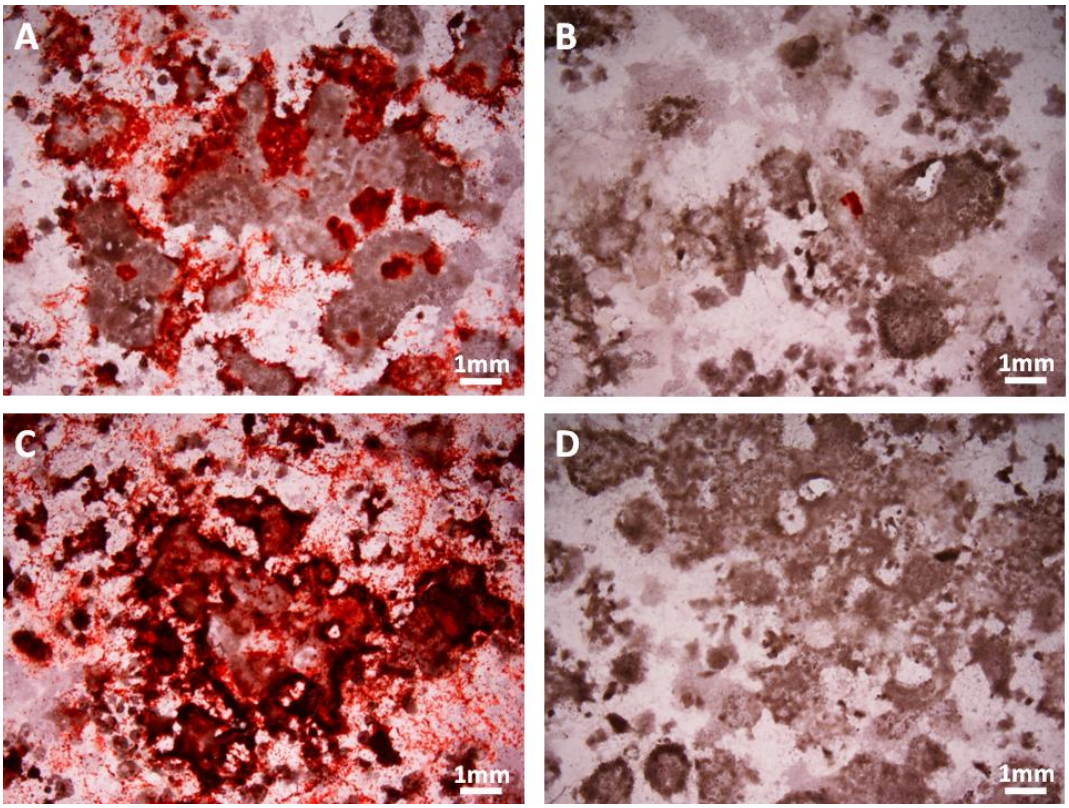

Figure 5.13: Effect of extended bone nodule formation. Engineered (A and B) and control 1 (C and D) ES cells were seeded into mass suspension at 5 x 10^4 cells/mL rotated at 16rpm for 6hrs and cultured for 3 days at 37°C and 5% CO_2 in a humidified atmosphere. After 3 days, EBs were transferred to gelatin-coated plates and cultured in either osteo-inductive (A and C) or control (B and D) media for 4 weeks. After 4 weeks, osteogenic differentiation was identified by Alizarin Red stained bone nodules.

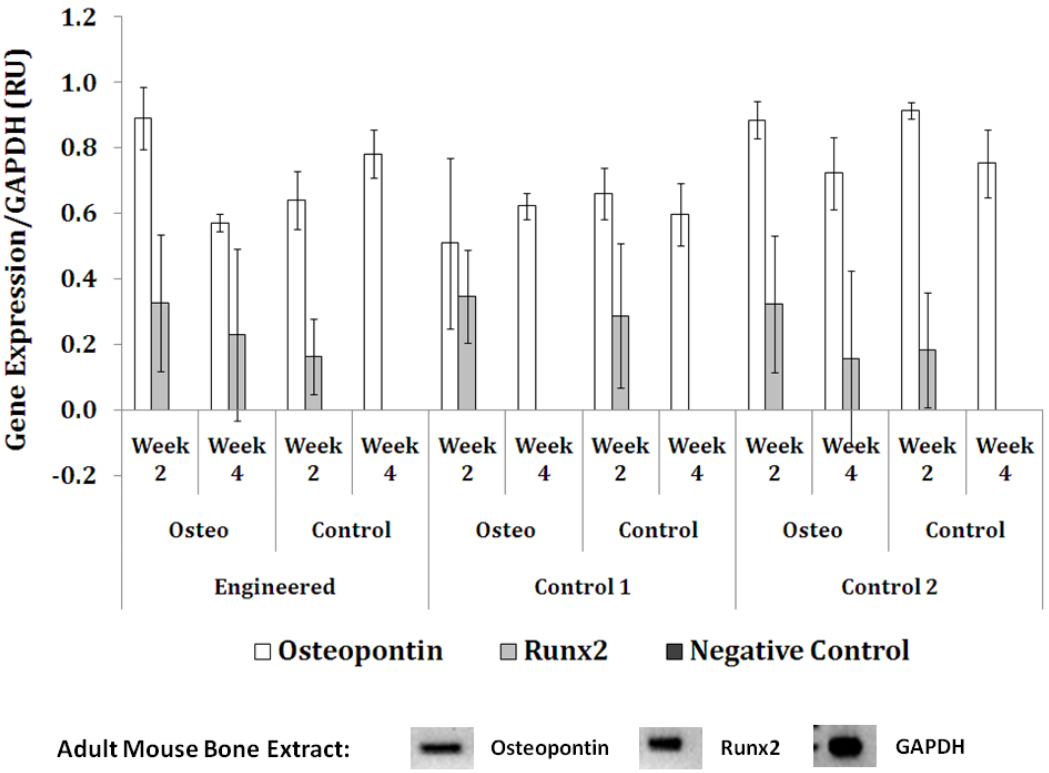

Figure 5.14: Osteogenic differentiation over time; assessed by PCR amplification. Engineered and control ES cells were seeded into mass suspension at 5 x 10^4 cells/mL rotated at 16rpm for 6hrs and cultured for 3 days at 37°C and 5% CO_2 in a humidified atmosphere. After 3 days, EBs were transferred to gelatin-coated plates and cultured in either osteo-inductive or control media for 4 weeks. After 2 and 4 weeks, EBs were incubated in papain buffer and whole lysates were analyzed by PCR amplification for osteogenic markers Runx2 and OPN. GAPDH was used as a quality control. Bands were scanned using densiometric analysis and equalized between samples using GAPDH expression levels. Cell extracts from adult mouse femurs were used as a positive control. Negative controls were prepared by not adding cDNA templates to the PCR mix before amplification. Error bars = standard deviation.

engineered and control samples exhibited OPN expression after 2 and 4 weeks in either osteo-inductive or control media. Both engineered and control samples exhibited Runx2 expression after 2 weeks which decreased after 4 weeks, in both osteo-inductive and control media. GAPDH expression and positive controls showed that the primer pairs and reverse transcription had worked efficiently. Duplicate engineered and control ES cell cultures seeded at 5 x 10^4 cells/mL and aggregated for 3 days, were stained with Alcian Blue solution after 4 weeks incubation in osteo-inductive or control media (Fig 5.15). Positive stain was observed in both engineered and control samples cultured in both osteo-inductive and control media. Staining appeared speckled and widespread throughout all cultures (Fig 5.15D). However, concentrated regions of positive staining were located at sites of initial attachment and within thick accumulations of cells (Figs 5.15A and B).

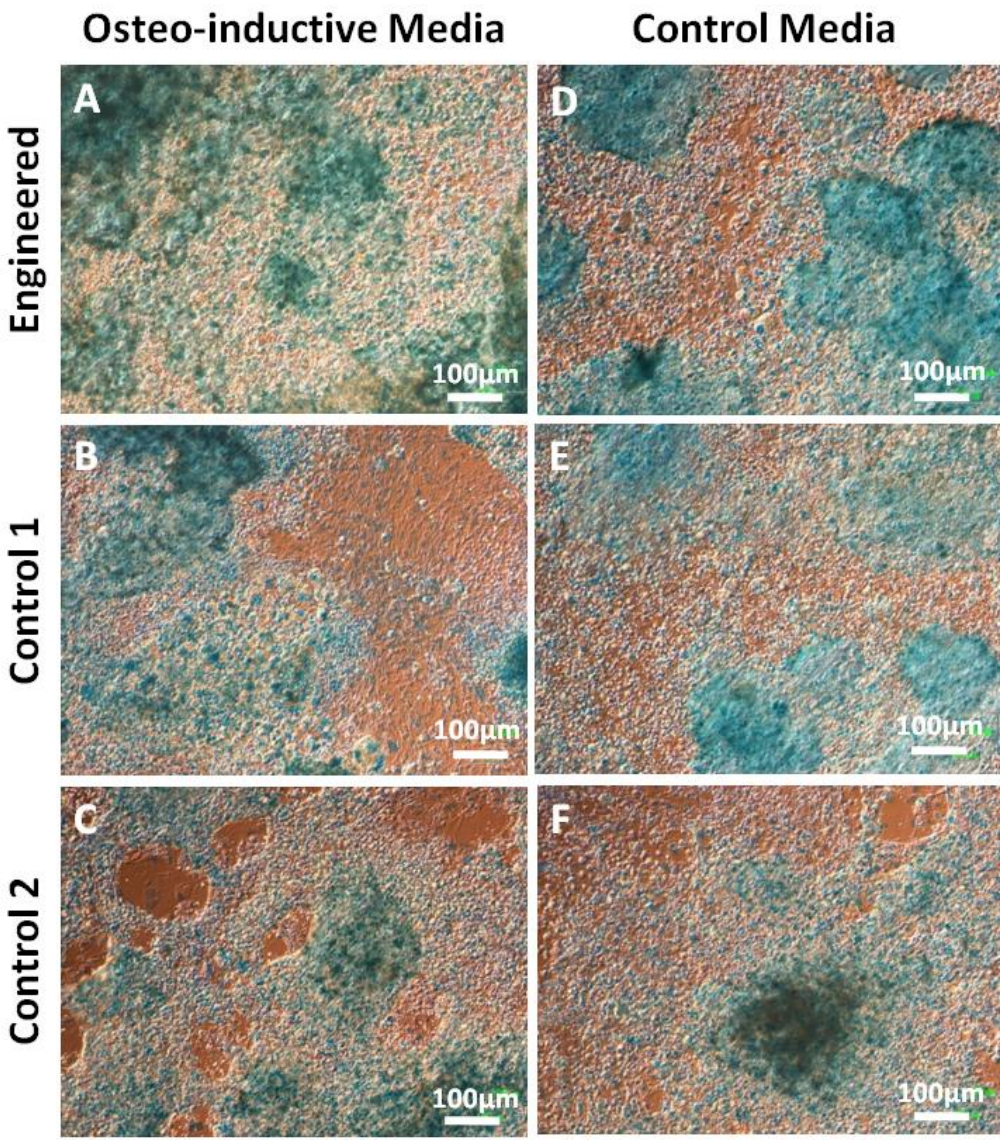

Figure 5.15: EB differentiation and chondrogenesis; assessed by Alcian Blue stain. Engineered and control ES cells were seeded into mass suspension at 5 x 10^4 cells/mL rotated at 16rpm for 6hrs and cultured for 3 days at 37°C and 5% CO_2 in a humidified atmosphere. After 3 days, EBs were transferred to gelatin-coated plates and cultured in either osteo-inductive or control media for 4 weeks. After 4 weeks, cultures were stained with Alcian Blue solution to label GAGs and mucopolysaccharides within deposited collagen matrix, an indicator of chondrogenic differentiation.

5.4. Discussion

Many studies have investigated osteogenic differentiation and the events involved in bone development with the intention of understanding the underlying mechanisms (Buttery et al., 2001). ES cell differentiation has been effectively directed towards the osteogenic lineage through the combination of EB formation and exogenously added growth factors (Bellows et al., 1990). However, due to a lack of understanding concerning mechanisms occurring within the EB and their effect on ES cell differentiation, it is difficult to decipher essential parameters which affect osteogenic differentiation. Controlled ES cell aggregation and formation of EBs exhibiting specified properties, afforded by the previously described surface engineering, could provide a means to understanding early events in osteogenic differentiation. Here it is shown that engineered EBs significantly ($P \leq 0.001$) increased osteogenic differentiation in comparison to control samples. Characterization of the EB stage and investigation of ALP activity, bone nodule formation and osteogenic markers indicated susceptibility to osteo-induction within engineered samples. This may have been the consequence of increased cell number, accelerated EB formation, altered ES cell-ES cell interaction, and/or altered ES cell-ECM interaction. Although these results do not definitively identify parameters of EB formation which affect osteogenic differentiation and their mode of action, they do warrant further investigation of engineered ES cell aggregation.

5.4.1. Embryoid Body Adhesion and Growth

One major similarity between engineered and control samples was that neither had adhered to collagen-coated wells whether cultured in osteo-inductive or control-

media. EBs appeared inhibited or unable to interact with the collagen even though both medias contained Asc to aid ECM production and adhesion. It may be that the differentiated surface cells did not express the required surface integrins. It may also be possible that there was interaction with the type I collagen which caused differentiation towards non-adherent cell types. However, previous studies have shown that interaction with type I collagen does not induce differentiation of mouse ES cells (Hayashi et al., 2007).

Control EBs appeared to dissociate over time forming single cell suspensions by day 28 when cultured on collagen-coated plates, suggestive of cell death. Engineered samples however, exhibited intact EBs by day 28 due to the increased structural integrity afforded by engineered intercellular interaction. Although EBs were intact they exhibited a darkened appearance, far different from that of their initial translucent appearance. This darkening/blackening effect may have been an artefact of cell death within the core. Alternatively, it may simply have been due to refraction of the light as a result of cell proliferation and changing density, or differentiation towards perhaps pigmented cells. The fact that darkened areas also appeared in EBs which had adhered and thrived lends support to the idea that cell density and/or differentiation explains their presence and not cell death. The collagen employed was acid-soluble and therefore required an acidic environment to be solubilized and coat the wells. It may have been that the acid solvent was not sufficiently washed away before EBs were seeded into suspension. This would have altered local pH levels affecting cell adhesion.

Similar observations were made in samples seeded onto uncoated plates. Engineered EBs cultured in osteo-inductive and control media, and control EBs cultured in control media all remained free-floating after 28 days. They also exhibited the

characteristic darkened appearance as few as 7 days after initial seeding. Some EBs were intact after 28 days, but large quantities had dissociated into single cell suspensions. This may be a consequence of EBs remaining in suspension. Free-floating EBs would have undergone extensive cell death within their cores over 28 days of culture due to decreased nutrient and gaseous exchange. Therefore, lack of adhesion would indirectly cause advanced ES cell death within the EB samples at large. Control EBs cultured on uncoated plates in osteo-inductive media had adhered and spread out during 28 days of culture. This may be due to a number of reasons including increased ECM deposition when cultured in osteo-inductive media or affected natural adhesion by engineering. However, the reason may be more complicated and remains unclear. Ultimately, it was concluded that both uncoated and collagen-coated plates were not sufficient for EB adhesion and growth.

Both engineered and control EBs had adhered to fibronectin and gelatin-coated plates after 7 days in osteo-inductive media, and 14 days in control media. Osteo-inductive media had therefore accelerated ES cell-matrix interaction and adhesion. EBs maintained a translucent appearance throughout, although some darkened patches were observed. This was most likely due to extensive ECM deposition causing refraction of the light. By day 28, EBs had adhered and spread outwards. It appeared that integrins expressed on the EB surface were specific for both fibronectin and gelatin (Critchley et al., 1999). Gelatin was chosen to coat plates for all subsequent experiments.

EB adhesion and spreading occurred in stages depicted in Fig 5.4. EBs were seeded into suspension and were heavy enough to sink to the bottom. Once in contact with the gelatin-coated surface the EBs made initial attachment. This attachment was weak and could easily be broken by vigorous shaking of the whole suspension. After

initial attachment EBs became adhered to the well surface (Fig 5.4B). Prior to adherence, EBs exhibited a ringed structure around their core (Fig 5.4A). The core appeared dense and spherical, but the surface appeared random and uneven. However, smaller EBs did not exhibit this ring structure. They were simply ES cell accumulations resembling the surface of larger EBs. The ringed appearance illustrated the structural differences within EBs discussed in Chapter 4. The fact that smaller EBs did not exhibit structural differences showed that EB reorganisation was associated with size. After adherence, EBs began to flatten and spread outwards. Expansion from the site of initial attachment was also due to cell proliferation and highly mobile cells. Differentiating cells from the EB surface would have been the first to migrate outwards since undifferentiated ES cells exhibit characteristic nucleated growth (Stewart et al., 2008, Stojkovic et al., 2004, Imreh et al., 2004, Heng et al., 2005). These migrating cells had a flattened and stretched appearance similar to that of cultured fibroblasts (Fig 5.4D). These initial outgrowing cells provided a platform for further spreading and proliferation of the EB mass. After 7 days in culture, the central EB mass had spread out and begun to form a thick fringe of newly proliferated and/or differentiated cells (Fig 5.4E). However, the original mass of the EB was not completely lost and could still be distinguished by eye (Fig 5.4F). Differentiating cells within the EB may not have been mobile enough to migrate further away and therefore remained at the site of attachment. Alternatively, extensive ECM deposition between ES cells during the EB stage and initial adhesion could have trapped constituent cells and inhibited their migration. This also indicated that remodelling of ECM was either not occurring or not occurring fast enough to have been observed over 28 days. Engineered EBs appeared to exhibit accelerated adhesion as depicted in Figs 5.4G to L.

5.4.2. Embryoid Body Differentiation

5.4.2.1. Embryonic Stem Cell 'vs' Embryoid Body Osteogenic Differentiation

Previous studies have shown that ES cells differentiate towards the osteogenic lineage without prior EB formation (Hwang et al., 2008b, Karp et al., 2006). However, these studies employed EBs aggregated for the standard 5 days and therefore were subject to any inhibitory effects of core necrosis on osteogenic differentiation. This may have accounted for the difference observed between samples with and without prior EB formation. To investigate whether EB formation was an essential step, both ES cells without an aggregation step and EBs were investigated for osteogenic differentiation. Both engineered and control samples with prior EB formation exhibited significantly ($P \leq 0.001$) increased osteogenic differentiation (Figs 5.5A and B). However, osteogenic differentiation was still observed in ES cell samples without prior EB formation (Figs 5.6A and B). Consequently, EB formation enhanced osteogenic differentiation but was not essential. However, this enhancement was only observed in samples cultured in osteo-inductive media. EB formation may therefore have made ES cells more sensitive to osteo-induction rather than actually driving or stimulating osteogenic differentiation. If engineering drove osteogenic differentiation then enhancement would have been expected in all engineered samples regardless of exogenous cues. Osteogenic differentiation in control samples with and without prior EB formation and cultured in control media was not significantly different (Figs 5.5C and D). Engineered samples with prior EB formation exhibited significantly ($P \leq 0.001$) increased ALP activity and bone nodule formation than those without prior EB formation. This suggested engineered EBs may drive osteogenic differentiation of constituent ES cells whereas control EBs simply

increase sensitivity or responsiveness to exogenous osteo-inductive cues. A major difference between engineered and control EBs was their constituent ES cell densities. It may be that tighter adhesion between ES cells and mechanical stresses emanating from being in a high density environment drove osteogenic differentiation. *In vivo* osteogenesis involves environmental cues such as compaction and condensation which may occur from high density mechanical stress (Hall and Miyake, 1992, Titushkin and Cho, 2007). Therefore, engineered EBs may to some extent replicate this environment *in vitro*.

At higher seeding densities (above 2.5 x 10^5 cells/mL) engineered EBs did not exhibit significantly increased osteogenic differentiation compared to control EB samples. ES cell suspensions at high density have previously been shown to generate larger EBs comprising more ES cells than those at 5 x 10^4 cells/mL (Chapter 4: Fig 4.4). No significant difference was observed between the ES cell densities of engineered EBs at both 5 x 10^4 and 2.5 x 10^5 cells/mL. The only difference observed was in constituent ES cell number. Therefore, osteogenic differentiation may be directly linked to ES cell number. Greater ES cell numbers may have had a negative effect on osteogenic differentiation. The increased number of EBs at high initial seeding density may have caused increased inter-EB signalling. This may have had a negative effect on osteogenic differentiation. Alternatively, larger EBs from engineered samples at 2.5 x 10^5 cells/mL would have taken longer to spread out after adhesion or shown restricted spreading. Lateral migration, monolayer formation and minimal 3D interaction involved in spreading after the EB stage may therefore have been important in osteogenic differentiation. Previous studies have highlighted the importance of cell shape on cell function and therefore on cell differentiation (Chen et al., 1998). The change from EB to monolayer culture (3D to 2D) would have had

considerable effect on ES cell shape. In summary, engineered EBs may have provided internal dynamics that had a positive effect on osteogenic differentiation, but were sensitive to initial seeding density.

5.4.2.2. Settled 'vs' Dissociated Embryoid Body Osteogenic Differentiation

Previous studies have shown that dissociating EBs prior to osteo-induction aids osteogenic differentiation (Woll et al., 2006). Both intact and dissociated EBs were consequently investigated for their effects on osteogenic differentiation (Figs 5.7 and 5.8). Settled EBs exhibited significantly ($P \leq 0.001$) increased osteogenic differentiation compared to dissociated EBs in both engineered and control samples when cultured in osteo-inductive media at both 5×10^4 and 2.5×10^5 cells/mL (Figs 5.7A and B). Clearly, enhancement provided by the EB stage was detrimentally affected by dissociation. However, dissociated samples still exhibited greater osteogenic differentiation than samples without prior EB formation, indicating that enhancement during the EB stage was not completely lost as a consequence of dissociation. Continued 3D interaction between ES cells within the EB structure may be beneficial to osteogenic differentiation (Tian et al., 2008, Purpura et al., 2004). However, it was previously shown that a transition from 3D to 2D culture demonstrated increased osteogenic differentiation (Bourne et al., 2004, Buttery et al., 2001). Dissociation would inevitably cause the formation of a 2D culture. Therefore, an alternative explanation is required for the difference between settled and dissociated EBs. Dissociation not only destroys 3D interaction between ES cells but also removes any ECM made during the EB stage. ECM acts as a scaffold and provides the basis for shape and structure of constituent proliferating and differentiating ES cells (Sachlos and Auguste, 2008, Prestwich, 2008, Prestwich,

2007). As stated previously, the shape and morphology of cells affects their function and differentiation (Thomas et al., 2002). It is possible that the continued ES cell-ECM interaction afforded by settled EB culture helped in promoting cell-cell signalling for osteo-induction. When the same samples were cultured in control media there was no observed difference between settled and dissociated EBs. Therefore, it is unlikely that continued ES cell-ECM interaction alone efficiently induces osteogenic differentiation. Instead, it could cause responsiveness to exogenous osteo-inductive cues. However, settled EBs within engineered samples at 5 x 10^4 cells/mL did exhibit significantly ($P \leq 0.001$) increased osteogenic differentiation compared to equivalent dissociated EBs when cultured in control media (Figs 5.7C and 5.8C). These dissociated EBs also showed significant ($P \leq 0.001$) increase in osteogenic differentiation compared to equivalent control samples demonstrating that engineered samples enhanced osteogenic differentiation with or without exogenous osteo-induction. Engineering increased the interaction between ES cells and accelerated EB formation. It is possible that accelerated ES cell-ECM interaction was more advanced than that in control samples. The lack of increased osteogenic differentiation between settled and dissociated EBs in control samples cultured in control media may have therefore been due to a lack of advanced ES cell-ECM interaction. Three days of aggregation appeared to have been insufficient for control samples to reach the advanced stage of ES cell-ECM interaction which was observed in engineered EBs over the same time period.

The lack of enhancement in engineered samples at 2.5 x 10^5 cells/mL could have been the effect of exceeding a critical cell number within the EB beyond which had a negative effect on osteogenic differentiation. Cell number can affect many properties including density (Carpenedo et al., 2007), cell-cell interaction (Chen et al., 2008),

cell-matrix interaction (Giancotti and Ruoslahti, 1999), viability (Cormier et al., 2006) and differentiation (Kurosawa, 2007, Kim et al., 2007a, Koike et al., 2007). Altering of any or all of these properties may have had drastic effects on ES cell differentiation (Ng et al., 2005). Overall, engineered samples exhibited advanced ES cell-ES cell and ES cell-ECM interactions which may have caused increased sensitivity to exogenous osteo-induction.

Bone nodule formation is strictly a function of osteoblasts and is therefore a relatively accurate measurement for osteogenic differentiation quantification (Cao et al., 2005, Buttery et al., 2001). On the other hand, other cell types including the liver, kidney and intestinal epithelium have been shown to exhibit ALP activity (Fernandez and Kidney, 2007, Martins et al., 2001, Wood et al., 2003). ALP activity is also a standard pluripotency marker for undifferentiated ES cells (Berrill et al., 2004). Therefore, ALP activity must not accurately represent the true level of osteogenic differentiation. A new study has proven that ALP activity is in fact not proportional to mineralization (Hoemann et al., 2008). However, the study investigated adult bone cells and bone marrow stromal cells. Therefore it is only suggestive that ALP activity is not proportional to bone nodule formation within ES cell samples. Osteogenic differentiation within all investigated samples was far from homogeneous. Therefore, the ALP assays conducted may have measured ALP activity from these contaminating ALP-positive cells in addition to that from osteoblasts. Bone nodules were chosen for osteogenic differentiation quantification over ALP activity for all ensuing investigations.

5.4.3. Embryoid Body Development and Osteogenic Differentiation

To investigate the effect of EB stage on osteogenic differentiation, ES cells were aggregated between 1 and 9 days prior to 4 weeks incubation in osteo-inductive or control media (Fig 5.9). All samples exhibited purple background staining which may have interfered with absorbance readings after chemical leaching (Fig 5.10). Consequently, bone nodules were photographed and counted, rather than assayed to maintain accurate quantification of osteogenic differentiation. Both engineered and control EBs aggregated for 1 day exhibited significantly ($P \leq 0.001$) less bone nodule formation than those aggregated for longer time periods (Figs 5.9A and C). Samples aggregated for 3 days exhibited a significant ($P \leq 0.001$) increase in bone nodule formation. Clearly, enhancement of osteogenic differentiation via the formation of EBs was dependent on aggregation time. It was possible that 1 day was insufficient time for EBs to accumulate an appropriate number of ES cells, undergo spontaneous differentiation and/or produce suitable quantities of ECM. It has previously been mentioned that ES cell-ECM interaction has an important role to play in ES cell differentiation (Ilic, 2006). It appeared that 3 days of aggregation was sufficient time for the EB stage to affect constituent ES cell differentiation and cause significant ($P \leq 0.001$) increase in osteogenic differentiation. However, the trend between EB stage and osteogenic differentiation was not linear. After 3 days of aggregation all samples showed significant ($P \leq 0.001$) decrease in osteogenic differentiation up to 9 days. It has been shown that EBs aggregated for longer than 3 days begin to suffer core necrosis (Chapter 4). Cell death is an important event in embryogenesis and is involved in the differentiation of specific cell types (Hurle et al., 1995). Necrosis may therefore have triggered complex signalling for the differentiation of non-osteogenic cells (Yamashita et al., 2009, Trouillas et al., 2008). Longer aggregation periods have

also been shown to reduce osteogenic differentiation and increase cardiomyogenesis within resultant EBs (Hwang et al., 2006b). It is therefore possible that 3 days was optimum time for initiation of osteogenic differentiation prior to 2D culture, and that ≥ 5 days simply induced differentiation of constituent ES cells towards alternative cell lineages. The observation of beating cardiomyocytes within all samples supports this assumption (data not shown). Engineered samples exhibited significantly ($P \leq 0.001$) increased bone nodule formation compared to control samples when cultured in osteo-inductive media (Figs 5.10A and B). The increase in osteogenic differentiation in engineered EBs after 3 days may have been due to the increased number of ES cells which remained viable and the advanced ES cell-ECM interaction. However, this enhancement became gradually diminished beyond 3 days of aggregation. Again, this may have been due to the occurrence of core necrosis beyond 3 days.

An interesting observation was made when samples were cultured in control media (Figs 5.9B and D). At 2.5 x 10^5 cells/mL engineered EBs formed bone nodules (Fig 5.10D), whereas control EBs did not form bone nodules in samples cultured for more than 1 day (Fig 5.10H). However, control samples only exhibited one or two bone nodules in the whole sample and therefore may simply have been due to chance differentiation, rather than optimised parameters for osteogenic differentiation. The lack of bone nodule formation in all samples indicated that any enhancement was oriented towards sensitivity to osteo-induction rather than directed osteogenic differentiation. The lack of bone nodules also indicated that Alizarin Red absorbance readings in Figs 5.6 and 5.8 were potentially inaccurate. The absorbance readings may have been of background stain rather than positive stain. However, if we considered this to be true and subtracted the values for samples cultured at 2.5 x 10^5

cells/mL in control media from all others as a blank (background stain), the same trends would still be observed. It is also possible that bone nodules were too small to see within the samples since data in Fig 5.9 represented bone nodules counted by eye. Another interesting observation was made when samples were cultured at 5 x 10^4 cells/mL in control media (Fig 5.9B). Only engineered EBs exhibited bone nodule formation after the optimum 3 days of aggregation (Fig 5.10B). Clearly, engineered samples show directed osteogenic differentiation without exogenous osteo-induction. However, the increase was only 6% of that found in osteo-inductive media. Therefore, engineered samples could simply have directed differentiation of a progenitor cell toward the osteogenic lineage. The 6% observed in control media may therefore have been chance osteoblast differentiation after enhancement of progenitor cells. Overall, engineered samples exhibited significantly ($P \leq 0.001$) increased osteogenic differentiation compared to control samples after an optimum aggregation period of 3 days. However, enhancement was significantly ($P \leq 0.001$) reduced in control media at 5 x 10^4 cells/mL and completely lost in control media at 2.5 x 10^5 cells/mL.

5.4.4. Engineered Osteogenic Differentiation over Time

To investigate osteogenic differentiation within engineered and control samples over the 4 week incubation period, osteogenic differentiation was quantified every week during incubation (Fig 5.11). The number of bone nodules increased significantly ($P \leq 0.001$) over time, indicating that new ES cells were differentiating towards the osteogenic lineage. However, the same osteoblasts could simply have migrated and produced a second or third bone nodule. Migration was indicated by irregular shaped bone nodules (Fig 5.12E and K). If osteoblasts were stationary then nodules

would logically appear perfectly circular. Alternatively, if osteoblasts were mobile and migrating across the culture whilst mineralising, then nodules would logically become irregular and elongated in the direction of migration. Bone nodules also increased in size over time which may have caused overestimation of osteogenic differentiation when quantified by assay (Figs 5.12F, J and N). A more accurate method of quantification would have involved taking diameter measurements of individual bone nodules within a representative area and calculation of average bone nodule number against surface area coverage. Highly functional osteoblasts would mineralize more matrix generating larger bone nodules. Therefore, measurement of bone nodule size would provide indirect measurement of differentiated osteoblast function within engineered and control samples. Bone nodule counts give good estimation of individual occurrences of osteoblastic differentiation and bone nodule size measurements would illustrate continued function of these osteoblasts.

Migration of osteoblasts to a second deposition site and continued mineralization at established sites caused merging of individual bone nodules. Visualisation of bone nodules by eye was inadequate to distinguish between individual nodules at 2.5 x 10^5 cells/mL (Figs 5.13A and C). Samples were consequently viewed at 10x magnification. This helped resolve boundaries between separate bone nodules. However, some overlap remained and quantification was therefore subject to human error when attempting to visualise separate nodules.

When cultured in control media, only engineered samples formed bone nodules which again equated to ~5-6% of that when the same engineered samples were cultured in osteo-inductive media. Control samples did not exhibit any obvious bone nodules (Figs 5.12D, H, L and P). Engineered samples interestingly exhibited bone nodule formation after only 2 weeks in culture in either osteo-inductive or control

media compared to control samples taking 3 weeks (Fig 5.11A and B). This emphasized the idea that enhancement within engineered samples was partly due to accelerated ES cell aggregation, EB formation and ES cell-ECM interaction. The increase in bone nodule formation between weeks 2 and 3 was greater than the difference between weeks 3 and 4. This may have been due to limited space within the wells or complete differentiation of the sample. If the whole culture had differentiated then there would be no more spontaneous occurrence of osteoblasts and therefore a possible reduction in the number of new bone nodules. Alternatively, continued deposition and formation of new nodules may have filled available space by week 4 and caused the quantification trend to plateau. The increase in bone nodule formation in samples cultured in control media was linear, possibly due to less osteoblasts having more space in which to form new bone nodules, and more space for existing nodules to increase in size due to the inherent lower levels of osteogenic differentiation. At 2.5×10^5 cells/mL, there was a notable decrease in osteogenic differentiation as a result of decreased space between EBs and differentiated osteoblasts.

Limitations to the efficacy of both Alizarin Red assay and bone nodule count regarding osteogenic differentiation quantification have been identified. Therefore, samples were assessed for osteogenic differentiation by PCR amplification of the transcription factor related gene, Runx2 and the bone related gene, OPN (Valenti et al., 2008, Randle et al., 2007). Samples were taken after 2 weeks when osteogenic differentiation was first observed and then again after 4 weeks at the end of the incubation period (Fig 5.14). Engineered samples exhibited OPN expression after 2 and 4 weeks of culture in both osteo-inductive and control media. Runx2 expression was also observed, but reduced after 4 weeks. Control samples also exhibited both

OPN and Runx2 expression when cultured in osteo-inductive media which correlates with observations of bone nodule formation in Fig 5.11A. However, control samples also exhibited OPN and Runx2 expression when cultured in control media. This is inconsistent with observations made in Fig 5.11B. This may have been due to the increased sensitivity of PCR amplification compared to Alizarin Red stained bone nodules. Strong expression of OPN was observed after 2 and 4 weeks which was consistent with the presence of functional osteoblasts. Runx2 expression was present after 2 weeks but not as strongly as corresponding OPN expression. Runx2 has been shown to induce OPN expression (Valenti et al., 2008, Lee et al., 2008b). Runx2 may therefore have been present in samples between 1 and 2 weeks inducing strong OPN expression by week 2. However, continued Runx2 expression after osteoblast differentiation has an inhibitory effect on osteoblast function (Kanatani et al., 2006). Runx2 is auto-regulated by the production of OPN (Takahashi et al., 2005). As OPN expression increases, Runx2 expression is down-regulated. Down-regulation of Runx2 is critical to the maturation of osteoblasts and transition to osteocytes (Maruyama et al., 2007). Therefore, the observed decrease in Runx2 expression after 4 weeks in culture could have been the direct result of the observed strong OPN expression. Consequently, findings in Fig 5.14 were in agreement with current understanding of OPN and Runx2 function in bone development. In summary, Runx2 was possibly expressed between 1 and 2 weeks of culture. This induced osteoblast differentiation and OPN expression. Runx2 expression was down-regulated by the increased OPN expression. Down-regulation of Runx2 allowed maturation of the osteoblasts. Mature osteoblasts were fully functional and began to mineralize surrounding matrix.

Expression of Runx2 was arguably absent in control samples after 4 weeks of culture compared to engineered samples. This would imply that osteoblasts may have been more mature in control samples. Advanced maturation may also mean advanced transition from osteoblasts to osteocytes. Osteocytes do not mineralize surrounding matrix. Therefore, osteoblasts may have formed and become quickly trapped within mineralized matrix which was not detectable by Alizarin Red stain. These osteoblasts may have subsequently formed osteocytes which ceased to form new bone nodules, or possibly increase the size of existing nodules. This could explain the absence of bone nodules in control samples cultured in control media (Fig 5.11B). However, similar results would have been expected in control samples cultured in osteo-inductive media. The presence of bone nodules within these samples was most likely the result of Dex within the osteo-inductive media. Dex has been shown to cause osteoblast differentiation and up-regulation of type I collagen deposition (Jager and Krauspe, 2007). Osteo-inductive media would have caused differentiation of greater numbers of osteoblasts which would have mineralized substantial amounts of matrix to form bone nodules before becoming trapped and forming osteocytes. The strong expression of OPN after 4 weeks indicated that functional mineralizing osteoblasts were present in control samples cultured in control media. Consequently, the idea that osteoblasts became trapped and quickly formed osteocytes prior to detectable bone nodule formation must be incorrect. However, there are other explanations for the strong expression of OPN. Osteocytes have been shown to express OPN, especially when they are starved of oxygen or deprived of mechanical loading (Morinobu et al., 2003, Gross et al., 2005). The cultures were not placed under hypoxic conditions, but no mechanical loading was applied to the cultures either. Therefore, osteoblasts could have become trapped, formed osteocytes and ceased

forming a detectable level of bone nodule formation whilst OPN expression remained high. OPN has also been shown to up-regulate osteoclast function in bone remodelling (Terai et al., 1999). It is possible that control samples cultured in control media did not exhibit bone nodules because of strong OPN expression causing bone resorption through up-regulation of spontaneously differentiated osteoclasts. The presence of beating cardiac cells as contaminating cell types within all cultures provided evidence that HS cells were present. HS cells are progenitor cells of osteoclasts. It is also possible that greater numbers of progenitor cells within control samples cultured in control media differentiated to form chondrocytes instead of osteoblasts. Chondrocytes are closely related to osteoblasts and are essential to bone nodule formation. Without chondrocytes there would be no collagen matrix ready for mineralization. Alcian Blue stain revealed extensive collagen deposition throughout all cultures (Fig 5.15). This showed that cultures may have contained chondrocytes and that collagen matrix was not a limiting factor in bone nodule formation. Considerable matrix deposition was located at sites of initial EB attachment. Deposition was less dense further away from initial sites. This indicated that the initial migrating cells observed in Fig 5.4 may possibly have been chondrocytes depositing matrix as they migrated across the well surface. It is possible that chondrocytes within control samples did not produce enough matrix in which to be trapped and become hypertrophic when cultured in control media. Hypertrophic chondrocytes are essential in the differentiation of osteoblasts *in vivo* (Rich et al., 2008, Jukes et al., 2008). Dex within osteo-inductive media enhances collagen deposition (Jager and Krauspe, 2007, Tanaka et al., 2004). Therefore, samples cultured in osteo-inductive media may have exhibited an increase in trapped chondrocytes, which may have consequently become hypertrophic.

Increased ES cell-ECM interaction has been shown previously within engineered samples. Subsequently, there may also have been an increase in downstream trapped chondrocytes, hence the observed bone nodule formation (Fig 5.11B).

5.5. Conclusions

In summary, gelatin-coated plates provided an inexpensive method of enhancing EB adhesion and spreading. EB culture exhibited significantly ($P \leq 0.001$) increased osteogenic differentiation when compared to ES cell culture. Settled EBs exhibited significantly ($P \leq 0.001$) increased osteogenic differentiation when compared to dissociated EBs. Settled EBs rapidly attached to gelatin-coated plates and began to flatten and spread outwards through both constituent ES cell proliferation and structural reorganization. Initial migrating cells which may have been chondrocytes moved outwards forming a fringe around the EBs. Deposited collagen matrix provided (1) support for lateral expansion of the EB and constituent ES cells, and (2) a basis for osteoblast driven mineralization and bone nodule formation. ES cell suspensions seeded at 5×10^4 cells/mL and aggregated for 3 days generated EBs exhibiting the greatest levels of osteogenic differentiation following osteogenic culture for 4 weeks. Engineered samples exhibited enhanced osteogenic differentiation in all samples, regardless of culture in osteo-inductive or control media. Enhancement in engineered samples may have been due to accelerated ES cell-ES cell and/or ES cell-ECM interaction and consequent differentiation. Accordingly, osteogenic differentiation appeared subject to variables such as ES cell number and 3D interaction which can all potentially be controlled and fine tuned through the proposed engineered culture system.

Chapter 6

6. Results

Microparticle Incorporation

6.1. Introduction

EBs are employed in many differentiation protocols and show control over ES cell differentiation (Carpenedo et al., 2007). Controlled alterations made to EB formation afforded by engineering, have had an important effect on resultant osteogenic differentiation. However, contaminating cells types were still observed illustrating how little is understood about the control the EB stage has over ES cell differentiation. It is hypothesized that these contaminating cell types arise from random differentiation of internal ES cells which are not exposed to exogenous osteo-inductive factors. Many studies have utilized biodegradable polymer microparticles as a delivery system for growth factors and proteins (Suciati et al., 2006, Mantalaris et al., 1998, Sokolsky-Papkov et al., 2007). Here we show the delivery of internal osteo-induction to the EB via the release of Dex from incorporated PLGA/triblock microparticles.

6.2. Methods and Materials

6.2.1. Microparticle Fabrication

Microparticles were fabricated using a single emulsion system where polymer and Dex were dissolved and emulsified in dichloromethane (DCM, Fisher) (Xu et al., 2008, Morita et al., 2000, Choi and Park, 2006). The polymer was a blend of triblock with PLGA (30:70). To fabricate microparticles with a theoretical content of 1% Dex, 1g of polymer and 10mg of Dex were gently dissolved in 4mL DCM using a vortex mixer (VM20, Chiltern Scientific, Buckinghamshire U.K.) for 1min. Once dissolved, 4mL of 0.3% polyvinyl acetate (PVA) in dH_2O was carefully added to the 4mL DCM/polymer mix and emulsified using a vortex mixer for 1min. After emulsification the suspension was poured into a 100mL hardening bath of 0.3% PVA in dH_2O that was continually stirred at 300rpm using a magnetic stirrer for 3hrs. Microparticles were subsequently vacuum filtered using appropriate pore size filter paper once hardened. Residual water was removed by freeze drying over 48hrs. Duplicate microparticles were fabricated without the addition of Dex to the suspension as a control. After microparticles were dried they were fractionated using a Retsch AS 200 sieve set at 150 taps min^{-1} (1.6mm amplitude) and 280 horizontal oscillations min^{-1}. Fractionation was carried out for 20mins consisting of 40sec cycles with a 3sec pause between each cycle. Filtered microparticle fraction had a 50-100μm diameter. Microparticles were vacuum-packed and stored at 4°C in the dark.

DCM is an organic solvent which enables salvation of the polymer and Dex. Triblock is a polymer composed of three individual polymers joined together. The specific triblock used in the fabrication of these microparticles was PLGA-PEG-PLGA (Mw 7,500).

6.2.2. Dexamethasone Incorporation

6.2.2.1. Encapsulation Efficiency

20mg of the Dex-encapsulated microparticles was dissolved in 2mL of acetonitrile. After further dilution to 10mL, Dex content was measured using reverse phase high pressure liquid chromatography with U.V. detector (HPLC-U.V.) set at 246nm. HPLC-U.V. employed the use of a phenomenex C18 luna-column (4.6 x 150mm) on an Agilent 1090 machine. The mobile phase was 2mM acetate buffer (pH 4.8) and acetonitrile (58:42). Standards ranging from 0.2 to 100mg/mL Dex in acetonitrile were used to create a standard curve. Entrapment efficiency (%) was calculated through division of 'measured Dex concentration' by 'theoretical Dex concentration (1%)' and multiplication by 100. Results were taken in triplicate and an average calculated.

6.2.2.2. Controlled Release Assay

20mg of Dex-loaded microparticles was placed inside a flow chamber and attached to a syringe pump driver machine (PHD2000, Harvard, Kent U.K.) which applied a constant force on the syringes. Syringes were filled with PBS and the whole setup was incubated at 37°C. PBS was pushed through the flow chamber and eluted into a collection chamber. At regular intervals the eluted PBS was analyzed by HPLC-U.V. for Dex content. Standards were made ranging from 0 to 20μg/mL to create a standard curve. Dex content was calculated by converting the fluorescence reading to μg/mL using the standard curve and multiplying by the volume of PBS eluted. The volume of PBS varied between samples. Samples were taken in triplicate and an average calculated.

6.2.3. Microparticle Quantification: Particle Sizing System

The number of microparticles within each fractionated size range of microparticles was assessed using the PSS. 0 to 25mg of microparticles were suspended in 10mL of PBS containing 1% Tween 20. Weights increased with an increment of 5mg. Suspensions were gently inverted to ensure homogeneity prior to transfer into the glass holding vial of the PSS. The suspension volume was increased to 50mL with dH_2O whilst under rotation with a magnetic stirrer. The suspension was allowed to drain until the last few millilitres so as to not allow air bubbles to enter the PSS. The glass holding vial was thoroughly washed with PBS and dH_2O until the PSS measured ≤ 5 particles/sec both before and after each sample.

6.2.4. Microparticle Surface Analysis

Microparticles were imaged using SEM to assess surface topography and visualize morphology (Chapter 2). Images were taken at 12kV and a working distance of 38mm from the electron gun tungsten filament. Samples were gold sputtered once per sample for 4mins.

6.2.5. Microparticle Coating

Microparticles were coated in both ECM components and allylamine to improve ES cell attachment (Hamerli et al., 2003, Lu et al., 2008, Finke et al., 2007, Ren et al., 2008). After coating, microparticles were seeded at high density in 2mL SCM and allowed to settle. ES cells were seeded on top at low density and the suspension was incubated overnight. The suspension was left stationary for the majority of the incubation with occasional gentle shaking to turn microparticles. After 24hrs, microparticles were stained with May-Grünwald and Giemsa and imaged.

6.2.5.1. Gelatin and Foetal Calf Serum

Similar to the tissue culture plates for EB adhesion during osteo-induction, microparticles were pre-coated in gelatin and also FCS to enhance attachment of ES cells. PLGA is known to have high adsorption capacity for proteins such as gelatin and within FCS (Rouzes et al., 2000). Prior to coating, microparticles were sterilized by suspension in 5mL of dH_2O and irradiation for 20mins in U.V. light (Shearer et al., 2006, Moioli et al., 2006). Microparticles were subsequently transferred to an Eppendorf tube suspended in 1.5mL of PBS containing 1% gelatin or FCS. Suspensions were rotated for 1.5hrs at 37°C. FCS was employed to adsorb alternative adhesive proteins such as fibronectin and vitronectin to the microparticle surface (Garcia and Boettiger, 1999).

6.2.5.2. Plasma

Plasma coating can be used to modify surface chemistry by either etching or deposition of particular substances (Safinia et al., 2007). Microparticles were placed within a T-shaped borosilicate glass chamber and coated with plasma polymerized allylamine (ppAAm) for 4.5mins (Fig 6.1) (Barry et al., 2005). Plasma coating was repeated four times and degassed by one freeze-pump-thaw cycle after each coat. Between plasma coatings the chamber was cleaned by oxygen etching for 3mins. Both plasma polymerisation and oxygen etching were carried out at a power of 20W under a working pressure of 300mTorr. To prevent toxicity to the ES cells, plasma coated microparticles were left for 24hrs at room temperature. The process of plasma polymerisation sterilized the microparticles.

Studies have shown that ppAAm-coating enhances cell attachment to surfaces previously found to have low affinity (Dehili et al., 2006). The coating provides a

Figure 6.1: Plasma-polymerised allylamine-deposition within a borosilicate glass chamber.

uniform thin film of reactive allylamine species including functional amine and amide groups (Griesser et al., 1994). Consequently, the surface becomes hydrophilic and nitrogen rich resulting in high affinity for proteins and cell attachment. Alternatively the surface is capable of immobilizing biologically reactive compounds for ES cell interaction through ECM components (Siow et al., 2006).

6.2.6. Microparticle-Embryonic Stem Cell Aggregation

Sterile gelatin and FCS-coated microparticles were seeded into 6-well tissue culture plates in 2mL of AM or SCM at high density. ES cells were seeded at 5 x 10^4 cells/mL. Seeding ratios ranged from 1:1 to 40:1 for ES cells to microparticles. Plates were either rotated at 15rpm for 6hrs or left stationary with a gentle shake after 3hrs. Plates were subsequently incubated at 37°C and 5% CO_2 in a humidified atmosphere for 3 days in SCM to allow for aggregation and EB formation. Further optimization involved alteration of the initial step. Microparticles were seeded with ES cells into a 1.5mL Eppendorf tube in 1mL SCM and rotated for 3hrs prior to transfer to tissue culture plates. Seeding ratios included 1:1, 2.5:1 and 5:1, ES cells to microparticles respectively. Suspensions were then incubated at 37°C and 5% CO_2 in a humidified atmosphere for 3 days. EB suspensions were imaged at 10x magnification.

6.3. Results

6.3.1. Fabricated Microparticles

After fractionation both Dex-loaded and plain microparticles were analyzed by SEM for any differences in morphology and surface topography (Fig 6.2). Clearly, fractionation had been sufficient enough to separate out all microparticles with a diameter ≤ 100μm (Figs 6.2A and C). There were however, microparticles with a diameter < 50μm were found in both samples, present due to electrostatic interaction which fractionation did not overcome. The majority of microparticles in both samples had a spherical morphology with a smooth unblemished surface ideal for uniform degradation and release. No morphological differences were observed between Dex-loaded and plain microparticles. However, Dex-loading appeared to have a negative effect on microparticle size, with greater numbers at the lower end of the 50-100μm range compared to plain microparticles (Figs 6.2B and D). Dex-loaded microparticles therefore exhibited a tighter size distribution than plain microparticles. Some microparticles did not exhibit a spherical morphology due to a fabrication defect, or that they simply collapsed before hardening in the 0.3% PVA solution (Figs 6.2E and F, respectively). Other defects included rippling across the surface, presence of holes with a diameter ≤ 1μm, surface cracks and thick polymer deposits. Although, defects were at a low frequency in the whole samples there was no way to separate out affected microparticles. Consequently, a certain level of error within the following data was expected.

Following the observation that Dex-loading appeared to have a negative effect on microparticle size, samples were analyzed by PSS to assess microparticle number in a given weight (Fig 6.3). This analysis was also performed for ensuing experiments

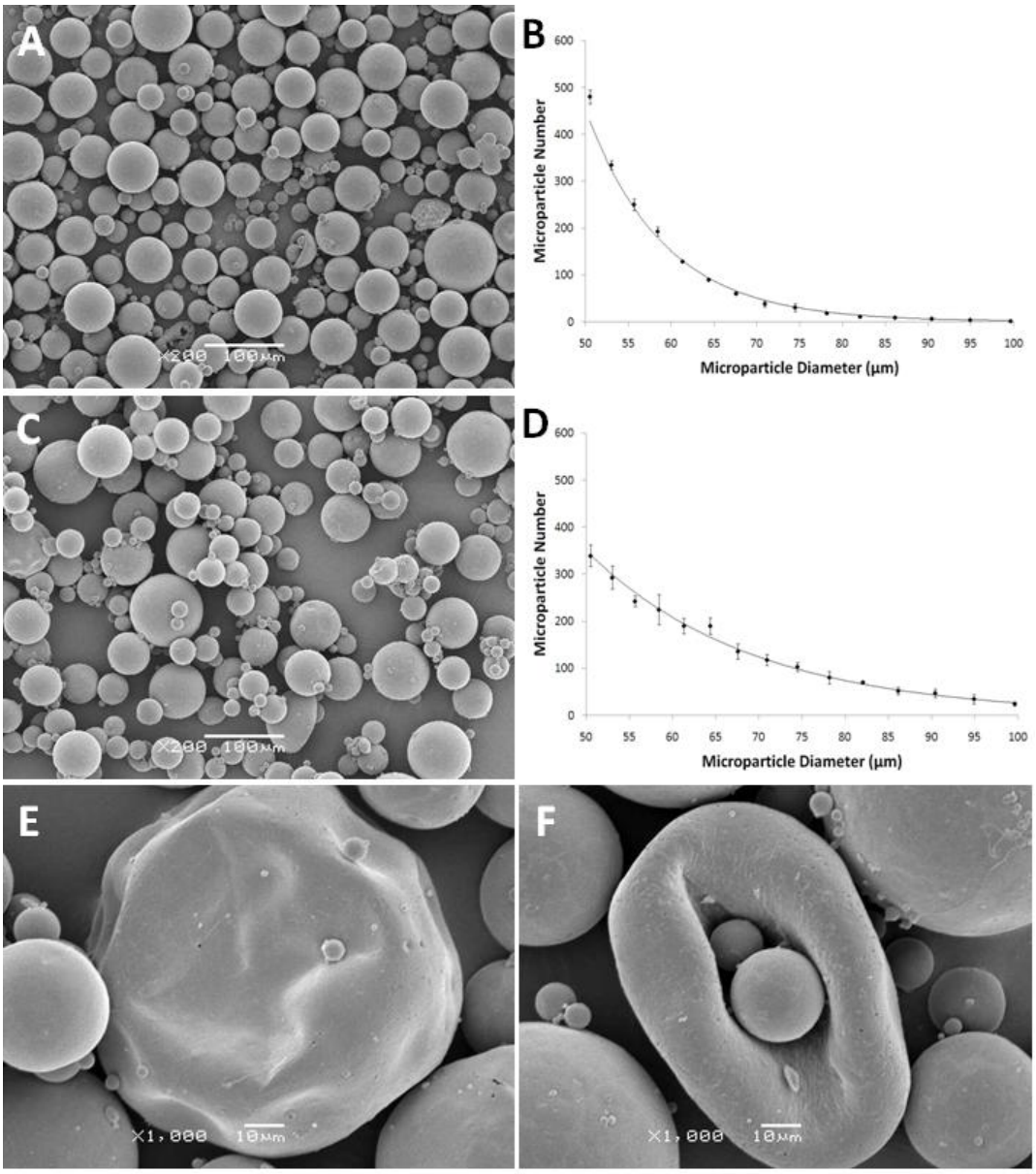

Figure 6.2: Surface morphology and size distribution of fabricated microparticles with a diameter range of 50-100µm. Once fabricated, both Dex-loaded (A and B) and plain (C and D) microparticles were analyzed by SEM (A and C) to assess surface morphology, and by PSS (B and D) to assess size distribution within the 50-100µm range. PSS analyzed all microparticles within 1mg of each sample. E and F show examples of deformed or collapsed microparticles.

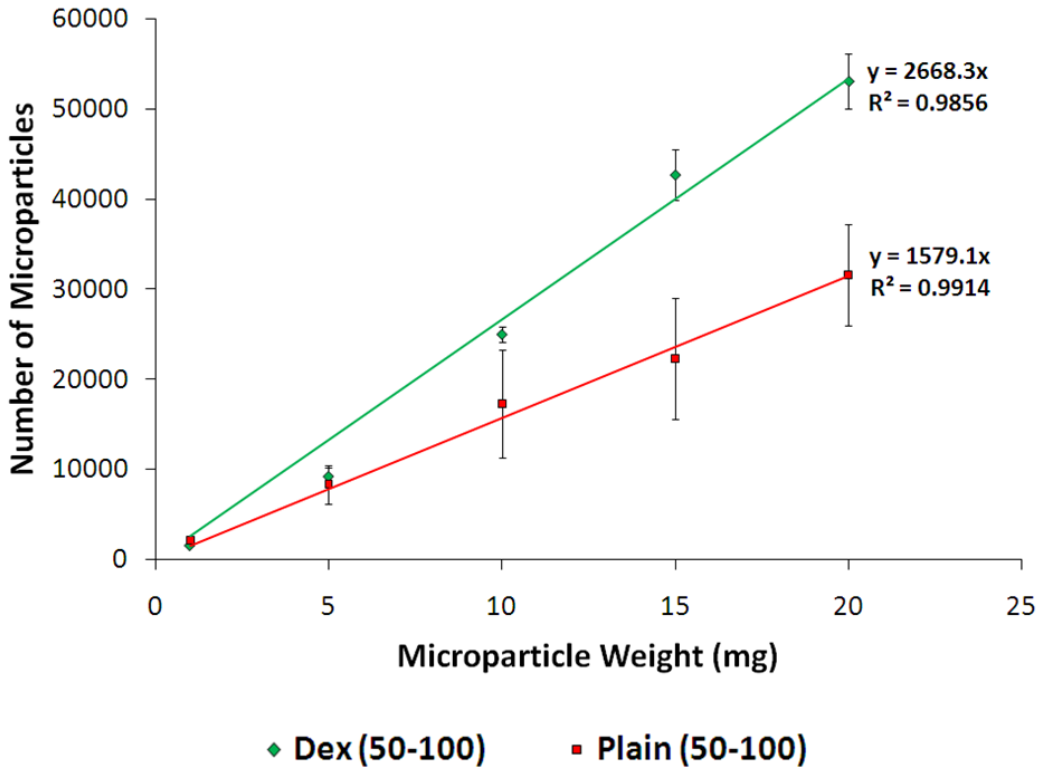

Figure 6.3: Number of microparticles with increasing weight. Once fabricated, both Dex-loaded and plain microparticles from the fractionated 50-100µm range were analyzed by PSS over a range of weights including 1, 5, 10, 15 and 20mg. Experiments were repeated in triplicate and all EBs were counted per sample; *n* = 3. Error bars = S.E.M.

requiring exact ratios of microparticles to ES cells. Supporting previous observations, Dex-loaded samples generated significantly ($P \leq 0.001$) greater numbers of microparticles within the 50-100μm range. Both Dex-loaded and plain samples exhibited a linear trend in microparticle weight to number. However, plain microparticles showed considerable variability in number indicating that Dex-loading may have had a positive effect on reproducibility concerning microparticle number during fabrication.

6.3.2. Dexamethasone Entrapment

Standard curves for Dex concentration in both acetonitrile and PBS are shown in Figs 6.4A and B, respectively. Both show a linear relationship between increasing Dex concentration and peak area (detected by HPLC-U.V.). To calculate entrapment efficiency 20mg of Dex-loaded microparticles was dissolved in 2mL of acetonitrile which was diluted by 5 prior to HPLC-U.V. analysis. Average peak area was 185.9 which was converted to 3.63μg/mL Dex using the standard curve in Fig 6.4A. Multiplication by the dilution factor of 10 equalled 36.3μg/mL Dex within 20mg of microparticles. Theoretical loading was 1% therefore 20mg of microparticles would have been expected to hold 200μg Dex. Entrapment efficiency was subsequently calculated to be 18.16%.

The next step was to analyze the release profile of the microparticles (Fig 6.5). Peak area measurements were converted to Dex concentrations using the standard curve in Fig 6.4B. Concentrations were multiplied by a dilution factor and the PBS volume eluted to calculate Dex release over time. There was an initial burst release phase in the first 3 days releasing ~30% of the encapsulated Dex. Dex release was then linear and constant up to day 14 where ~80% had been released. Linear release between

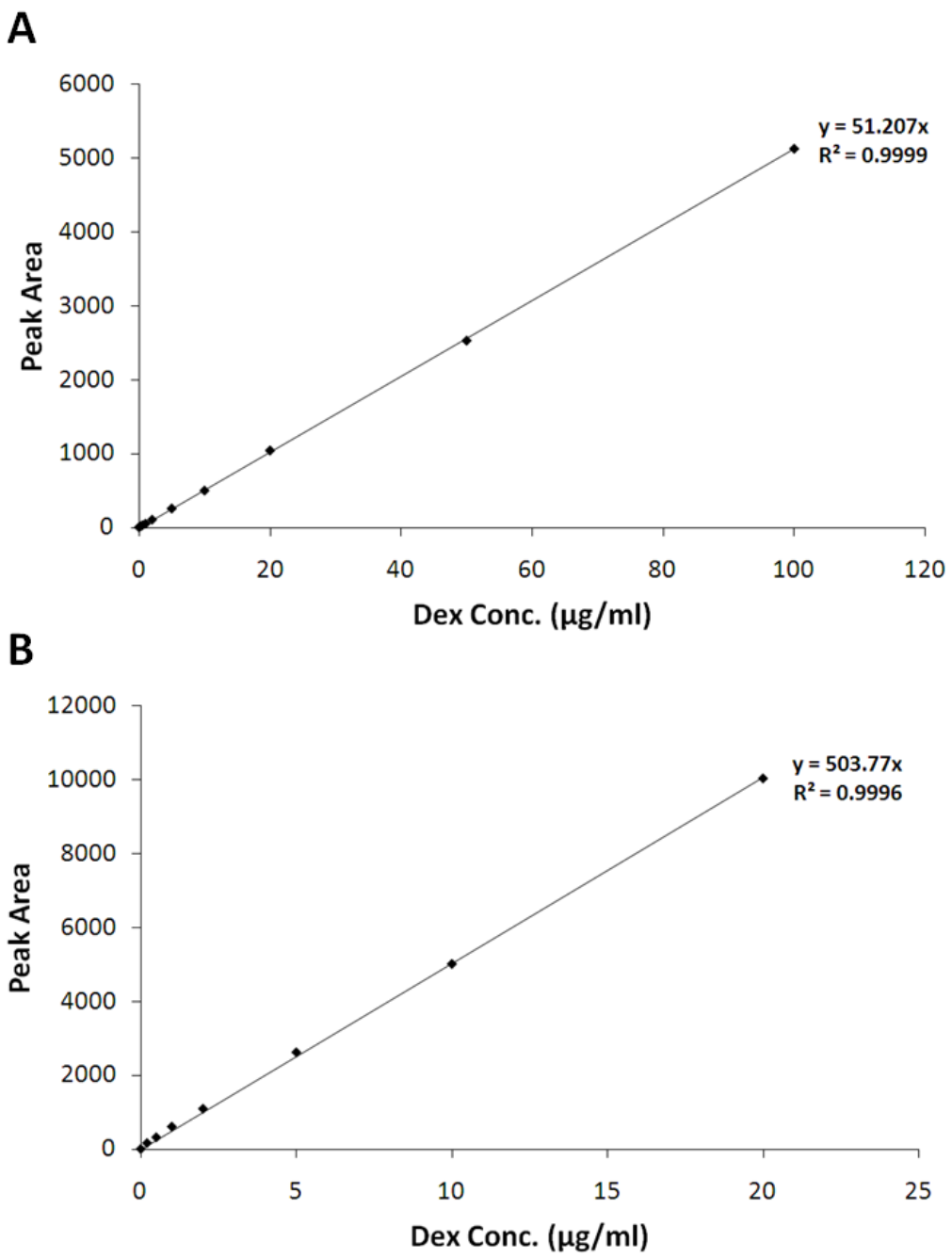

Figure 6.4: Dex concentration standard curves. Dex was dissolved in both acetonitrile (A) and PBS (B) at varying concentrations including 0.2, 0.5, 1, 2, 5, 10, 20, 50 and 100µg/mL. Samples were analyzed by HPLC-U.V. set at 246nm. All samples were taken in triplicate and averages calculated; *n* =3. Error bars = S.E.M.

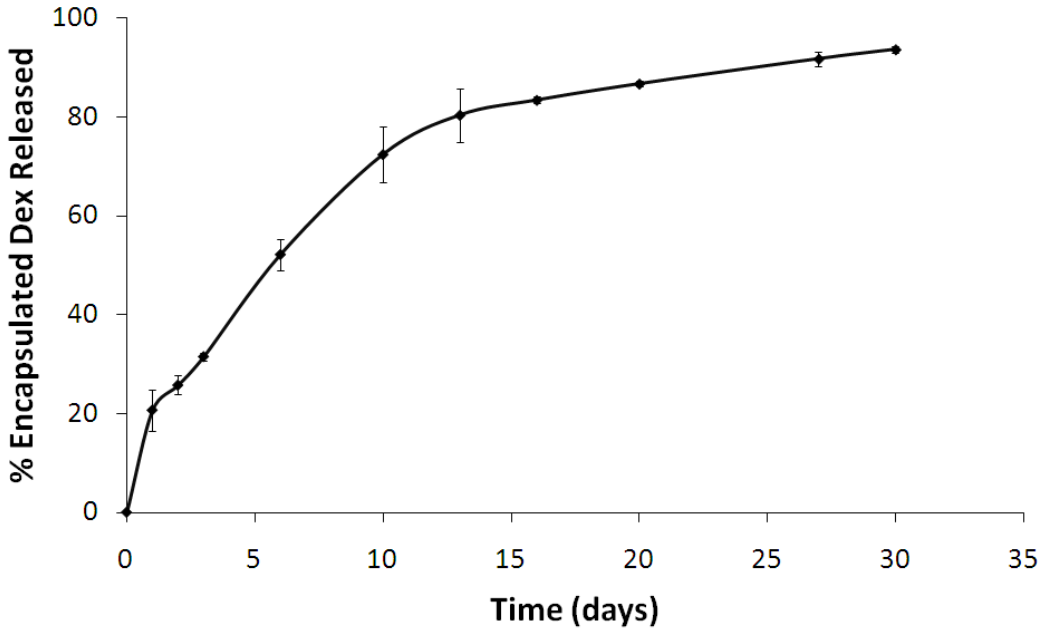

Figure 6.5: Release profile of Dex-loaded microparticles in PBS over time. Once fabricated, microparticles were placed within a flow chamber suspended in PBS and incubated for 30 days at 37°C and 5% CO_2 in a humidified atmosphere. The flow chamber was under continual PBS perfusion at 2µl/min. Flow through was collected and analyzed by HPLC-U.V. set at 246nm. Experiment was repeated in triplicate; *n* = 3. Error bars = S.E.M.

day 3 and 14 was ~1.3μg/mL every day. Beyond 14 days Dex release remained linear but at a reduced rate. 93% of the encapsulated Dex was released by day 30. Therefore, linear release between day 14 and 30 was ~0.3μg/mL every day. Consequently, Dex-loaded microparticles were capable of providing osteo-induction over the full 28 days of osteogenic culture. The release profile can be altered by mixing combinations of different sized microparticles. Small microparticles may limit the quantity of Dex delivered, but provide rapid release. Large microparticles would increase the quantity of Dex delivered, but release more slowly. Alternatively, the release profile can be altered by adjusting the degradation rate of the polymer. High molecular weight polymers would release slowly due to slow degradation, and low molecular weight polymers would release quickly due to rapid degradation. Degradation rate could also be controlled by blending of hydrophobic polymers with hydrophilic substances.

6.3.3. Embryonic Stem Cell Adhesion

Microparticles were coated in gelatin, FCS and ppAAm to enhance ES cell adhesion (Fig 6.6). Clearly, ES cells attached to microparticles with all 3 coatings. At sites of attachment ES cells subsequently became well spread out indicating a level of biocompatibility and support for colonization. ES cells showed a marked decrease in attachment to control uncoated microparticles (Fig 6.6D). Low level attachment was observed on few microparticles. However, this may be residual stain that was not sufficiently removed during washing.

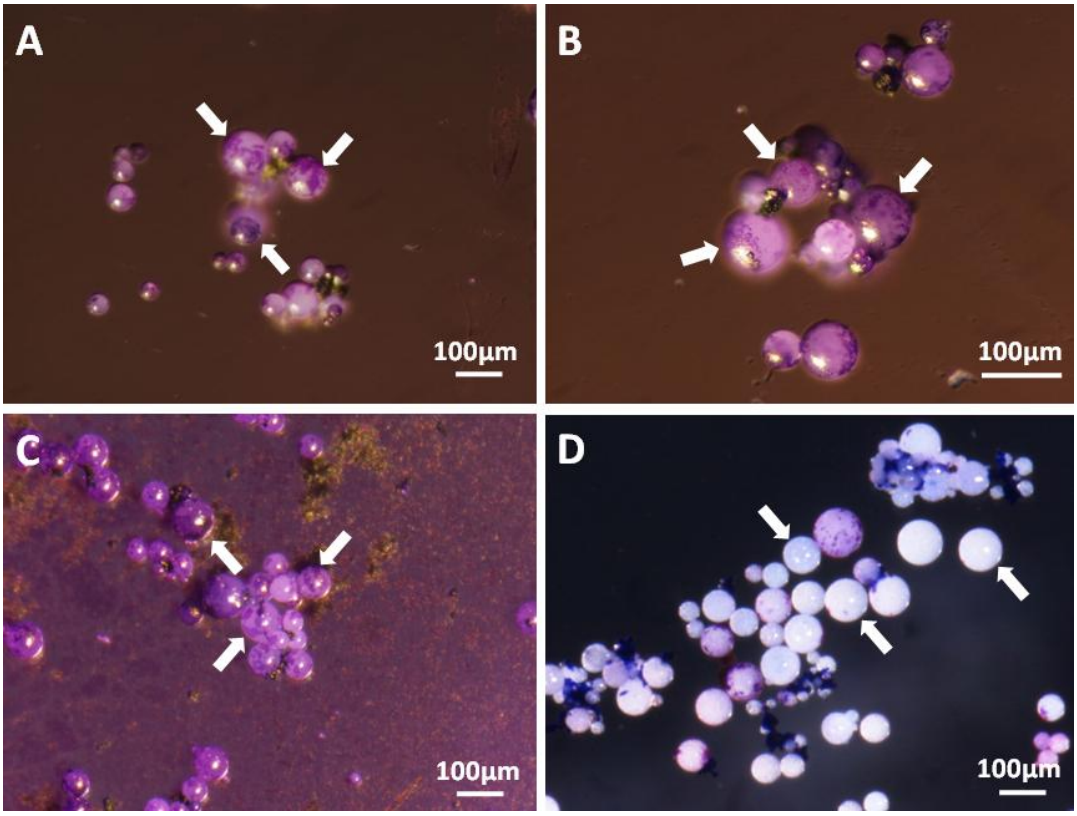

Figure 6.6: Microparticle coating and ES cell attachment. Appropriate quantities of plain microparticles were suspended in 0.1% gelatin (A) or 10% FCS (B) and agitated at room temperature for 30mins. Suspensions were washed and suspended in PBS and sterilized by U.V. irradiation for 20mins at room temperature. An alternative microparticle coating was ppAAm (C). Once coated, microparticles were washed in PBS, seeded into SCM and allowed to settle before addition of ES cells at 5 x 10^4 cells/mL. Cultures were incubated at 37°C and 5% CO_2 in a humidified atmosphere for 24hrs. Control microparticles were left uncoated (D). After 24hrs, samples were carefully washed and ES cells were visualized with May-Grünwald and Giemsa stain.

6.3.4. Microparticle Incorporated Embryoid Bodies

6.3.4.1. High Density Microparticles in Mass Suspension

Microparticles were seeded into suspension with ES cells during aggregation to assess the efficiency of their incorporation within resultant EBs. Initially, microparticles were seeded over a wide range of ratios from 1:1 to 40:1 (Fig 6.7). At 40:1 microparticle incorporation within EBs was not observed. Clearly, ratios above 20:1 inhibited microparticle incorporation (Fig 6.7C). ES cells within these samples had adhered to the well surface and begun to proliferate outwards with free floating microparticles suspended above (Figs 6.7D). However, at low seeding densities of 1:1 and 10:1, microparticles were incorporated within EBs (Figs 6.7A and B). Microparticles were visualized as opaque spheres embedded in translucent EBs. Microparticle incorporation occurred at low frequency, with the majority of EBs not containing any microparticles. The results indicate that microparticles coated with 0.1% gelatin did lead to EB incorporation, but inefficiently. Observations also showed that microparticle incorporation was highly variable between EBs which would have affected localized concentrations of Dex during release.

6.3.4.2. Low Density Microparticles in Mass Suspension

To assess the efficiency of microparticle incorporation at low seeding ratio, suspensions were seeded at 1:1, 2.5:1 and 5:1 (Fig 6.8). Microparticles were coated in FCS, seeded with ES cells into SCM, rotated at 15rpm for 6hrs before 3 days incubation at 37°C and 5% CO_2 in a humidified atmosphere. Microparticle incorporation was observed at all three densities. However, 2.5:1 exhibited a marked increase in microparticle incorporation and therefore chosen for all subsequent

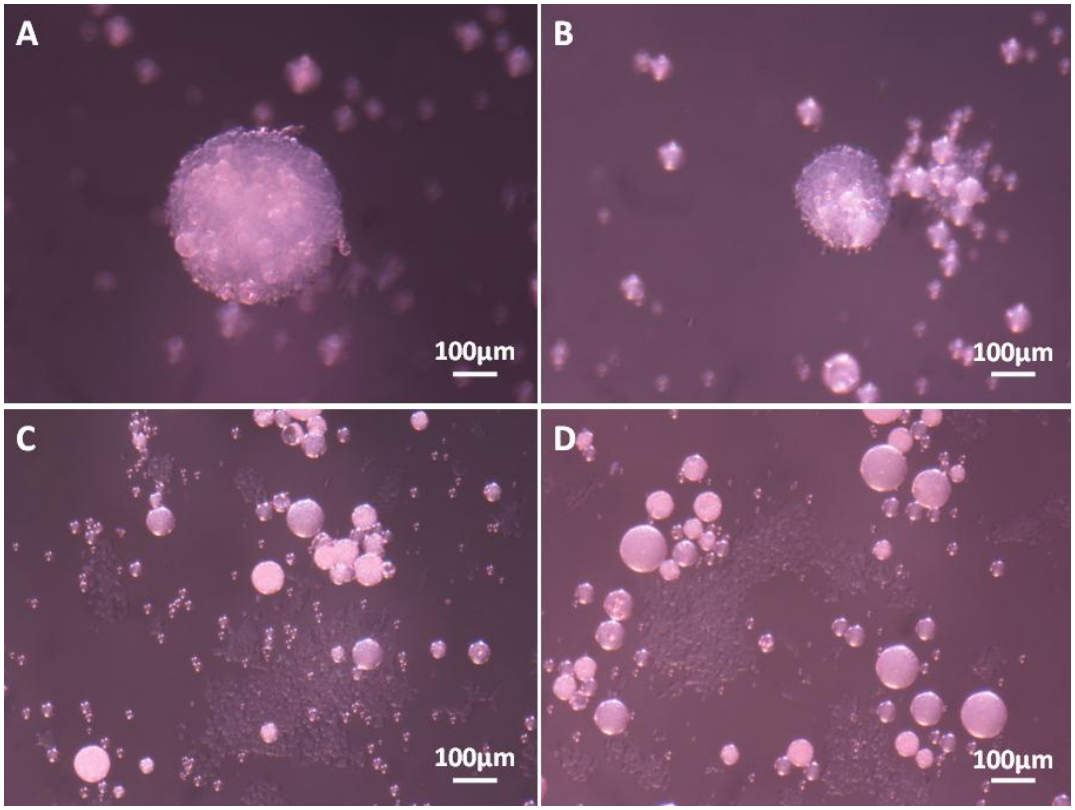

Figure 6.7: Effect of 'microparticle to ES cell' seeding ratio on aggregation. Plain microparticles were suspended in 0.1% gelatin solution and gently agitated for 20mins at room temperature. Microparticles were then washed and suspended in PBS and sterilized by U.V. irradiation for 20mins at room temperature. Coated microparticles were transferred to mass suspension with control 1 ES cells seeded at 5 x 10^4 cells/mL. Suspensions were rotated at 15rpm for 6hrs then cultured for 3 days in SCM at 37°C and 5% CO_2 in a humidified atmosphere. Microparticles were seeded with ES cells over a range of ratios including 1:1 (A), 10:1 (B), 20:1 (C) and 40:1 (D) (microparticles to ES cells). Suspensions were imaged after 3 days of culture.

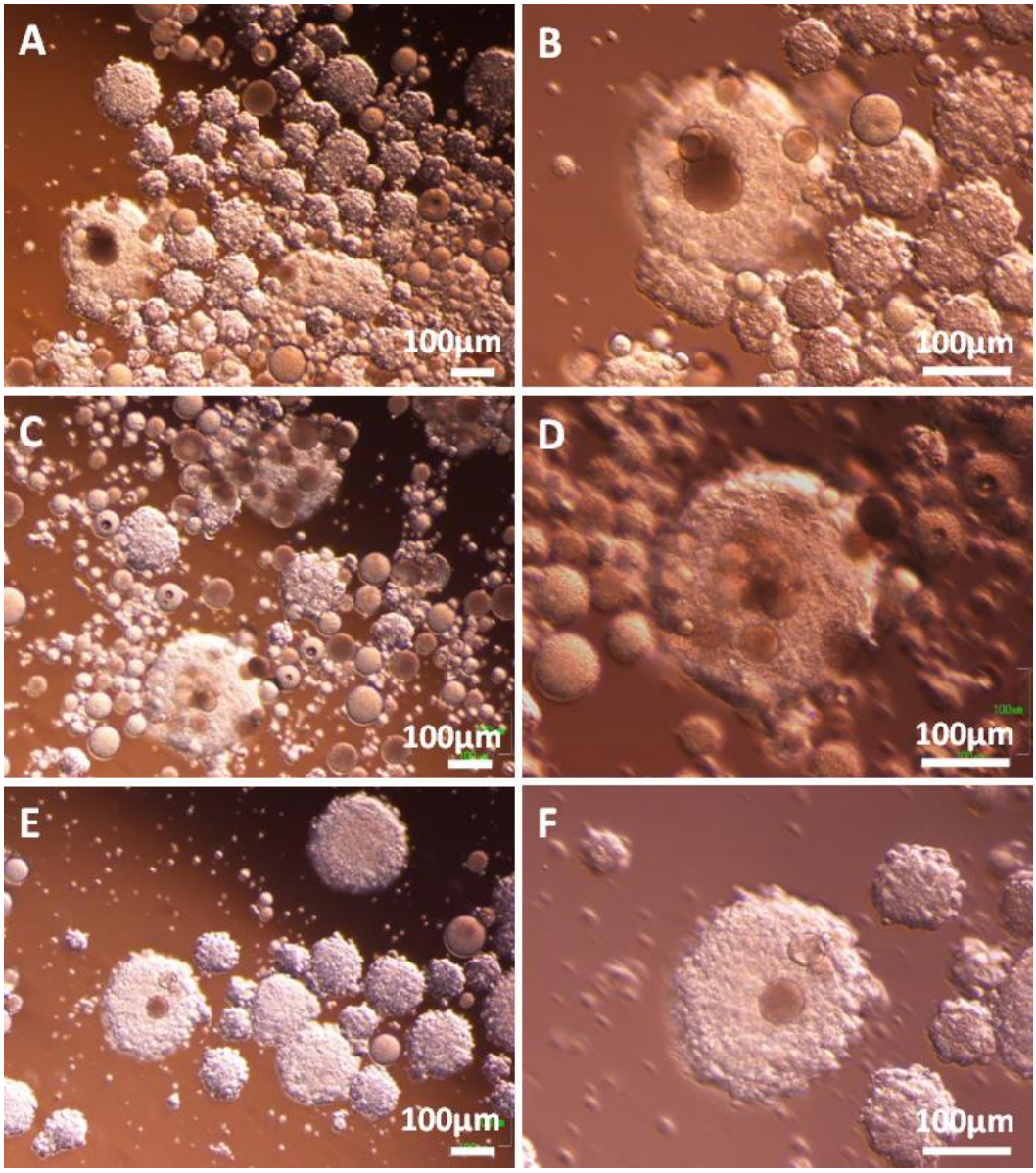

Figure 6.8: Effect of low 'microparticle to ES cell' seeding ratios on microparticle incorporation. Appropriate quantities of plain microparticles were suspended in 10% FCS and agitated for 30mins at room temperature. Microparticles were then washed and suspended in PBS and sterilized by U.V. irradiation for 20mins at room temperature. Microparticles then were seeded with control 1 ES cells (5 x 10^4 cells/mL) at 5:1 (A and B), 2.5:1 (C and D) and 1:1 (E and F) in SCM, rotated at 15rpm for 6hrs and cultured for 3 days at 37°C and 5% CO_2 in a humidified atmosphere. Suspensions were imaged after 3 days.

experiments (Fig 6.8C). Many microparticles remained in suspension indicating that although incorporation efficiency had improved, it was still not optimal. At both 1:1 and 5:1, microparticles were observed within EBs however, many EBs did not exhibit any microparticle incorporation (Figs 6.8A and E). Higher magnification showed that the number of incorporated microparticles between EBs was highly variable indicating a lack of control over incorporation. FCS-coating appeared to have little or no effect on incorporation efficiency in comparison to gelatin-coating.

6.3.4.3. Eppendorf-Based Embryoid Body Formation

The low frequency of microparticle incorporation may have been due to reduced interaction between ES cells and microparticles within culture wells and/or adhesive properties of gelatin and FCS. Microparticles were subsequently coated in ppAAm and seeded with ES cells into a 1mL volume of SCM in a 1.5mL Eppendorf tube (Fig 6.9). Due to the Eppendorf tube being a sealed unit, the rotation time was reduced from 6hrs to 3hrs to avoid hypoxic conditions. The cap was removed from the Eppendorf tubes once every half to allow for fresh gaseous exchange and then resealed. The majority of EBs exhibited microparticle incorporation over all seeding ratios investigated observed as black spheres embedded within light and transparent aggregates. Clearly, a reduced suspension volume afforded by the Eppendorf method, appeared to enhance microparticle incorporation. Coating with ppAAm provided microparticles with sufficient adhesive properties for increased incorporation compared to both gelatin and FCS-coating. It therefore appears that the ability of ES cells to adhere to the microparticle surface did not directly correlate with microparticle incorporation. 2.5:1 was chosen as the optimum seeding ratio for all subsequent experiments. Microparticles were shown to be spread throughout the

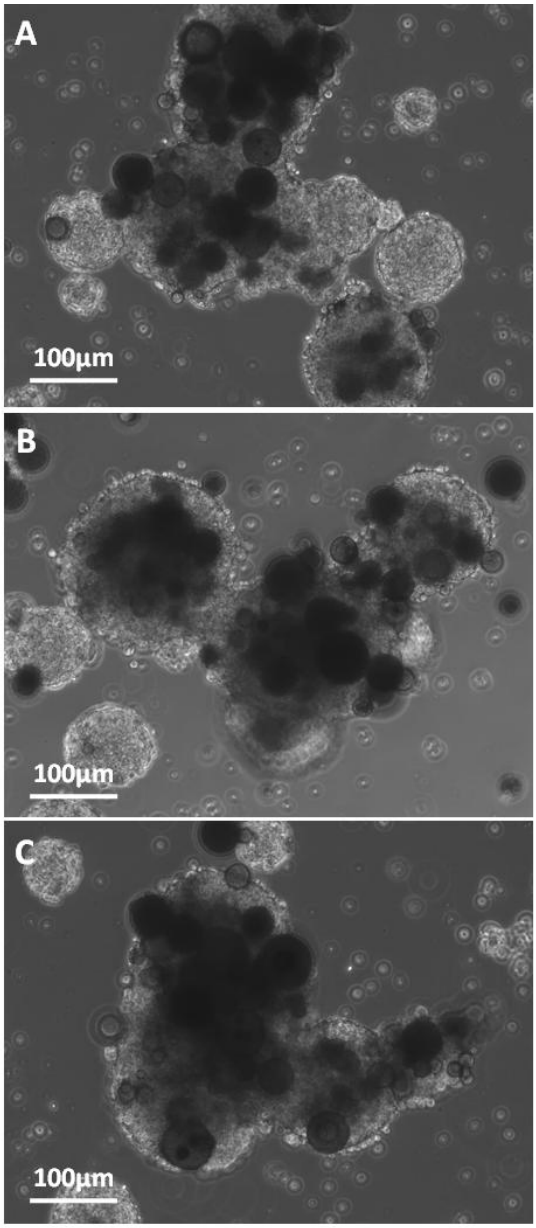

Figure 6.9: Microparticle incorporation within Eppendorf derived EBs. Appropriate quantities of plain microparticles were coated with ppAAm and suspended in AM. Microparticles were then seeded with control 1 ES cells (5 x 10^4 cells/mL) at 5:1 (A), 2.5:1 (B) and 1:1 (C) (microparticles to ES cells) into an Eppendorf tube suspended in AM. Suspensions were agitated at 15rpm for 6hrs (cap was opened and closed after 3hrs for exchange of gases as Eppendorf tube was a sealed unit) before transfer to mass suspension and culture in SCM for 24hrs before imaging.

EB structure in both engineered and control ES cell samples (Fig 6.10). The presence of DAPI stained cell nuclei covering the location of a microparticle indicated that the microparticle was embedded within the EB (Fig 6.10A). Other microparticle locations showed minimal or no cell nuclei coverage, indicating that the microparticle was at the surface of the EB (Fig 6.10B).

6.3.5. Embryonic Stem Cell Viability

Plain microparticles with ppAAm-coating were seeded in a 1.5mL Eppendorf tube with both engineered and control ES cells at a ratio of 2.5:1 (Fig 6.11). After 5 days of culture EBs were labelled with Live/Dead™ stain and imaged. Strong green fluorescence was observed in all samples illustrating the fact that the majority of ES cells were alive and thriving. Microparticle incorporation was therefore found to not have a detrimental effect on ES cell viability. However, there were areas of red fluorescence indicating the presence of dead or necrotic ES cells. Red fluorescence was mainly restricted to the centre of EBs as depicted by the overlay images in Fig 6.11. Suspensions were incubated for 5 days instead of 3 days for increased EB stability during Live/Dead™ stain and sequential PBS washing. Red fluorescence was randomly spaced throughout the centre of the EB structure and not located in proximity to microparticles. No measurable difference was observed in ES cell viability between engineered and control samples. Microparticle incorporation appeared similar in all samples being randomly distributed both within an individual EB and between EBs. Microparticles were not auto-fluorescent.

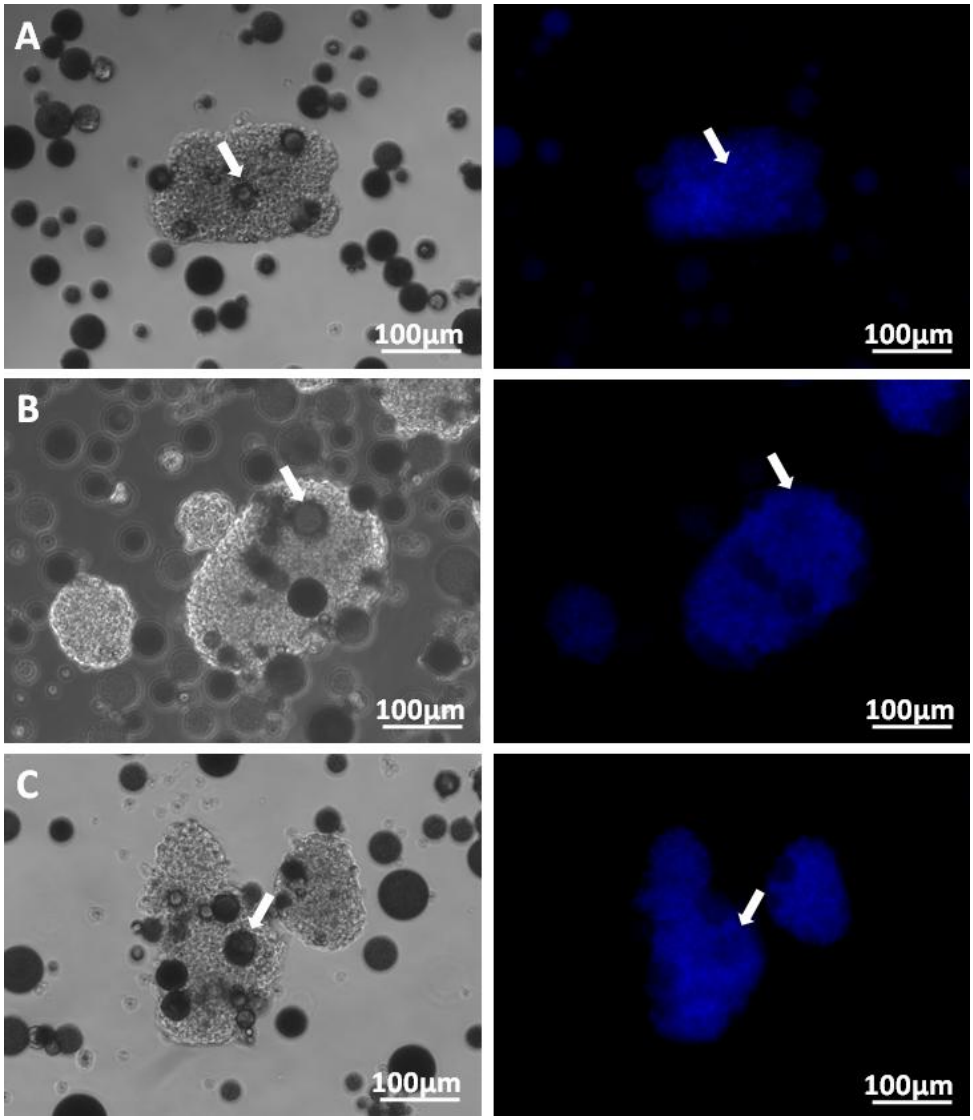

Figure 6.10: Microparticle location within Eppendorf derived EBs. Appropriate quantities of plain microparticles were coated with ppAAm and suspended in AM. Microparticles were then seeded with engineered (A), control 1 (B) and control 2 ES cells (5 x 10^4 cells/mL) (C) at an optimal ratio of 2.5:1 (microparticles to ES cells) into an Eppendorf tube suspended in AM. Suspensions were agitated at 15rpm for 6hrs (cap was opened and closed after 3hrs for exchange of gases as Eppendorf tube was a sealed unit) before transfer to mass suspension and culture in SCM for 24hrs. After 24hrs, microparticle incorporation was assessed by DAPI staining and fluorescence imaging at ex/em 358/461nm.

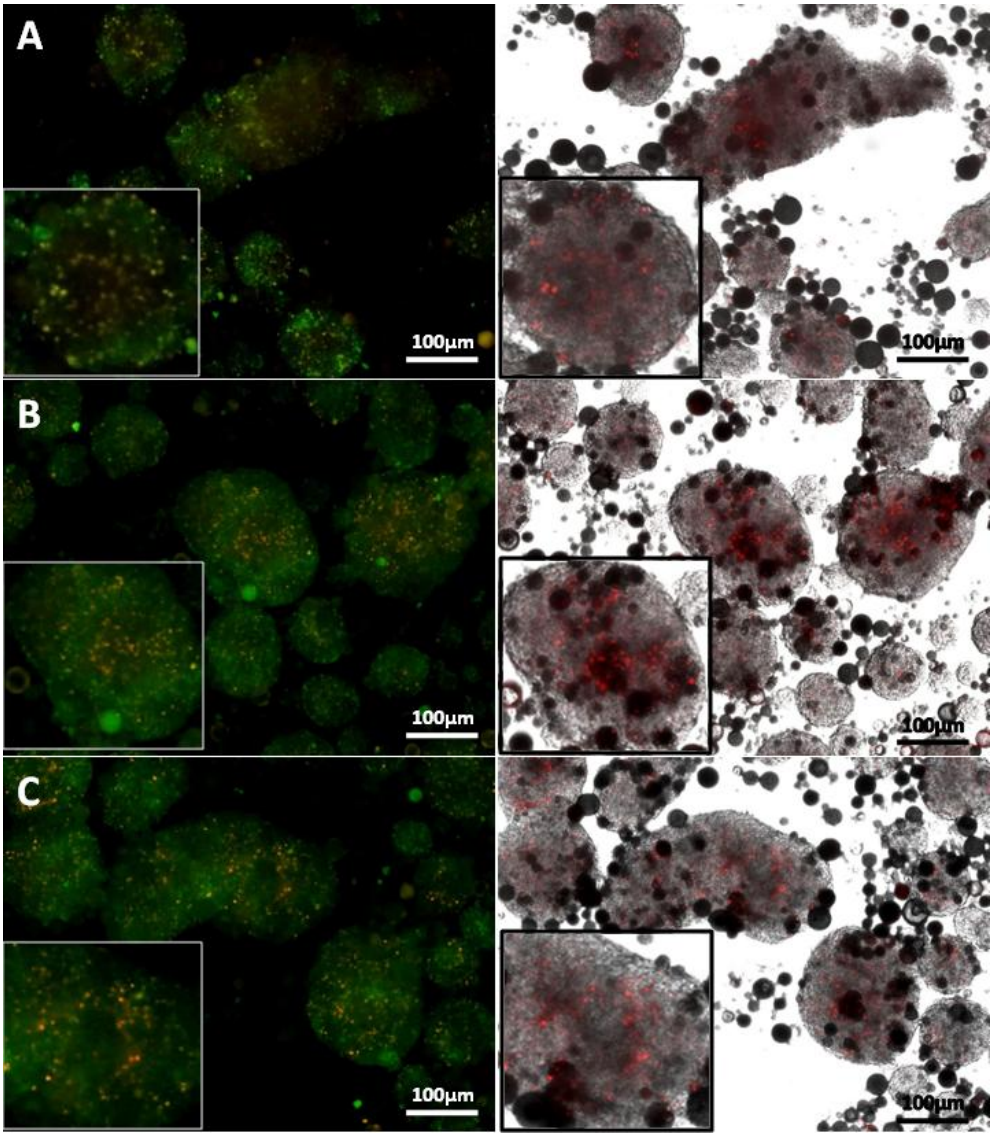

Figure 6.11: ES cell viability within microparticle-incorporated EBs. Appropriate quantities of Dex-loaded microparticles were coated with ppAAm and suspended in AM. Microparticles were seeded with engineered (A), control 1 (B) and control 2 ES cells (5 x 10^4 cells/mL) (C) at a ratio of 2.5:1 (microparticles to ES cells) into an Eppendorf tube suspended in AM. Suspensions were agitated at 15rpm for 6hrs (cap was opened and closed after 3hrs for exchange of gases as Eppendorf tube was a sealed unit) before transfer to mass suspension and culture in SCM for 5 days. After 5 days, ES cell viability within resultant EBs was assessed by Live/Dead™ stain. Box inserts were imaged at 20x magnification.

6.4. Discussion

It has been shown that the aggregation step of EB formation has important ramifications on downstream differentiation of constituent ES cells. Alteration of the aggregation step afforded by the proposed engineered 3D culture system has been shown to increase osteogenic differentiation in differentiated ES cell cultures (Chapter 5). However, cultures were heterogeneous and contained contaminating cell types such as cardiomyocytes. This was due to random uncontrolled ES cell differentiation within the EBs prior to osteo-induction. One solution would be to aggregate ES cells in osteo-inductive media. However, this may only cause appropriate differentiation in ES cells located at the EB surface since the osteo-inductive factors may not be able to permeate through the whole EB structure. Microparticles provide a means of delivering osteo-inductive factors such as Dex directly within the EB structure. By releasing Dex internally, it is hypothesized that most or all ES cells would be exposed during aggregation and EB formation (Fig 6.12). This may aid osteogenic differentiation throughout the EB structure and minimize the occurrence of contaminating cell types in downstream cultures. However, microparticles had to be fabricated and assessed for both Dex encapsulation and release during degradation. Here is shown, efficient incorporation of Dex-loaded microparticles into the EB structure and evaluation of their effect on ES cell aggregation and constituent ES cell viability.

6.4.1. Fabricated Microparticle Analysis

Microparticles exhibited the stereotypical spherical shape expected in micelle formation during the oil/water phase (Fig 6.2). The polymer is hydrophobic and therefore orientates itself away from contact with surrounding water molecules. The

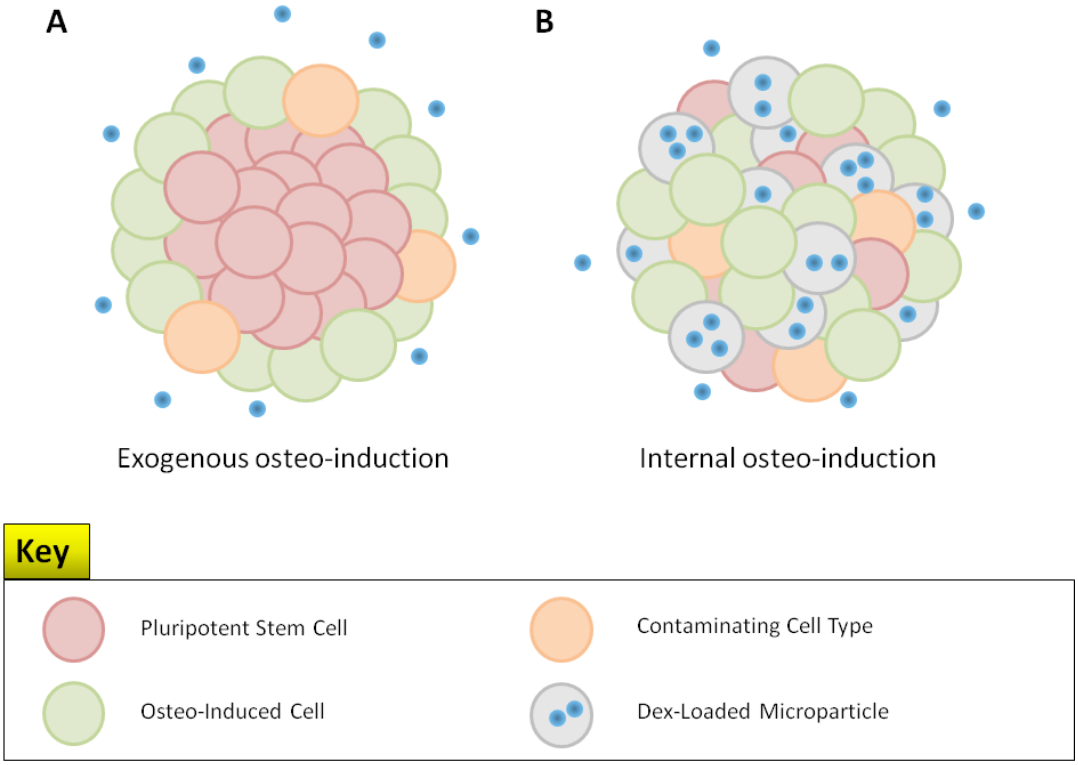

Figure 6.12: Dex-loaded microparticle incorporation and ES cell differentiation. Only ES cells located at the EB surface become differentiated when inductive factors are added exogenously within the surrounding media (A). These create a barrier against inductive factors and permeation internally is restricted. Dex-loaded microparticles can be incorporated within the EBs generating a mixed structure. The released Dex no longer needs to diffuse across the EB structure as it will be released from numerous locations throughout the EB. ES cells throughout the EB structure would become differentiated due to osteo-induction from these Dex-loaded microparticles (B).

least chaotic conformation to achieve this is a sphere where the pressure to move away from the water is equal between adjacent polymer molecules. Microparticles also exhibited a smooth and solid surface morphology from which a uniform release of Dex would be permitted. A smooth surface may also have reduced interaction between microparticles due to a lack of aberrations with which to link together. Interaction between microparticles was still possible through electrostatic attraction between hydrophilic surfaces. No major difference was observed between plain and Dex-loaded microparticles. However, Dex-loaded microparticles did exhibit a tighter size distribution compared to plain microparticles (Figs 6.2B and D, respectively). It was possible that solubilized Dex within the oil phase reduced chance interaction between polymer molecules when agitated using a vortex machine. Reduced chance interactions would lead to fewer polymer molecules within individual micelles and result in smaller microparticles. However, this was only an observation made during SEM imaging and would require verification by further analysis. Microparticles exhibited holes with a diameter measuring ≤ 1μm in all samples. Holes are an artefact of the fabrication process. The DCM solvent requires an escape route in order to evaporate. Consequently, tiny channels are formed as the DCM evaporates and the microparticles harden. Microparticles are thought of as solid structures encapsulating a solid core of Dex, much like an egg (polymer = white, and Dex = yolk). However, DCM evaporation reveals microparticles are actually porous. This is beneficial to Dex release as it allows solution to enter the microparticles and aid both internal and external degradation. The majority of microparticles exhibited a spherical shape and smooth surface morphology (Figs 6.2A and C) however, a minority exhibited surface defects and imperfections. The larger proportion of these microparticles exhibited minor imperfections such as a rippled surface morphology.

The rippled effect was most likely due to uneven distribution of polymer. This would have effectively slowed Dex release since degradation time would have increased with polymer thickness. The smaller proportion of these microparticles exhibited large defects including partial to complete collapse (Figs 6.2E and F, respectively). This is suggestive of damage to the microparticle during fabrication. During hardening, the microparticles may have ruptured and become deflated whilst still supple. Complete evaporation of the solvent would therefore have left the microparticle in a hardened and permanently collapsed conformation. In all images, tiny microparticles with a diameter < 50μm were observed. Tiny microparticles were present even after fractionation to acquire a diameter range of 50-100μm. It appears that the force of gravity acting on these tiny microparticles was overcome by their electrostatic interaction with larger microparticles. Consequently, the 50-100μm fraction contained an unknown proportion of contaminating tiny microparticles. Their presence was unaccounted for and therefore so too was the amount of Dex they released. This would require further analysis for accurate quantification. However, since calculation of Dex encapsulation involved these tiny microparticles, the Dex they released was partly quantified as part of the whole fraction.

Ensuing experiments required precise numbers of microparticles to ES cells. Therefore microparticle number within the 50-100μm fraction was quantified by PSS (Fig 6.3). Both plain and Dex-loaded samples exhibited a linear trend between microparticle number and weight showing a direct correlation. However, Dex-loaded samples exhibited an increased number of microparticles within a given weight. This supports the observation of smaller microparticles within Dex-loaded samples compared to plain samples in Fig 6.2. Since the amount of polymer was constant and the weight from the 50-100μm fraction was the same, then the only explanation for

increased microparticle number was that there must have been more microparticles at the low end (50μm) of the fraction than at the high end (100μm). Plain microparticles exhibited larger error in microparticle number which indicated a wider size distribution than Dex-loaded microparticles.

6.4.2. Release Profile of Dexamethasone-Loaded Microparticles

Entrapment efficiency was calculated as 18.16% which would mean that 1g of microparticles contained 1.8mg of Dex. This could possibly be increased by adding more Dex to the initial mixture. However, it has been suggested that the addition of Dex has an effect of microparticle size. Therefore, simply adding more Dex may hinder fabrication of microparticles with the required diameter range of 50-100μm. The 50-100μm range was chosen for practical reasons concerning fractionation and because of the need to avoid internalization within the ES cell. Subsequently, the release profile of Dex-loaded microparticles was assessed over a 30 day period (Fig 6.5). There appeared to be an initial burst release phase followed by a steady release phase over 14 days which then decreased as encapsulated Dex became diminished. The initial burst release was mainly due to diffusion of Dex close to the surface and from evaporation channels (Yeo and Park, 2004). The rapid release could have caused a build up of Dex in the local vicinity that exceeded biologically acceptable levels, leading to toxicity and cell death. Many methods have been employed to reduce or stop this well recorded phenomenon (Allison, 2008). One such method involves cross-linking of the surface to reduce the dissolution of encapsulated drug (Thote et al., 2005). However, there are drawbacks with all attempts including a delayed steady release phase which is the most important part of drug release. Rather than altering parameters to reduce the initial burst release, microparticles

were simply incubated in PBS for 3 days prior to the addition of ES cells therefore bypassing the initial burst release. After the initial burst release, further Dex release slowed and exhibited a linear relationship with incubation time and therefore polymer degradation. This steady release phase lasted for 14 days and produced ~1.3μg/mL/day Dex. The steady and slow release of Dex was ideal for sustained osteo-induction without exceeding non-toxic levels. Beyond 14 days, release decreased due to exhaustion of encapsulated Dex. However, release remained linear and persisted to 30 days providing osteo-induction for the full 4 week incubation period. Also, high but steady release of Dex would really only be required until terminal ES cell differentiation towards the osteoblastic lineage. Since osteoblast function in the form of bone nodules was observed within engineered samples after 2 weeks, the release profile of Dex-loaded microparticles is ideal for osteo-induction without localized concentrations reaching cytotoxic levels.

6.4.3. Microparticle Coating and Embryonic Stem Cell Attachment

The next step was to investigate the adhesive properties of the microparticles concerning ES cell attachment. The hydrophobic properties of PLGA proved a hindrance towards ES cell attachment (Fig 6.6D). Therefore, different coatings that would bind to the hydrophobic surface and express adhesive molecules recognised by ES cells were investigated (Neff et al., 1998). The coatings included gelatin, FCS and ppAAm. Gelatin was used as it was found to improve EB adhesion to culture wells during previous osteogenic differentiation experiments and also to PLGA microparticles (Tsung and Burgess, 2001). FCS was used as it contains many components conducive to cell attachment such as fibronectin and vitronectin (Norris et al., 1990, Blanquet, 1982). Coating with ppAAm provides a synthetic method for

enhancing cell attachment (Hamerli et al., 2003). Initially, uncoated microparticles were assessed as a control for other coatings and showed minimal to no cell attachment after 24hrs incubation. All coatings enhanced cell attachment and spreading as observed by the presence of labelled cells on the microparticle surface (Figs 6.6A, B and C). No significant difference was observed between coatings however, results were qualitative not quantitative. Further analysis may have highlighted substantial differences.

6.4.4. Microparticle and Embryonic Stem Cell Aggregation

To determine the correct ratio of microparticles to ES cells for optimum microparticle incorporation within EBs a wide range was investigated from 1:1 to 40:1, respectively (Fig 6.7). Microparticles were gelatin-coated and seeded into suspension with control ES cells in a volume of 2mL AM. At high seeding ratios ≥ 20:1, microparticles were not incorporated within EBs. Microparticles remained free floating in suspension whereas ES cells attached to the culture well surface and proliferated to form colonies (Figs 6.7C and D). Due to the large number of microparticles in suspension the chance collisions between them would also have been high. These collisions could easily have damaged attached ES cells on the microparticle surface. Alternatively, ES cells may have attached to the microparticles but due to the high microparticle numbers it was difficult to find those that exhibited ES cell attachment. The lack of EB formation would therefore simply be due to the lack of interaction between microparticles exhibiting ES cell attachment. Previous experiments have shown that ES cells migrate and spread outwards once adhered to the well surface. This would explain the generation of 2D cell colonies observed in Figs 6.7C and D. In suspensions at low seeding density ≤ 10:1, microparticles were

incorporated within the EB structure, as observed by opaque spheres embedded in translucent EBs (Figs 6.7A and B). The decreased number of microparticles would have lowered the chance of collisions between microparticles. Due to the lower number of microparticles, ES cell coverage would have been relatively higher than that with greater microparticle numbers. Consequently, chance collisions between ES cell attached microparticles would have been increased. As a result, ES cells coalesced and proliferated across the surface of the adhered microparticles generating microparticle embedded EBs. These observations warranted further analysis of low seeding ratios. However, the methodology was not optimal due to the low frequency of EB formation. Only two or three EBs were observed in whole samples. Many ES cells had attached to the well surface and microparticles were free floating. To address this problem, gelatin-coating was replaced with FCS-coating. Initial aggregation which was carried out in AM containing 1% FCS was subsequently carried out in SCM containing 10% FCS to both maintain coating on microparticles and also decrease possible stress from nutrient competition between ES cells.

FCS-coated microparticles were seeded into suspension with control ES cells at low seeding ratios of 5:1, 2.5:1 and 1:1 (Fig 6.8). The most striking difference observed was that considerably more EBs formed at these low ratios. Evidently, high microparticle numbers hinder ES cell aggregation. However, the increased number of EBs did not exhibit increased microparticle incorporation. The majority of EBs comprised solely of ES cells with most microparticles free floating in suspension (Figs 6.8A and E). Consequently, low seeding ratio was essential for EB formation but had little or no effect on microparticle incorporation. The low number of microparticles allowed for increased ES cell-ES cell interaction and resultant EB formation. Another observation was that only large EBs contained microparticles

(Fig 6.8C). It was therefore possible that during rotation, ES cells attached to microparticles and formed EBs which continued to increase in size during stationary culture for 3 days. The presence of small EBs without microparticle incorporation developed from those ES cells that were not attached to microparticles during rotation. During stationary culture their chance of interaction with microparticles was reduced. These EBs may eventually have incorporated microparticles if given longer incubation periods. Alternatively, microparticles may not have been incorporated within EBs during initial aggregation. It is possible that EBs form from ES cells alone and proliferate until they reach a critical size. Once EBs reached a size which was larger than adjacent microparticles, microparticles became attached and 'engulfed' by the EB. It has been shown that EBs are capable of structural reorganization and could therefore have reshaped and proliferated around the microparticle. This would explain why only larger EBs contained microparticles and why so many microparticles remained in suspension. However, further analysis of initial aggregation during rotation and immediately after would be required to vindicate this hypothesis.

FCS-coated microparticles have been shown to enhance ES cell attachment however, this was within static culture. It was possible that rotation provided microparticles with too much kinetic energy so that interaction between microparticles and ES cells was not long enough for attachment. This supported the idea that microparticles were 'engulfed' within existing EBs and provides explanation as to why minimal EB formation was observed in suspensions with gelatin-coated microparticles. Both gelatin and FCS notably enhance ES cell attachment, but only in static culture when ES cells and microparticles can be held in close proximity for long time periods. Both gelatin and FCS-coated microparticles were sterilized by U.V. irradiation for 20mins

prior to seeding into suspension with ES cells. It has been shown that U.V. exposure can increase the adsorption properties of gelatin and ECM components within FCS (Stevens et al., 1998). Therefore, ES cell attachment to U.V. irradiated gelatin and FCS-coated microparticles would have been greatly enhanced. It was therefore safe to assume that some attachment did occur. The absence of microparticle-incorporated EBs therefore required alternative explanation. It was possible that the increased volume and decreased ES cell-ES cell interaction due to the addition of a microparticle suspension may have had a detrimental effect on EB formation. ES cell adhesion to the microparticles still occurred, but ES cell-ES cell attachment was reduced.

Aggregation was transferred to an Eppendorf tube and microparticles were coated in ppAAm to enhance microparticle incorporation during the aggregation step (Dehili et al., 2006, Barry et al., 2005). Rotation speed remained at 15rpm but time was reduced to 3hrs to avoid hypoxia within the samples since the Eppendorf tubes were sealed. All samples generated microparticle-incorporated EBs as observed by black spheres within almost transparent ES cell aggregates (Fig 6.8). Coating with ppAAm enhanced microparticle incorporation. However, small EBs did not contain microparticles. This was due to proliferation of ES cells which had remained in suspension after the rotation period. The vessel shape also appeared to have had an effect on the efficiency of aggregation and EB formation. The culture well was cylindrical and rotation caused fluid movement such that a vortex was created. The vessel shape of an Eppendorf is also cylindrical however the tube was long and thin and placed on the rotating platform on its side. Consequently, fluid movement no longer formed a vortex but was rather reduced to a gentle unidirectional flow from one end of the tube to the other. The simple fluid movement may therefore have

been adequate to mobilize microparticles and ES cells enabling interaction without too much shear stress. Therefore, vessel shape was shown to control fluid flow which had a direct effect on EB formation. There was no observed difference between seeding ratios and therefore an arbitrary ratio of 2.5:1 was chosen for all subsequent experiments. Further analysis involved the use of both engineered and control ES cells (Fig 6.10). Microparticles were positioned within the EBs rather than adhered to the surface. The presence of DAPI stained ES cell nuclei in front of microparticles during imaging demonstrated the fact that they encased the microparticle. Microparticles that did not have ES cells in front were either embedded in the surface or not attached. Both engineered and control samples formed microparticle-incorporated EBs. It was found that engineered ES cells no longer aggregated efficiently without the addition of avidin (Chapter 3). The advantage of ppAAm-coating was that it would have adsorbed avidin protein to the microparticle surface which would therefore have enhanced direct adhesion of engineered ES cells. The presence of amine groups on the surface could also have caused direct adhesion to the reactive aldehyde groups on the engineered ES cell surface via reductive amination (Griesser et al., 1994, Myung and Choi, 2006). Gelatin and FCS-coating enhanced attachment of ES cells via recognition of natural adhesion molecules (Nagaoka et al., 2006, Pokutta and Weis, 2007, Muller et al., 2008). Engineered ES cells may have been temporarily unable to recognise these, until membrane renewal replaced the surface modification.

6.4.5. Embryonic Stem Cell Viability

ES cell viability was assessed within both engineered and control EBs containing microparticles (Fig 6.11). The majority of ES cells were alive and thriving.

Consequently, the Eppendorf-based method did not have a detrimental effect on ES cell viability. It was also suggestive that shear force and microparticle-microparticle collisions did not cause lethal damage to the ES cells during aggregation. ES cell viability also demonstrated the non-toxic effect of ppAAm. The most important finding was that the Dex release did not appear to build up to toxic levels. However, there were dead ES cells present within the EB, but their location did not correlate with that of the microparticles. It is possible that dead ES cells were simply reorganized to the core during EB restructuring.

6.5. Conclusions

In summary, PLGA and triblock microparticles with a diameter of 50-100μm were fabricated using a single emulsion method. Dex was encapsulated within these microparticles with an efficiency of 18.16%, and release was linear and constant providing osteo-induction over 30 days after an initial burst release for 3 days. These microparticles were incorporated within both engineered and control EBs for the intention of delivering osteo-induction during EB formation. Ideal seeding ratio was found to be 2.5:1, microparticles to ES cells. However, mass suspension culture was found to be inadequate for microparticle incorporation. Introduction of an Eppendorf-based method increased the efficiency of microparticle incorporation and yielded high quantities of ES cell/microparticle EBs. Characterisation revealed that microparticles were randomly positioned throughout the EB structure and that neither their presence nor the potential released Dex caused noticeable cell death. However, the addition of microparticles resulted in the formation of larger EBs which in turn increased the surface to core distance. Consequently, efficient nutrient and gaseous exchange was decreased and microparticle incorporated EBs tended to suffer a higher frequency of core necrosis. However, control afforded by engineering provides the ability to alter aggregation kinetics and could therefore be employed to resolve this problem. Further analysis would be required to assess the impact of Dex-loaded microparticle incorporation on osteogenic differentiation.

Chapter 7

7. Conclusions

To summarize, aggregation occurred via a rapid but weak initial attachment. These temporary connections were susceptible to breaking as a result of environmental stresses during initial rotation. However, once under stationary conditions ES cell clusters formed through further aggregation and structural reorganization to a less chaotic conformation. ES cell clusters developed into EBs through a complex interaction between ES cell aggregation, proliferation, death, cluster agglomeration and ECM deposition. Engineered EBs were significantly ($P \leq 0.001$) larger in size and exhibited improved constituent ES cell viability.

Engineered EBs were both larger and denser than control EBs. However, ES cell viability remained unaffected demonstrating that engineering may have enhanced ES cell-ES cell adhesion in such a way to as improve nutrient and gaseous exchange across the entire EB structure. Extended culture beyond 3 days resulted in core necrosis. Core necrosis caused EBs to exhibit a layered structure where the innermost region composed of necrotic cells and the surface composed of alive and thriving ES cells. These surface ES cells were subject to environmental cues such as exogenous growth factors and began to spontaneously differentiate. A range of cell morphologies were observed on both engineered and control EBs illustrating the fact that chemical modification did not have a detrimental effect on ES cell differentiation

potential. This is extremely important if the proposed methodology were to be expanded to an industrial scale. All three germ layers were found to be present on the EB surface with a noticeable increase in mesoderm differentiation on engineered EBs. Cadherin-11 expression on the engineered EB surface indicated a potential for enhanced osteogenic differentiation.

Further investigation revealed that cultures originating from engineered EBs exhibited enhanced levels of osteogenic differentiation, quantified by ALP activity, bone nodule counts and OPN/Runx2 expression. Osteogenic differentiation also appeared enhanced in ES cell cultures involving EB formation, and where EBs were not dispersed prior to osteo-induction. These observations indicated that ES cell-ES cell and ES cell-ECM interactions were highly prevalent in osteogenic differentiation. Surface cells were the first to migrate outwards from settled EBs and were thought to be chondrocytes. The ECM they deposited provided a platform for cell proliferation and eventual osteoblast-driven mineralization. Improved viability within engineered EBs also appeared to enhance osteogenic differentiation. It appeared that engineering simply enhanced mesoderm differentiation, which increased relative ES cell proportions susceptible to osteo-induction.

Cultures exhibited contaminating cell types including beating cardiomyocytes. It was hypothesised that these arose from randomly differentiated internal progenitor cells within the EB during aggregation where there was no osteo-induction. Although engineering allowed for control of EB formation, it is believed that inductive signals may still be required for the generation of homogenously differentiated cell populations. The next step was to introduce osteo-inductive factors to the ES cells during the EB stage. Dex-loaded microparticles were chosen as a delivery system and their incorporation within the EB was investigated. The microparticles exhibited an

entrapment efficiency of 18.16% and a steady release of Dex over a 4 week period. Analysis revealed that microparticle incorporation was optimum when microparticles were ppAAm-coated and seeded at 2.5:1 with ES cells. The suspension volume and vessel shape were crucial to efficient microparticle incorporation, affecting parameters such as fluid motion, shear stress and field flow. Microparticles were randomly spaced throughout the EB structure resulting in uneven distribution of released Dex. However, levels were low enough to avoid cytotoxic effects. Further analysis would be required to assess control over spatial orientation of microparticles within the EB. The effect of microparticle incorporation on osteogenic differentiation was unfortunately not examined due to time restraints during the study.

In conclusion, chemical modification of the ES cell surface has proven to exhibit a high degree of control over aggregation and EB formation. The proposed engineered 3D culture system provided a reliable, reproducible and non-cytotoxic methodology for the controlled and enhanced production of EBs compared to control samples. The methodology also showed potential economic benefits via a reduction in the required incubation time due to accelerated ES cell aggregation. There will be many obstacles to overcome, but this novel aggregation method could be transferred to a human ES cell line (Ginis et al., 2004). These standardised EBs could provide a valuable tool in the field of tissue engineering and regenerative medicine (Griffith and Naughton, 2002, Rose and Oreffo, 2002).

Chapter 8

8. Further Work

Although the proposed 3D culture system holds great promise for the field of tissue engineering and regenerative medicine, many facets of the process still require investigation and resolution. Engineered EBs exhibited enhanced ES cell viability compared to control EBs. However, all EBs began to show signs of necrosis within their core after ~5 days in culture due to an ever increasing surface to core distance for efficient nutrient and gaseous exchange. Investigation revealed that EBs cultured for < 5 days exhibited the greatest levels of osteogenic differentiation providing a convenient solution to this problem. However, increased EB diameter via incorporation of microparticles appeared to accelerate core necrosis. Furthermore, the generation of other cell types may require extended culture during the EB stage beyond 3 days. Consequently, there is a distinct need for improved nutrient and gaseous exchange throughout the EB structure. One solution currently under investigation is vascularization of the EB structure. Many methods exist for effective vasculogenesis and angiogenesis within the EB involving addition of exogenous growth factors, co-culture and biodegradable scaffolds (Boyd et al., 2007, Wenger et al., 2005, Luong and Gerecht, 2008). It is hoped that vascularization will effectively generate an invasive network through which nutrients and growth factors can be

pumped into the EB structure maintaining ES cell viability and inducing differentiation. However, the obvious problem with this methodology is the generation of heterogeneous cell populations if the desired cell type is not endothelium. Engineered aggregation has shown influence over such EB properties that could aid in effective nutrient and gaseous exchange, including density and diameter. Therefore, fine tuning of affecting parameters, such as extent of biotinylation, exogenous avidin concentration and cell seeding density may provide control over EB structure and viability enabling longer incubation periods.

In vivo embryogenesis involves countless intricately controlled interactions between numerous cell types. It is unknown how these interactions eventuate in the formation of specific cell types. Engineered EBs would provide an ideal means to investigate these interactions under controlled parameters. However, if heterogeneous populations are required for the efficient generation of desired cell types then these would require effective isolation in preparation for clinical application (Kim et al., 2007b, Kumashiro et al., 2005, Shamblott et al., 2001). Isolation techniques would also be required to extract desired cell types from cultures originating from vascularized EBs.

Clinical application would require large quantities of biological material for transplantation. Consequently, the proposed 3D culture system would need to be scaled-up to an industrial level that is cost effective, whilst maintaining any observed enhancement to ES cell differentiation. One leading method of increasing production is the use of bioreactors (Dang et al., 2004, Botta et al., 2007, Come et al., 2008, Yin et al., 2007, Hwang et al., 2009). However, changing the aggregation method may have detrimental effects on the observed osteogenic differentiation enhancement within engineered samples. Further investigation would be required to assess bioreactors

as a viable option for increased production of desired biological material. Interestingly, bioreactor-based 3D models have been previously utilized to investigate cancer signalling (Mastro and Vogler, 2009). It may therefore be possible to use a similar model to investigate the signalling involved within engineered EB formation and how this affects observed osteogenic differentiation.

Ultimately, the whole system would have to be transferred to a human ES cell line for the controlled investigation of early steps involved in human embryogenesis. Understanding the fundamental ES cell-ES cell and ES cell-ECM interactions involved in organogenesis is crucial to *in vitro* generation of potentially homogeneous cell populations for tissue regeneration, repair or replacement (Leahy et al., 1999). One drawback is that any biological material generated would inevitably lack *in vivo* architecture. To engineer tissues exhibiting *in vivo* architecture within the laboratory, ES cells can be cultured on biodegradable polymer scaffolds providing both chemical and spatial cues (Nichols and Cortiella, 2008, Fromstein et al., 2008, Lee et al., 2006).

Since microparticles were successfully incorporated within the EB structure the next step would be to investigate their potential as a delivery system for internally released Dex and their consequent impact on downstream osteogenic differentiation.

Chapter 9

9. References

ABDI, R., FIORINA, P., ADRA, C. N., ATKINSON, M. & SAYEGH, M. H. (2008) Immunomodulation by mesenchymal stem cells: a potential therapeutic strategy for type 1 diabetes. *Diabetes,* 57**,** 1759-1767.

ABE, K., NIWA, H., IWASE, K., TAKIGUCHI, M., MORI, M., ABE, S. I., ABE, K. & YAMAMURA, K. I. (1996) Endoderm-Specific Gene Expression in Embryonic Stem Cells Differentiated to Embryoid Bodies. *Experimental Cell Research,* 229**,** 27-34.

ABILEZ, O., BENHARASH, P., MEHROTRA, M., MIYAMOTO, E., GALE, A., PICQUET, J., XU, C. & ZARINS, C. (2006) A novel culture system shows that stem cells can be grown in 3D and under physiologic pulsatile conditions for tissue engineering of vascular grafts. *The Journal of Surgical Research,* 132**,** 170-178.

ALI, S. Y., SAJDERA, S. W. & ANDERSON, H. C. (1970) Isolation and Characterization of Calcifying Matrix Vesicles from Epiphyseal Cartilage. *Proceedings of the National Academy of Sciences of the United States of America,* 67**,** 1513-1520.

ALLISON, S. D. (2008) Analysis of initial burst in PLGA microparticles. *Expert Opinion on Drug Delivery,* 5**,** 615-628.

ALTMAN, J. (1962) Are New Neurons Formed in the Brains of Adult Mammals? *Science,* 135**,** 1127-1128.

AMIT, M. (2007) Feeder-layer free culture system for human embryonic stem cells. *Methods in Molecular Biology,* 407**,** 11-20.

AMIT, M., MARGULETS, V., SEGEV, H., SHARIKI, K., LAEVSKY, I., COLEMAN, R. & ITSKOVITZ-ELDOR, J. (2003) Human Feeder Layers for Human Embryonic Stem Cells. *Biology of Reproduction,* 68**,** 2150-2156.

ANDERSON, C. & DANYLCHUK, K. D. (1977) The effect of chronic low level lead intoxication on the Haversian remodeling system in dogs. *Laboratory Investigation,* 37**,** 466-469.

ANDERSON, C. & DANYLCHUK, K. D. (1978) Effect of chronic low level cadmium intoxication on the Haversian remodeling system in dogs. *Calcified Tissue Research,* 26**,** 143-148.

ANDERSON, H. C. (2003) Matrix vesicles and calcification. *Current rheumatology reports,* 5**,** 222-226.

ANDERSON, J. M. & SHIVE, M. S. (1997) Biodegradation and biocompatibility of PLA and PLGA microspheres. *Advanced Drug Delivery Reviews,* 28**,** 5-24.

ANDREWS, P. W. (2002) From teratocarcinomas to embryonic stem cells. *Philosophical transactions of the Royal Society of London. Series B,* 357**,** 405-417.

ARNAOUT, A. A., GOODMAN, S. & XIONG, J. P. (2007) Structure and mechanics of integrin-based cell adhesion. *Current Opinion in Cell Biology,* 19**,** 495-507.

ASCENZI, A. & BONUCCI, E. (1976) Relationship between ultrastructure and "pin test" in osteons. *Clinical Orthopaedics and Related Research,* 121**,** 275-294.

ASCENZI, A., BONUCCI, E., RIPAMONTI, A. & ROVERI, N. (1978) X-ray diffraction and electron microscope study of osteons during calcification. *Calcified Tissue Research,* 25**,** 133-143.

AWAD, H. A., WICKHAM, M. Q., LEDDY, H. A., GIMBLE, J. M. & GUILAK, F. (2004) Chondrogenic differentiation of adipose-derived adult stem cells in agarose, alginate, and gelatin scaffolds. *Biomaterials,* 25**,** 3211-3222.

BABIS, G. C. & SOUCACOS, P. N. (2005) Bone scaffolds: the role of mechanical stability and instrumentation. *Injury-International Journal of the Care of the Injured,* 365**,** S38-S44.

BADYLAK, S. F. (2004) Xenogeneic extracellular matrix as a scaffold for tissue reconstruction. *Transplant Immunology,* 12**,** 367-377.

BAGCHI, B., KUMAR, M. & MANI, S. (2006) CMV promotor activity during ES cell differentiation: potential insight into embryonic stem cell differentiation. *Cell Biology International,* 30**,** 505-513.

BAIN, G., KITCHENS, D., YAO, M., HUETTNER, J. E. & GOTTLIEB, D. I. (1995) Embryonic stem cells express neuronal properties in vitro. *Developmental Biology,* 168**,** 342-357.

BAKER, S. C. & SOUTHGATE, J. (2008) Towards control of smooth muscle cell differentiation in synthetic 3D scaffolds. *Biomaterials,* 29**,** 3357-3366.

BALAKRISHNAN, B. & JAYAKRISHNAN, A. (2005) Self-cross-linking biopolymers as injectable in situ forming biodegradable scaffolds. *Biomaterials,* 26**,** 3941-3951.

BARRILEAUX, B., PHINNEY, D. G., PROCKOP, D. J. & O'CONNOR, K. C. (2006) Review: ex vivo engineering of living tissues with adult stem cells. *Tissue Engineering,* 12**,** 3007-3019.

BARRY, J. J. A., SILVA, M. M. C. G., POPOV, V. K., SHAKESHEFF, K. M. & HOWDLE, S. M. (2006) Supercritical carbon dioxide: putting the fizz into biomaterials. *Philosophical Transactions: Series A: Maths, Physics and Engineering Sciences,* 364**,** 249-261.

BARRY, J. J. A., SILVA, M. M. C. G., SHAKESHEFF, K. M., HOWDLE, S. M. & ALEXANDER, R. A. (2005) Using Plasma Deposits to Promote Cell Population of the Porous Interior of Three-Dimensional Poly (D,L-Lactic Acid) Tissue-Engineering Scaffolds. *Advanced Functional Materials,* 15**,** 1134-1140.

BASMANAV, F. B., KOSE, G. T. & HASIRCI, V. (2008) Sequential growth factor delivery from complexed microspheres for bone tissue engineering. *Biomaterials,* 29**,** 4195-4205.

BAUWENS, C. L., PEERANI, R., NIEBRUEGGE, S., WOODHOUSE, K. A., KUMACHEVA, E., HUSAIN, M. & ZANDSTRA, P. W. (2008) Control of human embryonic stem cell colony and aggregate size heterogeneity influences differentiation trajectories. *Stem Cells,* 26**,** 2300-2310.

BELANGER, L. F. (1969) Osteocytic osteolysis. *Calcified Tissue Research,* 4**,** 1-12.

BELLOWS, C. G., AUBIN, J. E. & HEERSCHE, J. N. M. (1987) Physiological concentrations of glucocorticoids stimulate formation of bone nodules from isolated rat calvaria cells in vitro. *Endocrinology,* 121**,** 1985-1992.

BELLOWS, C. G., HEERSCHE, J. N. M. & AUBIN, J. E. (1990) Determination of the capacity for proliferation and differentiation of osteoprogenitor cells in the presence and absence of dexamethasone. *Developmental Biology,* 140**,** 1320138.

BENJAMIN, M. & EVANS, E. J. (1990) Research Review: Fibrocartilage. *Journal of Anatomy,* 171**,** 1-15.

BERRILL, A., TAN, H., WUANG, S., FONG, W., CHOO, A. B. & OH, S. K. (2004) Assessment of Stem Cell Markers During Long-Term Culture of Mouse Embryonic Stem Cells. *Cytotechnology,* 44**,** 77-91.

BHAGAVATI, S. (2008) Stem cell based therapy for skeletal muscle diseases. *Current Stem Cell Research Therapy,* 3**,** 219-28.

BIELBY, R. C., BOCCACCINI, A. R., POLAK, J. M. & BUTTERY, L. D. K. (2004) In Vitro Differentiation and In Vivo Mineralization of Osteogenic Cells Derived from Human Embryonic Stem Cells. *Tissue Engineering,* 10**,** 1518-1528.

BIGDELI, N., ANDERSSON, M., STREHL, R., EMANUELSSON, K., KILMARE, E., HYLLNER, J. & LINDAHL, A. (2008) Adaptation of human embryonic stem cells to feeder-free and matrix-free culture conditions directly on plastic surfaces. *Journal of Biotechnology,* 133**,** 146-153.

BISHOP, A. E., BUTTERY, L. D. K. & POLAK, J. M. (2002) Embryonic stem cells. *The Journal of Pathology,* 197**,** 424-429.

BLACKWOOD, K. A., MCKEAN, R., CANTON, I., FREEMAN, C. O., FRANKLIN, K. L., COLE, D., BROOK, I., FARTHING, P., RIMMER, S., HAYCOCK, J. W., RYAN, A. J. & MACNEIL, S. (2008) Development of biodegradable electrospun scaffolds for dermal replacement. *Biomaterials,* 29**,** 3091-3104.

BLANQUET, P. R. (1982) Unrelated Surface Control of Commitment to Growth and Attachment in Isolated Adult Rat Hepatocytes. *Journal of Cell Science,* 56**,** 40-69.

BLUM, B. & BENVENISTY, N. (2008) The tumorigenicity of human embryonic stem cells. *Advances in Cancer Research,* 100**,** 133-58.

BLUMER, M. J. F., LONGATO, S. & FRITSCH, H. (2008) Structure, formation and role of cartilage canals in the developing bone. *Annals of Anatomy,* 190**,** 305-315.

BLUTHMANN, H., VOGT, E., HOSLI, P., STEVENS, L. C. & ILLMENSEE, K. (1983) Enzyme activity profiles in mouse teratocarcinomas. A quantitative ultramicroscale analysis. *Differentiation,* 24**,** 65-73.

BOIS, P. R., O'HARA, B. P., NIETISPACH, D., KIRKPATRICK, J. & IZARD, T. (2006) The vinculin binding site of talin and alpha actin are sufficient to activate vinculin. *Journal of Biological Chemistry,* 281**,** 7228-7236.

BONEWALD, L. (2006) Osteocytes as multifunctional cells. *Journal of Musculoskeletal and Neuronal Interactions,* 6**,** 331-333.

BONFIELD, W. (2006) Designing porous scaffolds for tissue engineering. *Philisophical Transactions of the Royal Society Part A,* 364**,** 227-232.

BOONTHEEKUL, T., KONG, H. J. & MOONEY, D. J. (2005) Controlling alginate gel degradation utilizing partial oxidation and bimodal molecular weight distribution. *Biomaterials,* 26**,** 2455-2465.

BOTTA, G. P., MANLEY, P., MILLER, S. & LELKES, P. I. (2007) Real-time assessment of three-dimensional cell aggregation in rotating wall vessel bioreactors *in vitro*. *Nature,* 1**,** 2116-2127.

BOURNE, S., POLAK, J. M., HUGHES, S. P. F. & BUTTERY, L. D. K. (2004) Osteogenic differentiation of mouse embryonic stem cells: differential gene expression analysis by cDNA microarray and purification of osteoblasts by cadherin-11 magnetically activated cell sorting. *Tissue Engineering,* 10**,** 796-807.

BOYD, N. L., DHARA, S. K., REKAYA, R., GODBEY, E. A., HANSEEN, K., RAO, R. R., WEST, F. D. R., GERWE, B. A. & STICE, S. L. (2007) BMP4 promotes formation of primitive vascular networks in human embryonic stem cell-derived embryoid bodies. *Experimental Biology in Medicine,* 232**,** 833-843.

BOYD, S. M., HOOPER, M. L. & WYLLIE, A. H. (1984) The mode of cell death associated with cavitation in teratocarcinoma-derived embryoid bodies. *Journal of Embryology and Experimental Morphology,* 80**,** 63-74.

BOYDE, A., DILLON, C. E. & JONES, S. J. (1990) Measurement of osteoclastic resorption pits with a tandem scanning microscope. *Journal of Microscopy,* 158**,** 261-265.

BRATT-LEAL, A. M., CARPENEDO, R. L. & MCDEVITT, T. C. (2009) Engineering the embryoid body microenvironment to direct embryonic stem cell differentiation. *Biotechnology Progress,* 25**,** 43-51.

BRINSTER, R. L. (1974) The effect of cells transferred into the mouse blastocyst on subsequent development. *Journal of Experimental Medicine,* 140**,** 1049-1055.

BUDYANTO, L., GOH, Y. Q. & OOI, C. P. (2008) Fabrication of porous poly (L-lactide) (PLLA) scaffolds for tissue engineering using liquid-liquid phase separation and freeze extraction. *Journal of Materials Science:Materials in Medicine*.

BULIC-JAKUS, F., ULAMEC, M., VLAHOVIC, M., SINCIC, N., KATUSIC, A., JURIC-LEKC, G., SERMAN, L., KRUSLIN, B. & BELICZA, M. (2006) Of mice and men: teratomas and teratocarcinomas. *Collegium antropologicum,* 30**,** 921-4.

BURDICK, J. A. & VUNJAK-NOVAKOVIC, G. (2008) Review: Engineered Microenvironments for Controlled Stem Cell Differentiation. *Tissue Engineering Part A*.

BURDON, T., STRACEY, C., CHAMBERS, I., NICHOLS, J. & SMITH, A. (1999) Suppression of SHP-2 and ERK signalling promotes self-renewal of mouse embryonic stem cells. *Developmental Biology,* 210**,** 30-43.

BURRIDGE, P. W., ANDERSON, D., PRIDDLE, H., MUNOZ, M. D. B., CHAMBERLAIN, S., ALLEGRUCCI, C., YOUNG, L. E. & DENNING, C. (2007) Improved human embryonic stem cell embryoid body homogeneity and cardiomyocyte differentiation from a novel V-96 plate aggregation system highlights interline variability. *Stem Cells,* 25**,** 929-938.

BURT, R. K., SLAVIN, S., BURNS, W. H. & MARMONT, A. M. (2002) Induction of tolerance in autoimmune diseases by hematopoietic stem cells. *Blood,* 99**,** 768-784.

BURT, R. K., TRAYNOR, A. & STATKUTE, L. (2006) Nonmyeloablative hematopoietic stem cell transplantation for systemic lupus erythematosus. *Journal of the American Medical Association,* 295**,** 527-535.

BUTLER, D. L., GOLDSTEIN, S. A. & GUILAK, F. (2000) Functional tissue engineering: the role of biomechanics. *Journal of biomechanical engineering,* 122**,** 570-5.

BUTTERY, L. D. K., BOURNE, S., XYNOS, J. D., WOOD, H., HUGHES, F. J., HUGHES, S. P. F., EPISKOPOU, V. & POLAK, J. M. (2001) Differentiation of Osteoblasts and in Vitro Bone Formation from Murine Embryonic Stem Cells. *Tissue Engineering,* 7**,** 89-99.

CAI, H., AZANGWE, G. & SHEPHERD, D. E. T. (2005) Skin cell culture on an ear-shaped scaffold created by fused deposition modelling. *Bio-Medical Materials and Engineering,* 15**,** 375-380.

CAO, T., HENG, B. C., YE, C. P., LIU, H., TOH, W. S., ROBSON, P., LI, P., HONG, Y. H. & STANTON, L. W. (2005) Osteogenic differentiation within intact human embryoid bodies result in a marked increase in osteocalcin secretion after 12 days of in vitro culture, and formation of morphologically distinct nodule-like structures. *Tissue and Cell,* 37**,** 325-334.

CAPO-CHICHI, C. D., RULA, M. E., SMEDBERG, J. L., VANDERVEER, L., PARMACEK, M. S., MORRISEY, E. E., GODWIN, A. K. & XU, X. X. (2005) Perception of differentiation cues by GATA factors in primitive endoderm lineage determination of mouse embryonic stem cells. *Developmental Biology,* 286**,** 574-586.

CARPENEDO, R. L., SARGENT, C. Y. & MCDEVITT, T. C. (2007) Rotary Suspension Culture Enhances the Efficiency, Yield, and Homogeneity of Embryoid Body Differentiation. *Stem Cells,* 25**,** 2224-2234.

CARTMELL, S. (2008) Controlled Release Scaffolds for Bone Tissue Engineering. *Journal of Pharmaceutical Sciences*.

CEDAR, S. H., COOKE, J. A., PATEL, M. R., LUO, Z. & MINGER, S. L. (2007) The therapeutic potential of human embryonic stem cells. *The Indian Journal of Medical Research,* 125**,** 17-24.

CHAMBERS, I. & SMITH, A. (2004) Self-renewal of teratocarcinoma and embryonic stem cells. *Oncogene,* 23**,** 7150-7160.

CHAMBERS, T. J., DARBY, J. A. & FULLER, K. (1985) Mammalian collagenase predisposes bone surfaces to osteoclastic resorption. *Cell and Tissue Research,* 241**,** 671-675.

CHAN, G. & MOONEY, D. J. (2008) New materials for tissue engineering: towards greater control over the biological response. *Trends in Biotechnology,* 26**,** 382-392.

CHANG, Y. L., STANFORD, C. M. & KELLER, J. C. (2000) Calcium and phosphate supplementation promotes bone cell mineralization: implications for hydroxyapatite (HA)-enhanced bone formation. *Journal of Biomedical Materials Research Part A,* 52**,** 270-278.

CHAUDHRY, G. R., YAO, D., SMITH, A. & HUSSAIN, A. (2004) Osteogenic cells derived from embryonic stem cells produced bone nodules in three-dimensional scaffolds. *Journal of Biomedicine and Biotechnology,* 2004**,** 203-210.

CHAZAUD, C., YAMANAKA, Y., PAWSON, T. & ROSSANT, J. (2006) Early lineage segregation between epiblast and primitive endoderm in mouse blastocysts through the Grb2-MAPK pathway. *Developmental Cell,* 10**,** 615-624.

CHEN, C. S., MRKSICH, M., HUANG, S., WHITESIDES, G. M. & INGBER, D. E. (1998) Micropatterned Surfaces for Control of Cell Shape, Position, and Function. *Biotechnology Progress,* 14**,** 356-363.

CHEN, C. S., PEGAN, J., LUNA, J., XIA, B., MCCLOSKEY, K., CHIN, W. C. & KHINE, M. (2008) Shrinky-dink hanging drops: a simple way to form and culture embryoid bodies. *Journal of Visualized Experiments,* 13**,** pii: 692.

CHENG, L., GEARING, D. P., WHITE, L. S., COMPTON, D. L., SCHOOLEY, K. & DONOVAN, P. J. (1994) Role of leukemia inhibitory factor and its receptor in mouse primordial germ cell growth. *Development,* 120**,** 3145-3153.

CHIM, H., SCHANTZ, J. T. & GOSAIN, A. K. (2008) Beyond the vernacular: new sources of cells for bone tissue engineering. *Plastic and Reconstructive Surgery,* 122**,** 755-64.

CHOI, K. M., SEO, Y. K., YOON, H. H., SONG, K. Y., KWON, S. Y., LEE, H. S. & PARK, J. K. (2008a) Effect of ascorbic acid on bone marrow-derived mesenchymal stem cell proliferation and differentiation. *Journal of Bioscience and Bioengineering,* 105**,** 586-594.

CHOI, S. H. & PARK, T. G. (2006) G-CSF loaded biodegradable PLGA nanoparticles prepared by a single oil-in-water emulsion method. *International Journal of Pharmaceutics,* 311**,** 223-228.

CHOI, Y. S., NOH, S. E., LIM, S. M., LEE, C. W., KIM, C. S., IM, M. W., LEE, M. H. & KIM, D. I. (2008b) Multipotency and growth characteristic of periosteum-derived progenitor cells for chondrogenic, osteogenic, and adipogenic differentiation. *Biotechnology Letters,* 30**,** 593-601.

CHOO, A., NGO, A. S., DING, V., OH, S. K. & KIANG, L. S. (2008) Autogeneic feeders for the culture of undifferentiated human embryonic stem cells in feeder and feeder-free conditions. *Methods in Cell Biology,* 86**,** 15-28.

CHU, G. (2003) Embryonic stem-cell research and the moral status of embryos. *Internal Medicine Journal,* 33**,** 530-531.

COHEN, S. & BANO, M. C. (1993) Design of synthetic polymeric structures for cell transplantation and tissue engineering. *Clinical Materials,* 13**,** 3-10.

COME, J., NISSAN, X., AUBRY, L., TOURNOIS, J., GIRARD, M., PERRIER, A. L., PESCHANSKI, M. & CAILLERET, M. (2008) Improvement of culture conditions of human embryoid bodies using a controlled perfused and dialyzed bioreactor system. *Tissue Engineering Part C,* 14**,** 289-298.

CONLEY, B. J., DENHAM, M., GULLUYAN, L., OLSSON, F., COLE, T. J. & MOLLARD, R. (2005) Mouse embryonic stem cell derivation, and mouse and human embryonic stem cell culture and differentiation as embryoid bodies. *Current Protocols in Cell Biology,* 23**,** Unit 23.2.

CORMIER, J. T., ZUR NIEDEN, N. I., RANCOURT, D. E. & KALLOS, M. S. (2006) Expansion of undifferentiated murine embryonic stem cells as aggregates in suspension culture bioreactors. *Tissue Engineering,* 12**,** 3233-3245.

COURJEAN, O., CHEVREUX, G., PERRET, E., MOREL, A., SANGLIER, S., POTIER, N., ENGEL, J., VAN DORSSELAER, A. & FERACCI, H. (2008) Modulation of E-Cadherin Monomer Folding by Cooperative Binding of Calcium Ions. *Biochemistry (Washington),* 47**,** 2339-2349.

CRITCHLEY, D. R., HOLT, M. R., BARRY, S. T., PRIDDLE, H., HEMMINGS, L. & NORMAN, J. (1999) Integrin-mediated cell adhesion: the cytoskeletal connection. *Biochemical Society Symposium,* 65**,** 79-99.

CUKIERMAN, E., PANKOV, R., STEVENS, D. R. & YAMADA, K. M. (2001) Taking cell-matrix adhesions to the third dimension. *Science,* 294**,** 1708-1712.

CULLINANE, D. M. (2002) The role of osteocytes in bone regulation: mineral homeostasis versus mechanoreception. *Journal of Musculoskeletal and Neuronal Interactions,* 2**,** 242-244.

CURTIS, A. & RIEHLE, M. (2001) Tissue engineering: the biophysical background. *Physics in Medicine and Biology,* 46**,** 47-65.

DAI, J. & RABIE, A. B. (2007) VEGF: an essential mediator of both angiogenesis and endochondral ossification. *Journal of Dental Research,* 86**,** 937-950.

DAI, W. (1994) Cell binding peptides conjugate to poly(ethylene glycol) promote neural cell aggregation. *Nature Biotechnology,* 12**,** 797-801.

DAI, W. & SALTZMAN, W. M. (1996) Fibroblast Aggregation by Suspension with Conjugates of Poly(ethylene glycol) and RGD. *Biotechnology and Bioengineering,* 50**,** 349-356.

DANG, S. M., GERECHT-NIR, S., CHEN, J., ITSKOVITZ-ELDOR, J. & ZANDSTRA, P. W. (2004) Controlled, scalable embryonic stem cell differentiation culture. *Stem Cells,* 22**,** 275-282.

DANG, S. M., KYBA, M., PERLINGEIRO, R., DALEY, G. Q. & ZANDSTRA, P. W. (2002) Efficiency of embryoid body formation and hematopoietic development from embryonic stem cells in different culture systems. *Biotechnology and Bioengineering,* 78**,** 442-453.

DANI, C., CHAMBERS, I., JOHNSTONE, S., ROBERTSON, M., EBRAHIMI, B., SAITO, M., TAGA, T., LI, M., BURDON, T., NICHOLS, J. & SMITH, A. (1998) Paracrine induction of stem cell renewal by LIF-deficient cells: a new ES cell regulatory pathway. *Developmental Biology,* 203**,** 149-162.

DAWSON, J. L. & OREFFO, R. O. C. (2008) Bridging the regeneration gap: Stem cell, biomaterials and clinical translation in bone tissue engineering. *Archives of Biochemistry and Biophysics,* 473**,** 124-131.

DE BANK, P. A., HOU, Q., WARNER, R. M., WOOD, I. V., ALI, B. E., MACNEIL, S., KENDALL, D. A., KELLAM, B., SHAKESHEFF, K. M. & BUTTERY, L. D. K. (2007) Accelerated formation of

multicellular 3-D structures by cell-to-cell cross-linking. *Biotechnology and Bioengineering,* 97**,** 1617-1625.

DE BANK, P. A., KELLAM, B., KENDALL, D. A. & SHAKESHEFF, K. M. (2003) Surface engineering of living myoblasts via selective periodate oxidation. *Biotechnology and Bioengineering,* 81**,** 800-808.

DE SMEDT, A., STEEMANS, M., DE BOECK, M., PETERS, A. K., VAN DER LEEDE, B. J., VAN GOETHEM, F., LAMPO, A. & VANPARYS, P. (2008) Optimisation of the cell cultivation methods in the embryonic stem cell test results in an increased differentiation potential of the cells into strong beating myocard cells. *Toxicology in Vitro,* 22**,** 1789-1796.

DEB, K. D., JAYAPRAKASH, A. D., SHARMA, V. & TOTEY, S. (2008) Embryonic stem cells: from markers to market. *Rejuvenation research,* 11**,** 19-37.

DEHILI, C., LEE, P., SHAKESHEFF, K. M. & ALEXANDER, R. A. (2006) Comparison of Primary Rat Hepatocyte Attachment to Collagen and Plasma-Polymerised Allylamine on Glass. *Plasma Processes and Polymers,* 3**,** 474-484.

DOMOQATSKAYA, A., RODIN, S., BOUTAUD, A. & TRYQQVASON, K. (2008) Laminin-511 but not -332, -111, or -411 enables mouse embryonic stem cell self-renewal in vitro. *Stem Cells,* 26**,** 2800-2809.

DOTY, S. B. (1981) Morphological evidence of gap junctions between bone cells. *Calcified Tissue International,* 33**,** 509-512.

DOUNCHIS, J. S., BAE, W. C., CHEN, A. C., SAH, R. L., COUTTS, R. D. & AMIEL, D. (2000) Cartilage repair with autogenic perichondrium cell and polylactic acid grafts. *Clinical Orthopaedics and Related Research***,** 248-64.

DROBINSKAYA, I., LINN, T., SARIC, T., BRETZEL, R. G., BOHLEN, H., HESCHELER, J. & KOLOSSOV, E. (2008) Scalable selection of hepatocyte- and hepatocyte precursor-like cells from culture of differentiating transgenically modified murine embryonic stem cells. *Stem Cells,* 26**,** 2245-2256.

DRUGARIN, D., DRUGARIN, M., NEGRU, S. & CIOACA, R. (2003) RANKL-RANKL/OPG Molecular Complex - Control Factors in Bone Remodeling. *Timisoara Medical Journal,* 53**,** 297-302.

DRURY, J. L. & MOONEY, D. J. (2003) Hydrogels for tissue engineering: Scaffold design variables and applications. *Biomaterials,* 24**,** 4337-4351.

DUNN, J. C. Y. (2008) Tissue Engineering and Regenerative Science in Pediatrics. *Pediatric Research,* 63**,** 459-460.

DUPLOMB, L., DAGOUASSAT, M., JOURDON, P. & HEYMANN, D. (2007) Concise Review: Embryonic Stem Cells: A New Tool to Study Osteoblast and Osteoclast Differentiation. *Stem Cells,* 25**,** 544-552.

DUQUE, G., HUANG, D. C., MACORITTO, M., RIVAS, D., YANG, X. F., STE-MARIE, L. G. & KREMNER, R. (2008) Autocrine regulation of interferon (gamma) in mesenchymal stem cells plays a role in early osteoblastogenesis. *Stem Cells*.

DUTOUR-SIKIRIC, M. & FUREDI-MILHOFER, H. (2006) The influence of surface active molecules on the crystallization of biominerals in solution. *Advances in Colloid and Interface Science,* 128**,** 135-158.

DUTY, A. O., OEST, M. E. & GULDBERG, R. E. (2007) Cyclic Mechanical Compression Increases Mineralization of Cell-Seeded Polymer Scaffolds In Vivo. *Journal of Biomechanical Engineering, Transactions of the ASME,* 129**,** 531-539.

DYSON, J. A., GENEVER, P. G., DALGARNO, K. W. & WOOD, D. J. (2007) Development of Custom-Built Bone Scaffolds Using Mesenchymal Stem Cells and Apatite-Wollastonite Glass-Ceramics. *Tissue Engineering,* 13**,** 2891-2901.

ECAROT-CHARRIER, B., GLORIEUX, F. H., VAN DER REST, M. & PEREIRA, G. (1983) Osteoblasts isolated from mouse calvaria initiate matrix mineralization in culture. *Journal of Cell Biology,* 96**,** 639-643.

EGGLI, P. S., HERRMANN, W., HUNZIKER, E. B. & SCHENK, R. K. (1985) Matrix compartments in the growth plate of the proximal tibia of rats. *The Anatomical Record,* 211**,** 246-257.

EL HAJ, A. J., WOOD, M. A., THOMAS, P. & YANG, Y. (2005) Controlling cell biomechanics in orthopaedic tissue engineering and repair. *Pathology Biology (Paris),* 53**,** 581-589.

ENGEL, E., DEL VALLE, S., APARICIO, C., ALTANKOV, G., ASIN, L., PLANELL, J. A. & GINEBRA, M. P. (2008) Discerning the Role of Topography and Ion Exchange in Cell Response of Bioactive Tissue Engineering Scaffolds. *Tissue Engineering, Part A,* 14**,** 1341-1352.

ENMON, R. M., JR., O'CONNOR, K. C., LACKS, D. J., SCHWARTZ, D. K. & DOTSON, R. S. (2001) Dynamics of spheroid self-assembly in liquid-overlay culture of DU 145 human prostate cancer cells. *Biotechnology and Bioengineering,* 72**,** 579-591.

EVANS, E. J. & KAUFMAN, M. H. (1981) Establishment in culture of pluripotential cells from mouse embryos. *Nature,* 292**,** 154-156.

FENG, G., WAN, Y., BALIAN, G., LAURENCIN, C. T. & LI, X. (2008) Adenovirus-mediated expression of growth and differentiation factor-5 promotes chondrogenesis of adipose stem cells. *Growth factors,* 26**,** 132-42.

FERAUD, O., CAO, Y. & VITTET, D. (2001) Embryonic stem cell-derived embryoid bodies development in collagen gels recapitulates sprouting angiogenesis. *Laboratory Investigation,* 81**,** 1669-1681.

FERNANDEZ, N. J. & KIDNEY, B. A. (2007) Alkaline phosphatase: beyond the liver. *Veterinary clinical pathology / American Society for Veterinary Clinical Pathology,* 36**,** 223-33.

FILIP, S., MOKRY, J., ENGLISH, D. & VOJACEK, J. (2005) Stem cell plasticity and issues of stem cell therapy. *Folia Biologica (Praha),* 51**,** 180-187.

FINCH, B. W. & EPHRUSSI, B. (1967) Retention of multiple developmental potentialities by cells of a mouse testicular tetracarcinoma during prolonged culture in vitro and their extinction upon hybridization with cells of permanent lines. *Proceedings of the National Academy of Sciences of the United States of America,* 57**,** 615-621.

FINKE, B., LUETHEN, F., SCHROEDER, K., MUELLER, P. D., BERGEMANN, C., FRANT, M., OHL, A. & NEBE, B. J. (2007) The effect of positively charged plasma polymerization on initial osteoblastic focal adhesion on titanium surfaces. *Biomaterials,* 28**,** 4521-4534.

FODOR, W. L. (2003) Tissue engineering and cell based therapies, from the bench to the clinic: the potential to replace, repair and regenerate. *Reproductive Biology and Endocrinology,* 1**,** 102-108.

FOK, E. Y. L. & ZANDSTRA, P. W. (2005) Shear-Controlled Single-Step Mouse Embryonic Stem Cell Expansion and Embryoid Body-Based Differentiation. *Stem Cells,* 23**,** 1333-1342.

FOX, J. L. (1999) Stem cell hearing stirs bioethics debate. *Nature Biotechnology,* 17**,** 11.

FRATZL-ZELMAN, N., FRATZL, P., HORANDNER, H., GRABNER, B., VARGA, F., ELLINGER, A. & KLAUSHOFER, K. (1998) Matrix mineralization in MC3T3-E1 cell cultures initiated by beta-glycerophosphate pulse. *Bone,* 23**,** 511-20.

FREED, L. E., VUNJAK-NOVAKOVIC, G., BIRON, R. J., EAGLES, D. B., LESNOY, D. C., BARLOW, S. K. & LANGER, R. (1994) Biodegradable polymer scaffolds for tissue engineering. *Nature Biotechnology,* 12**,** 689-693.

FROMSTEIN, J. D., ZANDSTRA, P. W., ALPERIN, C., ROCKWOOD, D., RABOLT, J. F. & WOODHOUSE, K. A. (2008) Seeding bioreactor-produced embryonic stem cell-derived cardiomyocytes on different porous, degradable, polyurethane scaffolds reveals the effect of scaffold architecture on cell morphology. *Tissue Engineering Part A,* 14**,** 369-378.

FUKADA, T., HIBI, M., YAMANAKA, Y., TAKAHASHI-TEZUKA, M., FUJITANI, Y., YAMAGUCHI, T., NAKAJIMA, K. & HIRANO, T. (1996) Two signals are necessary for cell proliferation induced by a cytokine receptor gp130: Involvement of STAT3 in anti-apoptosis. *Immunity,* 5**,** 449-460.

FULLER, K. & CHAMBERS, T. J. (1995) Localisation of mRNA for collagenase in osteocytic, bone surface and chondrocytic cells but not osteoclasts. *Journal of Cell Science,* 108**,** 2221-2230.

FURUE, M., OKAMOTO, T., HAYASHI, Y., OKOCHI, H., FUJIMOTO, M., MYOISHI, Y., ABE, T., OHNUMA, K., SATO, G. H., ASASHIMA, M. & SATO, J. D. (2005) Leukemia inhibitory factor as an anti-apoptotic mitogen for pluripotent mouse embryonic stem cells in a serum-free medium without feeder cells. *In Vitro Cellular & Developmental Biology. Animal,* 41**,** 19-28.

GARCIA, A. J. & BOETTIGER, D. (1999) Integrin-fibronectin interactions at the cell-material interface: initial integrin binding and signaling. *Biomaterials,* 20**,** 2427-2433.

GARIMELLA, R., BI, X., ANDERSON, H. C. & CAMACHO, N. P. (2006) Nature of phosphate substrate as a major determinant of mineral type formed in matrix vesicle-mediated in vitro mineralization: An FTIR imaging study. *Bone,* 38**,** 811-817.

GARRETA, E., GENOVE, E., BORROS, S. & SEMINO, C. E. (2006) Osteogenic differentiation of mouse embryonic stem cells and mouse embryonic fibroblasts in a three-dimensional self-assembling peptide scaffold. *Tissue Engineering,* 12**,** 2215-2227.

GERECHT-NIR, S., COHEN, S. & ITSKOVITZ-ELDOR, J. (2004) Bioreactor cultivation enhances the efficiency of human embryoid body (hEB) formation and differentiation. *Biotechnology and Bioengineering,* 86**,** 493-502.

GERECHT-NIR, S., DAZARD, J. E., GOLAN-MASHIACH, M., OSENBERG, S., BOTVINNIK, A., AMARIGLIO, N., DOMANY, E., RECHAVI, G., GIVOL, D. & ITSKOVITZ-ELDOR, J. (2005) Vascular gene expression and phenotypic correlation during differentiation of human embryonic stem cells. *Developmental Dynamics,* 232**,** 487-497.

GHOSH, K. & INGBER, D. E. (2007) Micromechanical control of cell and tissue development: Implications for tissue engineering. *Advanced Drug Delivery Reviews,* 59**,** 1306-1318.

GIANCOTTI, F. G. & RUOSLAHTI, E. (1999) Integrin signaling. *Science,* 285**,** 1028-1032.

GINIS, I., LUO, Y., MIURA, T., THIES, S., BRANDENBERGER, R., GERECHT-NIR, S., AMIT, M., HOKE, A., CARPENTER, M. K., ITSKOVITZ-ELDOR, J. & RAO, M. S. (2004) Differences between human and mouse embryonic stem cells. *Developmental Biology,* 269**,** 360-380.

GOESSLER, U. R., BUGERT, P., BIEBACK, K., STERN-STRAETER, J., BRAN, G., SADICK, H., HORMANN, K. & RIEDEL, F. (2008) In vitro-analysis of integrin-expression in stem-cells from bone marrow and cord blood during chondrogenic differentiation. *Journal of Cellular and Molecular Medicine*.

GOH, Y. Q. & OOI, C. P. (2008) Fabrication and characterization of porous poly(l-lactide) scaffolds using solid-liquid phase separation. *Journal of Materials Science: Materials in Medicine,* 19**,** 2445-2452.

GOODWIN, A. M. (2007) In vitro assays of angiogenesis for assessment of angiogenic and anti-angiogenic agents. *Microvascular Research,* 74**,** 172-183.

GOUMANS, M. J., WARD-VAN OOSTWAARD, D., WIANNY, F., SAVATIER, P., ZWIJSEN, A. & MUMMERY, C. (1998) Mouse embryonic stem cells with aberrant transforming growth factor beta signalling exhibit impaired differentiation in vitro and in vivo. *Differentiation,* 63**,** 101-113.

GRAYSON, W. L., MARTENS, T. P., ENG, G. M., RADISIC, M. & VUNJAK-NOVAKOVIC, G. (2008) Biomimetic approach to tissue engineering. *Seminars in Cell and Developmental Biology*.

GREEN, D., WALSH, D., MANN, S. & OREFFO, R. O. C. (2002) The potential of biomimesis in bone tissue engineering: Lessons from the design and synthesis of invertebrate skeletons. *Bone,* 30**,** 810-815.

GREEN, D. W. (2008) Tissue bionics: examples in biomimetic tissue engineering. *Biomedical Materials,* 3**,** 11 pages.

GREGORY, C. A., GUNN, W. G., PEISTER, A. & PROCKOP, D. J. (2004) An alizarin red-based assay of mineralization by adherent cells in culture: comparison with cetylpyridinium chloride extraction. *Analytical Biochemistry,* 329**,** 77-84.

GREGORY, K. E., KEENE, D. R., TUFA, S. F., LUNSTRUM, G. P. & MORRIS, N. P. (2001) Developmental Distribution of Collagen Type XII in Cartilage: Association with Articular Cartilage and the Growth Plate. *Journal of Bone and Mineral Research,* 16**,** 2005-2016.

GRIESSER, H. J., CHATELIER, R. C., GENGENBACH, T. R., JOHNSON, G. & STEELE, J. G. (1994) Growth of human cells on plasma polymers: putative role of amine and amide groups. *Journal of biomaterials science. Polymer edition,* 5**,** 531-54.

GRIFFITH, L. G. & NAUGHTON, G. (2002) Tissue Engineering--Current Challenges and Expanding Opportunities. *Science,* 295**,** 1009-1010.

GRIGORIADIS, A. E., HEERSCHE, J. N. M. & AUBIN, J. E. (1988) Differentiation of muscle, fat, cartilage, and bone from progenitor cells present in a bone-derived clonal cell population: Effect of dexamethasone. *Journal of Cell Biology,* 106**,** 2139-2152.

GROSS, T. S., KING, K. A., RABAIA, N. A., PATHARE, P. & SRINIVASAM, S. (2005) Upregulation of osteopontin by osteocytes deprived of mechanical loading or oxygen. *Journal of Bone and Mineral Research,* 20**,** 250-256.

GRUEN, L. & GRABEL, L. (2006) Concise review: scientific and ethical roadblocks to human embryonic stem cell therapy. *Stem cells,* 24**,** 2162-2169.

GUAN, J., SACKS, M. S., BECKMAN, E. J. & WAGNER, W. R. (2004) Biodegradable poly)ether ester urethane)urea elastomers based on poly(ether ester) triblock copolymers and putrescine: synthesis, characterization and cytocompatibility. *Biomaterials,* 25**,** 85-96.

HABIB, M., CASPI, O. & GEPSTEIN, L. (2008) Human embryonic stem cells for cardiomyogenesis. *Journal of Molecular and Cellular Cardiology,* 45**,** 462-74. Epub: 2008 Aug 30.

HAISCH, A., WANJURA, F., RADKE, C., LEDER-JOHRENS, K., GROGER, A., ENDRES, M., KLAERING, S., LOCH, A. & SITTINGER, M. (2004) Immunomodulation of tissue-engineered transplants: in vivo bone generation from methylprednisolone-stimulated chondrocytes. *European archives of oto-rhino-laryngology,* 261**,** 216-24.

HALL, B. K. & MIYAKE, T. (1992) The membranous skeleton: the role of cell condensations in vertebrate skeletogenesis. *Anatomy and Embryology,* 186**,** 107-124.

HAMAZAKI, T., OKA, M., YAMANAKA, S. & TERADA, N. (2004) Aggregation of embryonic stem cells induces Nanog repression and primitive endoderm differentiation. *Journal of Cell Science,* 117**,** 5681-5686.

HAMERLI, P., WEIGEL, T., GROTH, T. & PAUL, D. (2003) Surface properties of and cell adhesion onto allylamine-plasma-coated polyethylenterephtalat membranes. *Biomaterials,* 24**,** 3989-3999.

HANDSCHEL, J., BERR, K., DEPPRICH, R., KUBLER, N. R., NAUJOKS, C., WIESMANN, H. P., OMMERBORN, M. A. & MEYER, U. (2008a) Induction of osteogenic markers in differentially treated cultures of embryonic stem cells. *Head and Face Medicine,* 4.

HANDSCHEL, J., BERR, K., DEPPRICH, R., NAUJOKS, C., KUBLER, N. R., MEYER, U., OMMERBORN, M. & LAMMERS, L. (2008b) Compatibility of Embryonic Stem Cells with Biomaterials. *Journal of Biomaterials Applications*.

HARTSOCK, A. & NELSON, W. J. (2008) Adherens and tight junctions: Structure, function and connections to the actin cytoskeleton. *Biochimica et Biophysica Acta,* 1778**,** 660-669.

HATANO, S. Y., TADA, M., KIMURA, H., YAMAGUCHI, S., KONO, T., NAKANO, T., SUEMORI, H., NAKATSUJI, N. & TADA, T. (2005) Pluripotential competence of cells associated with Nanog activity. *Mechanisms of Development,* 122**,** 67-79.

HAYASHI, Y., FURUE, M. K., OKAMOTO, T., OHNUMA, K., MYOISHI, Y., FUKUHARA, Y., ABE, T., SATO, J. D., HATA, R. I. & ASASHIMA, M. (2007) Integrins regulate mouse embryonic stem cell self-renewal. *Stem Cells,* 25**,** 3005-3015.

HE, L. J., NAN, X., WANG, Y. F., GUAN, L. D., BAI, C. X., SHI, S. S., YUAN, H. F., CHEN, L., LIU, D. Q. & PEI, X. T. (2007) Full-thickness tissue engineered skin constructed with autogenic bone marrow mesenchymal stem cells. *Science in China Series C: Life Sciences,* 50**,** 429-437.

HELFRITCH, M. H., NESBITT, S. A., DOREY, E. L. & HORTON, M. A. (1992) Rat osteoclasts adhere to a wide range of RGD (Arg-Gly-Asp) peptide-containing proteins, including the bone sialoproteins and fibronectin, via a beta 3 integrin. *Journal of Bone and Mineral Research,* 7**,** 335-343.

HENG, B. C., CAO, T., LIU, H. & RUFAIHAH, A. J. (2005) Reduced mitotic activity at the periphery of human embryonic stem cell colonies cultured in vitro with mitotically-inactivated murine embryonic fibroblast feeder cells. *Cell Biochemistry and Function,* 23**,** 141-146.

HENG, B. C., CAO, T., STANTON, L. W., ROBSON, P. & OLSEN, B. (2004) Strategies for directing the differentiation of stem cells into the osteogenic lineage in vitro. *Journal of Bone and Mineral Research,* 19**,** 1379-1394.

HILLEL, A. T., VARQHESE, S., PETSCHE, J., SHAMBLOTT, M. J. & ELISSEEFF, J. H. (2009) Embryonic germ cells are capable of adipogenic differentiation in vitro and in vivo. *Tissue Engineering Part A,* 15**,** 479-486.

HIRAGA, K. & KIKUCHI, G. (1980) The Mitochondrial Glycine Cleavage System. *Journal of Biological Chemistry,* 255**,** 11671-11676.

HIRT-BURRI, N., SCALETTA, C., GERBER, S., PIOLETTI, D. P. & APPLEGATE, L. A. (2008) Wound-healing gene family expression differences between fetal and foreskin cells used for bioengineered skin substitutes. *Artificial Organs,* 32**,** 509-518.

HOEMANN, C. D., EL-GABALAWY, H. & MCKEE, M. D. (2008) In vitro osteogenesis assays: influence of the primary cell source on alkaline phosphatase activity and mineralization. *Pathology Biology (Paris)*.

HOLLINGER, J. O. (1983) Preliminary report on the osteogenic potential of a biodegradable copolymer of polylactide (PLA) and polygylcolide (PGA). *Journal of Biomedical Materials Research,* 17**,** 71-82.

HORCH, R. E. (2006) Future perspectives in tissue engineering. *Journal of Cellular and Molecular Medicine,* 10**,** 4-6.

HORTON, M. A., NESBITT, M. A. & HELFRITCH, M. H. (1995) Interaction of osteopontin with osteoclast integrins. *Annals of the New York Academy of Sciences,* 760**,** 190-200.

HORVATH, L., SMIT, I., SIKIRIC, M. & FILIPOVIC-VINCEKOVIC, N. (2000) Effect of cationic surfactant on the transformation of octacalcium phosphate. *Journal of Crystal Growth,* 219**,** 91-97.

HOWARD, D., BUTTERY, L. D. K., SHAKESHEFF, K. M. & ROBERTS, S. J. (2008) Tissue engineering: strategies, stem cells and scaffolds. *Journal of Anatomy,* 213**,** 66-72.

HOWELL, D. S., PITA, J. C., MARQUEZ, J. F. & MADRUGA, J. E. (1968) Partition of Calcium, Phosphate, and Protein in the Fluid Phase Aspirated at Calcifying Sites in Epiphyseal Cartilage. *The Journal of Clinical Investigation,* 47**,** 1121-1132.

HUANG, H. I. (2007) Isolation of human placenta-derived multipotent cells and in vitro differentiation into hepatocyte-like cells. *Current Protocols in Stem Cell Biology,* Chapter 1**,** Unit 1E.1.

HUANG, Y. C., KHAIT, L. & BIRLA, R. K. (2008) Modulating the functional performance of bioengineered heart muscle using growth factor stimulation. *Annals of Biomedical Engineering,* 36**,** 1372-1382.

HURLE, J. M., ROS, M. A., GARCIA-MARTINEZ, V., MACIAS, D. & GANAN, Y. (1995) Cell death in the embryonic limb. *Scanning Microscopy,* 9**,** 519-533.

HWANG, N. S., KIM, M. S., SAMPATTAVANICH, S., BAEK, J. H., ZHANG, Z. & ELISSEEFF, J. (2006a) Effects of Three-Dimensional Culture and Growth Factors on the Chondrogenic Differentiation of Murine Embryonic Stem Cells. *Stem Cells,* 24**,** 284-291.

HWANG, Y. S., CHO, J., TAY, F., HENG, J. Y. Y., HO, R., KAZARIAN, S. G., WILLIAMS, D. R., BOCCACCINI, A. R., POLAK, J. M. & MANTALARIS, A. (2009) The use of murine embryonic stem cells, alginate encapsulation, and rotary microgravity bioreactor in bone tissue engineering. *Biomaterials,* 30**,** 499-507.

HWANG, Y. S., POLAK, J. M. & MANTALARIS, A. (2008a) In vitro direct chondrogenesis of murine embryonic stem cells by bypassing embryoid body formation. *Stem Cells and Development,* 17**,** 971-978.

HWANG, Y. S., POLAK, J. M. & MANTALARIS, A. (2008b) In vitro direct osteogenesis of murine embryonic stem cells without embryoid body formation. *Stem Cells and Development,* 17**,** 963-970.

HWANG, Y. S., RANDLE, W. L., BIELBY, R. C., POLAK, J. M. & MANTALARIS, A. (2006b) Enhanced derivation of osteogenic cells from murine embryonic stem cells after treatment with HepG2-conditioned medium and modulation of the embryoid body formation period: application to skeletal tissue engineering. *Tissue Engineering,* 12**,** 1381-1392.

IANNACCONE, P. M., TABORN, G. U., GARTON, R. L., CAPLICE, M. D. & BRENIN, D. R. (1994) Pluripotent embryonic stem cells from the rat are capable of producing chimeras. *Developmental Biology,* 163**,** 288-292.

ILIC, D. (2006) Culture of human embryonic stem cells and the extracellular matrix microenvironment. *Regenerative Medicine,* 1**,** 95-101.

IMREH, M. P., WOLBANK, S., UNGER, C., GERTOW, K., AINTS, A., SZELES, A., IMREH, S., HOVATTA, O., FRIED, G., DILBER, S. & AHRLUND- RICHTER, L. (2004) Culture and expansion of the

human embryonic stem cell line HS181, evaluated in a double-color system. *Stem Cells and Development,* 13**,** 337-343.

INANC, B., ELCIN, A. E. & ELCIN, Y. M. (2007) Effect of osteogenic induction on the in vitro differentiation of human embryonic stem cells cocultured with peridontal ligament fibroblasts. *Artificial Organs,* 31**,** 792-800.

INANC, B., ELCIN, A. E. & ELCIN, Y. M. (2008) Human Embryonic Stem Cell Differentiation on Tissue Engineering Scaffolds: Effects of NGF and Retinoic Acid Induction. *Tissue Engineering, Part A,* 14**,** 955-964.

IRVINE, D. J., STACHOWIAK, A. N. & HORI, Y. (2008) Lymphoid tissue engineering: Invoking lymphoid tissue neogenesis in immunotherapy and models of immunity. *Seminars in Immunology,* 20**,** 137-146.

ITSKOVITZ-ELDOR, J., SCHULDINER, M., KARSENTI, D., EDEN, A., YANUKA, O., AMIT, M., SOREQ, H. & BENVENISTY, N. (2000) Differentiation of human embryonic stem cells into embryoid bodies compromising the three embryonic germ layers. *Molecular Medicine,* 6**,** 88-95.

IZUMI, N., ERA, T., AKIMARU, H., YASUNAGA, M. & NISHIKAWA, S. I. (2007) Dissecting the molecular hierarchy for mesendoderm differentiation through a combination of embryonic stem cell culture and RNA interference. *Stem Cells,* 25**,** 1664-1674.

JACOBS, C. L., YAREMA, K. J., MAHAL, L. K., NAUMAN, D. A., CHARTERS, N. W. & BERTOZZI, C. R. (2000) Metabolic labeling of glycoproteins with chemical tags through unnatural sialic acid biosynthesis. *Methods in Enzymology,* 327**,** 260-275.

JAGER, M. & KRAUSPE, R. (2007) Antigen expression of cord blood derived stem cells under osteogenic stimulation in vitro. *Cell Biology International,* 31**,** 950-957.

JIANG, Y., PJESIVAC-GRBOVIC, J., CANTRELL, C. & FREYER, J. P. (2005) A multiscale model for avascular tumor growth. *Biophysical Journal,* 89**,** 3884-3894.

JIMI, E., AKIYAMA, S., TSURUKAI, T., OKAHASHI, N., KOBAYASHI, K., UDAGAWA, N., NISHIHARA, T., TAKAHASHI, N. & SUDA, T. (1999) Osteoclast differentiation factor acts as a multifunctional regulator in murine osteoclast differentiation and function. *Journal of Immunology,* 163**,** 434-442.

JUKES, J. M., BOTH, S. K., LEUSINK, A., STERK, L. M. T., VAN BLITTERSWIJK, C. A. & DE BOER, J. (2008) Endochondral bone tissue engineering using embryonic stem cells. *Proceedings of the National Academy of Sciences of the United States of America,* 105**,** 6840-6845.

KALAJZIC, I., BRAUT, A., GUO, D., JIANG, X., KRONENBERG, M. S., MINA, M., HARRIS, M. A., HARRIS, S. E. & ROWE, D. W. (2004) Dentin matrix protein 1 expression during osteoblastic differentiation, generation of an osteocyte GFP-transgene. *Bone,* 35**,** 74-82.

KANATANI, N., FUJITA, T., FUKUYAMA, R., LIU, W., YOSHIDA, C. A., MORIISHI, T., YAMANA, K., MIYAZAKI, T., TOYOSAWA, S. & KOMORI, T. (2006) Cbf beta regulates Runx2 function isoform-dependently in postnatal bone development. *Developmental Biology,* 296**,** 48-61.

KANCZLER, J. M. & OREFFO, R. O. C. (2008) Osteogenesis and Angiogenesis: The Potential for Engineering Bone. *European Cells and Materials,* 15**,** 100-114.

KARAGEORGIOU, V. & KAPLAN, D. (2005) Porosity of 3D biomaterial scaffolds and osteogenesis. *Biomaterials,* 26**,** 5474-5491.

KARAGIOSIS, S. A. & KARIN, N. J. (2007) Lysophosphatidic acid induces osteocyte dendrite outgrowth. *Biochemical and Biophysical Research Communications,* 357**,** 194-199.

KARAMUK, E., MAYER, J., WINTERMANTEL, E. & AKAIKE, T. (1999) Partially Degradable Film/Fabric Composites: Textile Scaffolds for Liver Cell Culture. *Artificial Organs,* 23**,** 881-887.

KARBANOVA, J. & MORKRY, J. (2002) Histological and histochemical analysis of embryoid bodies. *Acta Histochemica,* 104**,** 361-365.

KARLSSON, K. R., COWLEY, S., MARTINEZ, F. O., SHAW, M., MINGER, S. L. & JAMES, W. (2008) Homogeneous monocytes and macrophages from human embryonic stem cells following coculture-free differentiation in M-CSF and IL-3. *Experimental Hematology,* 36**,** 1167-1175.

KARNER, E., UNGER, C., SLOAN, A. J., AHRLUND- RICHTER, L., SUGARS, R. V. & WENDEL, M. (2007) Bone matrix formation in osteogenic cultures derived from human embryonic stem cells in vitro. *Stem Cells and Development,* 16**,** 39-52.

KARP, J. M., FERREIRA, L. S., KHADEMHOSSEINI, A., KWON, A. H., YEH, J. & LANGER, R. S. (2006) Cultivation of Human Embryonic Stem Cells Without the Embryoid Body Step Enhances Osteogenesis In Vitro. *Stem Cells,* 24**,** 835-843.

KARP, J. M., YEH, J., ENG, G., FUKUDA, J., BLUMLING, J., SUH, K. Y., CHENG, J., MAHDAVI, A., BORENSTEIN, J., LANGER, R. & KHADEMHOSSEINI, A. (2007) Controlling size, shape and homogeneity of embryoid bodies using poly(ethylene glycol) microwells. *The Royal Society of Chemistry,* 7**,** 786-794.

KAWAGUCHI, J., KII, I., SUGIYAMA, Y., TAKESHITA, S. & KUDO, A. (2001) The transition of cadherin expression in osteoblast differentiation from mesenchymal cells: consistent expression of cadherin-11 in osteoblast lineage. *Journal of Bone and Mineral Research,* 16**,** 260-269.

KAWATE, K., YAJIMA, H., OHGUSHI, H., KOTOBUKI, N., SUGIMOTO, K., OHMURA, T., KOBATA, Y., SHIGEMATSU, K., KAWAMURA, K., TAMAI, K. & TAKAKURA, Y. (2006) Tissue-engineered approach for the treatment of steroid-induced osteonecrosis of the femoral head: Transplantation of autologous mesenchymal stem cells cultured with beta-tricalcium phosphate ceramics and free-vascularized fibula. *Artificial Organs,* 30**,** 960-962.

KELLAM, B., DE BANK, P. A. & SHAKESHEFF, K. M. (2003) Chemical modification of mammalian cell surfaces. *Chemical Society Reviews,* 32**,** 327-337.

KELLER, G. & SNODGRASS, H. R. (1999) Human embryonic stem cells: The future is now. *Nature Medicine,* 5**,** 151-152.

KELLER, G. M. (1995) In vitro differentiation of embryonic stem cells. *Current Opinion in Cell Biology,* 7**,** 862-869.

KELLOUCHE, S., MARTIN, C., KORB, G., REZZONICO, R., BOUARD, D., BENBUNAN, M., DUBERTRET, L., SOLER, C., LEGRAND, C. & DOSQUET, C. (2007) Tissue engineering for full-thickness burns: a dermal substitute from bench to bedside. *Biochemical and Biophysical Research Communications,* 363**,** 472-478.

KENT, D., DYKSTRA, B. & EAVES, C. (2007) Isolation and assessment of long-term reconstituting hematopoietic stem cells from adult mouse bone marrow. *Curr Protoc Stem Cell Biol,* Chapter 2**,** Unit 2A.4.

KERR, C. L., HILL, C. M., BLUMENTHAL, P. D. & GEARHART, J. D. (2008a) Expression of pluripotent stem cells markers in the human fetal ovary. *Human Reproduction,* 23**,** 589-599.

KERR, C. L., HILL, C. M., BLUMENTHAL, P. D. & GEARHART, J. D. (2008b) Expression of pluripotent stem cells markers in the human fetal testis. *Stem Cells,* 26**,** 412-421.

KII, I., AMIZUKA, N., SHIMOMURA, J., SAGA, Y. & KUDO, A. (2004) Cell-Cell Interaction Mediated by Cadherin-11 Directly Regulates the Differentiation of Mesenchymal Cells Into the Cells of the Osteo-Lineage and the Chondro-Lineage. *Journal of Bone and Mineral Research,* 19**,** 1840-1849.

KIKUCHI, G. & HIRAGA, K. (1982) The mitochondrial gylcine cleavage system. Unique features of the glycine decarboxylation. *Molecular and Cellular Biochemistry,* 45**,** 137-149.

KIM, C., LEE, I. H., LEE, K., RYU, S. S., LEE, S. H., LEE, K. J., LEE, J., KANG, J. Y. & KIM, T. S. (2007a) Multi-well chip for forming a uniform embryoid body in a tiny droplet with mouse embryonic stem cells. *Bioscience, Biotechnology, and Biochemistry,* 71**,** 2985-2991.

KIM, G. D., KIM, G. J., SEOK, J. H., CHUNG, H. M., CHEE, K. M. & RHEE, G. S. (2008) Differentiation of endothelial cells derived from mouse embryoid bodies: a possible in vitro vasculogenesis model. *Toxicology Letters,* 180**,** 166-173.

KIM, H. S., OH, S. K., PARK, Y. B., AHN, H. J., SUNG, K. C., KANG, M. J., LEE, L. A., SUH, C. S., KIM, S. H., KIM, D. W. & MOON, S. Y. (2005) Methods for derivation of human embryonic stem cells. *Stem Cells,* 23**,** 1228-1233.

KIM, J., MOON, S. H., LEE, S. H., LEE, D. R., KOH, G. Y. & CHUNG, H. M. (2007b) Effective isolation and culture of endothelial cells in the embryoid body differentiated from human embryonic stem cells. *Stem Cells and Development,* 16**,** 269-280.

KIMURA, T., SUZUKI, A., FUJITA, Y., YOMOGIDA, K., LOMELI, H., ASADA, N., IKEUCHI, M., NAGY, A., MAK, T. W. & NAKANO, T. (2003) Conditional loss of PTEN leads to testicular teratoma and enhances embryonic germ cell production. *Development,* 130**,** 1691-1700.

KIMURA, T., TOMOOKA, M., YAMANO, N., MURAYAMA, K., MATOBA, S., UMEHARA, H., KANAL, Y. & NAKANO, T. (2008) AKT signaling promotes derivation of embryonic germ cells from primordial germ cells. *Development,* 135.

KLIMANSKAYA, I., CHUNG, Y., BECKER, S., LU, S. J. & LANZA, R. (2006) Human embryonic stem cell lines derived from single blastomeres. *Nature,* 444**,** 481-485.

KLIMANSKAYA, I., CHUNG, Y., MEISNER, L., JOHNSON, J., WEST, M. D. & LANZA, R. (2005) Human embryonic stem cells derived without feeder cells. *Lancet,* 365**,** 1636-1641.

KO, K. S., ARORA, P. D., BHIDE, V., CHEN, A. & MCCULLOCH, C. A. (2001) Cell-cell adhesion in human fibroblasts requires calcium signaling. *Journal of Cell Science,* 114**,** 1155-1167.

KOIKE, M., SAKAKI, S., AMANO, Y. & KUROSAWA, H. (2007) Characterization of Embryoid Bodies of Mouse Embryonic Stem Cells Formed under Various Culture Conditions and Estimation of Differentiation Status of Such Bodies. *Journal of Bioscience and Bioengineering,* 104**,** 294-299.

KOLLER, M. R., PALSSON, M. A., MANCHEL, I. & PALSSON, B. (1995) Long-term culture-initiating cell expansion is dependent on frequent medium exchange combined with stromal and other accessory cell effects. *Blood,* 86**,** 1784-1793.

KOROSSIS, S. A., BOOTH, C., WILCOX, H. E., WATTERSON, K. G., KEARNEY, J. N., FISHER, J. & INGHAM, E. (2002) Tissue engineering of cardiac valve prostheses II: biomechanical characterization of decellularized porcine aortic heart valves. *Journal of Heart Valve Disease,* 11**,** 463-471.

KRONENBERG, H. M. (2003) Developmental regulation of the growth plate. *Nature,* 423**,** 332-336.

KUMASHIRO, Y., TERAMOTO, K., SHIMIZU-SAITO, K., ASAHINA, K., TERAOKA, H. & ARII, S. (2005) Isolation of hepatocyte-like cells from mouse embryoid body cells. *Transplantation Proceedings,* 37**,** 299-300.

KUO, H. C., PAU, K. Y., YEOMAN, R. R., MITALIPOV, S. M., OKANO, H. & WOLF, D. P. (2003) Differentiation of monkey embryonic stem cells into neural lineages. *Biology of Reproduction,* 68**,** 1727-1735.

KUROSAWA, H. (2007) Methods for inducing embryoid body formation: *In Vitro* differentiation system of embryonic stem cells. *Journal of Bioscience and Bioengineering,* 103**,** 398-398.

LABOSKY, P. A., BARLOW, D. P. & HOGAN, B. L. M. (1994) Mouse embryonic germ (EC) cell lines: transmission through the germline and differences in the methylation imprint of insulin-like growth factor 2 receptor (*Igf2r*) gene compared with embryonic stem (ES) cell lines. *Development,* 120**,** 3197-3204.

LAI, B., MAO, X. O., GREENBERG, D. A. & JIN, K. (2008) Endothelium-induced proliferation and electrophysiological differentiation of human embryonic stem cell-derived neuronal precursors. *Stem cells and development,* 17**,** 565-72.

LAKKAKORPI, P. T. & VAANANEN, H. K. (1991) Kinetics of the osteoclast cytoskeleton during the resorption cycle in vitro. *Journal of Bone and Mineral Research,* 6**,** 817-826.

LANGER, R. & VACANTI, J. P. (1993) Tissue Engineering. *Science,* 260**,** 920-926.

LASCHKE, M. W., RUCKER, M., JENSEN, G., CARVALHO, C., MULHAUPT, R., GELLRICH, N. C. & MENGER, M. D. (2008) Incorporation of growth factor containing Matrigel promotes vascularization of porous PLGA scaffolds. *Journal of Biomedical Materials Research Part A,* 85**,** 397-407.

LAVERY, K., SWAIN, P., FALB, D. & ALAOUI-ISMAILI, M. H. (2008) BMP-2/4 and BMP-6/7 differentially utilize cell surface receptors to induce osteoblastic differentiation of human bone marrow-derived mesenchymal stem cells. *Journal of Biological Chemistry,* 283**,** 20948-20958.

LEAHY, A., XIONG, J. W., KUHNERT, F. & STUHLMANN, H. (1999) Use of developmental marker genes to define temporal and spatial patterns of differentiation during embryoid body formation. *Journal of Experimental Zoology,* 284**,** 67-81.

LEE, C. N., CHENG, W. F., CHANG, M. C., SU, Y. N., CHEN, C. A. & HSIEH, F. J. (2005) Hypoxia-induced apoptosis in endothelial cells and embryonic stem cells. *Apoptosis,* 10**,** 887-894.

LEE, H. J., YU, C., CHANSAKUL, T., VARGHESE, S., HWANG, N. S. & ELISSEEFF, J. H. (2008a) Enhanced chondrogenic differentiation of embryonic stem cells by coculture with hepatic cells. *Stem Cells and Development,* 17**,** 555-563.

LEE, H. W., SUH, J. H., KIM, H. N., KIM, A. Y., PARK, S. Y., SHIN, C. S., CHOI, J. Y. & KIM, J. B. (2008b) Berberine promotes osteoblast differentiation by Runx2 activation with p38 MAPK. *Journal of Bone and Mineral Research,* 23**,** 1227-1237.

LEE, J. D. & ANDERSON, K. V. (2008) Morphogenesis of the Node and Notochord: The Cellular Basis for the establishment and Maintenance of Left–Right Asymmetry in the Mouse. *Developmental Dynamics,* 237**,** 3464-3476.

LEE, K. D. (2008) Applications of mesenchymal stem cells: an updated review. *Chang Gung Medical Journal,* 31**,** 228-236.

LEE, K. L., AUBIN, J. E. & HEERSCHE, J. N. M. (1992) beta -Glycerophosphate-induced mineralization of osteoid does not alter expression of extracellular matrix components in fetal rat calvarial cell cultures. *Journal of Bone and Mineral Research,* 7**,** 1211-1219.

LEE, S. J., LIM, G. J., LEE, J. W., ATALA, A. & YOO, J. J. (2006) In vitro evaluation of a poly(lactide-co-glycolide)-collagen composite scaffold for bone regeneration. *Biomaterials,* 27**,** 3466-3472.

LEHMAN, J. M., SPEERS, W. C., SWARTZENDRUBER, D. E. & PIERCE, G. B. (1974) Neoplastic differentiation: characteristics of cell lines derived from a murine teratocarcinoma. *Journal of Cell Physiology,* 84**,** 13-27.

LEI, H., OH, S. P., OKANO, M., JUETTERMANN, R., GOSS, K. A., JAENISCH, R. & LI, E. (1996) De novo DNA cytosine methyltransferase activities in mouse embryonic stem cells. *Development,* 122**,** 3195-3205.

LENDLEIN, A., NEUENSCHWANDER, P. & SUTER, U. W. (1998) Tissue-compatible multiblock copolymers for medical applications, controllable in degradation rate and mechanical properties. *Macromolecular Chemistry and Physics,* 199**,** 2785-2796.

LEVENBERG, S. (2005) Engineering blood vessels from stem cells: recent advances and applications. *Current Opinion in Biotechnology,* 16**,** 516-523.

LEVENBERG, S., HUANG, N. F., LAVIK, E., ROGERS, A. B., ITSKOVITZ-ELDOR, J. & LANGER, R. (2003) Differentiation of human embryonic stem cells on three-dimensional polymer scaffolds. *Proceedings of the National Academy of Sciences of the United States of America,* 100**,** 12741-12746.

LIAO, C. J., CHEN, C. F., CHEN, J. H., CHIANG, S. F., LIN, Y. J. & CHANG, K. Y. (2002) Fabrication of porous biodegradable scaffolds using a solvent merging/particle leaching method. *Journal of Biomedical Materials Research,* 59**,** 676-681.

LING, V. & NEBEN, S. (1997) In vitro differentiation of embryonic stem cells: immunophenotypic analysis of cultured embryoid bodies. *Journal of Cellular Physiology,* 171**,** 104-115.

LOWRY, W. E., RICHTER, L., YACHECHKO, R., PYLE, A. D., TCHIEU, J., SRIDHARAN, R., CLARK, A. T. & PLATH, K. (2008) Generation of human induced pluripotent stem cells from dermal fibroblasts. *Proceedings of the National Academy of Sciences of the United States of America,* 105**,** 2883-2888.

LU, H. F., CHAUA, K. N., ZHANG, P. C., LIM, W. S., RAMAHRISHNA, S., LEONG, K. W. & MAO, H. Q. (2005) Three-dimensional co-culture of rat hepatocyte spheroids and NIH/3T3 fibroblasts enhances hepatocyte functional maintenance. *Acta Biomaterialia,* 1**,** 399-410.

LU, Y., SUN, J. & SHEN, J. (2008) Cell adhesion properties of patterned poly(acrylic acid)/poly(allylamine hydrochloride) multilayer films created by room-temperature imprinting technique. *Langmuir,* 24**,** 8050-8055.

LUDWIG, H., METZGER, H. & HAFEZ, E. S. (1976) Critical-point drying and gold sputtering as applied to scanning electron microscopy of human reproductive tissues. *Acta Anatomica (Basel),* 96**,** 469-477.

LUONG, E. & GERECHT, S. (2008) Stem Cells and Scaffolds for Vascularizing Engineered Tissue Constructs. *Advances in Biochemical Engineering/Biotechnology*.

LUTOLF, M. P. & HUBBELL, J. A. (2005) Synthetic biomaterials as instructive extracellular microenvironments for morphogenesis in tissue engineering. *Nature Biotechnology,* 23**,** 47-55.

MA, P. X. (2008) Biomimetic Materials for Tissue Engineering. *Advanced Drug Delivery Reviews,* 60**,** 184-198.

MA, W., TAVAKOLI, T., DERBY, E., SEREBRYAKOVA, Y., RAO, M. S. & MATTSON, M. P. (2008) Cell-extracellular matrix interactions regulate neural differentiation of human embryonic stem cells. *BMC Developmental Biology,* 8.

MACDONALD, B. R., TAKAHASHI, N., MCMANUS, L. M., HOLAHAN, J., MUNDY, G. R. & ROODMAN, G. D. (1987) Formation of a multinucleated cell that responds to osteotropic hormones in long term human bone marrow cultures. *Endocrinology,* 120**,** 2326-2333.

MAHERALI, N., SRIDHARAN, R., XIE, W., UTIKAL, J., EMINLI, S., ARNOLD, K., STADFELD, M., YACHECHKO, R., TCHIEU, J., JAENISCH, R., PLATH, K. & HOCHEDLINGER, K. (2007) Directly reprogrammed fibroblasts show global epigenetic remodeling and widespread tissue contribution. *Cell Stem Cell,* 1**,** 55-70.

MAHMUTEFENDIC, H., BLAGOJEVIC, G., KUCIC, N. & LUCIN, P. (2007) Constitutive internalization of murine MHC class I molecules. *Journal of Cellular Physiology,* 210**,** 445-455.

MANSERGH, F. C., DALY, C. S., HURLEY, A. L., WRIDE, M. A., HUNTER, S. M. & EVANS, M. J. (2009) Gene expression profiles during early differentiation of mouse embryonic stem cells. *BMC Developmental Biology,* 9.

MANTALARIS, A., KENG, P., BOURNE, P., CHANG, A. Y. & WU, J. H. (1998) Engineering a human bone marrow model: a case study on ex vivo erythropoiesis. *Biotechnology Progress,* 14**,** 126-133.

MARCU, A. C., PACCIONE, K. E., BARBEE, R. W., DIEGELMANN, R. F., IVATURY, R. R., WARD, K. R. & LORIA, R. M. (2007) Androstenetriol immunomodulation improves survival in a severe trauma hemorrhage shock model. *The Journal of trauma,* 63**,** 662-9.

MARKS, D. I. (2008) The role of allografting in adults with acute leukaemia. *Bone marrow transplantation,* 41**,** 413-4.

MARQUIS, M. E., LORD, E., BERGERON, E., DREVELLE, O., PARK, H., CABANA, F., SENTA, H. & FAUCHEUX, N. (2009) Bone cells-biomaterials interactions. *Frontiers in Bioscience,* 14**,** 1023-1067.

MARSH, J. L., SLONGO, T. F., AGEL, J., BRODERICK, J. S., CREEVEY, W., DECOSTER, T. A., PROKUSKI, L., SIRKIN, M. S., ZIRAN, B., HENLEY, B. & AUDIGE, L. (2007) Fracture and dislocation classification compendium - 2007: Orthopaedic Trauma Association classification, database and outcomes committee. *Journal of Orthopaedic Trauma,* 21**,** S1-133.

MARTIN, G. (1981) Isolation of a pluripotent cell line from early mouse embryos cultured in medium conditioned by teratocarcinoma stem cells. *Proceedings of the National Academy of Sciences of the United States of America,* 78**,** 7634-7638.

MARTIN, G. R. (1975) Teratocarcinomas as a model system for the study of embryogenesis and neoplasia. *Cell,* 5**,** 229-243.

MARTIN, G. R. (1980) Teratocarcinomas and Mammalian Embryogenesis. *Science,* 209**,** 768-776.

MARTIN, M. J., MUOTRI, A., GAGE, F. & VARKI, A. (2005) Human embryonic stem cells express an immunogenic nonhuman sialic acid. *Nature Medicine,* 11**,** 228-232.

MARTIN, R. B. & ISHIDA, J. (1989) The relative effects of collagen fiber orientation, porosity, density, and mineralization of on bone strength. *Journal of Biomechanics,* 22**,** 419-426.

MARTINS, M. J., NEGRAO, M. R. & HIPOLITO-REIS, C. (2001) Alkaline phosphatase from rat liver and kidney is differentially modulated. *Clinical biochemistry,* 34**,** 463-8.

MARUYAMA, Z., YOSHIDA, C. A., FURUICHI, T., AMIZUKA, N., ITO, M., FUKUYAMA, R., MIYAZAKI, T., KITAURA, H., NAKAMURA, K., FUJITA, T., KANATANI, N., MORIISHI, T., YAMANA, K., LIU, W., KAWAGUCHI, H., NAKAMURA, K. & KOMORI, T. (2007) Runx2 determines bone maturity and turnover rate in postnatal bone development and is involved in bone loss in estrogen deficiency. *Developmental Dynamics,* 236**,** 1876-1890.

MASTRO, A. M. & VOGLER, E. A. (2009) A three-dimensional osteogenic tissue model for the study of metastatic tumor cell interactions with bone. *Cancer Research,* 69**,** 4097-4100.

MATEIZEL, I., DE BECKER, A., VAN DE VELDE, H., DE RYCKE, M., VAN STEIRTEGHEM, A., CORNELISSEN, R., VAN DER ELST, J., LIEBAERS, I., VAN RIET, I. & SERMON, K. (2008) Efficient differentiation of human embryonic stem cells into a homogeneous population of osteoprogenitor-like cells. *Reproductive Biomedicine Online,* 16**,** 741-753.

MATSUBARA, T., TSUTSUMI, S., PAN, H., HIRAOKA, H., ODA, R., NISHIMURA, M., KAWAGUCHI, H., NAKAMURA, K. & KATO, Y. (2004) A new technique to expand human mesenchymal stem cells using basement membrane extracellular matrix. *Biochemical and Biophysical Research Communications,* 313**,** 503-508.

MATSUDA, T., NAKAMURA, T., NAKAO, K., ARAI, T., KATSUKI, M., HEIKE, T. & YOKOTA, T. (1999) STAT3 activation is sufficient to maintain an undifferentiated state of mouse embryonic stem cells. *EMBO Journal,* 18**,** 4261-4269.

MATSUI, Y., TOKSOZ, D., NISHIKAWA, S., NISHIKAWA, S. I., WILLIAMS, D., ZSEBO, K. & HOGAN, B. L. M. (1991) Effect of *Steel* factor and leukaemia inhibitory factor on murine primordial germ cells in culture. *Nature,* 353**,** 750-752.

MCLAREN, A. & DURCOVA-HILLS, G. (2001) Germ cells and pluripotent stem cells in the mouse. *Reproduction,* 13**,** 661-664.

MCMAHON, L. A., O'BRIEN, F. J. & PRENDERGAST, P. J. (2008) Biomechanics and mechanobiology in osteochondral tissues. *Regenerative Medicine,* 3**,** 743-759.

MEIER, K., LEHR, C. M. & DAUM, N. (2008) Differentiation potential of human pancreatic stem cells for epithelial- and endothelial-like cell types. *Annals of Anatomy*.

MENDERES, A., BAYTEKIN, C., TOPCU, A., YILMAZ, M. & BARUTCU, A. (2004) Craniofacial reconstruction with high-density porous polyethylene implants. *Journal of Craniofacial Surgery,* 15**,** 719-724.

MEYER, J. R. (2000) Human embryonic stem cells and respect for life. *Journal of Medical Ethics,* 26**,** 166-170.

MICALLEF, S. J., LI, X., ELEFANTY, A. G. & STANLEY, E. G. (2007) Pancreas differentiation of mouse ES cells. *Current Protocols in Stem Cell Biology,* Chapter 1**,** Unit 1G.2.

MIGEON, B. R., CHOWDHURY, A. K., DUNSTON, J. A. & MCINTOSH, I. (2001) Identification of TSIX, Encoding an RNA Antisense to Human XIST, Reveals Differences from its Murine Counterpart: Implications for X Inactivation. *American Journal of Human Genetics,* 69**,** 951-960.

MITALPOVA, M., CALHOUN, J., SHEN, S., WININGER, D., SCHULZ, T., NOGGLE, S., VENABLE, A., LYONS, I., ROBINS, A. & STICE, S. (2003) Human Embryonic Stem Cell Lines Derived from Discarded Embryos. *Stem Cells,* 21**,** 521-526.

MITCHELL, N., SHEPARD, N. & HAAROD, J. (1982) The measurement of proteoglycan in the mineralizing region of the rat growth plate. *Journal of Bone and Joint Surgery: American volume,* 64**,** 32-38.

MOELLER, H. C., MIAN, M. K., SHRIVASTAVA, S., CHUNG, B. G. & KHADEMHOSSEINI, A. (2008) A microwell array system for stem cell culture. *Biomaterials,* 29**,** 752-763.

MOGI, A., ICHIKAWA, H., MATSUMOTO, C., HIEDA, T., TOMOTSUNE, D., SAKAKI, S., YAMADA, S. & SASAKI, K. (2009) The method of mouse embryoid body establishment affects structure and developmental gene expression. *Tissue and Cell,* 41**,** 79-84.

MOHAN, N., NAIR, P. D. & TABATA, Y. (2008) A 3D biodegradable protein based matrix for cartilage tissue engineering and stem cell differentiation to cartilage. *Journal of Materials Science:Materials in Medicine*.

MOHR, J. C., DE PABLO, J. J. & PALECEK, S. P. (2006) 3-D microwell culture of human embryonic stem cells. *Biomaterials,* 27**,** 6032-6042.

MOIOLI, E. K., HONG, L., GUARDADO, J., CLARK, P. A. & MAO, J. J. (2006) Sustained release of TGFbeta3 from PLGA microspheres and its effect on early osteogenic differentiation of human mesenchymal stem cells. *Tissue Engineering,* 12**,** 537-546.

MOON, S. Y., PARK, Y. B., KIM, D. S., OH, S. K. & KIM, D. W. (2006) Generation, culture, and differentiation of human embryonic stem cells for therapeutic applications. *Molecular Therapy,* 13**,** 5-14.

MORINOBU, M., ISHIJIMA, M., RITTLING, S. R., TSUJI, K., YAMAMOTO, H., NIFUJI, A., DENHARDT, D. T. & NODA, M. (2003) Osteopontin Expression in Osteoblasts and Osteocytes During Bone Formation Under Mechanical Stress in the Calvarial Suture In Vivo. *Journal of Bone and Mineral Research,* 18**,** 1706-1715.

MORITA, T., SAKAMURA, Y., HORIKIRI, Y., SUZUKI, T. & YOSHINO, H. (2000) Protein encapsulation into biodegradable microspheres by a novel S/O/W emulsion method using poly(ethylene glycol) as a protein micronization adjuvant. *Journal of Controlled Release,* 69**,** 435-444.

MORRIS, D. C., MASUHARA, K., TAKAOKA, K., ONO, K. & ANDERSON, H. C. (1992) Immunolocalization of alkaline phosphatase in osteoblasts and matrix vesicles of human fetal bone. *Bone and Mineral,* 19**,** 287-298.

MORRISEY, E. E., MUSCO, S., CHEN, M. Y., LU, M. M., LEIDEN, J. M. & PARMACEK, M. S. (2000) The gene encoding the mitogen-responsive phosphoprotein Dab2 is differentially regulated by GATA-6 and GATA-4 in the visceral endoderm. *Journal of Biological Chemistry,* 275**,** 19949-19954.

MULLER, E. J., WILLIAMSON, L., KOLLY, C. & SUTER, M. M. (2008) Outside-in signaling through integrins and cadherins: a central mechanism to control epidermal growth and differentiation? *The Journal of Investigative Dermatology,* 128**,** 501-516.

MURASHOV, A. K., PAK, E. S., HENDRICKS, W. A. & TATKO, L. M. (2004) 17beta-Estradiol enhances neuronal differentiation of mouse embryonic stem cells. *FEBS Letters,* 569**,** 165-168.

MURATA, M., YUDOH, K. & MASUKO, K. (2008) The potential role of vascular endothelial growth factor (VEGF) in cartilage: how the angiogenic factor could be involved in the pathogenesis of osteoarthritis? *Osteoarthritis and Cartilage,* 16**,** 279-286.

MURPHY, W. L. & MOONEY, D. J. (1999) Controlled delivery of inductive proteins, plasmid DNA and cells from tissue engineering matrices. *Journal of periodontal research,* 34**,** 413-9.

MURRELL, W., FERON, F., WETZIG, A., CAMERON, N., SPLATT, K., BELLETTE, B., BIANCO, J., PERRY, C., LEE, G. & A., M.-S. (2005) Multipotent stem cells from adult olfactory mucosa. *Developmental Dynamics,* 233**,** 496-515.

MURUGANANDAN, S., ROMAN, A. A. & SINAI, C. J. (2008) Adipocyte differentiation of bone marrow-derived mesenchymal stem cells: Cross talk with the osteoblastogenic program. *Cellular and Molecular Life Sciences*.

MYUNG, S. W. & CHOI, H. S. (2006) Chemical structure and surface morphology of plasma polymerised-allylamine film. *Korean Journal of Chemical Engineering,* 23**,** 505-511.

NAGAOKA, M., KOSHIMIZU, U., YUASA, S., HATTORI, F., CHEN, H., TANAKA, T., OKABE, M., FUKUDA, K. & AKAIKE, T. (2006) E-cadherin-coated plates maintain pluripotent ES cells without colony formation. *PLoS ONE,* 1**,** e15.

NAGY, A., ROSSANT, J., NAGY, R., ABRAMOW-NEWERLY, W. & RODER, J. C. (1993) Derivation of completely cell culture-derived mice from early-passage embryonic stem cells. *Proceedings of the National Academy of Sciences of the United States of America,* 90**,** 8424-8428.

NAKAGAWA, M., KOYANAGI, M., TANABE, K., TAKAHASHI, K., ICHISAKA, T., AOI, T., OKITA, K., MOCHIDUKI, Y., TAKIZAWA, N. & YAMANAKA, S. (2008) Generation of induced pluripotent stem cells without Myc from mouse and human fibroblasts. *Nature Biotechnology,* 26**,** 101-106.

NAKASHIMA, K., ZHOU, X., KUNKEL, G., ZHANG, Z., DENG, J. M., BEHRINGER, R. R. & DE CROMBRUGGHE, B. (2002) The novel zinc finger-containing transcription factor osterix is required for osteoblast differentiation and bone formation. *Cell,* 108**,** 17-29.

NATION, J. L. (1983) A new method using hexamethyldisilazane fro preparation of soft insect tissues for scanning electron microscopy. *Stain Technology,* 58**,** 347-351.

NAVARRO-ALVAREZ, N., SOTO-GUTIERREZ, A., YUASA, T., YAMATSUJI, T., SHIRAKAWA, Y., NAGASAKA, T., SUN, S. D., JAVED, M. S., TANAKA, N. & KOBAYASHI, N. (2008) Long-term culture of Japanese human embryonic stem cells in feeder-free conditions. *Cell Transplantation,* 17**,** 27-33.

NEFF, J. A., CALDWELL, K. D. & TRESCO, P. A. (1998) A novel method for surface modification to promote cell attachment to hydrophobic substrates. *Journal of Biomedical Materials Research,* 40**,** 511-519.

NESTI, L. J., LI, W. J., SHANTI, R. M., JIANG, Y. J., JACKSON, W., FREEDMAN, B. A., KUKLO, T. R., GIULIANI, J. R. & TUAN, R. S. (2008) Intravertebral disc tissue engineering using a novel hyaluronic acid-nanofibrous scaffold (HANFS) amalgam. *Tissue Engineering Part A*.

NG, E. S., DAVIS, R. P., AZZOLA, L., STANLEY, E. G. & ELEFANTY, A. G. (2005) Forced aggregation of defined numbers of human embryonic stem cells into embryoid bodies fosters robust, reproducible hematopoietic differentiation. *Blood,* 106**,** 1601-1603.

NGIAM, M., LIAO, S. & PATEL, A. J. (2008) Fabrication of mineralized polymeric nanofibrous composites for bone graft materials. *Tissue Engineering Part A*.

NICHOLS, J., CHAMBERS, I., TAGA, T. & SMITH, A. (2001) Physiological rationale for responsiveness of mouse embryonic stem cells to gp130 cytokines. *Development,* 128**,** 2333-2339.

NICHOLS, J., DAVIDSON, D., TAGA, T., YOSHIDA, K., CHAMBERS, I. & SMITH, A. (1996) Complementary tissue-specific expression of LIF and LIF-receptor mRNAs in early mouse embryogenesis. *Mechanisms of Development,* 57**,** 123-131.

NICHOLS, J., EVANS, E. P. & SMITH, A. G. (1990) Establishment of germ-line-competent embryonic stem (ES) cells using differentiation inhibiting activity. *Development,* 110**,** 1341-1348.

NICHOLS, J. E. & CORTIELLA, J. (2008) Engineering of a complex organ: progress toward development of a tissue-engineered lung. *Proceedings of the American Thoracic Society,* 5**,** 723-730.

NIE, D., GENGE, B. R., WU, L. N. & WUTHIER, R. E. (1995) Defect in formation of functional matrix vesicles by growth plate chondrocytes in avian tibial dyschondroplasia: evidence of defective tissue vascularization. *Journal of Bone and Mineral Research,* 10**,** 1625-1634.

NIEBRUEGGE, S., NEHRING, A., BAER, H., SCHROEDER, M., ZWEIGERDT, R. & LEHMANN, J. (2008) Cardiomyocyte Production in Mass Suspension Culture: Embryonic Stem Cells as a Source for Great Amounts of Functional Cardiomyocytes. *Tissue Engineering, Part A,* 14**,** 1591-1602.

NIIDA, S., KAKU, M., AMANO, H., YOSHIDA, H., KATAOKA, H., NISHIKAWA, S., TANNA, K., MAEDA, M., NISHIKAWA, S. & KODAMA, H. (1999) Vascular endothelial growth factor can substitute for macrophage colony-stimulating factor in the support of osteoclastic bone resorption. *Journal of Experimental Medicine,* 190**,** 293-298.

NIWA, H. (2001) Molecular mechanism to maintain stem cell renewal of ES cells. *Cell Structure and Function,* 26**,** 137-148.

NIWA, H., BURDON, T., CHAMBERS, I. & SMITH, A. (1998) Self-renewal of pluripotent embryonic stem cells is mediated via activation of STAT3. *Genes & Development,* 12**,** 2048-2060.

NORRIS, W. D., STEELE, J. G., JOHNSON, G. & UNDERWOOD, P. A. (1990) Serum enhancement of human endothelial cell attachment to and spreading on collagens I and IV does not require serum fibronectin or vitronectin. *Journal of Cell Science,* 95**,** 255-262.

O'BRIEN, J., WILSON, I., ORTON, T. & POGNAN, F. (2000) Investigation of the Alamar Blue (resazurin) fluorescent dye for the assessment of mammalian cell cytotoxicity. *European journal of biochemistry / FEBS,* 267**,** 5421-6.

O'NEILL, H. C. (2006) Dendritic Cell Therapy for Tolerance Induction to Stem Cell Transplants. *Current Stem Cell Research and Therapy,* 1**,** 121-125.

OCCLESTON, N. L., DANIELS, J. T., TARNUZZER, R. W., SETHI, K. K., ALEXANDER, R. A., BHATTACHARYA, S. S., SCHULTZ, G. S. & KHAW, P. T. (1997) Single Exposures to Antiproliferatives: Long-Term Effects on Ocular Fibroblast Wound-Healing Behavior. *Investigative Ophthalmology and Visual Science,* 38**,** 1998-2007.

ODORICO, J. S., KAUFMAN, D. S. & THOMSON, J. A. (2001) Multilineage differentiation from human embryonic stem cell lines. *Stem Cells,* 19**,** 193-204.

OGAWA, K., NISHINAKAMURA, R., IWAMATSU, Y., SHIMOSATO, D. & NIWA, H. (2006) Synergistic action of Wnt and LIF in maintaining pluripotency of mouse ES cells. *Biochemical and Biophysical Research Communications,* 343**,** 159-166.

OKA, M., TAGOKU, K., RUSSELL, T. L., NAKANO, Y., HAMAZAKI, T., MEYER, E. M., YOKOTA, T. & TERADA, N. (2002) CD9 is associated with leukemia inhibitory factor-mediated maintenance of embryonic stem cells. *Molecular Biology of the Cell,* 13**,** 1274-1281.

OKITA, K., ICHISAKA, T. & YAMANAKA, S. (2007) Generation of germline-competent induced pluripotent stem cells. *Nature,* 448**,** 313-317.

ONYANGO, P., JIANG, S., UEJIMA, H., SHAMBLOTT, M. J., GEARHART, J. D., CUI, H. & FEINBERG, A. P. (2002) Monoallelic expression and methylation of imprinted genes in human and mouse embryonic germ cell lineages. *Proceedings of the National Academy of Sciences of the United States of America,* 99**,** 10599-10604.

PANOSKALTSIS, N., MANTALARIS, A. & WU, J. H. (2005) Engineering a mimicry of bone marrow tissue ex vivo. *Journal of Bioscience and Bioengineering,* 100**,** 28-35.

PANSERI, S., CUNHA, C., LOWERY, J., DEL CARRO, U., TARABALLI, F., AMADIO, S., VESCOVI, A. & GELAIN, F. (2008) Electrospun micro- and nanofiber tubes for functional nervous regeneration in sciatic nerve transections. *BMC Biotechnology,* 8**,** 39.

PAPPALARDO, S., PUZZO, S., CARLINO, V. & CAPPELLO, V. (2007) Bone substitutes in oral surgery. *Minerva Stomatologica,* 56**,** 541-557.

PAREKKADAN, B., BERDICHEVSKY, Y., IRIMIA, D., LEEDER, A., YARMUSH, G., TONER, M., LEVINE, J. B. & YARMUSH, M. L. (2008) Cell-cell interaction modulates neuroectodermal specification of embryonic stem cells. *Neuroscience Letters,* 438**,** 190-195.

PAREKKADAN, B., VAN POLL, D., MEGEED, Z., KOBAYASHI, N., TILLES, A. W., BERTHIAUME, F. & YARMUSH, M. L. (2007) Immunomodulation of activated hepatic stellate cells by mesenchymal stem cells. *Biochemical and Biophysical Research Communications,* 363**,** 247-252.

PARK, I. H., LEROU, P. H., ZHAO, R., HUO, H. & DALEY, G. Q. (2008a) Generation of human-induced pluripotent stem cells. *Nature Protocols,* 3**,** 1180-1186.

PARK, I. H., ZHAO, R., WEST, J. A., YABUUCHI, A., HUO, H., INCE, T. A., LEROU, P. H., LENSCH, M. W. & DALEY, G. Q. (2008b) Reprogramming of human somatic cells to pluripotency with defined factors. *Nature,* 451**,** 141-146.

PARK, J., SETTER, V., WIXLER, V. & SCHNEIDER, H. (2008c) Umbilical cord blood stem cells: induction of differentiation into mesenchymal lineages by cell-cell contacts with various mesenchymal cells. *Tissue Engineering Part A*.

PARK, K. H. & NA, K. (2008) Effect of growth factors on chondrogenic differentiation of rabbit mesenchymal cells embedded in injectable hydrogels. *Journal of Bioscience and Bioengineering,* 106**,** 74-79.

PARK, S., KIM, G., JEON, Y. C., KOH, Y. & KIM, W. (2008d) 3D polycaprolactone scaffolds with controlled pore structure using a rapid prototyping system. *Journal of Materials Science:Materials in Medicine*.

PATIL, N., LEE, K. & GOODMAN, S. B. (2009) Porous tantalum in hip and knee reconstructive surgery. *Journal of Biomedical Materials Research, Part B, Applied Biomaterials,* 89**,** 242-251.

PERA, M. F., REUBINOFF, B. & TROUNSON, A. (2000) Human embryonic stem cells. *Journal of Cell Science,* 113**,** 5-10.

PHILLIPS, J. E. & GARCIA, A. J. (2008) Retroviral-mediated gene therapy for the differentiation of primary cells into a mineralizing osteoblastic phenotype. *Methods in Molecular Biology,* 434**,** 333-354.

PHILLIPS, J. E., GULDBERG, R. E. & GARCIA, A. J. (2007) Dermal Fibroblasts Genetically Modified to Express Runx2/Cbfa1 as a Mineralizing Cell Source for Bone Tissue Engineering. *Tissue Engineering,* 13**,** 2029-2040.

PIQUET-PELLORCE, C., GREY, L., MEREAU, A. & HEATH, J. K. (1994) Are LIF and related cytokines functionally equivalent? *Experimental Cell Research,* 213**,** 340-347.

PLACZEK, M. R., CHUNG, I. M., MACEDO, H. M., ISMAIL, S., MORTERA, B. T., LIM, M., CHA, J. M., FAUZI, I., KANG, Y., YEO, D. C., MA, C. Y., POLAK, J. M., PANOSKALTSIS, N. & MANTALARIS, A. (2009) Stem cell bioprocessing: fundamentals and principles. *The Journal of Royal Society - Interface,* 6**,** 209-232.

PLUCHINO, S. & MARTINO, G. (2008) Neural stem cell-mediated immunomodulation: repairing the haemorrhagic brain. *Brain,* 131**,** 604-605.

PLUSA, B., PILISZEK, A., FRANKENBERG, S., ARTUS, J. & HADJANTONAKIS, A. K. (2008) Distinct sequential cell behaviours direct primitive endoderm formation in the mouse blastocyst. *Development,* 135**,** 3081-3091.

POKUTTA, S. & WEIS, W. I. (2007) Structure and mechanism of cadherins and catenins in cell-cell contacts. *Annual Review of Cell and Developmental Biology,* 23**,** 237-261.

POLAK, J. M. & MANTALARIS, A. (2008) Stem cells bioprocessing: an important milestone to move regenerative medicine research into the clinical arena. *Paediatric Research,* 63**,** 461-466.

POLIARD, A., LAMBLIN, D., MARIE, P. J., BUC CARON, M. H. & KELLERMANN, O. (1993) Commitment of the teratocarcinoma-derived mesodermal clone C1 towards terminal osteogenic differentiation. *Journal of Cell Science,* 106**,** 503-511.

POTTER, W., KALIL, R. E. & KAO, W. J. (2008) Biomimetic material systems for neural progenitor cell-based therapy. *Frontiers in Bioscience : A Journal and Virtual Library,* 13**,** 806-821.

PRABHA, S. & VERGHESE, S. (2008) Existence of proviral porcine endogenous retrovirus in fresh and decellularised porcine tissues. *Indian journal of medical microbiology,* 26**,** 228-32.

PRESTWICH, G. D. (2007) Simplifying the extracellular matrix for 3-D cell culture and tissue engineering: a pragmatic approach. *Journal of Cellular Biochemistry,* 101**,** 1370-1383.

PRESTWICH, G. D. (2008) Evaluating drug efficacy and toxicology in three dimensions: using synthetic extracellular matrices in drug discovery. *Accounts of Chemical Research,* 41**,** 139-148.

PROKHOROVA, T. A., HARKNESS, L. M., FRANDSEN, U., DITZEL, N., BURNS, J. S., SCHROEDER, H. D. & KASSEM, M. (2008) Teratoma Formation by Human Embryonic Stem Cells is site-dependent and enhanced by the presence of Matrigel. *Stem Cells and Development*.

PURPURA, K. A., AUBIN, J. E. & ZANDSTRA, P. W. (2004) Sustained in vitro expansion of bone progenitors is cell density dependent. *Stem Cells,* 22**,** 39-50.

QUAGLIA, F. (2008) Bioinspired tissue engineering: The great promise of protein delivery technologies. *International Journal of Pharmaceutics,* 364**,** 281-297.

RADISIC, M., PARK, H., CHEN, F., SALAZAR-LAZZARO, J. E., WANG, Y., DENNIS, R., LANGER, R., FREED, L. E. & VUNJAK-NOVAKOVIC, G. (2006) Biomimetic Approach to Cardiac Tissue Engineering: Oxygen Carriers and Channeled Scaffolds. *Tissue Engineering,* 12**,** 2077.

RAIKWAR, S. P., MUELLER, T. & ZAVAZAVA, N. (2006) Strategies for Developing Therapeutic Application of Human Embryonic; Stem Cells. *Physiology,* 21**,** 19-28.

RANDLE, W. L., CHA, J. M., HWANG, Y. S., CHAN, K. L., KAZARIAN, S. G., POLAK, J. M. & MANTALARIS, A. (2007) Integrated 3-dimensional expansion and osteogenic differentiation of murine embryonic stem cells. *Tissue Engineering,* 13**,** 2957-2970.

RATAJCZAK, M. Z., MACHALINSKI, B., WOJAKOWSKI, W., RATAJCZAK, J. & KUCIA, M. (2007) A hypothesis for an embryonic origin of pluripotent Oct-4(+) stem cells in adult bone marrow and other tissues. *Leukemia : Official Journal of the Leukemia Society of America,* 21**,** 860-867.

RATHJEN, P. D., LAKE, J., WHYATT, L. M., BETTESS, M. D. & RATHJEN, J. (1998) Properties and uses of embryonic stem cells: prospects for application to human biology and gene therapy. *Reproduction,* 10**,** 31-47.

REN, T. B., WEIGEL, T., GROTH, T. & LENDLEIN, A. (2008) Microwave plasma surface modification of silicone elastomer with allylamine for improvement of biocompatibility. *Journal of Biomedical Materials Research Part A,* 86**,** 209-219.

RESNICK, J. L., BIXLER, L. S., CHENG, L. & DONOVAN, P. J. (1992) Long-term proliferation of mouse primordial germ cells in culture. *Nature,* 359**,** 550-551.

REUBINOFF, B. E., PERA, M. F., FONG, C.-Y., TROUNSON, A. & BONGSO, A. (2000) Embryonic stem cell lines from human blastocysts: somatic differentiation in vitro. *Nature Biotechnology,* 18**,** 399-404.

REYES, C. D., PETRIE, T. A. & GARCIA, A. J. (2008) Mixed extracellular matrix ligands synergistically modulate integrin adhesion and signaling. *Journal of Cellular Physiology,* 217**,** 450-458.

RICH, J. T., ROSOVA, I., NOLTA, J. A., MYCKATYN, T. M., SANDELL, L. J. & MCALINDEN, A. (2008) Upregulation of Runx2 and Osterix during in vitro chondrogenesis of human adipose-derived stromal cells. *Biochemical and Biophysical Research Communications,* 372**,** 230-235.

ROBERTSON, J. A. (2001) Human embryonic stem cell research: ethical and legal issues. *Nature Reviews Genetics,* 2**,** 74-78.

ROHANI, L., KARBALAIE, K., VAHDATI, A., HATAMI, M., NASR-ESFAHANI, M. H. & BAHARVAND, H. (2008) Embryonic stem cell sphere: a controlled method for production of mouse embryonic stem cell aggregates for differentiation. *International Journal of Artificial Organs,* 31**,** 258-265.

ROSE, F. R. & OREFFO, R. O. (2002) Bone Tissue Engineering: Hope vs Hype. *Biochemical and Biophysical Research Communications,* 292**,** 1-7.

ROSENSTRAUCH, D., CANIC, S., PAN, T. W., GLOWINSKI, R., GUIDOBONI, G., GILL, J., MONCIVAIS, K., JOSEF, T. & HARTLEY, C. (2007) Genetically Engineered Mammalian Cells could Improve the Biocompatibility of Implantable Cardiovascular Devices. *Heart, Lung and Circulation,* 16**,** S31-S38.

ROSKELLEY, C. D., SREBROW, A. & BISSELL, M. J. (1995) A hierarchy of ECM-mediated signalling regulates tissue-specific gene expression. *Current Opinion in Cell Biology,* 7**,** 736-747.

ROUZES, C., GREF, R., LEONARD, M., DE SOUSA DELGADO, A. & DELLACHERIE, E. (2000) Surface modification of poly(lactic acid) nanospheres using hydrophobically modified dextrans as stabilizers in an o/w emulsion/evaporation technique. *Journal of Biomedical Materials Research,* 50**,** 557-565.

RULA, M. E., CAI, K. Q., MOORE, R., YANG, D. H., STAUB, C. M., CAPO-CHICHI, C. D., JABLONSKI, S. A., HOWE, P. H., SMITH, E. R. & XU, X. X. (2007) Cell autonomous sorting and surface positioning in the formation of primitive endoderm in embryoid bodies. *Genesis,* 45**,** 327-338.

RUST, W. L., SADASIVAM, A. & DUNN, N. R. (2006) Three-dimensional extracellular matrix stimulates gastrulation-like events in human embryoid bodies. *Stem Cells and Development,* 15**,** 889-904.

SACHLOS, E. & AUGUSTE, D. T. (2008) Embryoid body morphology influences diffusive transport of inductive biochemicals: a strategy for stem cell differentiation. *Biomaterials,* 29**,** 4471-4480.

SAFINIA, L., WILSON, K., MANTALARIS, A. & BISMARCK, A. (2007) Through-thickness plasma modification of biodegradable and nonbiodegradable porous polymer constructs. *Journal of Biomedical Materials Research Part A,* 87**,** 632-642.

SAKAGUCHI, T., SEKIYA, I., YAGISHITA, K., ICHINOSE, S., SHINOMIYA, K. & MUNETA, T. (2004) Suspended cells from trabecular bone by collagenase digestion become virtually identical to mesenchymal stem cells obtained from marrow aspirates. *Blood,* 104**,** 2728-2735.

SALES, V. L., ENGELMAYR, G. C. J., JOHNSON, J. A. J., GAO, J., WANG, Y., SACKS, M. S. & MAYER, J. E. J. (2007) Protein Precoating of Elastomeric Tissue-Engineering Scaffolds Increased Cellularity, Enhanced Extracellular Matrix Protein Production, and Differentially Regulated the Phenotypes of Circulating Endothelial Progenitor Cells. *Circulation,* 116**,** I-55-I-63.

SARRAF, C. E., HARRIS, A. B., MCCULLOCH, A. D. & EASTWOOD, M. (2005) Cell proliferation rates in an artificial tissue-engineered environment. *Cell proliferation,* 38**,** 215-21.

SAUER, G. R. & WUTHIER, R. E. (1988) Fourier transform infrared characterization of mineral phases formed during induction of mineralization by collagenase-released matrix vesicles in vitro. *Journal of Biological Chemistry,* 263**,** 13718-13724.

SCHAUSS, S. M., HINZ, M., MAYR, E., BACH, C. M., KRISMER, M. & FISCHER, M. (2006) Inferior stability of a biodegradable cement plug. 122 total hip replacements randomized to degradable or non-degradable cement restrictor. *Archives of Orthopaedic and Trauma Surgery,* 126**,** 324-329.

SCHNEIDER, A., GARLICK, J. A. & EGLES, C. (2008) Self-assembling peptide nanofiber scaffolds accelerate wound healing. *PLoS ONE,* 3**,** e1410.

SCHNEIDER, D. & ENGELMAN, D. M. (2004) Involvement of transmembrane domain interactions in signal transduction by alpha/beta integrins. *The Journal of Biological Chemistry,* 279**,** 9840-9846.

SCHOPPET, M., PREISSNER, K. T. & HOFBAUER, L. C. (2002) RANK ligand and osteoprotegrin: paracrine regulators of bone metabolism and vascular function. *Arteriosclerosis, Thrombosis and Vascular Biology,* 22**,** 549-553.

SCHULDINER, M., YANUKA, O., ITSKOVITZ-ELDOR, J., MELTON, D. A. & BENVENISTY, N. (2000) Effects of eight growth factors on the differentiation of cells derived from human embryonic stem cells. *Proceedings of the National Academy of Sciences of the United States of America,* 97**,** 11307-11312.

SCHWARZKOPF, M., KNOBELOCH, K. P., ROHDE, E., HINDERLICH, S., WIECHENS, N., LUCKA, L., HORAK, I., REUTTER, W. & HORSTKORTE, R. (2002) Sialylation is essential for early development in mice. *Proceedings of the National Academy of Sciences of the United States of America,* 99**,** 5267-5270.

SEMINO, C. E. (2008) Self-assembling peptides: from bio-inspired materials to bone regeneration. *Journal of Dental Research,* 87**,** 606-616.

SHAMBLOTT, M. J., AXELMAN, J., LITTLEFIELD, J. W., BLUMENTHAL, P. D., HUGGINS, G. R., CUI, Y., CHENG, L. & GEARHART, J. D. (2001) Human embryonic germ cell derivatives express a broad range of developmentally distinct markers and proliferate extensively in vitro. *Proceedings of the National Academy of Sciences of the United States of America,* 98**,** 113-118.

SHAMBLOTT, M. J., AXELMAN, J., WANG, S., BUGG, E. M., LITTLEFIELD, J. W., DONOVAN, P. J., BLUMENTHAL, P. D., HUGGINS, G. R. & GEARHART, J. D. (1998) Derivation of pluripotent stem cells from cultured human primordial germ cells. *Proceedings of the National Academy of Sciences of the United States of America,* 95**,** 13726-13731.

SHEARER, H., ELLIS, M. J., PERERA, S. P. & CHAUDHURI, J. B. (2006) Effects of common sterilization methods on the structure and properties of poly(D,L lactic-co-glycolic acid) scaffolds. *Tissue Engineering,* 12**,** 2717-2727.

SHIN, H., JO, S. & MIKOS, A. G. (2003) Biomimetic materials for tissue engineering. *Biomaterials,* 24**,** 4353-4364.

SHINOKA, T. & BREUER, C. (2008) Tissue-engineered blood vessels in pediatric cardiac surgery. *Yale Journal of Biology and Medicine,* 81**,** 161-166.

SHINOKA, T., SHUM-TIM, D., MA, P. X., TANEL, R. E., ISOGAI, N., LANGER, R., VACANTI, J. P. & MAYER, J. E. (1998) Creation of viable pulmonary artery autografts through tissue engineering. *The Journal of thoracic and cardiovascular surgery,* 115**,** 536-45; discussion 545-6.

SHUM-TIM, D., STOCK, U., HRKACH, J., SHINOKA, T., LIEN, J., MOSES, M. A., STAMP, A., TAYLOR, G., MORAN, A. M., LANDIS, W., LANGER, R., VACANTI, J. P. & MAYER, J. E. (1999) Tissue engineering of autologous aorta using a new biodegradable polymer. *The Annals of Thoracic Surgery,* 68**,** 2298-2304; discussion 2305.

SIERRA, J., MARTINO, R., SANCHEZ, B., PINANA, J. L., VALCARCEL, D. & BRUNET, S. (2008) Hematopoietic transplantation from adult unrelated donors as treatment for acute myeloid leukemia. *Bone Marrow Transplantation,* 41**,** 425-437.

SILBERGELD, E. K., SAUK, J., SOMERMAN, M., TODD, A., MCNEILL, F., FOWLER, B., FONTAINE, A. & VAN BUREN, J. (1993) Lead in bone: Storage site, exposure source, and target organ. *Neurotoxicology,* 14**,** 225-236.

SILBERGELD, E. K., SCHWARTZ, J. & MAHAFFEY, K. (1988) Lead and Osteoporosis: Mobilization of Lead from Bone in Postmenopausal Women. *Environmental Research,* 47**,** 79-94.

SIOW, K. S., BRITCHER, L., KUMAR, S. & GRIESSER, H. J. (2006) Plasma Methods for the Generation of Chemically Reactive Surfaces for Biomolecule Immobilization and Cell Colonization - A Review. *Plasma Processes and Polymers,* 3**,** 392-418.

SMITH, A. G. (2001) Embryo-derived stem cells: Of mice and men. *Annual Review of Cell and Developmental Biology,* 17**,** 435-462.

SMITH, J. R., VALLIER, L., LUPO, G., ALEXANDER, M., HARRIS, W. A. & PEDERSEN, R. A. (2008) Inhibition of Activin/Nodal signaling promotes specification of human embryonic stem cells into neuroectoderm. *Developmental Biology,* 313**,** 107-117.

SOKOLSKY-PAPKOV, M., AGASHI, K., OLAYE, A. E., SHAKESHEFF, K. M. & DOMB, A. J. (2007) Polymer carriers for drug delivery in tissue engineering. *Advanced Drug Delivery Reviews,* 59**,** 187-206.

SOMMERFELDT, D. W. & RUBIN, C. T. (2001) Biology of bone and how it orchestrates the form and function of the skeleton. *European Spine Journal,* 10**,** S86-S95.

SONG, H., O'CONNOR, K. C., LACKS, D. J., ENMON, R. M. & JAIN, S. K. (2003) Monte Carlo Simulation of LNCaP Human Prostate Cancer Cell Aggregation in Liquid-Overlay Culture. *Biotechnology Progress,* 19**,** 1742-1749.

SOTTILE, V., THOMSON, A. & MCWHIR, J. (2003) In vitro osteogenic differentiation of human ES cells. *Cloning and Stem Cells,* 5**,** 149-155.

SROUJI, S., MAURICE, S. & LIVNE, E. (2005) Microscopy analysis of bone marrow-derived osteoprogenitor cells cultured on hydrogel 3-D scaffold. *Microscopy Research and Technique,* 66**,** 132.

STAMM, C., KHOSRAVI, A., GRABOW, N., SCHMOHL, K., TRECKMANN, N., DRECHSEL, A., NAN, M., SCHMITZ, K. P., HAUBOLD, A. & STEINHOFF, G. (2004) Biomatrix/polymer composite material for heart valve tissue engineering. *The Annals of Thoracic Surgery,* 78**,** 2084-2092; discussion 2092-3.

STARR, R., NOVAK, U., WILLSON, T. A., INGLESE, M., MURPHY, V., ALEXANDER, W. S., METCALF, D., NICOLA, N. A., HILTON, D. J. & ERNST, M. (1997) Distinct roles for leukemia inhibitory factor receptor alpha -chain and gp130 in cell type-specific signal transduction. *Journal of Biological Chemistry,* 272**,** 19982-19986.

STEVENS, P. V., NYSTRAM, M. & EHSANI, N. (1998) Modification of ultrafiltration membrane with gelatin protein. *Biotechnology and Bioengineering,* 57**,** 26-34.

STEWART, M. H., BENDALL, S. C. & BHATIA, M. (2008) Deconstructing human embryonic stem cell cultures: niche regulation of self-renewal and pluripotency. *Journal of Molecular Medicine,* 86**,** 875-886.

STOJKOVIC, M., LAKO, M., STOJKOVIC, P., STEWART, R., PRZYBORSKI, S., ARMSTRONG, L., EVANS, J., HERBERT, M., HYSLOP, L., AHMAD, S., MURDOCH, A. & STRACHAN, T. (2004) Derivation of human embryonic stem cells from day-8 blastocysts recovered after three-step in vitro culture. *Stem Cells,* 22**,** 790-797.

STUART, K. & PANITCH, A. (2008) Influence of Chondroitin Sulfate on Collagen Gel Structure and Mechanical Properties at Physiologically Relevant Levels. *Biopolymers,* 89**,** 841-851.

SUCIATI, T., HOWARD, D., BARRY, J. J. A., EVERITT, N. M., SHAKESHEFF, K. M. & ROSE, F. R. A. J. (2006) Zonal release of proteins within tissue engineering scaffolds. *Journal of Materials Science,* 17**,** 1049-1056.

SULTANA, N. & WANG, M. (2008) Fabrication of HA/PHBV composite scaffolds through the emulsion freezing/freeze-drying process and characterisation of the scaffolds. *Journal of Materials Science. Materials in Medicine,* 19**,** 2555-2561.

SUMMER, R. & FINE, A. (2008) Mesenchymal progenitor cell research: limitations and recommendations. *Proceedings of the American Thoracic Society,* 5**,** 707-710.

SUN, W., DARLING, A., STARLY, B. & NAM, J. (2004) Computer-aided tissue engineering: overview, scope and challenges. *Biotechnology and Applied Biochemistry,* 39**,** 29-47.

TAI, G., POLAK, J. M., BISHOP, A. E., CHRISTODOULOU, I. & BUTTERY, L. D. K. (2004) Differentiation of Osteoblasts from Murine Embryonic Stem Cells by Overexpression of the Transcriptional Factor Osterix. *Tissue Engineering,* 10**,** 1456-1466.

TAKAHASHI, K., TANABE, K., OHNUKI, M., NARITA, M., ICHISAKA, T., TOMODA, K. & YAMANAKA, S. (2007) Induction of Pluripotent Stem Cells from Adult Human Fibroblasts by Defined Factors. *Cell,* 131**,** 861-872.

TAKAHASHI, K. & YAMANAKA, S. (2006) Induction of Pluripotent Stem Cells from Mouse Embryonic and Adult Fibroblast Cultures by Defined Factors. *Cell,* 126**,** 663-676.

TAKAHASHI, T., KATO, S., SUZUKI, N., KAWABATA, N. & TAKAGI, M. (2005) Autoregulatory mechanism of Runx2 through the expression of transcription factors and bone matrix proteins in multipotential mesenchymal cell line, ROB-C26. *Journal of Oral Science,* 47**,** 199-207.

TAKASHIMIZU, I., TANAKA, Y., YOSHIE, S., KANO, Y., ICHIKAWA, H., CUI, L., OQIWARA, N., JOHKURA, K. & SASHI, K. (2009) Localization of Liv2 as an immature hepatocyte marker in EB outgrowth. *Scientific World Journal,* 9**,** 190-199.

TAKIMOTO, Y., DIXIT, V. K., ARTHUR, M. & GITNICK, G. (2003) De novo liver tissue formation in rats using a novel collagen-polypropylene scaffold. *Cell Transplantation,* 12**,** 413-421.

TANAKA, H., MURPHY, C. L., MURPHY, C., KIMURA, M., KAWAI, S. & POLAK, J. M. (2004) Chondrogenic differentiation of murine embryonic stem cells: effects of culture conditions and dexamethasone. *Journal of Cellular Biochemistry,* 93**,** 454-462.

TANG, X. & WEAVERS, L. K. (2007) Decomposition of hydrolysates of chemical warfare agents using photoactivated periodate. *Journal of Photochemistry and Photobiology A: Chemistry,* 187**,** 311-318.

TARALLO, L., ZAFFE, D., ADANI, R., KRAJEWSKI, A. & RAVAGLIOLI, A. (2008) Extracorporeal hydroxyapatite-chamber for bone and biomaterial studies. *Journal of Materials Science: Materials in Medicine,* 19**,** 159-166.

TATEISHI, K., TAKEHARA, N., MATSUBARA, H. & OH, H. (2008) Stemming heart failure with cardiac- or reprogrammed-stem cells. *Journal of Cellular and Molecular Medicine*.

TAUCHMANOVA , L., SERIO, B., DEL PUENTE, A., RISITANO, A. M., ESPOSITO, A., DE ROSA, G., LOMBARDI, G., COLAO, A., ROTOLI, B. & SELLERI, C. (2002) Long-lasting bone damage detected by dual-energy x-ray absorptiometry, phalangeal osteosonogrammetry, and in vitro growth of marrow stromal cells after allogeneic stem cell transplantation. *Journal of Clinical Endocrinology and Metabolism,* 87**,** 5058-5065.

TERAI, K., TAKANO-YAMAMOTO, T., OHBA, Y., HIURA, K., SUGIMOTO, M., SATO, M., KAWAHATA, H., INAGUMA, N., KITAMURA, Y. & NOMURA, S. (1999) Role of Osteopontin in Bone Remodeling Caused by Mechanical Stress. *Journal of Bone and Mineral Research,* 14**,** 839-849.

THOMAS, C. H., COLLIER, J. H., SFEIR, C. S. & HEALY, K. E. (2002) Engineering gene expression and protein synthesis by modulation of nuclear shape. *Proceedings of the National Academy of Sciences of the United States of America,* 99**,** 1972-1977.

THOMAS, R. J., BENNETT, A., THOMSON, B. & SHAKESHEFF, K. M. (2006) Hepatic stellate cells on poly(DL-lactic acid) surfaces control the formation of 3D hepatocyte co-culture aggregates in vitro. *European Cells and Materials,* 11**,** 16-26; discussion 26.

THOMSON, J. A., ITSKOVITZ-ELDOR, J., SHAPIRO, S. S., WAKNITZ, M. A., SWIERGIEL, J. J., MARSHALL, V. S. & JONES, J. M. (1998) Embryonic stem cell lines derived from human blastocysts. *Science,* 282**,** 1145-1147.

THOMSON, J. A., KALISHMAN, J., GOLOS, T. G., DURNING, M., HARRIS, C. P., BECKER, R. A. & HEARN, J. P. (1995) Isolation of a primate embryonic stem cell line. *Proceedings of the National Academy of Sciences of the United States of America,* 92**,** 7844-7848.

THOMSON, J. A. & ODORICO, J. S. (2000) Human embryonic stem cell and embryonic germ cell lines. *Trends in Biotechnology,* 18**,** 53-57.

THOTE, A. J., CHAPPELL, J. T. J., GUPTA, R. B. & KUMAR, R. (2005) Reduction in the initial-burst release by surface cross-linking of PLGA microparticles containing hydrophilic or hydrophobic drugs. *Drug Development and Industrial Pharmacy,* 31**,** 43-57.

TIAN, X. F., HENG, B. C., GE, Z., LU, K., RUFAIHAH, A. J., FAN, V. T., YEO, J. F. & CAO, T. (2008) Comparison of osteogenesis of human embryonic stem cells within 2D and 3D culture systems. *Scandinavian Journal of Clinical and Laboratory Investigation,* 68**,** 58-67.

TITUSHKIN, I. & CHO, M. (2007) Modulation of cellular mechanics during osteogenic differentiation of human mesenchymal stem cells. *Biophysical Journal,* 93**,** 3693-3702.

TOSATTI, S., SCHWARTZ, Z., CAMPBELL, C., COCHRAN, D. L., VANDEVONDELE, S., HUBBELL, J. A., DENZER, A., SIMPSON, J., WIELAND, M., LOHMANN, C. H., TEXTOR, M. & BOYAN, B. D. (2004) RGD-containing peptide GCRGYGRGDSPG reduces enhancement of osteoblast differentiation by poly(L-lysine)-graft-poly(ethylene glycol)-coated titanium surfaces. *Journal of Biomedical Materials Research. Part A,* 68**,** 458-472.

TRISH, E., DIMOS, J. & EGGAN, K. (2006) Passaging HuES human embryonic stem cell-lines with trypsin. *Journal of Visualized Experiments***,** 49.

TROUILLAS, M., SAUCOURT, C., DUVAL, D., GAUTHEREAU, X., THIBAULT, C., DEMBELE, D., FERAUD, O., MENAGER, J., RALLU, M., PRADIER, L. & BOEUF, H. (2008) Bcl2, a transcriptional target of p38alpha, is critical for neuronal commitment of mouse embryonic stem cells. *Cell Death and Differentiation,* 15**,** 1450-1459.

TSAI, M., WEDEMEYER, J., GANIATSAS, S., TAM, S., ZON, L. I. & GALLI, S. J. (2000) In vivo immunological function of mast cells derived from embryonic stem cells: An approach for the rapid analysis of even embryonic lethal mutations in adult mice in vivo. *Proceedings of the National Academy of Sciences of the United States of America,* 97**,** 9186-9190.

TSUNG, M. S. & BURGESS, D. J. (2001) Preparation and Characterization of Gelatin Surface Modified PLGA Microparticles. *American Association of Pharmaceutical Scientists,* 3**,** 1-11.

UNGRIN, M. D., JOSHI, C., NICA, A., BAUWENS, C. & ZANDSTRA, P. W. (2008) Reproducible, ultra high-throughput formation of multicellular organization from single cell suspension-derived human embryonic stem cell aggregates. *PLoS ONE,* 3**,** e1565.

UTTARWAR, M. & ASWATH, P. (2008) Fabrication of porous, drug-releasing, biodegradable, polymer scaffolds for sustained drug release. *Journal of Biomedical Materials research. Part B,* 87**,** 121-131.

VACANTI, C. A. (2006) The history of tissue engineering. *Journal of Cellular and Molecular Medicine,* 10**,** 569-576.

VACCARO, A. R., CHIBA, K., HELLER, J. G., PATEL, T. C., THALGOTT, J. S., TRUUMEES, E., FISCHGRUND, J. S., CRAIG, M. R., BERTA, S. C. & WANG, J. C. (2002) Bone grafting alternatives in spinal surgery. *Spine Journal,* 2**,** 206-215.

VALENTI, M. T., CARBONARE, L. D., DONATELLI, L., BERTOLDO, F., ZANATTA, M. & CASCIO, V. L. (2008) Gene expression analysis in osteoblastic differentiation from peripheral blood mesenchymal stem cells. *Bone,* 43**,** 1084-1092.

VALLIER, L., REYNOLDS, D. & PEDERSEN, R. A. (2004) Nodal inhibits differentiation of human embryonic stem cells along the neuroectodermal default pathway. *Developmental Biology,* 275**,** 403-421.

VEMURI, M. C., SCHIMMEL, T., COLLS, P., MUNNE, S. & COHEN, J. (2007) Derivation of human embryonic stem cells in xeno-free conditions. *Methods in Molecular Biology,* 407**,** 1-10.

VENO, P. A. (2006) Live imaging of osteocytes within their lacunae reveals cell body and dendrite motions. *Journal of Bone and Mineral Research,* 21**,** S38-S39.

VISWANATHAN, S., BENATAR, T., ROSE-JOHN, S., LAUFFENBURGER, D. A. & ZANDSTRA, P. W. (2002) Ligand/receptor signaling threshold (LIST) model accounts for gp130-mediated embryonic stem cell self-renewal responses to LIF and HIL-6. *Stem Cells,* 20**,** 119-138.

VOLTARELLI, J. C., COURI, C. E. B., STRACIERI, A. B. P. L., OLIVEIRA, M. C., MORAES, D. A., PIERONI, F., COUTINHO, M., MALMEGRIM, K. C. R., FOSS-FREITAS, M. C., SIMOES, B. P., FOSS, M. C., SQUIERS, E. & BURT, R. K. (2007) Autologous Nonmyeloablative Hematopoietic Stem Cell Transplantation in Newly Diagnosed Type 1 Diabetes Mellitus. *Journal of the American Medical Association,* 297**,** 1568-1576.

WANG, F., WEAVER, V. M., PETERSEN, O. W., LARABELL, C. A., DEDHAR, S., BRIAND, P., LUPU, R. & BISSELL, M. J. (1998) Reciprocal interactions between beta1-integrin and epidermal growth factor receptor in three-dimensional basement membrane breast cultures: a different perspective in epithelial biology. *Proceedings of the National Academy of Sciences of the United States of America,* 95**,** 14821-14826.

WANG, H., YOSHIDA, Y., YAMAMOTO, R., MINAMIZAKI, T., KOZAI, K., TANNE, K., AUBIN, J. E. & MAEDA, M. (2008) Overexpression of fibroblast growth factor 23 suppresses osteoblast differentiation and matrix mineralization in vitro. *Journal of Bone and Mineral Research,* 23**,** 939-948.

WARE, C. B., HOROWITZ, M. C., RENSHAW, B. R., HUNT, J. S., LIGGITT, D., KOBLAR, S. A., GLINIAK, B. C., MCKENNA, J. H. & PAPAYANNOPOULOU, T. (1995) Targeted disruption of the low-affinity leukemia inhibitory factor receptor gene causes placental, skeletal, neural and metabolic defects and results in perinatal death. *Development,* 121**,** 1283-1299.

WARTENBERG, M., GUNTHER, J., HESCHELER, J. & SAUER, H. (1998) The embryoid body as a novel in vitro assay system for antiangiogenic agents. *Laboratory Investigation,* 78**,** 1301-1314.

WATT, F. M. & HOGAN, B. L. M. (2000) Out of Eden: Stem cells and their niches. *Science,* 287**,** 1427-1430.

WDZIEKONSKI, B., VILLAGEOIS, P., VERNOCHET, C., PHILLIPS, B. & DANI, C. (2006) Use of differentiating embryonic stem cells in pharmacological studies. *Methods in Molecular Biology,* 329**,** 341-351.

WEAVER, V. M., PETERSEN, O. W., WANG, F., LARABELL, C. A., BRIAND, P., DAMSKY, C. & BISSELL, M. J. (1997) Reversion of the malignant phenotype of human breast cells in three-

dimensional culture and in vivo by integrin blocking antibodies. *Journal of Cell Biology,* 137**,** 231-245.

WEBER, M., STEINERT, A., JORK, A., DIMMLER, A., THUERMER, F., SCHUETZE, N., HENDRICH, C. & ZIMMERMANN, U. (2002) Formation of cartilage matrix proteins by BMP-transfected murine mesenchymal stem cells encapsulated in a novel class of alginates. *Biomaterials,* 23**,** 2003-2013.

WEINER, S., TRAUB, W. & WAGNER, H. D. (1999) Lamellar bone: structure-function relations. *Journal of Structural Biology,* 126**,** 241-255.

WENGER, A., KOWALEWSKI, N., STAHL, A., MEHLHORN, A. T., SCHMAL, H., STARK, G. B. & FINKENZELLER, G. (2005) Development and characterization of a spheroidal coculture model of endothelial cells and fibroblasts for improving angiogenesis in tissue engineering. *Cells,* 181**,** 80-88.

WENGER, A., STAHL, A., WEBER, H., FINKENZELLER, G., AUGUSTIN, H. G., STARK, G. B. & KNESER, U. (2004) Modulation of In Vitro Angiogenesis in a Three-Dimensional Spheroidal Coculture Model for Bone Tissue Engineering. *Tissue Engineering,* 10**,** 1536-1547.

WERNIG, M., MEISSNER, A., FOREMAN, R., BRAMBRINK, T., KU, M., HOCHEDLINGER, K., BERNSTEIN, B. E. & JAENISCH, R. (2007) In vitro reprogramming of fibroblasts into a pluripotent ES-cell-like state. *Nature,* 448**,** 318-324.

WIECHULA, D., JURKIEWICZ, A. & LOSKA, K. (2008) An assessment of natural concentrations of selected metals in the bone tissues of the femur head. *Science of the Total Environment,* 406**,** 161-167.

WILES, M. V. & JOHANSSON, B. M. (1999) Embryonic stem cell development in a chemically defined medium. *Experimental Cell Research,* 247**,** 241-248.

WILSON, J. H., PATURZO, F. X., JOHNSON, L. K., CARREIRO, M. P., HIXSON, D. C., A, M., BOYER, J. L., POBER, J. S. & HARDING, M. J. (2006) Rat hepatocyte engraftment in severe combined immunodeficient x beige mice using mouse-specific anti-fas antibody. *Xenotransplantation,* 13**,** 53-62.

WISSINK, M. J., BEERNINK, R., POOT, A. A., ENGBERS, G. H., BEUGELING, T., VAN AKEN, W. G. & FEIJEN, J. (2000) Improved endothelialization of vascular grafts by local release of growth factor from heparinized collagen matrices. *Journal of Controlled Release,* 64**,** 103-114.

WOLL, N. L., HEANEY, J. D. & BRONSON, S. K. (2006) Osteogenic nodule formation from single embryonic stem cell-derived progenitors. *Stem Cells and Development,* 15**,** 865-879.

WOO, G. L. Y., YANG, M. L., YIN, H. Q., JAFFER, F., MITTELMAN, M. W. & SANTERRE, J. P. (2002) Biological characterization of a novel biodegradable antimicrobial polymer synthesized with fluoroquinolones. *Journal of Biomedical Materials Research,* 59**,** 35-45.

WOOD, S. R., ZHAO, Q., SMITH, L. H. & DANIELS, C. K. (2003) Altered morphology in cultured rat intestinal epithelial IEC-6 cells is associated with alkaline phosphatase expression. *Tissue & cell,* 35**,** 47-58.

WUTHIER, R. E. (1968) Lipids of mineralizing epiphyseal tissues in the bovine fetus. *Journal of Lipid Research,* 9**,** 68-78.

XIE, H., YANG, F., DENG, L., LUO, J., QIN, T., LI, X., ZHOU, G. Q. & YANG, Z. (2007) The performance of a bone-derived scaffold material in the repair of critical bone defects in a rhesus monkey model. *Biomaterials,* 28**,** 3314-3324.

XU, Q., CROSSLEY, A. & CZERNUSZKA, J. (2008) Preparation and Characterization of Negatively Charged Poly(Lacic-co-Glycolic Acid) Microspheres. *Journal of Pharmaceutical Sciences*.

XUE, H. H., SAKAGUCHI, T., FUJIE, M., OGAWA, H. & ICHIYAMA, A. (1999) Flux of the L-serine metabolism in rabbit, human, and dog livers. Substantial contributions of both mitochondrial and peroxisomal serine:pyruvate/alanine:glyoxylate aminotransferase. *Journal of Biological Chemistry,* 274**,** 16028-16033.

YAMADA, K. M. & CLARK, K. (2002) Survival in Three Dimensions. *Nature,* 419**,** 790-791.

YAMASHITA, A., KRAWETZ, R. & RANCOURT, D. E. (2009) Loss of discordant cells during micro-mass differentiation of embryonic stem cells into the chondrocyte lineage. *Cell Death and Differentiation,* 16**,** 278-286.

YANG, D. H., CAI, K. Q., ROLAND, I. H., SMITH, E. R. & XU, X. X. (2007) Disabled-2 is an epithelial surface positioning gene. *Journal of Biological Chemistry,* 282**,** 13114-13122.

YANG, D. H., SMITH, E. R., ROLAND, I. H., SHENG, Z., HE, J., MARTIN, W. D., HAMILTON, T. C., LAMBETH, J. D. & XU, X. X. (2002) Disabled-2 is essential for endodermal cell positioning and structure formation during mouse embryogenesis. *Developmental Biology,* 251**,** 27-44.

YANG, X., TARE, R. S., PARTRIDGE, K. A., ROACH, H. I., CLARKE, N. M. P., HOWDLE, S. M., SHAKESHEFF, K. M. & OREFFO, R. O. C. (2003) Induction of Human Osteoprogenitor Chemotaxis, Proliferation, Differentiation, and Bone Formation by Osteoblast Stimulating Factor-1/Pleiotrophin: Osteoconductive Biomimetic Scaffolds for Tissue Engineering. *Journal of Bone and Mineral Research,* 18**,** 47-57.

YAREMA, K. J., MAHAL, L. K., BRUEHL, R. E., RODRIGUEZ, E. C. & BERTOZZI, C. R. (1998) Metabolic delivery of ketone groups to sialic acid residues. Application To cell surface glycoform engineering. *The Journal of Biological Chemistry,* 273**,** 31168-31179.

YEO, Y. & PARK, K. H. (2004) Control of encapsulation efficiency and initial burst in polymeric microparticle systems. *Archives of Pharmacal Research,* 27**,** 1-12.

YIN, C. H., CHEN, W., HSIAO, C. C., KUO, C. Y., CHEN, C. L. & WU, W. T. (2007) Production of Mouse Embryoid Bodies with Hepatic Differentiation Potential by Stirred Tank Bioreactor. *Bioscience, Biotechnology, and Biochemistry,* 71**,** 728-734.

YING, Q. L., WRAY, J., NICHOLS, J., BATLLE-MORERA, L., DOBLE, B., WOODGETT, J., COHEN, P. & SMITH, A. (2008) The ground state of embryonic stem cell self-renewal. *Nature,* 453**,** 519-523.

YOSHIDA, K., TAGA, T., SAITO, M., SUEMATSU, S., KUMANOGOH, A., TANAKA, T., FUJIWARA, H., HIRATA, M., YAMAGAMI, T., NAKAHATA, T., HIRABAYASHI, T., YONEDA, Y., TANAKA, K., WANG, W. Z., MORI, C., SHIOTA, K., YOSHIDA, N. & KISHIMOTO, T. (1996) Targeted disruption of gp130, a common signal transducer for the interleukin 6 family of cytokines, leads to myocardial and hematological disorders. *Proceedings of the National Academy of Sciences of the United States of America,* 93**,** 407-411.

YOUNG, Y., LEE, S. W., YOUK, J. H., MIN, B. M., LEE, S. J. & PARK, W. H. (2005) In vitro degradation behaviour of non-porous ultra-fine poly(glycolic acid)/poly (L-lactic acid) fibres and porous ultra-fine poly (glycolic acid) fibres. *Polymer Degradation and Stability,* 90**,** 441-448.

YU, J., VODYANIK, M. A., SMUGA-OTTO, K., ANTOSIEWICZ-BOURGET, J., FRANE, J. L., TIAN, S., NIE, J., JONSDOTTIR, G. A., RUOTTI, V., STEWART, R., SLUKVIN, I. I. & THOMSON, J. A. (2007) Induced Pluripotent Stem Cell Lines Derived from Human Somatic Cells. *Science (Washington),* 318**,** 1917-1920.

ZALMAN, F., MALONEY, M. A. & PATT, H. M. (1979) Differential Response of Early Erythropoietic and Granulopoietic Progenitors to Dexamethasone and Cortisone. *Journal of Experimental Medicine,* 49**,** 67-72.

ZANDSTRA, P. W., EAVES, C. J. & PIRET, J. M. (1994) Expansion of hematopoietic progenitor cell populations in stirred suspension bioreactors of normal human bone marrow cells. *Biotechnology,* 12**,** 909-914.

ZANDSTRA, P. W., LE, H. V., DALEY, G. Q., GRIFFITH, L. G. & LAUFFENBURGER, D. A. (2000) Leukemia inhibitory factor (LIF) concentration modulates embryonic stem cell self-renewal and differentiation independently of proliferation. *Biotechnology and Bioengineering,* 69**,** 607-617.

ZHANG, J., WANG, M., CHA, J. M. & MANTALARIS, A. (2009) The incorporation of 70s bioactive glass to the osteogenic differentiation of murine embryonic stem cells in 3D bioreactors. *Journal of Tissue Engineering and Regenerative Medicine,* 3**,** 63-71.

ZHANG, Y., VENUGOPAL, J. R., EL-TURKI, A., RAMAKRISHNA, S., SU, B. & LIM, C. T. (2008) Electrospun biomimetic nanocomposite nanofibers of hydroxyapatite/chitosan for bone tissue engineering. *Biomaterials,* 29**,** 4314-4322.

ZHU, X. H., LEE, L. Y., JACKSON, J. S., TONG, Y. W. & WANG, C.-H. (2008) Characterization of porous poly(D,L-lactic-co-glycolic acid) sponges fabricated by supercritical CO2 gas-foaming method as a scaffold for three-dimensional growth of Hep3B cells. *Biotechnology and Bioengineering,* 100**,** 998-1009.

ZIEGLER, W. H., GINGRAS, A. R., CRITCHLEY, D. R. & EMSLEY, J. (2008) Integrin connections to the cytoskeleton through talin and vinculin. *Biochemical Society Transactions,* 36**,** 235-239.

ZWEIGERDT, R., BURG, M., WILLBOLD, E., ABTS, H. & RUEDIGER, M. (2003) Generation of confluent cardiomyocyte monolayers derived from embryonic stem cells in suspension: a cell source for new therapies and screening strategies. *Cytotherapy,* 5**,** 399-413.